GLIAL AND NEURAL STEM CELLS AS NEW THERAPEUTIC TARGETS FOR NEURODEGENERATIVE DISORDERS

EDITED BY: Sara Xapelli, Maria J. Diógenes, Vincenzo Crunelli, Carlos P. Fitzsimons and Sandra H. Vaz

PUBLISHED IN: Frontiers in Cellular Neuroscience

frontiers Research Topics

frontiers

ISSN 1664-8714
ISBN 978-2-88963-741-6
DOI 10.3389/978-2-88963-741-6

About Frontiers

Frontiers is more than just an open-access publisher of scholarly articles: it is a pioneering approach to the world of academia, radically improving the way scholarly research is managed. The grand vision of Frontiers is a world where all people have an equal opportunity to seek, share and generate knowledge. Frontiers provides immediate and permanent online open access to all its publications, but this alone is not enough to realize our grand goals.

Frontiers Journal Series

The Frontiers Journal Series is a multi-tier and interdisciplinary set of open-access, online journals, promising a paradigm shift from the current review, selection and dissemination processes in academic publishing. All Frontiers journals are driven by researchers for researchers; therefore, they constitute a service to the scholarly community. At the same time, the Frontiers Journal Series operates on a revolutionary invention, the tiered publishing system, initially addressing specific communities of scholars, and gradually climbing up to broader public understanding, thus serving the interests of the lay society, too.

Dedication to Quality

Each Frontiers article is a landmark of the highest quality, thanks to genuinely collaborative interactions between authors and review editors, who include some of the world's best academicians. Research must be certified by peers before entering a stream of knowledge that may eventually reach the public - and shape society; therefore, Frontiers only applies the most rigorous and unbiased reviews.
Frontiers revolutionizes research publishing by freely delivering the most outstanding research, evaluated with no bias from both the academic and social point of view. By applying the most advanced information technologies, Frontiers is catapulting scholarly publishing into a new generation.

What are Frontiers Research Topics?

Frontiers Research Topics are very popular trademarks of the Frontiers Journals Series: they are collections of at least ten articles, all centered on a particular subject. With their unique mix of varied contributions from Original Research to Review Articles, Frontiers Research Topics unify the most influential researchers, the latest key findings and historical advances in a hot research area! Find out more on how to host your own Frontiers Research Topic or contribute to one as an author by contacting the Frontiers Editorial Office: researchtopics@frontiersin.org

GLIAL AND NEURAL STEM CELLS AS NEW THERAPEUTIC TARGETS FOR NEURODEGENERATIVE DISORDERS

Topic Editors:
Sara Xapelli, Instituto de Medicina Molecular João Lobo Antunes, Faculdade de Medicina, Universidade de Lisboa, Portugal and Instituto de Farmacologia e Neurociências, Faculdade de Medicina, Universidade de Lisboa, Portugal
Maria J. Diógenes, Instituto de Medicina Molecular João Lobo Antunes, Faculdade de Medicina, Universidade de Lisboa, Portugal and Instituto de Farmacologia e Neurociências, Faculdade de Medicina, Universidade de Lisboa, Portugal
Vincenzo Crunelli, Neuroscience Division, School of Bioscience, Cardiff University, Cardiff, United Kingdom and Department of Physiology and Biochemistry, Malta University, Msida, Malta
Carlos P. Fitzsimons, Swammerdam Institute for Life Sciences, Center for Neuroscience, University of Amsterdam, Amsterdam, The Netherlands
Sandra H. Vaz, Instituto de Medicina Molecular João Lobo Antunes, Faculdade de Medicina, Universidade de Lisboa, Portugal and Instituto de Farmacologia e Neurociências, Faculdade de Medicina, Universidade de Lisboa, Portugal

Citation: Xapelli, S., Diógenes, M. J., Crunelli, V., Fitzsimons, C. P., Vaz, S. H., eds. (2020). Glial and Neural Stem Cells as New Therapeutic Targets for Neurodegenerative Disorders. Lausanne: Frontiers Media SA.
doi: 10.3389/978-2-88963-741-6

Table of Contents

04 ***Editorial: Glial and Neural Stem Cells as New Therapeutic Targets for Neurodegenerative Disorders***
Sara Xapelli, Maria J. Diógenes, Vincenzo Crunelli, Carlos P. Fitzsimons and Sandra H. Vaz

06 ***Permanent Whisker Removal Reduces the Density of c-Fos+ Cells and the Expression of Calbindin Protein, Disrupts Hippocampal Neurogenesis and Affects Spatial-Memory-Related Tasks***
Oscar Gonzalez-Perez, Verónica López-Virgen and Nereida Ibarra-Castaneda

20 ***On the Role of Basal Autophagy in Adult Neural Stem Cells and Neurogenesis***
Lucía Casares-Crespo, Isabel Calatayud-Baselga, Laura García-Corzo and Helena Mira

29 ***Switching of the Microglial Activation Phenotype is a Possible Treatment for Depression Disorder***
Lijuan Zhang, Jinqiang Zhang and Zili You

42 ***Clonal Glial Response in a Multiple Sclerosis Mouse Model***
Ana Bribian, Fernando Pérez-Cerdá, Carlos Matute and Laura López-Mascaraque

53 ***Evidence of Müller Glia Conversion Into Retina Ganglion Cells Using Neurogenin2***
Roberta Pereira de Melo Guimarães, Bruna Soares Landeira, Diego Marques Coelho, Daiane Cristina Ferreira Golbert, Mariana S. Silveira, Rafael Linden, Ricardo A. de Melo Reis and Marcos R. Costa

68 ***Brain-Derived Neurotrophic Factor (BDNF) Role in Cannabinoid-Mediated Neurogenesis***
Filipa Fiel Ferreira, Filipa F. Ribeiro, Rui S. Rodrigues, Ana Maria Sebastião and Sara Xapelli

84 ***Methyl 3,4-Dihydroxybenzoate Induces Neural Stem Cells to Differentiate Into Cholinergic Neurons* in vitro**
Jun-Ping Pan, Yang Hu, Jia-Hui Wang, Yi-Rong Xin, Jun-Xing Jiang, Ke-Qi Chen, Cheng-You Yang, Qin Gao, Fei Xiao, Li Yan and Huan-Min Luo

97 ***Astrocytes in Neuropathologies Affecting the Frontal Cortex***
Ulla-Kaisa Peteri, Mikael Niukkanen and Maija L. Castrén

106 ***Nrf2 Induction Re-establishes a Proper Neuronal Differentiation Program in Friedreich's Ataxia Neural Stem Cells***
Piergiorgio La Rosa, Marta Russo, Jessica D'Amico, Sara Petrillo, Katia Aquilano, Daniele Lettieri-Barbato, Riccardo Turchi, Enrico S. Bertini and Fiorella Piemonte

117 ***Fractalkine Modulates Microglia Metabolism in Brain Ischemia***
Clotilde Lauro, Giuseppina Chece, Lucia Monaco, Fabrizio Antonangeli, Giovanna Peruzzi, Serena Rinaldo, Alessio Paone, Francesca Cutruzzolà and Cristina Limatola

frontiers in Cellular Neuroscience

EDITORIAL
published: 03 April 2020
doi: 10.3389/fncel.2020.00071

Editorial: Glial and Neural Stem Cells as New Therapeutic Targets for Neurodegenerative Disorders

Sara Xapelli[1,2], *Maria J. Diógenes*[1,2], *Vincenzo Crunelli*[3,4], *Carlos P. Fitzsimons*[5] *and Sandra H. Vaz*[1,2]*

[1] *Instituto de Medicina Molecular João Lobo Antunes, Faculdade de Medicina, Universidade de Lisboa, Lisbon, Portugal,* [2] *Instituto de Farmacologia e Neurociências, Faculdade de Medicina, Universidade de Lisboa, Lisbon, Portugal,* [3] *Neuroscience Division, School of Bioscience, Cardiff University, Cardiff, United Kingdom,* [4] *Department of Physiology and Biochemistry, Malta University, Msida, Malta,* [5] *Swammerdam Institute for Life Sciences, Center for Neuroscience, University of Amsterdam, Amsterdam, Netherlands*

Keywords: neural stem/progenitor cells, glial cells, astrocytes, microglia, neurodegenenerative diseases

Editorial on the Research Topic

Glial and Neural Stem Cells as New Therapeutic Targets for Neurodegenerative Disorders

The gradual and progressive degeneration of neural cells is a common feature of different neurological disorders culminating in a disturbed neuronal communication. The remarkable discovery that adult brain has the capacity to develop new neurons, as well as new glial cells, raised the hope to restore neuronal communication. It is now accepted that adult neurogenesis occurs in neurogenic niches which are under the control of several factors including neurotrophins. These neurogenic niches contain multipotent neural stem/progenitor cells (NSPCs) which can differentiate into neurons, astrocytes and oligodendrocytes. Interestingly, different brain injuries or pathologies, such as epilepsy, head traumas and stroke, induce neurogenesis and/or astrogliogenesis. This increase in neurogenesis has been proposed as an endogenous attempt to repair and reduce brain damage. On the contrary, aging and several neurodegenerative disorders promote a decrease in neurogenesis. Nevertheless, NSPC-based therapy is, to date, not yet a satisfactory strategy due to poor survival and differentiation levels, as well as reduced synaptic plasticity either after transplantation or neural injury. Therefore, it is important to study the molecular and cellular mechanisms of NSPC's function in detail, and their potential therapeutic applicability to improve long-term survival, differentiation, and synaptic integration of derived newborn neural cells.

Classically, the studies in neurodegenerative disorders are mainly focused on neuronal abnormalities, while the non-neuronal cells were almost neglected. Nevertheless, there is increasing evidence that glial cells, and in particularly astrocytes and microglia, are very important in the pathology of these disorders. Astrocytes play important roles in neuronal synaptic activity by removing the majority of glutamate present at the synapse and also by releasing modulators/transmitters that interact with neuronal receptors. Moreover, in pathological conditions astrocytes have been implicated in the onset and progression of several diseases with reactive astrogliosis a common feature. In many neurodegenerative disorders, several changes in astrocytic function have been detected, namely in calcium signaling and in the release of inflammatory molecules. Furthermore, microglia plays an important role in managing neuronal cell death, neurogenesis, and synaptic interactions, besides their involvement in immune-response generating cytokines. Most likely astrocytes and microglia are possible candidates as new pharmacological targets that can ameliorate some of the features of neurological disorders.

This Research Topic containing 10 manuscripts highlights the role of glial and NSPCs in physiological and pathological conditions. La Rosa et al. showed that enhancing the expression and

OPEN ACCESS

Edited and reviewed by:
Enrico Cherubini, European Brain Research Institute, Italy

***Correspondence:**
Sandra H. Vaz
svaz@medicina.ulisboa.pt

Specialty section:
This article was submitted to Cellular Neurophysiology, a section of the journal Frontiers in Cellular Neuroscience

Received: *06 March 2020*
Accepted: *12 March 2020*
Published: *03 April 2020*

Citation:
Xapelli S, Diógenes MJ, Crunelli V, Fitzsimons CP and Vaz SH (2020) Editorial: Glial and Neural Stem Cells as New Therapeutic Targets for Neurodegenerative Disorders. Front. Cell. Neurosci. 14:71. doi: 10.3389/fncel.2020.00071

activity of the antioxidant response the master regulator nuclear factor erythroid 2–related factor 2 ameliorates the phenotypic defects observed in NSPCs, re-establishing a proper differentiation program. Lauro et al. reported that the chemokine CX3CL1 (fractalkine) protects against cerebral ischemia modulating the activation state of microglia and its metabolism in order to restrain inflammation and organize a neuroprotective response against the ischemic insult. The mini-review by Peteri et al. discussed that species-specificity of astrocytes poses a challenge in translating results obtained from animal studies to humans, and patient-derived induced pluripotent stem cells offer an alternative to disease modeling. The data described by Pereira de Melo Guimarães et al. revealed that neurogenin 2 induces lineage conversion of postnatal rodent müller glia cells into retinal ganglion cell-like induced neurons *in vitro* and resumes the generation of this neuronal type from late progenitors of the retina *in vivo*. Ferreira et al. described an interaction between brain-derived neurotrophic factor and endocannabinoid signaling in the control of neurogenesis at distinct levels, further contributing to highlight novel mechanisms in the emerging field of brain repair. In the review by Casares-Crespo et al. the role of basal autophagy in adult neural stem cells and neurogenesis was discussed. Bribian et al. detailed the clonal glial response in a multiple sclerosis mouse model. Pan et al. provided data showing that small molecule (Methyl 3,4-dihydroxybenzoate) promotes NSCs differentiation into cholinergic motor neurons by regulating cell cycle and the cholinergic neuronal differentiation Isl1 gene. Zhang et al. reviewed the relationship between microglia and depression, elucidating the mechanism by which microglia regulate inflammation and neurogenesis in response to major depression disorder. Gonzalez-Perez et al. showed that tactile inputs from vibrissal follicles strongly modify the expression of c-Fos and calbindin in the dentate gyrus, disrupt different aspects of hippocampal neurogenesis, and support the notion that spatial memory and navigation skills strongly require tactile information in the hippocampus.

Overall, the outstanding manuscripts including both reviews and original articles of this Research Topic provide evidence for a role of glial cells, namely microglia and astrocytes, and NSPCs in physiological and pathological conditions. The study of glial cells and NSPCs will continue to reveal novel and effective therapeutic mechanisms for disorders of the nervous system. We hope that this collection of articles will be highly attractive to the neuroscience community.

AUTHOR CONTRIBUTIONS

All authors listed have made a substantial, direct and intellectual contribution to the work, and approved it for publication.

ACKNOWLEDGMENTS

The authors would like to thank the following organizations for their funding: Fundação para a Ciência e Tecnologia (FCT) Portugal (LISBOA-01-0145-FEDER-031929; IF/01227/2015 and PTDC/BTM-SAL/32147/2017) and Santa Casa da Misericórdia de Lisboa (MB37-2017).

Conflict of Interest: The authors declare that the research was conducted in the absence of any commercial or financial relationships that could be construed as a potential conflict of interest.

frontiers in Cellular Neuroscience

ORIGINAL RESEARCH
published: 15 May 2018
doi: 10.3389/fncel.2018.00132

Permanent Whisker Removal Reduces the Density of c-Fos+ Cells and the Expression of Calbindin Protein, Disrupts Hippocampal Neurogenesis and Affects Spatial-Memory-Related Tasks

Oscar Gonzalez-Perez[1,2]*, *Verónica López-Virgen*[1,3] *and Nereida Ibarra-Castaneda*[1]

[1]*Laboratory of Neuroscience, School of Psychology, University of Colima, Colima, Mexico,* [2]*El Colegio de Colima, Colima, Mexico,* [3]*Medical Sciences PhD Program, School of Medicine, University of Colima, Colima, Mexico*

OPEN ACCESS

Edited by:
Sara Xapelli,
Universidade de Lisboa, Portugal

Reviewed by:
Carlos P. Fitzsimons,
University of Amsterdam, Netherlands
Helena Mira,
Instituto de Biomedicina de Valencia (IBV), Spain
Jorge Valero,
Achucarro Basque Center for Neuroscience, Spain

***Correspondence:**
Oscar Gonzalez-Perez
osglez@ucol.mx

Received: *23 January 2018*
Accepted: *27 April 2018*
Published: *15 May 2018*

Citation:
Gonzalez-Perez O, López-Virgen V and Ibarra-Castaneda N (2018) Permanent Whisker Removal Reduces the Density of c-Fos+ Cells and the Expression of Calbindin Protein, Disrupts Hippocampal Neurogenesis and Affects Spatial-Memory-Related Tasks. Front. Cell. Neurosci. 12:132. doi: 10.3389/fncel.2018.00132

Facial vibrissae, commonly known as whiskers, are the main sensitive tactile system in rodents. Whisker stimulation triggers neuronal activity that promotes neural plasticity in the barrel cortex (BC) and helps create spatial maps in the adult hippocampus. Moreover, activity-dependent inputs and calcium homeostasis modulate adult neurogenesis. Therefore, the neuronal activity of the BC possibly regulates hippocampal functions and neurogenesis. To assess whether tactile information from facial whiskers may modulate hippocampal functions and neurogenesis, we permanently eliminated whiskers in CD1 male mice and analyzed the effects in cellular composition, molecular expression and memory processing in the adult hippocampus. Our data indicated that the permanent deprivation of whiskers reduced in 4-fold the density of c-Fos+ cells (a calcium-dependent immediate early gene) in *cornu ammonis* subfields (CA1, CA2 and CA3) and 4.5-fold the dentate gyrus (DG). A significant reduction in the expression of calcium-binding proteincalbindin-D_{28k} was also observed in granule cells of the DG. Notably, these changes coincided with an increase in apoptosis and a decrease in the proliferation of neural precursor cells in the DG, which ultimately reduced the number of Bromodeoxyuridine (BrdU)+NeuN+ mature neurons generated after whisker elimination. These abnormalities in the hippocampus were associated with a significant impairment of spatial memory and navigation skills. This is the first evidence indicating that tactile inputs from vibrissal follicles strongly modify the expression of c-Fos and calbindin in the DG, disrupt different aspects of hippocampal neurogenesis, and support the notion that spatial memory and navigation skills strongly require tactile information in the hippocampus.

Keywords: subgranular zone, adult neurogenesis, whisker, tactile system, calbindin, hippocampus, memory, dentate gyrus

INTRODUCTION

Facial vibrissae, also referred to as whiskers, are the main sensitive tactile system in rodents. Each vibrissal follicle has a neuronal representation in the barrel cortex (BC), in layer IV of the somatosensory cortex (Woolsey and Van der Loos, 1970). Whisker stimulation increases the neuronal activity that, in turn, produces functional changes and neural plasticity in the BC (Lecrux et al., 2011). Some studies have shown that the whisker tactile information linked to fine discrimination increases the spiking rate in the CA1 hippocampal region (Pereira et al., 2007; Itskov et al., 2011). In fact, hippocampal place cells integrate tactile inputs from vibrissal follicles (Gener et al., 2013). Whisker elimination during early brain development reduces the activity of CA3 neurons, which induces CA3-CA1 synaptic facilitation (Milshtein-Parush et al., 2017). This evidence indicates that many of the tactile inputs from the vibrissal system are processed in the hippocampus, and this tactile information seems to play an important role in the creation of spatial maps (Pereira et al., 2007).

The CA1 hippocampal region contains pyramidal neurons that create spatial maps by integrating sensorial information (Muller and Kubie, 1987). Neuronal activity in CA1 is also modified by the electrical activity of the new neurons generated in the dentate gyrus (DG; Kitamura and Inokuchi, 2014). In the adult brain, the subgranular zone (SGZ) of DG produces new neurons that migrate shortly into the granular layer and spread their axons to CA3 (Kempermann et al., 2015). To date, it is well accepted that hippocampal neurogenesis modulates the processes of memory acquisition and retention (Aimone et al., 2006). Inputs from voluntary exercise, enriched environments and cognitive processes comprise a group of stimuli that control hippocampal functions in an activity-dependent manner that, in turn, modulates the adult neurogenesis (Kempermann et al., 1997; Pereira et al., 2007; Ma et al., 2009). Therefore, there is an exciting possibility that whisker-derived information modulates the neurogenic process in the DG. To assess this theory, we analyzed the effect of permanent whisker deprivation (WD) on the neuronal activity of hippocampal regions, adult neurogenesis in the DG and hippocampal functions. Our findings indicate that the permanent deprivation of whiskers strongly reduces the density of c-Fos+ cells (a calcium-dependent immediate early gene) and calbindin (a calcium-binding protein) in several hippocampal regions, including DG. WD is also associated with a dramatic decrease in several aspects of adult neurogenesis and produces a significant impairment of spatial memory and navigation. These data support the notion that tactile inputs are crucial to maintain the adult neurogenesis, create spatial maps in the hippocampus, and preserve memory performance.

MATERIALS AND METHODS

Animals

Eight-week-old male CD-1 mice were maintained at a constant room temperature (22 ± 2°C), 12-h light/dark cycle, with *ad libitum* access to food and water. All rodents were randomly assigned to experimental and control groups that were kept under the same biotery and handling conditions throughout the study. All procedures were in accordance with the Principles of Laboratory Animal Care (Mexican Official Norm [NOM] 062-ZOO-1999) and approved by the University of Colima, Animal Care Committee.

Whisker Deprivation (WD)

At the postnatal 60 (P60) day, the whisker-deprived group was intraperitoneally anesthetized with ketamine (10 mg/kg) plus xylazine (5 mg/kg) and the facial vibrissae were fulgurated under a surgical microscope (OPMI Vario/S88, Carl Zeiss Germany). Briefly, each whisker was gently pulled out and ablated with a surgical cautery device. The control group received the same pharmacological manipulation, but no whisker removal procedure was done. After that, the animals were placed in a pre-warmed cage until recovery. We quantified the bodyweight gain every 2 days and corroborated the fact that facial injuries healed in less than 72 h.

Bromodeoxyuridine (BrdU) Administration

Bromodeoxyuridine (BrdU) injections were used for two different experiments. To evaluate the short-term cell division, the animals (n = 5 per group) received an intraperitoneal injection of BrdU (50 mg/kg; Sigma B5002, St. Louis, MO, USA) dissolved in 0.007 N NaOH solution, 2 h before sacrifice (Xie et al., 2016). To label the cell proliferation at the long term, the mice (n = 5 per group) received an intraperitoneal injection of 50 mg/kg BrdU every 8 h for the first 3 days (Gonzalez-Perez et al., 2011). These BrdU injections were done 72 h after vibrissal fulguration to minimize the effect of inflammatory cytokines triggered by the surgical procedure.

Memory Test

Spatial memory was tested in the Barnes Maze (Barnes, 1979). The apparatus consisted of a circular platform (90-cm diameter) with 12 equally spaced holes (5.5-cm diameter) located at one centimeter from the edge of the platform. Visual cues consisted in four different geometrical pieces placed around the maze. Only one hole had access to the shelter hole, a black container (23 cm × 6 cm × 6 cm) attached under the platform. Twenty-four days after whisker elimination, the animals were covered with a black cylinder (the starting box), placed at the center of the maze and allowed to freely move onto the platform. The test consisted of three phases: habituation, acquisition and retention. For the habituation phase (experimental day 24), the mice were exposed to the components of the apparatus, platform, goal and starting box for 2 min, which helps reduce the anxiety induced by a novel environment. In the acquisition phase, the animal was placed at the center of the platform inside of the starting box for 15 s and allowed to move freely for 4 min. If the animal did not find the shelter hole in 4 min, it was guided and placed manually in the goal box for 1 min. After that, the mouse was returned to its home cage for 2 min, while the apparatus was cleaned with 70% ethanol solution to eliminate odor cues. This procedure was repeated four times per day for 3 days. For the retention phase or probe trial (48 h after the last trial), the

shelter box was removed, and mice were allowed to explore the maze for 4 min. For the acquisition trials, latency was defined as the time spent for the animal to enter the goal box. Instead, latency in the retention phase was defined as the time needed to reach the goal hole. We recorded the number of errors to the first encounter of the escape hole (primary errors) and path length for the entire duration of assays (total path length). The search strategy employed for the animals to solve the memory test during the acquisition phase was classified as: random, serial or spatial (Jašarević et al., 2011; Williams et al., 2013). The random strategy was characterized by multiple central crosses in the maze and random searching behavior. The serial strategy was defined as systematic searching behavior in consecutive holes and with maximum two central crosses. The spatial strategy was identified as navigation directed to the goal box without crossing the center of the platform more than once. All trials were recorded with a digital camera and analyzed using the EthoVision tracking system (Noldus Equipment, Wageningen, Netherlands).

Tissue Preparation

Animals were sacrificed with 100 mg/kg pentobarbital i.p. and perfused transcardially with 25 ml of 0.9% NaCl solution followed by 25 ml of 4% paraformaldehyde in 0.1 M phosphate buffer solution (PB), pH 7.4. The brains were extracted and post-fixed overnight in 50 ml of the same fixative solution. Then, we cut 20-μm coronal sections serially from −0.82 mm to −3.70 mm coordinates relative to Bregma (Paxinos and Watson, 2007) using a vibratome (Leica VT100S, Nussloch, Germany).

Cytochrome Oxidase Histochemistry

Cytochrome oxidase allows labeling the BC (Wong-Riley and Welt, 1980). Brain tissues were washed three times in 0.1 M PB saline solution (PBS) and incubated in cytochrome oxidase (0.5 mg sucrose, 0.6 mg diaminobenzidine (DAB) and 30 mg Cytochrome C; all from Sigma-Aldrich) in 10 ml of 0.2 M PB (pH = 7.4) for 4 h at 37°C. The samples were washed in 0.1 M PBS, mounted on glass slides, dehydrated and sealed with resin (Entellan, Millipore).

Immunohistochemistry

Brain sections were rinsed three times in 0.1 M PBS. To inactivate endogenous peroxidases, the sections were incubated in 3% hydrogen peroxide (H_2O_2) for 30 min and then washed three times (3×) in 0.1 M PBS. The samples were incubated in blocking solution (0.1 M PBS, 10% fetal bovine serum and 0.1% Triton X-100) for 40 min. Subsequently, the samples were incubated with the primary antibody rabbit anti-c-Fos (dilution 1:800; Cell Signaling Technology Cat # 2250, RRID:AB_2247211) and rabbit anti-Calbindin-D_{28k} (dilution 1:1000; Synaptic Systems Cat # 214002, RRID:AB_2068199) dissolved in blocking solution at 4°C overnight. The next day, the brain sections were rinsed 3× in 0.1 M PBS and incubated with the biotinylated secondary antibody (goat anti-rabbit IgG + IgM Biotin, dilution 1:200; Sigma-Aldrich; St. Louis, MO, USA) in 0.1 M PBS and 10% fetal bovine serum, for 1 h. Then, the samples were washed 3× and incubated with avidin-biotin complex (Vectastain Elite ABC kit, Vector Laboratories, Burlingame, CA, USA) for 60 min and rinsed in 0.1 M PBS. The sections were revealed for 5 min with 0.03% DAB solution (Sigma-Aldrich) plus 0.05% nickel ammonium sulfate (Sigma-Aldrich), washed 3× in 0.1 M PBS, mounted, dehydrated and sealed with resin (Entellan, Millipore, Billerica, MA, USA).

Immunofluorescence

For the BrdU immuno-labeling, the brain sections were rinsed three times in 0.1 M PBS and incubated in 2 N HCl at 37°C for 15 min, followed by 0.1 M borate buffer (pH = 8.6) for 10 min and washed 3× with 0.1 M PBS. Sections were incubated in blocking solution for 40 min. Then, sections were incubated with some combinations of the following primary antibodies: rat anti-BrdU (1:500; AbD Serotec Cat # OBT0030, RRID:AB_609568), mouse anti-NeuN (1:500; Millipore Cat # MAB377, RRID:AB_2298772), rabbit anti-GFAP (1:100; Dako Cat # Z0334, RRID:AB_10013382), rabbit anti-Sox2 (1:500, Abcam Cat # AB97959; RRID:AB_2341193), guinea pig anti-doublecortin (DCX, 1:1000: Millipore Cat# AB2253, RRID:AB_1586992) in blocking solution at 4°C overnight. Sections were rinsed 3× with 0.1 M PBS, and incubated in 0.1 M PBS containing 10% fetal bovine serum and conjugated secondary antibodies (Alexa Fluor® 488 anti-rat Cat # A-21208; Alexa Fluor® 594 anti-rat Cat # A-11007; Alexa Fluor® 488 anti-mouse Cat # A32723; Alexa Fluor® 594 anti-rabbit; Alexa Fluor® 594 Cat# R37117; anti-guinea pig Cat# A-11076; dilution 1:1000; Thermo Fisher) for 1 h at room temperature and washed 3× with 0.1 M PBS. Nuclear counterstaining was done with 4′,6-diamidino-2-phenylindole (DAPI; Abcam Cat # ab104139, Cambridge, MA, USA).

TUNEL Assay

TUNEL staining was performed using the *in situ* cell-death detection kit TMR red (Roche Cat # 12156792910) and following the manufacturer's directions. Briefly, the sections were fixed on a coverslip, washed 2× with 0.1 M PBS, and then incubated in a permeabilization solution (0.1 M PBS, 0.1% Triton X-100, 0.1% sodium citrate) for 15 min at 4°C. Samples were then washed 2× in 0.1 M PBS and blocked for 10 min in Tris-HCl (pH = 7.5) with 10% fetal bovine serum. Brain tissue was washed 2× and incubated in the TUNEL reaction mixture for 1 h at 37°C in the dark. Nuclear staining was performed with DAPI.

Quantification

To quantify the number cells per group, brain slices were consecutively numbered, and six sections (taken 120-μm apart) per animal were randomly selected along the rostro-caudal axis. Sectioning interval was from −0.82 mm to −3.70 mm and 0.38 mm to −1.94 mm coordinates relative to Bregma for hippocampus and BC, respectively. We only counted the c-Fos+ cells observed in the same focal plane. Quantifications were made under inverted bright-field microscopy (Zeiss Axio Observer D1, Germany) with the 20× objective (NA = 0.45; area = 0.63 mm^2 per field). To quantify double labeling, six slices by group were randomly selected in −0.82 mm to −3.70 mm coordinates relative to Bregma (Paxinos and Watson, 2007). For quantification purposes only, the dorsal aspect of the

hippocampus was analyzed. Double-labeled cells were quantified only when the DAPI staining colocalized with the cell marker expression and it was confirmed by the orthogonal views. For DCX, Sox2, GFAP cell counting was done in the SGZ along both upper and lower blades of the dorsal aspect of DG. The SGZ was defined as the two-nucleus-wide band below the evident border between the granule cell layer and the hilus. For NeuN, c-Fos, Calbindin and TUNEL, we included the granular zone of the DG. Double-staining quantifications were made with a confocal microscope (Zeiss LSM 700, Germany) with a 40× objective (NA = 1.3; area = 0.15 mm^2 per field). For confocal analyses, the number of double-labeled cells was quantified in at least 125 single-plane confocal pictures per region (CA1, CA2, CA3 and DG) in each group. To minimize the error for identifying double labeling in a single optical plane, 0.55-μm optical sections were used. To calculate the proliferation rate of SGZ progenitor cells, we determined the percentage of BrdU+ cells expressing a cell identity marker (GFAP, Sox2 or DCX) between the total number of cells expressing that marker. In all cases, these quantitative analyses were done by a researcher blinded to group assignments.

Densitometry (Relative Optical Density)

Tissue densitometry was used to establish the expression level of calbindin by quantifying the optical density as described previously (Kuchukhidze et al., 2015). Briefly, six brain sections per animal (n = 5 mice *per* group) were randomly selected by using the same strategy described above. At least eight pictures per brain section were taken along the whole DG with an inverted microscope (Zeiss Axio Observer D1, Germany) under the 40× objective (NA = 0.95). Images were processed with the software *IMAGEJ 1.46r*[1]. First, each picture was converted to an 8-bit image and the DG was delineated with the section tool of the software. We measured area integrated density and mean gray value in every antibody-treated section. Negative controls (with the omission of incubation with primary antibody) were included for each brain section analyzed. We calculated the corrected total marker expression with the following formula: Corrected marker expression = Integrated density (selected area × the mean intensity of background staining; McCloy et al., 2014). A blinded researcher to group assignment performed the densitometry measurement and calculations.

Statistical Analysis

We used the Shapiro-Wilk test to determine if the data were normally distributed and applied the appropriate statistical test to establish statistical differences. For the statistical analysis of histological quantifications, we used the Mann–Whitney "*U*" test. To determine intra group differences in the behavioral test we utilized Friedman's test, whereas intergroup differences (control vs. experimental) were calculated with the Mann-Whitney "*U*" test. *Chi*-square test was used for the analysis of the search strategies of memory test. Data are expressed as median (Mdn) and interquartile range (IQR). The level of confidence was set at 95% ($p < 0.05$).

[1]http://imagej.nih.gov/ij/

RESULTS

Whisker Fulguration Decreases Cytochrome C Oxidase and c-Fos-Expressing Cells in Barrel Cortex

c-Fos protein is coded by a calcium-dependent immediate early gene that is used as a marker of neuronal activity (Herrera and Robertson, 1996). Tactile experience and whisker stimulation increase c-Fos expression (Filipkowski et al., 2000), whereas whisker trimming reduces c-Fos expression in the BC (Filipkowski et al., 2001). To determine changes in the neuronal activity that occur after permanent WD, we fulgurated whiskers in P60 mice and analyzed the expression of cytochrome oxidase and c-Fos (n = 5 mice *per* group). At day 30 after WD, we stained brain sections to detect the activity of cytochrome C oxidase in the BC and found that the control group showed the typical barrel distribution (Wong-Riley and Welt, 1980), which was absent in the WD group (**Figures 1A,B,D**). We then quantified the density of c-Fos+ cells in the BC and observed that the WD group had a dramatic reduction in the density of c-Fos+ cells (Mdn = 104 cells/mm^2 of BC region, IQR: 66–139) as compared with the control group (Mdn = 497 cells/mm^2 of BC region, IQR: 381–597; $U = 0$, $p < 0.001$; **Figures 1C,E**). These findings indicate that whisker fulguration produces a persistent reduction in neural activity of the BC in the adult brain.

Long-Term WD Reduces the Density of c-Fos+ Cells and Calbindin in the Hippocampus

Adult hippocampus creates spatial maps by integrating multiple neural inputs from visual, olfactive and tactile clues (Pereira et al., 2007; Haggerty and Ji, 2015; Zhang and Manahan-Vaughan, 2015). Whisker information is partially processed in the hippocampus during texture discrimination tasks and memory integration (Grion et al., 2016). To determine whether permanent WD modified the neuronal activity in the adult hippocampus, we extended our analysis of the c-Fos-expressing cells to CA1, CA2 and CA3 regions. Our data indicated that WD produced a ∼4-fold reduction in the density of c-Fos+ neurons in the hippocampal regions (**Figures 2A–D,H–K**): CA1 (controls = 1020 cells/mm^2 of CA1 region, IQR: 531–1706 vs. WD = 113 cells/mm^2 of CA1 region, IQR: 73–151; $U = 22.5$, $p < 0.001$) CA2 (controls = 43 cells/mm^2 of CA2 region, IQR: 26–52 vs. WD = 18 cells/mm^2 of CA2 region, IQR: 4–35; $U = 73.5$, $p < 0.001$), and CA3 (controls = 119 cells/mm^2 of CA3 region, IQR: 70–157 vs. WD = 34 cells/mm^2 of CA3 region, IQR: 24–70; $U = 125.5$, $p < 0.001$). Remarkably, the density of c-Fos+ cells was significantly reduced in the DG (**Figures 2E,L,M**), a neurogenic region that importantly contributes to neural plasticity (Sahay et al., 2011). The upper blade of DG showed a significant decrease in the density of c-Fos+ cells in the WD group (Mdn = 186 cells/mm^2 of upper blade region, IQR: 127–197) as compared to the control group (Mdn = 354 cells/mm^2 of upper blade region, IQR: 348–387; $U = 0$, $p = 0.009$). No statistically significant

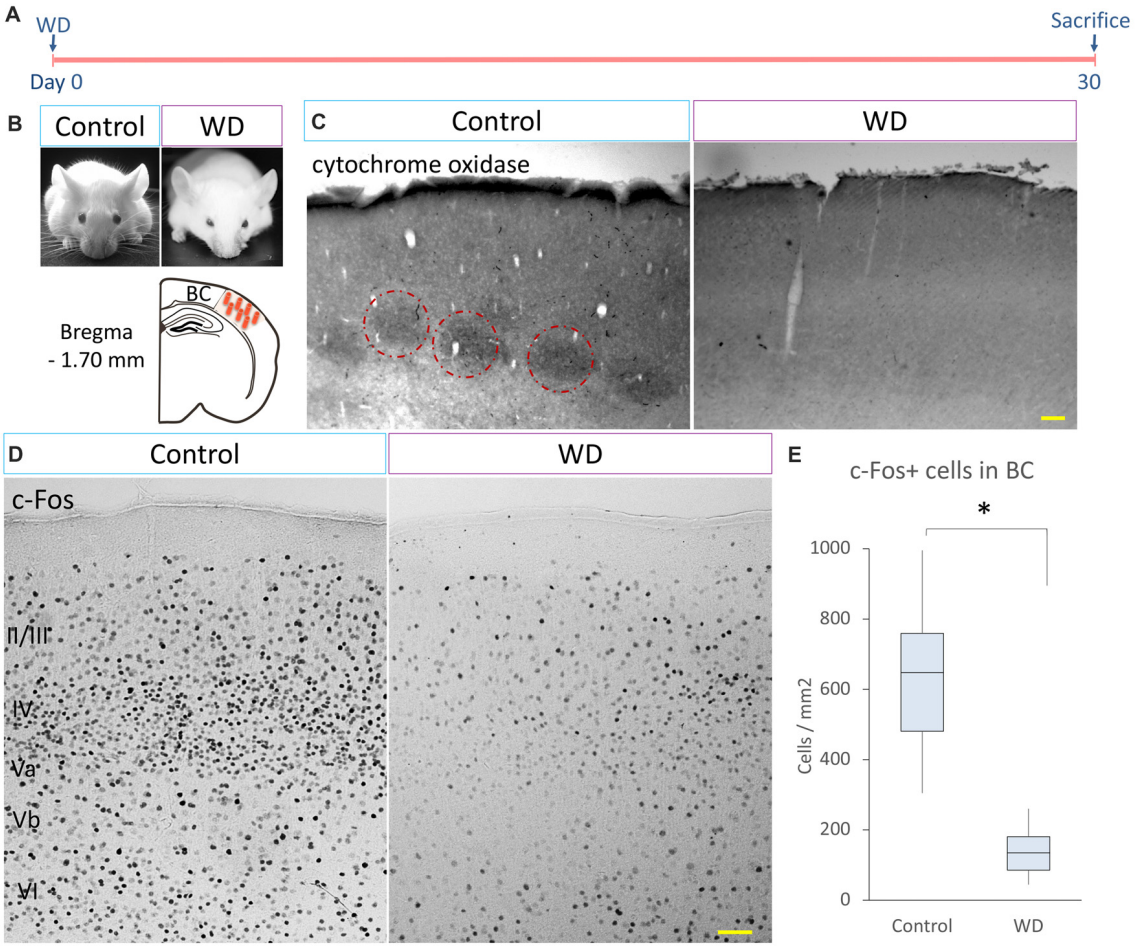

FIGURE 1 | Cytochrome C oxidase activity and c-Fos-expressing cells in the barrel cortex (BC). **(A)** Experimental design. **(B)** CD-1 mice 30 days after surgical manipulation (sham or whisker deprivation (WD)); below: representative coronal section at −1.70 mm coordinates relative to Bregma. **(C)** The control group shows the typical barrel pattern as identified by the cytochrome C activity staining (dotted circles). Note that the whisker-deprived (WD) group did not show cytochrome C activity staining. **(D)** Immunostaining for c-Fos (black dots) in the BC in controls and the WD group. **(E)** Quantification of c-Fos+ cells in the BC. The WD group showed a decrease in the density of c-Fos-expressing cells as compared to controls. Data are expressed as median and interquartile range (IQR). $^*U = 0$, $p < 0.001$; Mann-Whitney "*U*" test; $n = 5$ animals per group. Bars = 50 μm.

differences were found in the lower blade of DG: Controls (Mdn = 166 cells/mm^2 of lower blade region, IQR: 132–192) vs. WD animals (Mdn = 129 cells/mm^2 of lower blade region, IQR: 57–137; $U = 5$, $p = 0.11$). These findings indicate that permanent WD reduces the density of c-Fos+ cells, a calcium-dependent early gene product in the DG. To determine whether local calcium homeostasis was also altered by WD, we analyzed the expression of another calcium-dependent protein, the calcium-binding protein calbindin-D_{28k}, in the DG (**Figures 2F,G,N**). We observed that calbindin expression in granule cells was dramatically reduced in the WD group (Mdn = 9.5 densitometry units IQR: 7.9–18.2) as compared to the control group (Mdn = 40.2 densitometry units IQR: 39.1–46.3; $U = 0$, $P < 0.0001$). Taken together, our findings indicate that permanent vibrissal deprivation produces a sustained reduction in c-Fos and calbindin in the adult hippocampus, including the DG.

WD Reduces the Proliferation of Neural Progenitor Cells in the Hippocampus

The SGZ of DG is a discrete brain region that produces new neurons throughout life (Gonçalves et al., 2016). Activity-dependent inputs and calcium homeostasis modulate adult neurogenesis (Kempermann et al., 1997; Palop et al., 2003; Pereira et al., 2007; Ma et al., 2009). Our data indicated that the calcium-dependent neuronal activity in the DG is reduced by the effect of WD. These alterations may be due to functional variations (less neuronal activity) or structural changes (less neuronal production). To determine whether the whisker elimination affected the neuronal production in the SGZ, we injected BrdU 2 h before sacrifice ($n = 5$ mice *per* group) and studied the proliferation rate of hippocampal neural progenitors (Soto-Rodriguez et al., 2016; **Figures 3A–K**). We quantified the number of BrdU+ cells in the SGZ and found a statistically significant reduction in WD mice

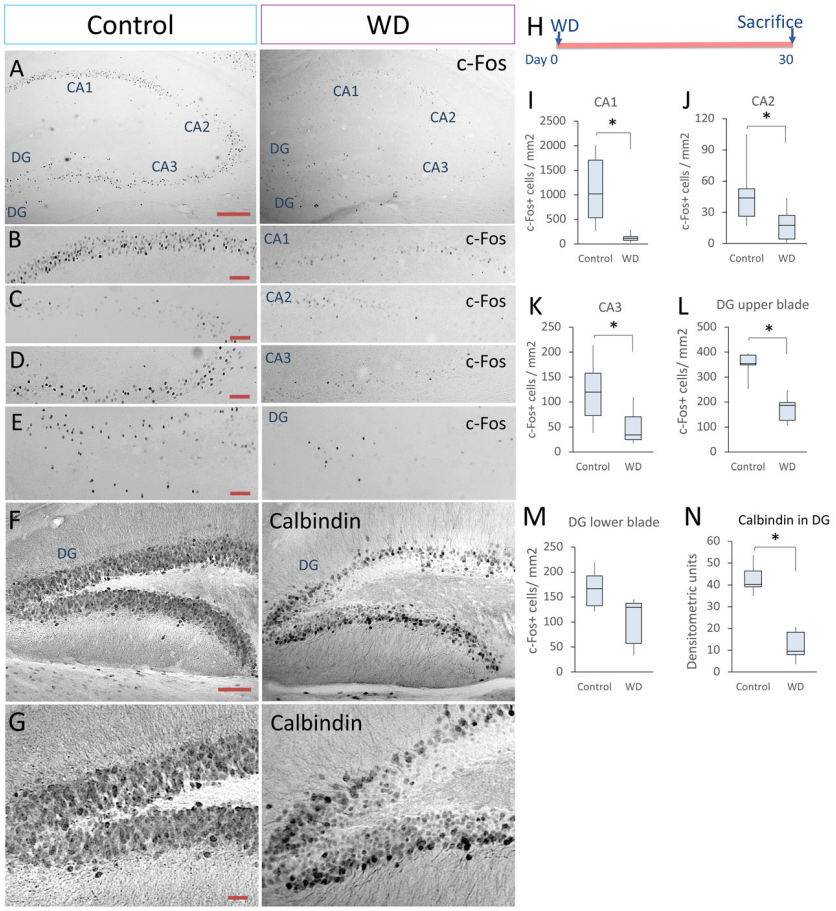

FIGURE 2 | Whisker elimination decreases the density of c-Fos+ cells and calbindin expression in the hippocampus. **(A)** Immunostaining of c-Fos+ cells in the hippocampus of both groups (black dots). **(B–E)** Higher magnifications of CA1, CA2, CA3 and dentate gyrus (DG). **(F)** Immunostaining of calbindin-D_{28k} in the hippocampus of both groups. **(G)** High magnifications of calbindin expression in DG. **(H)** Experimental design. **(I–L)** Quantification data of the c-Fos+ cells in CA1 **(I)**, CA2 **(J)**, CA3 **(K)**, upper blade of DG **(L)** and lower blade of DG **(M)**. **(N)** Quantification of the relative optical density of calbindin immunostaining in both groups. Data are expressed as median and IQR; $n = 5$ mice per group; $^*P < 0.01$; Mann-Whitney "*U*" test. Bars **(A,F)** = 50 μm. Bars **(B–E)** = 25 μm. Bar **(G)** = 15 μm.

(Mdn = 21.8 cells/mm^2 of SGZ area, IQR: 19.2–30.9) as compared with the control group (Mdn = 45.2 cells/mm^2 of SGZ area, IQR: 35.4–52.4; $U = 6$, $P = 0.001$; **Figure 3H**). We then investigated by confocal microscopy if some of these BrdU+ cells corresponded to hippocampal neural progenitors, i.e., radial-glia-like GFAP+ cells as confirmed by the presence of a pyramidal soma with a long vertical process extending from the SGZ towards the molecular layer and branching, as well as small horizontally oriented processes along the SGZ (Kosaka and Hama, 1986; Seri et al., 2001; Kronenberg et al., 2003; Steiner et al., 2006). We found that the WD group suffered a ∼3-fold decrease in the number of BrdU+GFAP+ cells with radial-glia morphology (Mdn = 3.7 cells/mm^2 of SGZ area, IQR: 3.2–4.3) as compared with controls (Mdn = 12.6 cells/mm^2 of SGZ area, IQR: 10.8–13.5; $U = 0$; $P = 0.004$). We then calculated the proliferation rate of radial-glia-like GFAP+ cells (**Figures 3A,B,I**). Our data indicate that the proliferation rate of radial-glia-like GFAP+ cells showed a statistically significant decrease in the WD group (Mdn = 10%, IQR: 8.5–10.1) as compared to controls (Mdn = 34%, IQR: 29–36; $U = 0$; $P = 0.004$).

To establish whether WD reduces the proliferation of other hippocampal progenitor cells (Kriegstein and Alvarez-Buylla, 2009; Gonçalves et al., 2016), we analyzed the expression of the Sox2 transcription factor in the SGZ (**Figures 3C,D**). Our data indicated that the WD group had a significant decrease in the number of BrdU+Sox2+ cells (Mdn = 1.5 cells/mm^2 of SGZ area, IQR: 1.5–5.5) respect to controls (Mdn = 28.5 cells/mm^2 of SGZ area, IQR: 20.2–37.3; $U = 0$, $p = 0.004$). We calculated the proliferation rate of Sox2+ progenitor cells (**Figure 3J**) and found that the WD group had a significant reduction in the percentage of Sox2+BrdU+/Sox2+ cells (Mdn = 3.3%, IQR: 1.1–7.7) when compared to the control group (Mdn = 15.6%, IQR: 10.7–17.1; $U = 3$; $P = 0.016$). Since these findings suggested that WD can affect the pool of radial-glia-like GFAP+ cells and Sox2-expressing progenitor cells, we decided to determine the percentage of Sox2+ cells that co-express GFAP with radial-glia-like morphology in the SGZ. Interestingly, we did

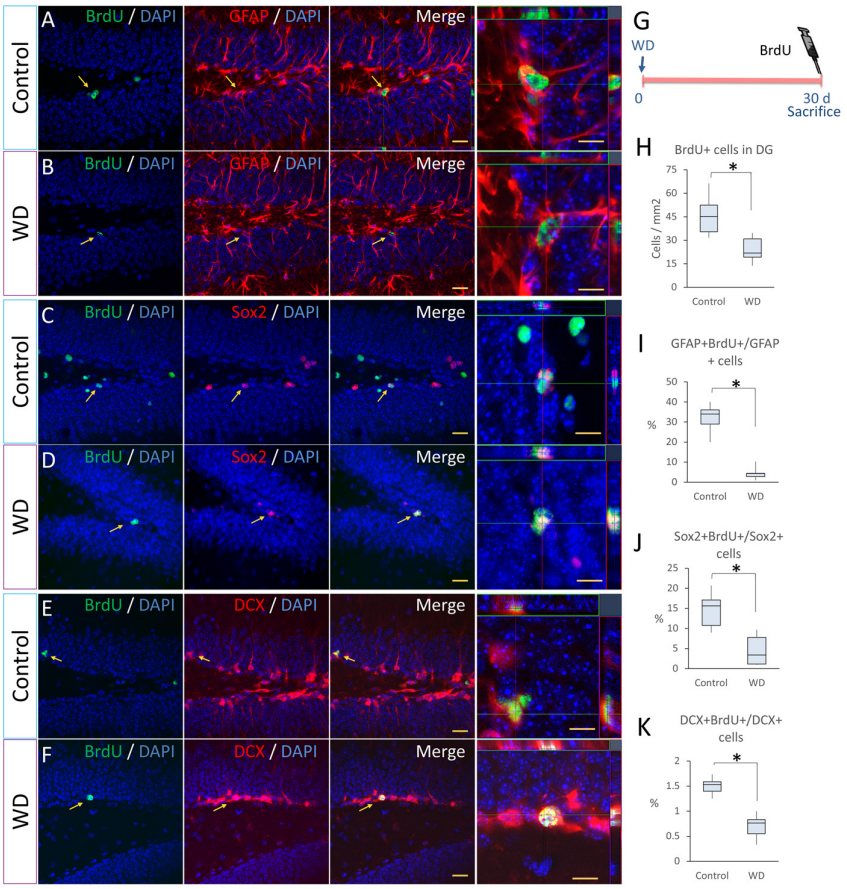

FIGURE 3 | Whisker elimination reduces the proliferation rate of primary progenitor cells and neuroblasts in the subgranular zone (SGZ). **(A–F)** Immunostaining of Bromodeoxyuridine (BrdU)+ (green)/GFAP+ (red), BrdU+/Sox+ (red) and BrdU+/doublecortin (DCX)+ (red) in control and WD groups. **(G)** Experimental design: at day 30 after WD, 50 mg/kg BrdU was injected intraperitoneally 2 h before sacrifice to determine the proliferation of neuronal progenitors. **(H)** Quantification of BrdU+ cells in the DG. **(I)** Percentage of GFAP+BrdU+/GFAP+ cells. **(J)** Percentage of Sox2+BrdU+/Sox2+ cells. **(K)** Percentage of DCX+BrdU+/DCX+ cells. All nuclei were stained with 4′,6-diamidino-2-phenylindole (DAPI; blue). Data are expressed as median and IQR. Insets show high magnification views. $n = 5$ animals per group; $^*P < 0.05$; Mann-Whitney "*U*" test. Bar **(A–F)** = 30 μm. Bar in orthogonal views = 10 μm. Optical section thickness = 0.55 μm.

not find statistically significant differences in the percentage of Sox2+GFAP+ radial-glia-like astrocytes between the WD group (Mdn = 18% IQR: 16.2–21.75%) and the control group (Mdn = 23% IQR: 20.2–27.7%; $U = 25$, $P = 0.065$). This evidence suggests that the reduction in the proliferation of Sox2+ cells found in the WD group is not due to a decrease in the density of radial-glia-like GFAP+ astrocytes.

To determinate whether the permanent WD affected the proliferation of neuroblasts in the SGZ (Song et al., 2012), we co-stained sections with BrdU and a neuroblast marker DCX and quantified the number of BrdU/DCX co-expressing cells in the SGZ (**Figures 3E,F**). We observed an important decrease in the number of co-labeled cells in WD animals (Mdn = 2.3 cells/mm^2 of SGZ area, IQR: 1.7–2.6) when compared to controls (Mdn = 6.9 cells/mm^2 of SGZ area, IQR: 5.2–7.5; $U = 0$, $p = 0.005$). We also calculated the proliferation rate of DCX+ cells (**Figure 3K**) and found that the WD group showed a significant reduction in the percentage of DCX+BrdU+/DCX+ cells (Mdn = 0.76%, IQR: 0.55–0.83) when compared to the control group (Mdn = 1.54%, IQR: 1.41–1.6; $U = 0$; $P = 0.004$). We then quantified the absolute number of neuroblasts found in both groups, we observed that the number of neuroblasts was significantly reduced by the whisker removal: WD mice (Mdn = 181 cells cells/mm^2 of SGZ area, IQR: 162–197) vs. controls (Mdn = 441 cells/mm^2 of SGZ area, IQR: 419–556; $U = 0$, $p = 0.004$). Taken together, these findings indicate that the permanent loss of tactile inputs from whiskers substantially affects the different aspect of the neurogenic process in the adult SGZ.

WD Affects the Proliferation and Maturation and Promotes Apoptosis in Dentate Gyrus

Our data indicated that WD affects the proliferation of SGZ progenitors. This event may affect the ultimate number of new-born neurons in the DG. To investigate this possibility,

at the 3rd day after whisker removal, we injected BrdU every 8 h for 3 days and sacrificed these mice 30 days later (n = 5 *per* group). We found that the number of BrdU+ cells that remained in the DG of WD group declined by approximately ∼3-fold (Mdn = 58 cells/mm^2 of DG area, IQR: 53–83) with respect to the control group (Mdn = 116 cells/mm^2 of DG area, IQR: 99–133; U = 2, P = 0.011; **Figures 4A,B,E–G**). To establish the number of BrdU+ cells that corresponded to NeuN+ mature neurons (Kempermann et al., 2015), we co-stained the sections with anti-NeuN antibodies and quantified BrdU/NeuN co-labeled cells. We found that the number of BrdU+NeuN+ cells in the control group (Mdn = 44 cells/mm^2 of DG area, IQR: 33–53) was significantly higher than that in the WD group (Mdn = 10 cells/mm^2 of DG area, IQR: 8–11; U = 0, P = 0.002; **Figures 4C,D,H**). These findings suggest that the cell survival of newborn neurons or a reduction in cell proliferation of precursor cells in the DG may be affected by the WD. We then estimated the percentage of BrdU+NeuN+/BrdU+ cells in the DG, our data indicated that the WD group showed a significant reduction in the percentage of co-labeled cells as compared to controls (WD: 17.7%, IQR 10.5–22.5% vs. controls 40.4%, IQR 39.3–40.9%; U = 0, P = 0.004). These findings suggest there is an alteration in the final proportion of new neurons produced in the hippocampus of WD animals. Thus,

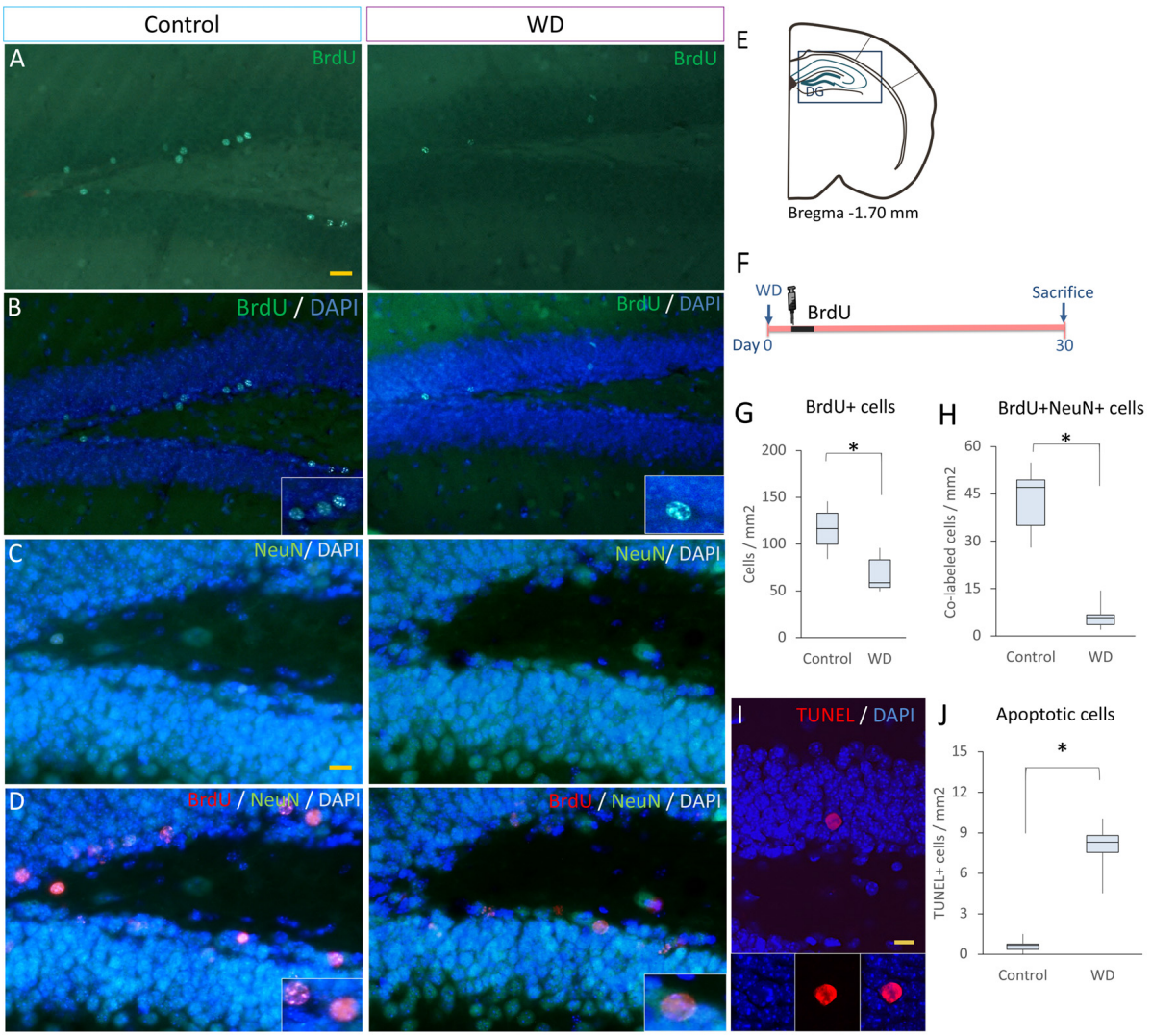

FIGURE 4 | The final number of newly generated neurons is decreased in whisker-deprived animals. **(A,B)** Immunostaining for BrdU (green) in the control and the whisker-deprived (WD) group. **(C,D)** Double immunostaining of NeuN+ (green)/BrdU+ (red). **(E)** A representative coronal section at −1.70 mm coordinate relative to Bregma. **(F)** Experimental design: 3 weeks after the last BrdU injection (50 mg kg^{-1} BrdU/8 h i.p. for 3 days), we determined the number of NeuN+ and BrdU+ cells. **(G)** BrdU+ cells in the DG, the analysis showed less BrdU+ cells in the WD group. **(H)** Quantification of BrdU+NeuN+ in the DG. **(I)** Confocal photography of a TUNEL positive cell and the results of TUNEL quantification in DG **(J)**. All nuclei were stained with DAPI (blue). Data are expressed as median and IQR. Insets: high magnification views. n = 5 per group; *P < 0.001; Mann-Whitney "U" test. Bar **(A,B)** = 20 μm; Bar **(C,D)** = 10 μm; Bar **(I)** = 10 μm. Optical section thickness = 0.55 μm.

we investigate whether this reduction in adult neurogenesis was partially due to a higher apoptosis rate. We analyzed the number of apoptotic cells (TUNEL+ cells; **Figures 4I,J**) in the DG (n = 5 mice *per* group). Our results showed that the WD group had ∼10-fold more apoptotic cells (Mdn = 8.2 cells/mm^2 of DG area, IQR: 7.5–8.7) as compared to the control group (Mdn = 0.7 cells/mm^2 of DG area, IQR: 0.4–0.75; U = 0, P = 0.009). Altogether, our findings indicate that permanent tactile deprivation significantly reduces the production of newly-generated neurons in the DG.

WD Affects the Spatial Memory

Visual information and the head-direction system are required for spatial learning (Knierim et al., 1995; Dombeck et al., 2010; Youngstrom and Strowbridge, 2012). While the role of these systems in acquisition of hippocampal-dependent memory has been extensively studied, the role of vibrissal system during spatial learning is not clear. To establish whether the hippocampal alterations induced by WD can affect spatial memory performance, we used the Barnes maze paradigm 24 days after WD to evaluate hippocampal-dependent memory (**Figures 5A–E**). We first analyzed whether animals learned the task by determining intragroup differences in the time spent to reach the goal box. Our data indicated that both controls (χ^2 = 5.33 s, p = 0.021, Friedman's test) and WD animals (χ^2 = 9 s, p = 0.003, Friedman's test) efficiently learned the task. Then, we examined intergroup differences and observed that the control group showed a continuous reduction in escape latency during the whole acquisition phase as compared to the WD group: day 1 (controls = 67 s, IQR: 39–122 vs. WD mice = 197 s, IQR: 44–240; U = 1420, p = 0.003); day 2 (controls = 34 s, IQR: 20–56 vs. WD mice = 106 s, IQR: 41–240; U = 1048, p < 0.001); day 3 (controls = 27 s, IQR: 18–45 vs. WD mice = 70 s, IQR: 26–240; U = 1113, p < 0.001; **Figure 5B**). We also recorded the total path length and the number of primary errors, two parameters indicative of spatial learning (Harrison et al., 2006). The control group presented path lengths shorter than those presented by the experimental group (**Figure 5C**): day 1 (controls = 643 cm, IQR: 604–674 vs. WD mice = 1016 cm, IQR: 881–1164; U = 0, p = 0.021); day 2 (controls = 491 cm, IQR: 388–531 vs. WD mice = 978 cm, IQR: 841–1076; U = 0, p = 0.021); day 3 (controls = 531 cm, IQR: 323–726 vs. WD mice = 818 cm, IQR: 795–862; U = 0, p = 0.021). Consistently, control animals also made significantly fewer primary errors than WD mice (**Figure 5D**): Day 1(WD = 1.6 errors, IQR: 1.3–1.7 vs. controls 0.6 errors, IQR: 0.5–0.6; U = 0, p = 0.02); day 2 (WD = 1.3 errors, IQR:

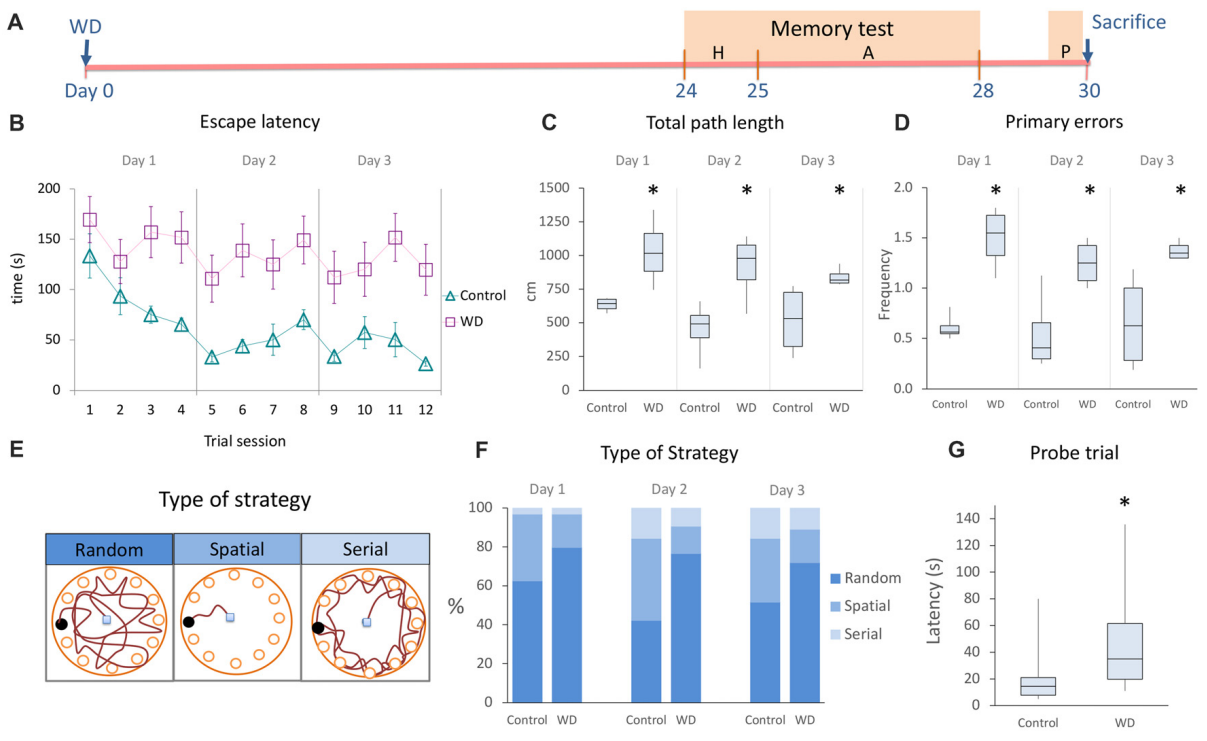

FIGURE 5 | The whisker elimination impairs the acquisition and retention of spatial memory in the Barnes Maze. **(A)** Experimental design of memory test. **(B)** Spatial memory acquisition by trial, escape latency represents the time employed to find the goal box. **(C)** Total path length (distance traveled by mice for the entire duration of assays). **(D)** Primary errors (number of errors to the first encounter of the escape hole). **(E)** Schematic drawings of the type of strategy used to solve the Barnes Maze. **(F)** Percentage of type of strategy used to find the escape hole during the acquisition period. Controls preferentially used the spatial strategy as compared to WD (χ^2 = 4.94, p = 0.026), whereas WD mice solve the task by using more frequently the random strategy than controls (χ^2 = 6.433, p = 0.011). **(G)** Probe trial: the WD group required more time to find the target hole. Habituation phase (H); memory acquisition phase (A); Probe trial (P). In the learning curve, data are expressed as mean ± SEM. The other plots show median and IQR; n = 16 per group. *P < 0.05; Mann-Whitney "U" test.

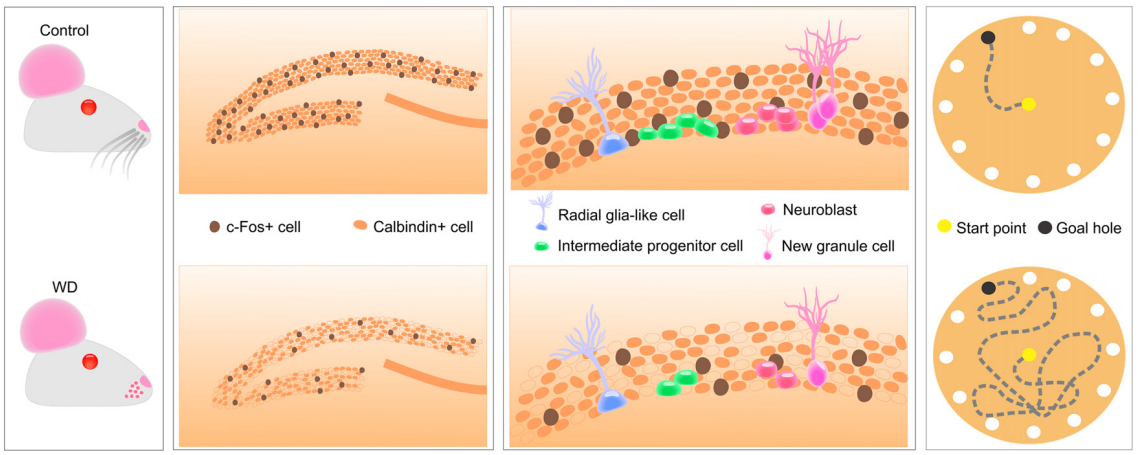

FIGURE 6 | Tactile information associated with fine whisker discrimination is a strong regulator of hippocampal activity that changes the expression of calcium-dependent proteins in DG, disrupts several aspects of hippocampal neurogenesis and impairs spatial memory acquisition and retention.

1–1.4 vs. controls 0.4 errors, IQR: 0.3–0.6; $U = 0$, $p = 0.021$); day 3 (WD = 1.4 errors, IQR: 1.3–1.45 vs. controls 0.6 errors, IQR: 0.28–0.6; $U = 0$, $p = 0.02$). Taken together, these data suggest that WD mice can learn, but their memory acquisition is deficient.

During the acquisition phase, we observed that our mice used different search strategies to solve the task. Hence, we analyzed the frequency of three well-known behavioral strategies: random, serial and spatial (Jašarević et al., 2011; **Figures 5E,F**). Our findings indicate that the spatial strategy (hippocampal-dependent task) was more frequently used by the control group (day 1 = 34.34%, day 2 = 42.2%, and day 3 = 34.4%) than WD animals (day 1 = 15.6%, day 2 = 14%, and day 3 = 17.1%; $\chi^2 = 4.94$, $p = 0.026$). In contrast, the random strategy (non-hippocampal-dependent task) was more frequently used by the WD group (day 1 = 81.3%, day 2 = 76.6%, and day 3 = 73.4%) than control animals (day 1 = 62.5%, day 2 = 42.2%, and day 3 = 51.6%; $\chi^2 = 6.433$, $p = 0.011$). No statistically significant differences were found for the use of serial strategy ($\chi^2 = 0.286$, $p = 0.593$). Taken together, these data indicate that WD animals tend to solve the behavioral paradigm with a non-hippocampal dependent strategy.

Our previous findings indicate that WD alters memory acquisition. To investigate whether the memory retention was also affected by whisker elimination, we repeated the behavioral task 48 h after the last trial (**Figure 5G**). We observed that WD animals needed more time to find the goal hole (Mdn = 35 s, IQR: 19.7–61.5) than controls (Mdn = 14.5 s, IQR: 7.7–21; $U = 47$, $p = 0.002$). Altogether, our data indicate that WD significantly impairs the hippocampal-dependent memory acquisition and retention.

DISCUSSION

In the present study, we produced tactile deprivation by cauterizing whisker follicles and evaluated whether these sensorial inputs can modify the hippocampal function. Our findings indicated that, 30 days after whisker removal, the cytochrome oxidase activity in the BC remains absent. This enzymatic activity reduction is associated with approximately 80% reduction in the density of c-Fos-expressing cells of the BC and the hippocampal CA1, CA2, and CA3 regions. Remarkably, the expression of c-Fos and calbindin in the DG was profoundly affected by whisker elimination. Thus, our next goal was to evaluate whether the low expression of these calcium-dependent proteins could be due to a decline in the hippocampal neurogenesis. Strikingly, we found that whisker elimination dramatically reduces the cell proliferation of neurogenic progenitors in the SGZ. We also observed that these histological abnormalities coincided with a defect in the hippocampal-dependent memory. Altogether, these findings indicate tactile deprivation reduces neuronal activity and some calcium-dependent proteins in the hippocampus, disrupts the hippocampal neurogenesis and impairs spatial memory (**Figure 6**).

Rodents need whiskers to acquire tactile information from the environment. These tactile inputs are processed in the BC, at layer IV of the somatosensory cortex (Petersen, 2007). We produced a chronic tactile deprivation by fulgurating the vibrissal follicles as previously described (Fetter-Pruneda et al., 2013) and used the expression of cytochrome oxidase to label the BC (Wong-Riley and Welt, 1980). At day 30 after WD, the expression of cytochrome oxidase was not observed in the BC, indicating that tactile inputs were permanently disrupted by our method. We then evaluated the number of neurons expressing the c-Fos protein, a calcium-dependent immediate early proto-oncogene that is triggered by a different stimulus and may change the structural and functional properties of neural cells (Miller et al., 1984; Herrera and Robertson, 1996). Our data indicated that the expression of c-Fos in the BC is dramatically reduced by whisker elimination. This evidence confirmed that tactile disruption produces a long-term reduction in the density

of c-Fos expressing cells. Short- and medium-term reductions in the c-Fos expression has been described with other models of tactile deprivation, such as: whisker plucking (Kaliszewska et al., 2012), whisker clipping (Filipkowski et al., 2001; Bisler et al., 2002) and whisker trimming (Staiger et al., 2002). In contrast, the c-Fos expression level in somatosensory cortex is increased by animal exposure to enriched environments or a direct stimulation of neural tissue (Mack and Mack, 1992; Filipkowski et al., 2000).

Electrical stimulation of the infraorbital nerve (that carries information from whiskers) and touch-guided behavior evoke neuronal firing in the CA1 hippocampal region (Pereira et al., 2007; Itskov et al., 2011). These tactile inputs increase the activity of CA1 hippocampal neurons the CA1 region through thalamocortical relays and are associated with fine sensorial discrimination (Pereira et al., 2007). During early brain development, WD reduces the activity of CA3 neurons that induces CA3-CA1 synaptic facilitation (Milshtein-Parush et al., 2017). For this reason, we decided to evaluate c-Fos expression in four hippocampal regions: CA1, CA2, CA3 and DG. Our findings indicate that long-lasting tactile deprivation reduces in approximately 80% the density of c-Fos+ cells in all these regions. Interestingly, we observed that c-Fos reduction was statistically significant only in the upper blade of DG in WD animals. The suprapyramidal (upper) blade, more than the infrapyramidal (lower) blade, is strongly activated by novel environment exploration (Guenthner et al., 2013). Therefore, our findings suggest that whisker activity triggered by environment exploration/navigation is modulating the neuronal activity in the suprapyramidal blade of DG.

We also found a significant reduction of the calcium-binding protein calbindin-D_{28k} in granule cells of the DG, which suggests that calcium homeostasis is strongly affected by permanent WD. Our experimental approach does not allow us to establish the biomolecular mechanism of these changes, but we hypothesize that WD may provoke hyper-excitability of hippocampal neurons as a homeostatic mechanism for sensorial deprivation. This kind of compensatory phenomenon has been previously reported and appears to be related to hypersensitivity to sensory inputs in the adult hippocampus (Zhang and Manahan-Vaughan, 2015). Interestingly, neuronal depletion of calcium-dependent proteins in the DG has also been tightly linked to cognitive impairment, neurodegeneration, aging and Alzheimer's disease (Palop et al., 2003; Moreno et al., 2012; Kook et al., 2014). However, we do not know whether the neuronal depletion of calcium-dependent proteins that follows permanent tactile deprivation is a predisposing condition for psychiatric disorders, cognitive decline and/or neurodegeneration. Our evidence indicates that whisker inputs may play an important role in neural plasticity, calcium homeostasis and synaptic connectivity of the adult hippocampus as that observed in cortical regions (Kaliszewska et al., 2012; Mangin et al., 2012; Pignataro et al., 2015).

The DG is a neurogenic region that produces new neurons in the adult brain throughout life. This specialized niche contains neural stem cells that originate neuroblasts, which migrate to the adjacent granular layer and spread their axons to local circuits in the adult hippocampus (Kempermann et al., 2015). Inputs from voluntary exercise, enriched environments, cognitive and emotional processes comprise the activity-dependent control of hippocampal functions that, in turn, modulates the adult neurogenesis (Kempermann et al., 1997; Pereira et al., 2007; Ma et al., 2009). Our results showed an important reduction in the density of c-Fos+ cells and calbindin expression in the DG after whisker elimination. Thus, we decided to investigate whether the long-term reduction in calbindin and c-Fos might affect the proliferation of primary neural progenitors (GFAP+ and Sox2+ cells) in the DG (Suh et al., 2007). Strikingly, WD animals show less number of BrdU+ neural progenitors. This reduction in the number of BrdU+Sox2+ cells was not due to a reduction in the pool of radial GFAP+ cells as indicated by the absent of significant changes in the number of Sox2+GFAP+ radial cells between groups. To verify if these cellular changes modified the final pool of new neurons that are continuously incorporated into the DG, we injected BrdU at day three and sacrificed the animals 30 days after whisker elimination. Strikingly, we found that the number of newly-generated mature neurons (NeuN+BrdU+) was reduced by 50%. This reduction was associated with an increase in the number of detectable apoptotic cells (TUNEL+ cells) in the WD group. Therefore, our data indicate that tactile information processed in the hippocampus regulates the addition of newly-generated neurons by reducing the proliferation of neural progenitor cells in the DG. WD induces presynaptic inhibition in CA3 and changes in the AMPA-mediated synaptic transmission (Milshtein-Parush et al., 2017). These changes are associated with a reduction in the AMPA/NMDA ratio and an increase in NR2B-containing NMDA receptors (Milshtein-Parush et al., 2017). Interestingly, *in vivo* administration of the NMDA receptor agonists reduce proliferation, whereas NMDA-receptor antagonists promote the proliferation of neural progenitor cells in the DG (Cameron et al., 1995; Kitayama et al., 2003; Halim et al., 2004). Therefore, this evidence excitingly suggests that WD may regulate the proliferation of hippocampal progenitor cells by maintaining the neurotransmitter balance in the adult hippocampus.

The adult hippocampus is a crucial region for the acquisition of spatial memory and navigation (Morris et al., 1982). The DG is a hippocampal region that regulates pattern separation, which helps distinguish similarly encoded contextual information (McHugh et al., 2007). Many studies have linked visual, self-motion and vestibular clues to spatial learning (Knierim et al., 1995; Dombeck et al., 2010; Youngstrom and Strowbridge, 2012), suggesting that spatial memories can be formed using visual information and the head-direction system. While spatial learning has been extensively studied, the role of vibrissal system during spatial learning was unclear. A previous report suggested that vibrissae trimming affected only the proprioceptive location of the escape platform in the Morris maze, without affecting memory acquisition (Grigoryan et al., 2005). Additionally, pharmacologically induced vibrissae paralysis did not affect the animal's ability to learn (Patarroyo et al., 2017). We used the

Barnes maze to evaluate both spatial memory and navigation (Barnes, 1979; Soto-Rodriguez et al., 2016). Our data indicated that the permanent deprivation of whiskers notably impairs the acquisition of spatial memory, as shown by longer latencies spent to find the goal holes. A possible explanation for some inconsistent findings between Morris and Barnes mazes in WD models may be due to the solving strategy for the Barnes maze requires both visual and tactile skills (Barnes, 1979; Soto-Rodriguez et al., 2016). Thus, Barnes may be a more sensitive behavioral paradigm to evaluate memory integration that is required to create spatial maps (Grion et al., 2016). Our data also indicated that 48 h after this acquisition deficit had a negative impact on memory retention in the whisker-deprived animals, which indicates a poor learning performance. Remarkably, whisker-deprived animals tend to solve the maze by using a random-based strategy, non-hippocampal dependent task (Harrison et al., 2006), more frequently than controls, while the control group preferentially used a spatial-based strategy, a hippocampus-dependent task, to solve the maze. Altogether, our findings indicate that whisker information is very important to create spatial memory and execute spatial navigation. Thus, our evidence strongly suggests that inputs from the tactile system and other sensorial modalities are integrated by hippocampus to form novel spatial memories. Nevertheless, it would be important to investigate whether these events can be reversed or compensated by whisker stimulation and whether partial whisker removal may also have significant consequences in the hippocampal cellularity and function.

CONCLUSION

Vibrissal fulguration is an efficient method of permanently removing facial whiskers and analyzing the effects of sensorial deprivation in the adult brain. Taken together, our findings indicate that tactile information associated with fine whisker discrimination is a strong regulator of hippocampal activity that changes the expression of calcium-dependent proteins, alters hippocampal neurogenesis and impairs spatial memory. These findings unveil the neurophysiological interactions among tactile information with the hippocampal neurogenesis and the creation of spatial maps in the adult brain.

AUTHOR CONTRIBUTIONS

OG-P: conception and design of experiments, data collection, analysis, interpretation, manuscript writing, final approval of manuscript and financial support. VL-V: data collection, analysis, interpretation and manuscript writing. NI-C: data collection, analysis and interpretation.

FUNDING

This work was kindly supported by grants from Consejo Nacional de Ciencia y Tecnología (CONACyT No. PN 2016-01-465 and INFR-280414), the CONACyT Fellowship grant (No. 660523), and PRODEP 2018-213544.

REFERENCES

Aimone, J. B., Wiles, J., and Gage, F. H. (2006). Potential role for adult neurogenesis in the encoding of time in new memories. *Nat. Neurosci.* 9, 723–727. doi: 10.1038/nn1707

Barnes, C. A. (1979). Memory deficits associated with senescence: a neurophysiological and behavioral study in the rat. *J. Comp. Physiol. Psychol.* 93, 74–104. doi: 10.1037/h0077579

Bisler, S., Schleicher, A., Gass, P., Stehle, J. H., Zilles, K., and Staiger, J. F. (2002). Expression of c-Fos, ICER, Krox-24 and JunB in the whisker-to-barrel pathway of rats: time course of induction upon whisker stimulation by tactile exploration of an enriched environment. *J. Chem. Neuroanat.* 23, 187–198. doi: 10.1016/s0891-0618(01)00155-7

Cameron, H. A., McEwen, B. S., and Gould, E. (1995). Regulation of adult neurogenesis by excitatory input and NMDA receptor activation in the dentate gyrus. *J. Neurosci.* 15, 4687–4692. doi: 10.1523/jneurosci.15-06-04687.1995

Dombeck, D. A., Harvey, C. D., Tian, L., Looger, L. L., and Tank, D. W. (2010). Functional imaging of hippocampal place cells at cellular resolution during virtual navigation. *Nat. Neurosci.* 13, 1433–1440. doi: 10.1038/nn.2648

Fetter-Pruneda, I., Geovannini-Acuna, H., Santiago, C., Ibarraran-Viniegra, A. S., Martinez-Martinez, E., Sandoval-Velasco, M., et al. (2013). Shifts in developmental timing and not increased levels of experience-dependent neuronal activity, promote barrel expansion in the primary somatosensory cortex of rats enucleated at birth. *PLoS One* 8:e54940. doi: 10.1371/journal.pone.0054940

Filipkowski, R. K., Rydz, M., Berdel, B., Morys, J., and Kaczmarek, L. (2000). Tactile experience induces c-fos expression in rat barrel cortex. *Learn. Mem.* 7, 116–122. doi: 10.1101/lm.7.2.116

Filipkowski, R. K., Rydz, M., and Kaczmarek, L. (2001). Expression of c-Fos, Fos, B., Jun, B. and Zif268 transcription factor proteins in rat barrel cortex following apomorphine-evoked whisking behavior. *Neuroscience* 106, 679–688. doi: 10.1016/s0306-4522(01)00310-4

Gener, T., Perez-Mendez, L., and Sanchez-Vives, M. V. (2013). Tactile modulation of hippocampal place fields. *Hippocampus* 23, 1453–1462. doi: 10.1002/hipo.22198

Gonçalves, J. T., Schafer, S. T., and Gage, F. H. (2016). Adult neurogenesis in the hippocampus: from stem cells to behavior. *Cell* 167, 897–914. doi: 10.1016/j.cell.2016.10.021

Gonzalez-Perez, O., Chavez-Casillas, O., Jauregui-Huerta, F., Lopez-Virgen, V., Guzman-Muniz, J., Moy-Lopez, N., et al. (2011). Stress by noise produces differential effects on the proliferation rate of radial astrocytes and survival of neuroblasts in the adult subgranular zone. *Neurosci. Res.* 70, 243–250. doi: 10.1016/j.neures.2011.03.013

Grigoryan, G., Hodges, I. H., and Gray, J. (2005). Effects of vibrissae removal on search accuracy in the water maze. *Neurosci. Behav. Physiol.* 35, 133–137. doi: 10.1007/s11055-005-0052-y

Grion, N., Akrami, A., Zuo, Y., Stella, F., and Diamond, M. E. (2016). Coherence between Rat sensorimotor system and hippocampus is enhanced during tactile discrimination. *PLoS Biol.* 14:e1002384. doi: 10.1371/journal.pbio.1002384

Guenthner, C. J., Miyamichi, K., Yang, H. H., Heller, H. C., and Luo, L. (2013). Permanent genetic access to transiently active neurons via TRAP: targeted recombination in active populations. *Neuron* 78, 773–784. doi: 10.1016/j.neuron.2013.03.025

Haggerty, D. C., and Ji, D. (2015). Activities of visual cortical and hippocampal neurons co-fluctuate in freely moving rats during spatial behavior. *Elife* 4:e08902. doi: 10.7554/eLife.08902

Halim, N. D., Weickert, C. S., McClintock, B. W., Weinberger, D. R., and Lipska, B. K. (2004). Effects of chronic haloperidol and clozapine treatment on neurogenesis in the adult rat hippocampus. *Neuropsychopharmacology* 29, 1063–1069. doi: 10.1038/sj.npp.1300422

Harrison, F. E., Reiserer, R. S., Tomarken, A. J., and McDonald, M. P. (2006). Spatial and nonspatial escape strategies in the Barnes maze. *Learn. Mem.* 13, 809–819. doi: 10.1101/lm.334306

Herrera, D. G., and Robertson, H. A. (1996). Activation of c-fos in the brain. *Prog. Neurobiol.* 50, 83–107. doi: 10.1016/S0301-0082(96)00021-4

Itskov, P. M., Vinnik, E., and Diamond, M. E. (2011). Hippocampal representation of touch-guided behavior in rats: persistent and independent traces of stimulus and reward location. *PLoS One* 6:e16462. doi: 10.1371/journal.pone.0016462

Jašarević, E., Sieli, P. T., Twellman, E. E., Welsh, T. H. Jr., Schachtman, T. R., Roberts, R. M., et al. (2011). Disruption of adult expression of sexually selected traits by developmental exposure to bisphenol A. *Proc. Natl. Acad. Sci. U S A* 108, 11715–11720. doi: 10.1073/pnas.1107958108

Kaliszewska, A., Bijata, M., Kaczmarek, L., and Kossut, M. (2012). Experience-dependent plasticity of the barrel cortex in mice observed with 2-DG brain mapping and c-Fos: effects of MMP-9 KO. *Cereb. Cortex* 22, 2160–2170. doi: 10.1093/cercor/bhr303

Kempermann, G., Kuhn, H. G., and Gage, F. H. (1997). More hippocampal neurons in adult mice living in an enriched environment. *Nature* 386, 493–495. doi: 10.1038/386493a0

Kempermann, G., Song, H., and Gage, F. H. (2015). Neurogenesis in the adult hippocampus. *Cold Spring Harb. Perspect. Biol.* 7:a018812. doi: 10.1101/cshperspect.a018812

Kitamura, T., and Inokuchi, K. (2014). Role of adult neurogenesis in hippocampal-cortical memory consolidation. *Mol. Brain* 7:13. doi: 10.1186/1756-6606-7-13

Kitayama, T., Yoneyama, M., and Yoneda, Y. (2003). Possible regulation by N-methyl-d-aspartate receptors of proliferative progenitor cells expressed in adult mouse hippocampal dentate gyrus. *J. Neurochem.* 84, 767–780. doi: 10.1046/j.1471-4159.2003.01567.x

Knierim, J. J., Kudrimoti, H. S., and McNaughton, B. L. (1995). Place cells, head direction cells and the learning of landmark stability. *J. Neurosci.* 15, 1648–1659. doi: 10.1523/jneurosci.15-03-01648.1995

Kook, S.-Y., Jeong, H., Kang, M. J., Park, R., Shin, H. J., Han, S.-H., et al. (2014). Crucial role of calbindin-D_{28k} in the pathogenesis of Alzheimer's disease mouse model. *Cell Death Differ.* 21, 1575–1587. doi: 10.1038/cdd.2014.67

Kosaka, T., and Hama, K. (1986). Three-dimensional structure of astrocytes in the rat dentate gyrus. *J. Comp. Neurol.* 249, 242–260. doi: 10.1002/cne.902490209

Kriegstein, A., and Alvarez-Buylla, A. (2009). The glial nature of embryonic and adult neural stem cells. *Annu. Rev. Neurosci.* 32, 149–184. doi: 10.1146/annurev.neuro.051508.135600

Kronenberg, G., Reuter, K., Steiner, B., Brandt, M. D., Jessberger, S., Yamaguchi, M., et al. (2003). Subpopulations of proliferating cells of the adult hippocampus respond differently to physiologic neurogenic stimuli. *J. Comp. Neurol.* 467, 455–463. doi: 10.1002/cne.10945

Kuchukhidze, G., Wieselthaler-Holzl, A., Drexel, M., Unterberger, I., Luef, G., Ortler, M., et al. (2015). Calcium-binding proteins in focal cortical dysplasia. *Epilepsia* 56, 1207–1216. doi: 10.1111/epi.13053

Lecrux, C., Toussay, X., Kocharyan, A., Fernandes, P., Neupane, S., Levesque, M., et al. (2011). Pyramidal neurons are "neurogenic hubs" in the neurovascular coupling response to whisker stimulation. *J. Neurosci.* 31, 9836–9847. doi: 10.1523/JNEUROSCI.4943-10.2011

Ma, D. K., Kim, W. R., Ming, G. L., and Song, H. (2009). Activity-dependent extrinsic regulation of adult olfactory bulb and hippocampal neurogenesis. *Ann. N Y Acad. Sci.* 1170, 664–673. doi: 10.1111/j.1749-6632.2009.04373.x

Mack, K. J., and Mack, P. A. (1992). Induction of transcription factors in somatosensory cortex after tactile stimulation. *Mol. Brain Res.* 12, 141–147. doi: 10.1016/0169-328x(92)90077-o

Mangin, J. M., Li, P., Scafidi, J., and Gallo, V. (2012). Experience-dependent regulation of NG2 progenitors in the developing barrel cortex. *Nat. Neurosci.* 15, 1192–1194. doi: 10.1038/nn.3190

McCloy, R. A., Rogers, S., Caldon, C. E., Lorca, T., Castro, A., and Burgess, A. (2014). Partial inhibition of Cdk1 in G 2 phase overrides the SAC and decouples mitotic events. *Cell Cycle* 13, 1400–1412. doi: 10.4161/cc.28401

McHugh, T. J., Jones, M. W., Quinn, J. J., Balthasar, N., Coppari, R., Elmquist, J. K., et al. (2007). Dentate gyrus NMDA receptors mediate rapid pattern separation in the hippocampal network. *Science* 317, 94–99. doi: 10.1126/science.1140263

Miller, A. D., Curran, T., and Verma, I. M. (1984). c-fos protein can induce cellular transformation: a novel mechanism of activation of a cellular oncogene. *Cell* 36, 51–60. doi: 10.1016/0092-8674(84)90073-4

Milshtein-Parush, H., Frere, S., Regev, L., Lahav, C., Benbenishty, A., Ben-Eliyahu, S., et al. (2017). Sensory deprivation triggers synaptic and intrinsic plasticity in the hippocampus. *Cereb. Cortex* 27, 3457–3470. doi: 10.1093/cercor/bhx084

Moreno, H., Burghardt, N. S., Vela-Duarte, D., Masciotti, J., Hua, F., Fenton, A. A., et al. (2012). The absence of the calcium-buffering protein calbindin is associated with faster age-related decline in hippocampal metabolism. *Hippocampus* 22, 1107–1120. doi: 10.1002/hipo.20957

Morris, R. G., Garrud, P., Rawlins, J. N., and O'Keefe, J. (1982). Place navigation impaired in rats with hippocampal lesions. *Nature* 297, 681–683. doi: 10.1038/297681a0

Muller, R. U., and Kubie, J. L. (1987). The effects of changes in the environment on the spatial firing of hippocampal complex-spike cells. *J. Neurosci.* 7, 1951–1968. doi: 10.1523/jneurosci.07-07-01951.1987

Palop, J. J., Jones, B., Kekonius, L., Chin, J., Yu, G. Q., Raber, J., et al. (2003). Neuronal depletion of calcium-dependent proteins in the dentate gyrus is tightly linked to Alzheimer's disease-related cognitive deficits. *Proc. Natl. Acad. Sci. U S A* 100, 9572–9577. doi: 10.1073/pnas.1133381100

Patarroyo, W. E., Garcia-Perez, M., Lamprea, M., Munera, A., and Troncoso, J. (2017). Vibrissal paralysis produces increased corticosterone levels and impairment of spatial memory retrieval. *Behav. Brain Res.* 320, 58–66. doi: 10.1016/j.bbr.2016.11.045

Paxinos, G., and Watson, C. (2007). *The Rat Brain in Stereotaxic Coordinates.* San Diego, CA: Academic Press.

Pereira, A., Ribeiro, S., Wiest, M., Moore, L. C., Pantoja, J., Lin, S. C., et al. (2007). Processing of tactile information by the hippocampus. *Proc. Natl. Acad. Sci. U S A* 104, 18286–18291. doi: 10.1073/pnas.0708611104

Petersen, C. C. (2007). The functional organization of the barrel cortex. *Neuron* 56, 339–355. doi: 10.1016/j.neuron.2007.09.017

Pignataro, A., Borreca, A., Ammassari-Teule, M., and Middei, S. (2015). CREB regulates experience-dependent spine formation and enlargement in mouse barrel cortex. *Neural Plast.* 2015:651469. doi: 10.1155/2015/651469

Sahay, A., Scobie, K. N., Hill, A. S., O'Carroll, C. M., Kheirbek, M. A., Burghardt, N. S., et al. (2011). Increasing adult hippocampal neurogenesis is sufficient to improve pattern separation. *Nature* 472, 466–470. doi: 10.1038/nature09817

Seri, B., Garcia-Verdugo, J. M., McEwen, B. S., and Alvarez-Buylla, A. (2001). Astrocytes give rise to new neurons in the adult mammalian hippocampus. *J. Neurosci.* 21, 7153–7160. doi: 10.1523/jneurosci.21-18-07153.2001

Song, J., Christian, K. M., Ming, G. L., and Song, H. (2012). Modification of hippocampal circuitry by adult neurogenesis. *Dev. Neurobiol.* 72, 1032–1043. doi: 10.1002/dneu.22014

Soto-Rodriguez, S., Lopez-Armas, G., Luquin, S., Ramos-Zuñiga, R., Jaureegui-Huerta, F., Gonzalez-Perez, O., et al. (2016). Rapid eye movement sleep deprivation produces long-term detrimental effects in spatial memory and modifies the cellular composition of the subgranular zone. *Front. Cell. Neurosci.* 10:132. doi: 10.3389/fncel.2016.00132

Staiger, J. F., Masanneck, C., Bisler, S., Schleicher, A., Zuschratter, W., and Zilles, K. (2002). Excitatory and inhibitory neurons express c-Fos in barrel-related columns after exploration of a novel environment. *Neuroscience* 109, 687–699. doi: 10.1016/s0306-4522(01)00501-2

Steiner, B., Klempin, F., Wang, L., Kott, M., Kettenmann, H., and Kempermann, G. (2006). Type-2 cells as link between glial and neuronal lineage in adult hippocampal neurogenesis. *Glia* 54, 805–814. doi: 10.1002/glia.20407

Suh, H., Consiglio, A., Ray, J., Sawai, T., D'Amour, K. A., and Gage, F. H. (2007). *in vivo* fate analysis reveals the multipotent and self-renewal capacities of Sox2+ neural stem cells in the adult hippocampus. *Cell Stem Cell* 1, 515–528. doi: 10.1016/j.stem.2007.09.002

Williams, S. A., Jasarevic, E., Vandas, G. M., Warzak, D. A., Geary, D. C., Ellersieck, M. R., et al. (2013). Effects of developmental bisphenol A exposure on reproductive-related behaviors in California mice (*Peromyscus californicus*): a monogamous animal model. *PLoS One* 8:e55698. doi: 10.1371/journal.pone.0055698

Wong-Riley, M. T., and Welt, C. (1980). Histochemical changes in cytochrome oxidase of cortical barrels after vibrissal removal in neonatal and adult mice. *Proc. Natl. Acad. Sci. U S A* 77, 2333–2337. doi: 10.1073/pnas.77.4.2333

Woolsey, T. A., and Van der Loos, H. (1970). The structural organization of layer IV in the somatosensory region (SI) of mouse cerebral cortex. The description of a cortical field composed of discrete cytoarchitectonic units. *Brain Res.* 17, 205–242. doi: 10.1016/0006-8993(70)90079-x

Xie, D., Croaker, G. D. H., Li, J., and Song, Z. M. (2016). Reduced cell proliferation and increased apoptosis in the hippocampal formation in a rat model of Hirschsprung's disease. *Brain Res.* 1642, 79–86. doi: 10.1016/j.brainres.2016.03.024

Youngstrom, I. A., and Strowbridge, B. W. (2012). Visual landmarks facilitate rodent spatial navigation in virtual reality environments. *Learn. Mem.* 19, 84–90. doi: 10.1101/lm.023523.111

Zhang, S., and Manahan-Vaughan, D. (2015). Spatial olfactory learning contributes to place field formation in the hippocampus. *Cereb. Cortex* 25, 423–432. doi: 10.1093/cercor/bht239

Conflict of Interest Statement: The authors declare that the research was conducted in the absence of any commercial or financial relationships that could be construed as a potential conflict of interest.

frontiers in Cellular Neuroscience

MINI REVIEW
published: 08 October 2018
doi: 10.3389/fncel.2018.00339

On the Role of Basal Autophagy in Adult Neural Stem Cells and Neurogenesis

Lucía Casares-Crespo†‡, Isabel Calatayud-Baselga†‡, Laura García-Corzo‡ and Helena Mira‡*

Stem Cells and Aging Unit, Instituto de Biomedicina de Valencia, Consejo Superior de Investigaciones Científicas, València, Spain

Adult neurogenesis persists in the adult mammalian brain due to the existence of neural stem cell (NSC) reservoirs in defined niches, where they give rise to new neurons throughout life. Recent research has begun to address the implication of constitutive (basal) autophagy in the regulation of neurogenesis in the mature brain. This review summarizes the current knowledge on the role of autophagy-related genes in modulating adult NSCs, progenitor cells and their differentiation into neurons. The general function of autophagy in neurogenesis in several areas of the embryonic forebrain is also revisited. During development, basal autophagy regulates Wnt and Notch signaling and is mainly required for adequate neuronal differentiation. The available data in the adult indicate that the autophagy-lysosomal pathway regulates adult NSC maintenance, the activation of quiescent NSCs, the survival of the newly born neurons and the timing of their maturation. Future research is warranted to validate the results of these pioneering studies, refine the molecular mechanisms underlying the regulation of NSCs and newborn neurons by autophagy throughout the life-span of mammals and provide significance to the autophagic process in adult neurogenesis-dependent behavioral tasks, in physiological and pathological conditions. These lines of research may have important consequences for our understanding of stem cell dysfunction and neurogenic decline during healthy aging and neurodegeneration.

Keywords: neural stem cell (NSC), adult neurogenesis, autophagy (macroautophagy), autophagy-lysosomal pathway, protein aggregate

OPEN ACCESS

Edited by:
Sara Xapelli,
Universidade de Lisboa, Portugal

Reviewed by:
Filipa Ferreira Ribeiro,
Instituto de Medicina Molecular (IMM), Portugal
Ana Martin-Villalba,
Deutsches Krebsforschungszentrum, Helmholtz-Gemeinschaft Deutscher Forschungszentren (HZ), Germany

***Correspondence:**
Helena Mira
hmira@ibv.csic.es

†Co-first authors

‡These authors have contributed equally to this work

***Received:** 26 July 2018*
***Accepted:** 13 September 2018*
***Published:** 08 October 2018*

Citation:
Casares-Crespo L, Calatayud-Baselga I, García-Corzo L and Mira H (2018) On the Role of Basal Autophagy in Adult Neural Stem Cells and Neurogenesis. Front. Cell. Neurosci. 12:339. doi: 10.3389/fncel.2018.00339

Abbreviations: ALP, autophagy-lysosomal pathway; Ambra1, activating molecule of Beclin 1-regulated autophagy; AMPK, AMP activated protein kinase; Atg, autophagy proteins; Beclin1, BCL-2 interacting moesin-like coiled-coil protein 1; DCX, doublecortin; GFAP, glial fibrillary acidic protein; HDAC6, histone deacetylase 6; IM, isolation membrane; LAMPs, lysosomal-associated membrane proteins; LC3, microtubule-associated protein light chain 3; MA, methyladenine; mTOR, mammalian target of rapamycin; NBR1, neighbor of BRCA1 gene 1; NSC, neural stem cell; NSPCs, neural stem and progenitor cells; OB, olfactory bulb; P, postnatal; PI3K, phosphatidylinositol 3 kinase; qNSC, quiescent neural stem cell; RAB7, ras-related protein; ROS, reactive oxygen species; RV, retroviral; SEZ, subependymal zone lining the lateral ventricles; SGZ, subgranular zone of the hippocampal dentate gyrus; SNAREs, soluble *N*-ethylmaleimide-sensitive fusion (NSF) attachment protein receptors; TFEB, transcription factor EB; TuJ1, beta tubulin III; Ub, ubiquitinated; ULK1, uncoordinated 51-like kinase 1; Vps, vacuolar protein sorting; VZ/SVZ, ventricular zone/subventricular zone.

INTRODUCTION

Autophagy ("self-eating" in greek) is a highly conserved intracellular catabolic pathway that occurs in response to different forms of stress such as starvation, hypoxia, drugs, infection, growth factor deprivation and ROS accumulation. The main function of autophagy is to provide nutrients for vital cellular functions during fasting and other stressors and selectively eliminate unwanted, potentially harmful cytosolic material, such as damaged mitochondria or protein aggregates. There are different forms of autophagy: microautophagy, chaperon-mediated autophagy, mitophagy and macroautophagy. The latter (in the following referred to as the ALP, or simply as autophagy), consists in degrading and recycling cell components by a vesicular structure called the autophagolysosome, that comes from the fusion of an autophagosome with a lysosome (Galluzzi et al., 2017).

Autophagy-lysosomal pathway plays a pivotal role in a wide range of physiological and pathological conditions and is fundamental for the nervous system. Terminally differentiated cells that no longer divide, such as neurons, depend on basal autophagy for the proper turnover of cytoplasmic contents and for protein quality control. Consequently, ALP-deficient mice accumulate ubiquitinated protein aggregates in neurons and suffer from neurodegeneration even in the absence of other pathological triggers (Hara et al., 2006; Komatsu et al., 2006). Autophagy is also required for proper membrane turnover in axon terminals (Komatsu et al., 2007) and for neurogenesis, the production of new neurons from neural stem cells (NSCs). Here we will provide a condensed review of the current knowledge about the physiological role of basal autophagy in neurogenesis, surveying the data available in embryonic development and the few studies conducted in adults. The general role of autophagy in neurogenesis and stem cell regulation has been the subject of other reviews, to which we would like to refer the reader for more extended information (Dhaliwal et al., 2017; Boya et al., 2018). For a better understanding of the topic, we will first give a brief overview of the main autophagy players in mammalian cells and their pharmacological manipulation.

THE AUTOPHAGY-LYSOSOMAL PATHWAY

Autophagy-lysosomal pathway is a step-wise procedure regulated by several protein complexes: the ULK1-Atg13-FIP200-Atg101 complex, required for autophagy induction; the class III phosphatidylinositol 3-kinase (PI3K) complex (PI3K/Vsp34, Beclin1, Atg14/Atg14L, Vps15, and Ambra1), responsible for autophagosome initiation and the Atg12-Atg5-Atg16L1 and LC3-I/LC3-II complexes, fundamental for the extension and closure of the autophagosome (Rodolfo et al., 2016) (**Figure 1**). We will next focus on how these proteins control ALP steps:

(1) *Autophagy induction* is tightly regulated by mTOR and AMPK, a metabolic sensor of the AMP/ATP ratio. Under nutrient deprivation, AMPK promotes autophagy through ULK1 phosphorylation at Ser317 and Ser777, whilst under nutrient sufficiency, high mTOR activity phosphorylates ULK1 at Ser757 preventing its activation (Kim et al., 2011). In addition, TFEB is normally phosphorylated by mTOR and is retained in the cytosol, but under fasting TFEB translocates to the nucleus to induce lysosomal gene expression (Napolitano and Ballabio, 2016), enhancing the cell's degradative capability (Sardiello et al., 2009). Autophagy induction can be modulated by several chemical compounds such as rapamycin, which inhibits mTOR (Benjamin et al., 2011) and metformin, an indirect activator of AMPK (Kim and Guan, 2015).

(2) *Vesicle nucleation (phagophore formation).* ULK1 activation leads to FIP200 and Atg13 phosphorylation, causing the assembly of the ULK1-Atg13-FIP200-Atg101 complex, which in turn triggers class III PI3K complex formation. The subsequent PI3-phosphate enrichment leads to formation of the endoplasmic reticulum cradle, from which an IM grows (Bissa and Deretic, 2018). The IM can be also originated from other sources (**Figure 1**) and forms a cup-shaped structure termed the phagophore that recruits autophagy (Atg)-related proteins (Dikic and Elazar, 2018). This step can be modulated by the class III PI3K inhibitors 3-methyladenine (3-MA) and wortmannin (Wu et al., 2010).

(3) *Vesicle elongation (autophagosome formation)* depends on two ubiquitin-like conjugating systems: Atg12-Atg5-Atg16L1 and LC3 (Wang et al., 2018). First, Atg5 binds to Atg12 in a reaction catalyzed by Atg7 and Atg10; the resulting complex is conjugated to Atg16L1 and is recruited to the pre-autophagosomal membrane by Eva1a/TMEM166 (Hu et al., 2016; Menzies et al., 2017). Atg12-Atg5-Atg16L1 assists in the recruitment of LC3, which gets cleaved by Atg4 to form LC3-I that in turn is conjugated to phosphatidylethanolamine by Atg3 and Atg7, generating lipidated LC3-II that participates in phagophore membrane elongation (Weidberg et al., 2010).

(4) *Cargo recruitment and completion.* Autophagy is a highly selective process that requires a variety of receptor proteins to recruit ubiquitinated (Ub)-cargoes to the forming autophagosomes, such as p62/SQSTM1, HDAC6 (Leyk et al., 2015) and NBR1 (Kirkin et al., 2009). P62 is a ubiquitin-binding protein that interacts with (Ub)-proteins and LC3 (Richter-Landsberg and Leyk, 2013), acting as a bridge between Ub-protein aggregates/autophagosomes and as a regulator of membrane formation around the sequestered cargoes (Tan and Wong, 2017a). HDAC6 mediates the transport of Ub-proteins along microtubules (Leyk et al., 2015) and the maturation of the autophagosome (Richter-Landsberg and Leyk, 2013). NBR1 also recruits Ub-protein aggregates and is degraded by autophagy depending on LC3 (Kirkin et al., 2009). Co-localization between aggregates and receptors like p62 or NBR1 is an indicator of selective autophagy (Tan and Wong, 2017b). Taking together the actions of the receptors and the role of Atg9 in lipid delivery, the loading and closure of

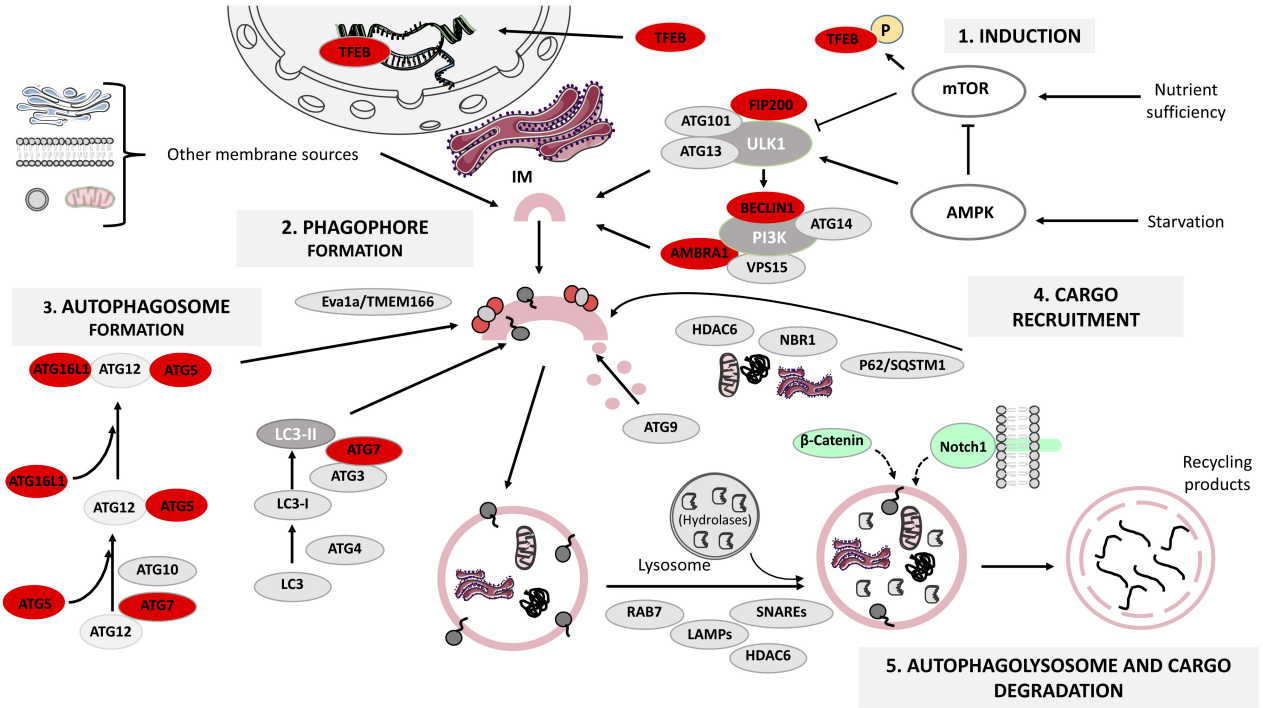

FIGURE 1 | The mammalian autophagy-lysosomal pathway (ALP). Under glucose starvation, AMP activated protein kinase (AMPK) promotes autophagy by directly activating uncoordinated 51-like kinase 1 (ULK1) and transcription factor EB (TFEB) translocates to the nucleus to induce the transcription of several lysosomal genes. Under nutrient sufficiency, high mammalian target of rapamycin (mTOR) activity prevents ULK1 activation and phosphorylates TFEB that remains in the cytoplasm. The ULK1 activation leads to the formation of ULK1-ATG13-FIP200-ATG101 complex, which in turn triggers the class III phosphatidylinositol 3-kinase (PI3K) complex formation. Both complexes participate in the formation of the endoplasmic reticulum cradle, from which the IM (isolation membrane) grows. Two ubiquitin-like conjugating systems are responsible for autophagosome formation: the ATG12-ATG5-ATG16L1 system and the microtubule-associated protein 1 light chain 3 (LC3) system, while ATG9 transmembrane protein collaborates in the delivery of lipids, and in the elongation and closure of the autophagosome. The ATG complex is recruited to the pre-autophagosomal membrane by Eva1a/TMEM166. Cargo recruitment is achieved thanks to a variety of receptor proteins for ubiquitinated proteins such as p62/SQSTM1, histone deacetylase 6 (HDAC6) and NBR1. Finally, the proteins LAMPs, RAB7 and HDAC6 regulate autophagosome fusion with lysosomes, and the lysosomal acidic hydrolases are responsible for degrading the autophagy cargo. Autophagy proteins whose function has been analyzed in relation to adult neurogenesis are highlighted in red (see also **Table 1**). β-catenin and Notch1 (signaling pathway components) are degraded through autophagy during embryonic neurogenesis and are shown in green. This figure was produced using images from Servier Medical Art, licensed under a Creative Commons Attribution 3.0 Unported License. http://smart.servier.com.

the autophagosome is achieved (Hurley and Young, 2017).

(5) *Autophagolysosome formation and cargo degradation* are controlled by regulators of autophagosome fusion with lysosomes, such as LAMPs, SNAREs, RAB7, HDAC6 and by lysosomal acidic hydrolases (Moreau et al., 2013; Boya et al., 2018). The fusion of the mature autophagosome's outer membrane with the lysosome's one leads to the degradation of the autophagosome's inner membrane as well as its contents, generating building blocks recycled by the cell (Rodolfo et al., 2016). This final step can be modulated by bafilomycin A1, a disruptor of autophagosome-lysosome fusion and autophagolysosome acidification (Mauvezin and Neufeld, 2015).

In the following sections, we will review the consequences of deleting autophagy-related genes or pharmacologically blocking autophagy in embryonic and adult NSPCs.

BASAL AUTOPHAGY AND NEUROGENESIS DURING DEVELOPMENT

Today we can safely say that constitutive autophagy is required for embryonic neurogenesis. The first evidences came from work showing that autophagic proteins increase during neuronal differentiation of fetal NSPCs. For instance, in NSPCs derived from the forebrain, Atg9a levels and the LC3-II/LC3-I ratio (a readout of autophagy) raised during neurogenesis (Morgado et al., 2015). A similar upregulation in the expression of other autophagy-related genes (coding for Atg7, Beclin1, Ambra1 and LC3) was described for the OB (Vázquez et al., 2012). The pattern was recapitulated in cultured OB-NSPCs and occurred concomitantly with an increase in the autophagic flux (Vázquez et al., 2012). Similarly, Atg5, Eva1a and LC3-II proteins raised in the mouse cerebral cortex during the neurogenic period (Lv et al., 2014; Li et al., 2016). Atg5 is highly expressed both in the cortical plate, where mature

TABLE 1 | Role of autophagy in adult neurogenesis.

		Cellular type/region	Species	Effect							Reference
				Self-renewal/ activation	Proliferation	Survival	Death	Differentiation	Migration	Maturation	
Genetic model	*FIP200* (hGFAP-Cre) cKO	Neurospheres and *in vivo* (SEZ, SGZ)	*Mus musculus*	↓ radial NSC maintenance	↓	↓	↑ apoptosis	↓ (infiltration and activation of microglia)			Wang et al., 2013, 2017a
	FIP200/Trp53 (hGFAP-Cre) dcKO	*In vivo* (SEZ, SGZ)	*Mus musculus*	rescue	rescue						Wang et al., 2013
	Atg5 (hGFAP-Cre) cKO	Neurospheres and *in vivo* (SEZ, SGZ)	*Mus musculus*	=	=	=	=	=			Wang et al., 2016
	Atg16L1 (hGFAP-Cre) cKO	Neurospheres and *in vivo* (SEZ, SGZ)	*Mus musculus*	=	=	=	=	=			
	Beclin $1^{+/-}$	Neurospheres and *in vivo* (SEZ)	*Mus musculus*		↓	↓	† apoptosis	↓			Yazdankhah et al., 2014
	Ambra1$^{+/-}$	Neurospheres and *in vivo* (SEZ)	*Mus musculus*		↓	↓	† apoptosis	↓			
	Let-7 (LV)	OB	*Mus musculus*						↓	↓	Petri et al., 2017
	Let-7/ Beclin o.e. (LV)	OB	*Mus musculus*						Rescue		
	Let-7/ TFEB o.e. (LV)	OB	*Mus musculus*						Rescue		
	Atg5 (RV-Cre) cKO	*In vivo* (SGZ)	*Mus musculus*		=	↓				↓ (delay)	Xi et al., 2016
	Atg5 (RV-Cre) cKO/*Bax*$^{-/-}$	*In vivo* (SGZ)	*Mus musculus*			Rescue				Rescue	
Treatment	Insulin withdrawal	Adherent NSPC cultures (Hippocampus)	*Rattus norvergicus*				↑ autophagic death				Chung et al., 2015; Ha et al., 2017; Yu et al., 2008
	Insulin withdrawal, Atg7 siRNA	Adherent NSPC cultures (Hippocampus)	*Rattus norvergicus*				rescue				Chung et al., 2015
	Oxygen-glucose deprivation	Adherent NSPC cultures (Hippocampus)	*Rattus norvergicus*				↑ autophagic death				Chung et al., 2018
	Nutrient deprivation/TFEB	Neurospheres (SEZ, young/old animals)	*Mus musculus*	↑ Quiescent NSC/NPC activation							Leeman et al., 2018
	Rapamycin	*In vivo* (SEZ, old animals)	*Mus musculus*	↑ Quiescent NSC/NPC activation							

cKO, conditional knockout; dcKO, double conditional knockout; LV, lentivirus; RV, retrovirus; o.e., overexpression.

neurons reside, and in the VZ/SVZ, where it co-localizes with the NSPC marker Sox2 (Lv et al., 2014), pointing to a role of autophagy in these two cell compartments. In line with this observation, Atg5 silencing impaired cortical neuronal differentiation while increasing proliferation of VZ/SVZ NSPCs (Lv et al., 2014).

Acute silencing of Class III PI3K (Vps34) during corticogenesis by in utero electroporation also affected neurogenesis, decreasing excitatory neuron migration and axonal growth without influencing the cell cycle of NSPCs at the VZ/SVZ (Inaguma et al., 2016). Pharmacological disruption of autophagy with PI3K inhibitors such as Wortmaninn or 3-MA impaired neuronal differentiation of OB-NSPCs by reducing newborn neuron numbers and their maturation. Moreover, neurogenesis was decreased in OB-NSPCs from Ambra1$^{+/gt}$ haploinsufficient mice and Atg5$^{-/-}$ mice, but supplementation with methylpyruvate (an analog for the citric acid cycle that restores ATP availability) rescued the phenotype, indicating that OB-NSPCs require autophagy as an energy source to differentiate into neurons (Vázquez et al., 2012). Wortmaninn, 3-MA or bafilomycin A1 also prevented neuronal differentiation of fetal forebrain NSPC cultures (Morgado et al., 2015) while overexpression of a microRNA (miR-34a) that downregulates Atg9 markedly affected neuronal differentiation and rapamycin-induced autophagy partly recovered the defect (Morgado et al., 2015).

Genetic manipulations of ALP selectively in NSPCs have also yielded interesting results. In Nestin-Cre driven Eva1a conditional knockout (cKO) embryos, the number of proliferative NSPCs and TuJ1^{+}BrdU^{+} newly generated neurons was greatly reduced (Li et al., 2016). This cortical phenotype correlated with an impaired autophagy, shown by a decrease in LC3-II levels, LC3 puncta and an increase in p62 and ubiquitin. *In vitro* neurosphere assays revealed a defect in NSC self-renewal with no change in apoptosis, while differentiation assays uncovered a reduction both in neurogenesis and neurite length (Li et al., 2016).

A few studies have addressed a more specific function of ALP in regulating components of signaling pathways that are key for brain development. For instance, Atg7 regulates the β-catenin-dependent branch of Wnt signaling (Petherick et al., 2013). Under normal physiological conditions, β-catenin limits basal autophagy in mammalian cell lines and functions as a transcriptional co-repressor of p62, but during nutrient deprivation, β-catenin is targeted for autophagic degradation and p62 is de-repressed (Petherick et al., 2013). In the embryonic brain, loss of Atg5 function decreases cortical neuronal differentiation and enhances progenitor proliferation through the stabilization of β-catenin, while Atg5 overexpression accelerates its degradation. Furthermore, the cortical phenotype observed following Atg5 silencing is fully rescued by β-catenin knockdown (Lv et al., 2014). On the other hand, it has been reported that Wnt3A decreases autophagy in mature neurons after traumatic brain injury while increasing hippocampal neurogenesis (Zhang et al., 2018a). In contrast, Wnt3A increases autophagy in embryonic rat hippocampal neuronal cultures through the activation of AMPK (Ríos et al., 2018). This effect is β-catenin-independent, uncovering an interesting connection between Wnt signaling, neuronal metabolism and autophagy that deserves further exploration.

Another key pathway regulated by autophagy is Notch signaling. Notch1 receptor is degraded via its uptake into pre-autophagosome vesicles in an Atg16L1-dependent manner (Wu et al., 2016). Atg7 and Atg16L1 knockdown increase Notch1 levels on the plasma membrane and Notch signaling, while Beclin1 overexpression has the opposite effect. Notch1 levels are increased in Atg16L1 hypomorphs (Wu et al., 2016) and in embryonic cortical primary cultures from these mice, there is an increase in the proportion of NSCs that is reversed with Notch inhibitors. *In vivo*, the VZ/SVZ of Atg16L1 hypomorphs is larger while the cortical plate is smaller compared to wild-type mice. Thus, increased Notch1 resulting from defective autophagy impairs neuronal differentiation and expands the NSC pool (Wu et al., 2016).

Altogether, the above studies combining pharmacological approaches and autophagy-deficient mouse models demonstrate that basal autophagy is required during embryonic neurogenesis and this is partly due to the regulation of key morphogen signaling pathways. In the next section, we will review the main findings regarding the role of ALP in neurogenesis during adulthood.

BASAL AUTOPHAGY AND ADULT NEUROGENESIS

Adult neurogenesis has been analyzed in animals deficient for ALP genes, with divergent results depending on which complex is targeted. Both direct (cell autonomous) effects on stem/progenitor cells and indirect (non-cell autonomous) niche-mediated effects have been identified. For the most part, the genetic strategies employed delete autophagy genes already at embryonic stages and the phenotype in the two adult neurogenic regions (the subependymal zone, SEZ, and the subgranular zone, SGZ) is analyzed in postnatal or young adults. Studies knocking out autophagy genes in stem or progenitor cells in adult mice are scarce.

Yu and co-workers first reported that insulin withdrawal induced an autophagic AMPK-dependent cell death in adult hippocampal NSPCs *in vitro* (Yu et al., 2008; Ha et al., 2017). The death correlated with the upregulation of Beclin1, LC3-II and the accumulation of autophagosomes, was partly rescued by Atg7 silencing and was enhanced with rapamycin. Later on, Chung and colleagues showed that low calpain activity underlied the switch from apoptosis to autophagic cell death (Chung et al., 2015). More recently it has been reported that oxygen-glucose deprivation (a cellular model of ischemia) also induces autophagic cell death in adult hippocampal NSPCs (Chung et al., 2018). These results suggest that blocking autophagy may be cytoprotective for insulin or oxygen-glucose deprived NSPCs.

In 2013, a seminal *in vivo* study demonstrated that FIP200-mediated autophagy is required for the maintenance and function of postnatal and adult NSPCs via the regulation of their oxidative state (Wang et al., 2013). Conditional deletion of FIP200 in

radial glia during development depleted postnatal SEZ and SGZ progenitors and decreased neurogenesis. The adult neurogenic niches appeared normal at postnatal day (P) 0, but at P28, the dentate gyrus shrunk, the number of radial NSCs was reduced and astrocytes populated the SGZ, forming a dense ribbon. At this stage, the SEZ appeared thinner and was depleted of both NSPCs and PSA-NCAM$^+$ neuroblasts. SEZ/SGZ proliferation became compromised and apoptosis was increased. *In vitro* neurosphere assays uncovered a reduced survival capacity of the NSCs and possibly a self-renewal defect. At P56, FIP200 deficiency raised mitochondrial mass and heterogeneity in the SEZ, increasing ROS and p53, a master regulator of cell cycle arrest and apoptosis in response to DNA damage (Ou and Schumacher, 2018). In double FIP200/p53 cKO animals, the apoptosis and proliferative defects were rescued yet differentiation was still affected, suggesting that the role of autophagy in the regulation of NSCs is uncoupled from its role in newborn neurons (Wang et al., 2013).

Neural stem cell maintenance, self-renewal and differentiation was unaffected in Atg5 and Atg16L1 cKO mice generated using the same mouse driver line employed for the FIP200 cKO (hGFAP-Cre) (Wang et al., 2016). This divergent result might be due to FIP200 functions beyond autophagy or to compensations for Atg5/Atg16L1 loss. Reinforcing the latter, p62 aggregates accumulated in the SEZ/SGZ of FIP200 cKO but not in Atg5 or Atg16L1 cKO mice; moreover, the decrease in NSPCs and proliferation was fully restored in double FIP200 and p62 cKO mice (Wang et al., 2016). At a mechanistic level, p62 aggregates reduced the activity of the superoxide dismutase SOD1, leading to oxidative stress and consequently to NSPC dysfunction. In addition, FIP200 indirectly regulated postnatal SEZ neurogenesis via microglia. Wang and colleagues demonstrated that p62 aggregates in FIP200-null NSPCs activate NF-κB and promote the production of Ccl5 and Cxcl110 chemokines, leading to microglia activation, niche infiltration and interference with NSPC differentiation (Wang et al., 2017a).

The role of the Beclin1-Atg14L1-Vps34 complex in the adult SEZ has been also analyzed (Yazdankhah et al., 2014). Ambra1 and Beclin1 are expressed in SEZ Nestin$^+$ NSPCs and DCX$^+$ neuroblasts and high levels of GFP-LC3 are detected in the SEZ of transgenic mice. In Beclin1$^{+/-}$ heterozygotes, proliferative cells and TuJ1$^+$ neurons decrease, while active caspase-3$^+$ cells increase throughout the SEZ (some co-localizing with TuJ1), evidencing a raise in apoptosis of the newly generated neurons. No *in vivo* analysis of the NSCs or intermediate progenitors using specific markers is so far available in these mice. Nevertheless, SEZ NSPC cultures from Beclin1$^{+/-}$ mutants were defective in neurosphere formation, neuronal differentiation and showed an increase in active caspase-3. NSPCs from Ambra1$^{+/-}$ mutants displayed a similar phenotype. Moreover, autophagy is required for radial migration of the SEZ newborn neurons upon their arrival to the OB. Lentiviral-mediated knockdown in migrating neuroblasts of a microRNA (let-7) targeting amino acid transporters [thus involved in ALP regulation (Nicklin et al., 2009)], impaired migration and autophagy, whilst overexpression of Beclin1 or TFEB restored both defects (Petri et al., 2017). Together, the data indicate that basal autophagy has a pro-survival role in adult SEZ newborn neurons *in vitro* and *in vivo* and point to an additional function in the maintenance of adult NSC pools and in the final migration of the adult-born neurons within the OB.

A recent report has knocked out an autophagy gene directly in actively proliferating NSPCs of the SGZ employing a retroviral (RV) strategy (Xi et al., 2016). Xi et al. (2016) injected a RV carrying an mCherry-EGFP-LC3 autophagy-sensing cassette in the dentate gyrus of young adult mice, traced the progeny of the transduced cells and found autolysosomes (mCherry$^+$ puncta) in progenitors and immature neurons at all stages of development, being the most prominent accumulation in the developing processes of young neurons (<30 days post RV injection). Next, they simultaneously tracked the autophagy flux and knocked out Atg5 in dividing NSCPs of Atg5$^{flox/flox}$ mice, by co-injecting a second RV directing the GFP-Cre expression. As expected, Atg5-null NSPCs had less autolysosomes and their survival was markedly compromised. Atg5-null neurons experienced a transient maturation delay, with a reduction in spine density and prolonged expression of the immature marker DCX at 30 days post injection. Dendritic arborization seemed normal, although subtle defects could have been missed. This phenotype is reminiscent of the age-related maturation delay of newborn neurons (Trinchero et al., 2017), suggesting that a cell-autonomous failure in autophagy could partly contribute to maturation impairments during aging. Of note, the survival and the maturation timing defects were rescued in mice lacking the pro-apoptotic protein Bax (Xi et al., 2016).

More recently, Leeman et al. (2018) found protein aggregates in quiescent NSCs from the SEZ of young adult mice. The aggregates were stored in large lysosomes and the expression of lysosome-associated genes with TFEB motifs was increased. Detection of LAMPs and autophagy-sensing constructs indicated that quiescent NCS contained more and larger lysosomes than actively dividing NSCs. Nutrient deprivation (a pro-ALP stimulus) improved quiescent NSC activation *in vitro*, and this was blocked by bafilomycin A1, suggesting that ALP provides a burst of energy for NSC division. With age, a subset of old quiescent NSCs had defects in their lysosomes and in ALP, accumulating higher levels of protein aggregates. This was counteracted by overexpression of a constitutive active TFEB, leading to quiescent NSC activation. *In vivo* administration of rapamycin also increased the frequency of active SEZ NSPCs expressing the epidermal growth factor receptor (EGFR) in old animals, as analyzed by FACS. Although the active NSC and progenitor populations were not clearly segregated in the analysis, since they are both EGFR$^+$, the finding suggests that clearing protein aggregates through ALP enhances NSC activity in the aged brain.

FUTURE PERSPECTIVES

Collectively, the above findings show a prevalent function for autophagy-related genes in embryonic neurogenesis and place autophagy at the crossroads between proteostasis and

developmental signaling pathways. During development, basal autophagy is mainly required for adequate neuronal differentiation and possibly to limit the expansion of the NSC population through the downregulation of the β-catenin/Wnt and Notch pathways. Commonalities and distinct features of ALP in adult *vs.* embryonic neurogenesis are also starting to emerge. The available data in the adult, summarized in **Table 1**, point to a distinctive role of ALP in the exit of NSCs from their predominant quiescent state (a property of adult NSCs that is not shared by their embryonic counterparts) and possibly to a shared role in the differentiation/maturation of the adult and embryonic newly born neurons. Basal autophagy has also a pro-survival role in adult neurogenesis. Nevertheless, to gain further insight into the function of ALP in adult neurogenesis, future studies using tamoxifen-inducible Cre/LoxP systems are required to delete autophagy genes during adulthood, bypassing confounding embryonic and postnatal effects.

A remaining challenge in the field is to solve whether ALP regulation is cell intrinsic/extrinsic and further refine its coupling to sequential cellular transitions of the neurogenic cascade. Moreover, little is known regarding the role of autophagy in the adult neurogenic response to external stimuli. Running increases autophagy in the brain (He et al., 2012) and Xi et al. (2016) showed that running could not rescue the survival deficits of Atg5-null newborn neurons, but further research in this direction is warranted. Exploring in the adult the interesting connections found in the embryo between niche signals such as Notch or Wnt, NSC expansion, neuronal metabolism and autophagy will also likely expand our knowledge on the coordination between extrinsic/intrinsic mechanisms regulating neurogenesis in the mature brain.

Finally, the activation of autophagy facilitates the clearing of intracellular protein aggregates and consequently the pharmacological enhancement of ALP is viewed as a promising neuroprotective approach for a variety of neurodegenerative proteinopathies (Menzies et al., 2017; Thellung et al., 2018). On the other hand, autophagy is involved in the pathophysiological changes induced in the brain upon ischemic stroke (Zhang et al., 2018b) and possibly in NSPC cell death following radiotherapy in malignant childhood brain tumors, including high-grade gliomas (Wang et al., 2017b). The potential impact of autophagy modulators on the regulation of either endogenous NSPCs/neurogenesis [controversial in humans at this point, see Kempermann et al. (2018) and references therein] or the possible outcome of modulating autophagy in combination with NSPC transplantation strategies for the treatment of some of these diseases has received little attention. Autophagy may play a dual role in NSPCs and immature neurons, being adaptive and cytoprotective in basal conditions, or detrimental following exposure to ischemic environments or irradiation. On the other hand, the neurogenesis studies performed in animal models predict that inducing autophagy would favor the survival and maturation of the newly generated neurons in grafts. Thus, it is tempting to speculate that enhancing autophagy in neurodegenerative pathologies could be beneficial both for the damaged neurons and to improve the efficacy of cell replacement strategies, so we anticipate that future research in this convergence zone may yield promising results.

AUTHOR CONTRIBUTIONS

LC-C and HM wrote the first draft of the manuscript. IC-B organized the database. LC-C and IC-B prepared **Figure 1**. IC-B and LG-C wrote sections of the manuscript. All authors contributed to manuscript revision, read and approved the submitted version.

FUNDING

We thank Dr. Marçal Vilar for critically reading the manuscript. This work was supported by the Spanish Ministerio de Economía y Competitividad (Grant No. SAF2015-70433-R).

REFERENCES

Benjamin, D., Colombi, M., Moroni, C., and Hall, M. N. (2011). Rapamycin passes the torch: a new generation of mTOR inhibitors. *Nat. Rev. Drug Discov.* 10, 868–880. doi: 10.1038/nrd3531

Bissa, B., and Deretic, V. (2018). Autophagosome formation: cutting the gordian knot at the ER. *Curr. Biol.* 28, R347–R349. doi: 10.1016/j.cub.2018.03.015

Boya, P., Codogno, P., and Rodriguez-Muela, N. (2018). Autophagy in stem cells: repair, remodelling and metabolic reprogramming. *Development* 145:dev146506. doi: 10.1242/dev.146506

Chung, H., Choi, J., and Park, S. (2018). Ghrelin protects adult rat hippocampal neural stem cells from excessive autophagy during oxygen-glucose deprivation. *Endocr. J.* 65, 63–73. doi: 10.1507/endocrj.EJ17-0281

Chung, K. M., Park, H., Jung, S., Ha, S., Yoo, S.-J., Woo, H., et al. (2015). Calpain determines the propensity of adult hippocampal neural stem cells to autophagic cell death following insulin withdrawal KYUNG. *Stem Cells* 33, 3052–3064. doi: 10.1634/stemcells.2008-0153

Dhaliwal, J., Trinkle-Mulcahy, L., and Lagace, D. C. (2017). Autophagy and adult neurogenesis: discoveries made half a century ago yet in their infancy of being connected. *Brain Plast.* 3, 99–110. doi: 10.3233/BPL-170047

Dikic, I., and Elazar, Z. (2018). Mechanism and medical implications of mammalian autophagy. *Nat. Rev. Mol. Cell Biol.* 19, 349–364. doi: 10.1038/s41580-018-0003-4

Galluzzi, L., Baehrecke, E. H., Ballabio, A., Boya, P., Bravo-San Pedro, J. M., Cecconi, F., et al. (2017). Molecular definitions of autophagy and related processes. *EMBO J.* 36, 1811–1836. doi: 10.15252/embj.201796697

Ha, S., Jeong, S.-H., Yi, K., Chung, K. M., Hong, C. J., Kim, S. W., et al. (2017). Phosphorylation of p62 by AMP-activated protein kinase mediates autophagic cell death in adult hippocampal neural stem cells. *J. Biol. Chem.* 292, 13795–13808. doi: 10.1074/jbc.M117.780874

Hara, T., Nakamura, K., Matsui, M., Yamamoto, A., Nakahara, Y., Suzuki-Migishima, R., et al. (2006). Suppression of basal autophagy in neural cells causes neurodegenerative disease in mice. *Nature* 441, 885–889. doi: 10.1038/nature04724

He, C., Sumpter, R. J., and Levine, B. (2012). Exercise induces autophagy in peripheral tissues and in the brain. *Autophagy* 8, 1548–1551. doi: 10.4161/auto.21327

Hu, J., Li, G., Qu, L., Li, N., Liu, W., Xia, D., et al. (2016). TMEM166/EVA1A interacts with ATG16L1 and induces autophagosome formation and cell death. *Cell Death Dis.* 7:e2323. doi: 10.1038/cddis.2016.230

Hurley, J. H., and Young, L. N. (2017). Mechanisms of autophagy initiation. *Annu. Rev. Biochem.* 86, 225–244. doi: 10.1146/annurev-biochem-061516-044820

Inaguma, Y., Matsumoto, A., Noda, M., Tabata, H., Maeda, A., Goto, M., et al. (2016). Role of class III phosphoinositide 3-kinase in the brain development: possible involvement in specific learning disorders. *J. Neurochem.* 139, 245–255. doi: 10.1111/jnc.13832

Kempermann, G., Gage, F. H., Aigner, L., Song, H., Curtis, M. A., Thuret, S., et al. (2018). Human adult neurogenesis: evidence and remaining questions. *Cell Stem Cell* 23, 25–30. doi: 10.1016/j.stem.2018.04.004

Kim, J., Kundu, M., Viollet, B., and Guan, K. L. (2011). AMPK and mTOR regulate autophagy through direct phosphorylation of Ulk1. *Nat. Cell Biol.* 13, 132–141. doi: 10.1038/ncb2152

Kim, Y. C., and Guan, K. L. (2015). MTOR: a pharmacologic target for autophagy regulation. *J. Clin. Invest.* 125, 25–32. doi: 10.1172/JCI73939

Kirkin, V., Lamark, T., Sou, Y. S., Bjørkøy, G., Nunn, J. L., Bruun, J. A., et al. (2009). A role for NBR1 in autophagosomal degradation of ubiquitinated substrates. *Mol. Cell* 33, 505–516. doi: 10.1016/j.molcel.2009.01.020

Komatsu, M., Waguri, S., Chiba, T., Murata, S., Iwata, J. I., Tanida, I., et al. (2006). Loss of autophagy in the central nervous system causes neurodegeneration in mice. *Nature* 441, 880–884. doi: 10.1038/nature04723

Komatsu, M., Wang, Q. J., Holstein, G. R., Friedrich, V. L., Iwata, J., Kominami, E., et al. (2007). Essential role for autophagy protein Atg7 in the maintenance of axonal homeostasis and the prevention of axonal degeneration. *Proc. Natl. Acad. Sci. U.S.A.* 104, 14489–14494. doi: 10.1073/pnas.0701311104

Leeman, D. S., Hebestreit, K., Ruetz, T., Webb, A. E., McKay, A., Pollina, E. A., et al. (2018). Lysosome activation clears aggregates and enhances quiescent neural stem cell activation during aging. *Science* 359, 1277–1283. doi: 10.1126/science.aag3048

Leyk, J., Goldbaum, O., Noack, M., and Richter-Landsberg, C. (2015). Inhibition of HDAC6 modifies tau inclusion body formation and impairs autophagic clearance. *J. Mol. Neurosci.* 55, 1031–1046. doi: 10.1007/s12031-014-0460-y

Li, M., Lu, G., Hu, J., Shen, X., Ju, J., Gao, Y., et al. (2016). EVA1A/TMEM166 regulates embryonic neurogenesis by autophagy. *Stem Cell Rep.* 6, 396–410. doi: 10.1016/J.STEMCR.2016.01.011

Lv, X., Jiang, H., Li, B., Liang, Q., Wang, S., Zhao, Q., et al. (2014). The crucial role of Atg5 in cortical neurogenesis during early brain development. *Sci. Rep.* 4:6010. doi: 10.1038/srep06010

Mauvezin, C., and Neufeld, T. P. (2015). Bafilomycin A1 disrupts autophagic flux by inhibiting both V-ATPase-dependent acidification and Ca-P60A/SERCA-dependent autophagosome-lysosome fusion. *Autophagy* 11, 1437–1438. doi: 10.1080/15548627.2015.1066957

Menzies, F. M., Fleming, A., Caricasole, A., Bento, C. F., Andrews, S. P., Ashkenazi, A., et al. (2017). Autophagy and neurodegeneration: pathogenic mechanisms and therapeutic opportunities. *Neuron* 93, 1015–1034. doi: 10.1016/j.neuron.2017.01.022

Moreau, K., Renna, M., and Rubinsztein, D. C. (2013). Connections between SNAREs and autophagy. *Trends Biochem. Sci.* 38, 57–63. doi: 10.1016/j.tibs.2012.11.004

Morgado, A. L., Xavier, J. M., Dionísio, P. A., Ribeiro, M. F. C., Dias, R. B., Sebastião, A. M., et al. (2015). MicroRNA-34a modulates neural stem cell differentiation by regulating expression of synaptic and autophagic proteins. *Mol. Neurobiol.* 51, 1168–1183. doi: 10.1007/s12035-014-8794-6

Napolitano, G., and Ballabio, A. (2016). TFEB at a glance. *J. Cell Sci.* 129, 2475–2481. doi: 10.1242/jcs.146365

Nicklin, P., Bergman, P., Zhang, B., Triantafellow, E., Wang, H., Yang, H., et al. (2009). NIH public access. *Cell* 136, 521–534. doi: 10.1016/j.cell.2008.11.044. Bidirectional

Ou, H.-L., and Schumacher, B. (2018). DNA damage responses and p53 in the aging process. *Blood* 131, 488–495. doi: 10.1182/blood-2017-07-746396

Petherick, K. J., Williams, A. C., Lane, J. D., Ordóñez-Morán, P., Huelsken, J., Collard, T. J., et al. (2013). Autolysosomal β-catenin degradation regulates Wnt-autophagy-p62 crosstalk. *EMBO J.* 32, 1903–1916. doi: 10.1038/emboj.2013.123

Petri, R., Pircs, K., Jönsson, M. E., Åkerblom, M., Brattås, P. L., Klussendorf, T., et al. (2017). Let-7 regulates radial migration of new-born neurons through positive regulation of autophagy. *EMBO J.* 36, 1379–1391. doi: 10.15252/embj.201695235

Richter-Landsberg, C., and Leyk, J. (2013). Inclusion body formation, macroautophagy, and the role of HDAC6 in neurodegeneration. *Acta Neuropathol.* 126, 793–807. doi: 10.1007/s00401-013-1158-x

Ríos, J. A., Godoy, J. A., and Inestrosa, N. C. (2018). Wnt3a ligand facilitates autophagy in hippocampal neurons by modulating a novel GSK-3β-AMPK axis. *Cell Commun. Signal.* 16:15. doi: 10.1186/s12964-018-0227-0

Rodolfo, C., Di Bartolomeo, S., and Cecconi, F. (2016). Autophagy in stem and progenitor cells. *Cell. Mol. Life Sci.* 73, 475–496. doi: 10.1007/s00018-015-2071-3

Sardiello, M., Palmieri, M., di Ronza, A., Medina, D. L., Valenza, M., Gennarino, V. A., et al. (2009). A gene network regulating lysosomal biogenesis and function. *Science* 325, 473–477. doi: 10.1126/science.1174447

Tan, S., and Wong, E. (2017a). *Kinetics of Protein Aggregates Disposal by Aggrephagy*, 1st Edn. New York, NY: Elsevier Inc., doi: 10.1016/bs.mie.2016.09.084

Tan, S., and Wong, E. (2017b). Mitophagy transcriptome: mechanistic insights into polyphenol-mediated mitophagy. *Oxid. Med. Cell. Longev.* 2017:9028435. doi: 10.1155/2017/9028435

Thellung, S., Scoti, B., Corsaro, A., Villa, V., Nizzari, M., Gagliani, M. C., et al. (2018). Pharmacological activation of autophagy favors the clearing of intracellular aggregates of misfolded prion protein peptide to prevent neuronal death. *Cell Death Dis.* 9:166. doi: 10.1038/s41419-017-0252-8

Trinchero, M. F., Buttner, K. A., Sulkes Cuevas, J. N., Temprana, S. G., Fontanet, P. A., Monzón-Salinas, M. C., et al. (2017). High plasticity of new granule cells in the aging hippocampus. *Cell Rep.* 21, 1129–1139. doi: 10.1016/j.celrep.2017.09.064

Vázquez, P., Arroba, A. I., Cecconi, F., De La Rosa, E. J., Boya, P., and De Pablo, F. (2012). Atg5 and ambra1 differentially modulate neurogenesis in neural stem cells. *Autophagy* 8, 187–189. doi: 10.4161/auto.8.2.18535

Wang, C., Chen, S., Yeo, S., Karsli-Uzunbas, G., White, E., Mizushima, N., et al. (2016). Elevated p62/SQS TM1 determines the fate of autophagy-deficient neural stem cells by increasing superoxide. *J. Cell Biol.* 212, 545–560. doi: 10.1083/jcb.201507023

Wang, C., Haas, M. A., Wang, C., Yeo, S., Haas, M. A., and Guan, J. L. (2017a). Autophagy gene FIP200 in neural progenitors non – cell autonomously controls differentiation by regulating microglia. *J. Cell Biol.* 216, 2581–2596. doi: 10.1083/jcb.201609093

Wang, C., Liang, C. C., Bian, Z. C., Zhu, Y., and Guan, J. L. (2013). FIP200 is required for maintenance and differentiation of postnatal neural stem cells. *Nat. Neurosci.* 16, 532–542. doi: 10.1038/nn.3365

Wang, Y., Zhou, K., Li, T., Xu, Y., Xie, C., Sun, Y., et al. (2017b). Inhibition of autophagy prevents irradiation-induced neural stem and progenitor cell death in the juvenile mouse brain. *Cell Death Dis.* 8:e2694. doi: 10.1038/cddis.2017.120

Wang, Y., Song, M., and Song, F. (2018). Neuronal autophagy and axon degeneration. *Cell. Mol. Life Sci.* 75, 2389–2406. doi: 10.1007/s00018-018-2812-1

Weidberg, H., Shvets, E., Shpilka, T., Shimron, F., Shinder, V., and Elazar, Z. (2010). LC3 and GATE-16/GABARAP subfamilies are both essential yet act differently in autophagosome biogenesis. *EMBO J.* 29, 1792–1802. doi: 10.1038/emboj.2010.74

Wu, X., Fleming, A., Ricketts, T., Pavel, M., Virgin, H., Menzies, F. M., et al. (2016). Autophagy regulates notch degradation and modulates stem cell development and neurogenesis. *Nat. Commun.* 7:10533. doi: 10.1038/ncomms10533

Wu, Y. T., Tan, H. L., Shui, G., Bauvy, C., Huang, Q., Wenk, M. R., et al. (2010). Dual role of 3-methyladenine in modulation of autophagy via different temporal patterns of inhibition on class I and III phosphoinositide 3-kinase. *J. Biol. Chem.* 285, 10850–10861. doi: 10.1074/jbc.M109.080796

Xi, Y., Dhaliwal, J. S., Ceizar, M., Vaculik, M., Kumar, K. L., and Lagace, D. C. (2016). Knockout of Atg5 delays the maturation and reduces the survival of adult-generated neurons in the hippocampus. *Cell Death Dis.* 7:e2127. doi: 10.1038/cddis.2015.406

Yazdankhah, M., Farioli-Vecchioli, S., Tonchev, A. B., Stoykova, A., and Cecconi, F. (2014). The autophagy regulators Ambra1 and beclin 1 are required for adult neurogenesis in the brain subventricular zone. *Cell Death Dis.* 5:e1403. doi: 10.1038/cddis.2014.358

Yu, S.-W., Baek, S.-H., Brennan, R. T., Bradley, C. J., Park, S. K., Lee, Y. S., et al. (2008). Autophagic death of adult hippocampal neural stem cells following insulin withdrawal. *Stem Cells* 26, 2602–2610. doi: 10.1634/stemcells.2008-0153

Zhang, J. Y., Lee, J., Gu, X., Wei, Z., Harris, M. J., Yu, S. P. P., et al. (2018a). Intranasally delivered Wnt3a improves functional recovery after traumatic brain injury by modulating autophagic, apoptotic and regenerative pathways in the mouse brain. *J. Neurotrauma* 35, 802–813. doi: 10.1089/neu.2016.4871

Zhang, T., Lu, D., Yang, W., Shi, C., Zang, J., Shen, L., et al. (2018b). HMG-CoA reductase inhibitors relieve endoplasmic reticulum stress by autophagy inhibition in rats with permanent brain ischemia. *Front. Neurosci.* 12:405. doi: 10.3389/fnins.2018.00405

Conflict of Interest Statement: The authors declare that the research was conducted in the absence of any commercial or financial relationships that could be construed as a potential conflict of interest.

frontiers in Cellular Neuroscience

REVIEW
published: 16 October 2018
doi: 10.3389/fncel.2018.00306

Switching of the Microglial Activation Phenotype Is a Possible Treatment for Depression Disorder

*Lijuan Zhang, Jinqiang Zhang and Zili You**

Center for Informational Biology, School of Life Science and Technology, University of Electronic Science and Technology of China, Chengdu, China

Major depressive disorder (MDD) is a common emotional cognitive disorder that seriously affects people's physical and mental health and their quality of life. Due to its clinical and etiological heterogeneity, the molecular mechanisms underpinning MDD are complex and they are not fully understood. In addition, the effects of traditional drug therapy are not ideal. However, postmortem and animal studies have shown that overactivated microglia can inhibit neurogenesis in the hippocampus and induce depressive-like behaviors. Nonetheless, the molecular mechanisms by which microglia regulate nerve regeneration and determine depressive-like behaviors remain unclear. As the immune cells of the central nervous system (CNS), microglia could influence neurogenesis through the M1 and M2 subtypes, and these may promote depressive-like behaviors. Microglia may be divided into four main states or phenotypes. Under stress, microglial cells are induced into the M1 type, releasing inflammatory factors and causing neuroinflammatory responses. After the inflammation fades away, microglia shift into the alternative activated M2 phenotypes that play a role in neuroprotection. These activated M2 subtypes consist of M2a, M2b and M2c and their functions are different in the CNS. In this article, we mainly introduce the relationship between microglia and MDD. Importantly, this article elucidates a plausible mechanism by which microglia regulate inflammation and neurogenesis in ameliorating MDD. This could provide a reliable basis for the treatment of MDD in the future.

Keywords: major depressive disorder, inflammation, microglia, neuroprotection, neurogenesis

OPEN ACCESS

Edited by:
Sandra Henriques Vaz, Instituto de Medicina Molecular (IMM), Portugal

Reviewed by:
Adelaide Fernandes, Universidade de Lisboa, Portugal
Luisa Pinto, University of Minho, Portugal

****Correspondence:***
Zili You
youzili@uestc.edu.cn

Received: *30 May 2018*
Accepted: *22 August 2018*
Published: *16 October 2018*

Citation:
Zhang L, Zhang J and You Z (2018) Switching of the Microglial Activation Phenotype Is a Possible Treatment for Depression Disorder. Front. Cell. Neurosci. 12:306. doi: 10.3389/fncel.2018.00306

INTRODUCTION

Major depressive disorder (MDD) is a common neuropsychiatric disorder with multiple contributing factors—both genetic and environmental—that now affects approximately 350 million people worldwide (Jo et al., 2015). In the past decades, many studies have focused on the monoamine hypothesis. The clinical use of tricyclic antidepressants (TCAs) or serotonin-selective reuptake inhibitors (SSRIs) is targeted at specific neurons and ignores the microenvironment of neurogenesis. Recently, there was a major breakthrough in our understanding of the mechanistic basis for MDD: "inflammatory hypothesis" (Dowlati et al., 2010). Cytokines are pleiotropic molecules with key roles in inflammatory responses and neuroinflammation is important not only in inflammatory responses but also in neurogenesis. Patients with MDD exhibit increased peripheral blood inflammatory biomarkers, including several inflammatory cytokines, such as interleukin (IL)-1β, tumor necrosis factor (TNF)-α and IL-6 (Kim et al., 2007; Dowlati et al., 2010).

Proinflammatory cytokines are closely associated with neurogenesis, in that proinflammatory receptors are highly aggregated in hippocampal regions with cognitive functions. For example, IL-1 receptors (IL-1Rs) are distributed in the central nervous system (CNS) of the human, mouse and rat, and they are modulated by various opposing factors including glucocorticoids and anti-inflammatory cytokines to ameliorate sickness behaviors (Parnet et al., 2002). Various studies suggest that proinflammatory cytokines exert harmful effects on cell survival and decrease neurite outgrowth and neural lineage commitment, and proinflammatory cytokines (MIP2, IL-1β, INOS and TNF-α) lead to microglial activation that reduce hippocampal neurogenesis (Monje et al., 2003; Farrell et al., 2016; Wang J. et al., 2018).

Microglial cells are the brain's immune cells in the CNS. While other major cell populations in the CNS share a neuroepithelial origin, microglia derive from myeloid progenitors, being more closely related to peripheral macrophages than to neurons, neighboring astrocytes, or oligodendrocytes (Ginhoux et al., 2010). They play a role in phagocytes, recognizing and scavenging dead cells and pathogens (Ajami et al., 2007; Casano and Peri, 2015). The presence of neurotransmitter receptors in microglia illustrates their functional connection to neurons and this receptor activation could cause microglial cells to perform different activation phenotypes (Pocock and Kettenmann, 2007). They are involved in various neural activities and immunological functions. Under normal physiological conditions, microglia remain in the resting phenotype involved in neuronal activities such as synaptogenesis, neurogenesis and the release of neurotrophic factors (Bilbo and Schwarz, 2009; Ferrini and De Koninck, 2013; Sato, 2015). However, when the brain is injured and the homeostasis of the microenvironment is disturbed, microglial cells shift into active phenotypes that can secrete proinflammatory cytokines, chemokines, and reactive oxidants (Harry and Kraft, 2008; Lehnardt, 2010). Increases in proinflammatory mediators are likely to damage normal tissues, as the uncontrolled and sustained inflammatory alterations have detrimental effects and further exacerbate the neuronal injury, thus increasing the susceptibility to MDD.

Microglia are characterized by strong plasticity and a diversified morphology and are capable of influencing complex moods, synaptic plasticity, neurogenesis, and memory; hence, some types of depression could be considered as microglial disease (i.e., microgliopathy; Yirmiya et al., 2015). Therefore, analyzing microglia morphology would be a good approach to better understanding the pathogenesis of depression. Here, we first review the potential phenotypic transformation mechanism of microglia, and then describe the impact of their different activation types on neurogenesis as related to depression. Next, we proceed to highlight the interplay between inflammation–microglia and neurogenesis–depression. Lastly, we explain how the key factors impact microglial activation in chronic neurological disorders. Understanding how microglia respond to different stimulators will thus have important implications for controlling the reactivity of these cells in MDD, as well as for treating more chronic neurodegenerative diseases.

MICROGLIA, NEUROINFLAMMATION AND MDD

MDD and Inflammatory Factors

MDD is a serious disease that globally affects many people often accompanied by abnormal behavior, anorexia, lethargy, weight loss, severe feelings of guilt and more sleep (Capuron et al., 2009). Because of its clinical and etiological heterogeneity, the molecular mechanisms underpinning depression are complex and not clearly understood. Inflammatory mediators have been proposed as causal links to MDD.

Bacterial endotoxin lipopolysaccharide (LPS), a potent activator of proinflammatory cytokines, was found to induce depressive-like behaviors (Medeiros et al., 2015). The sickness-related psychopathological symptoms during infection and inflammation are mediated by increasing multiple proinflammatory cytokines, namely IL-1ß, IL-6, TNF-α and IFN-γ. Intriguingly, an imbalance among them was detected in the serum of patients with MDD (Young et al., 2014; Mao et al., 2018). Some antidepressants have shown strong anti-inflammatory response, for example, selective serotonin and serotonin norepinephrine reuptake inhibitors (SSRI and SNRI, respectively) are the first choice pharmacological options for treating MDD. The transcription of TNF, IL11 and IL6 revealed significant expression differences at baseline and after escitalopram (SSRI antidepressant) treatment in depressed patients (Powell et al., 2013). Yet, it is increasingly apparent that these drugs also exert effects on inhibiting microglial activation (Tynan et al., 2012). The mechanism by which inflammation causes depressive-like behaviors likely involves one or more inflammatory molecules, such as C-reactive protein (CRP) or prostaglandin E2 (PGE2) and the hypothalamus–pituitary–adrenal (HPA) axis (**Figure 1**).

These observations suggest an interesting connection between microglial inflammatory responses and MDD.

Microglia Regulate Neuroinflammation in CNS

Although the level of inflammation in the brain is approximately as that in the peripheral areas, our work has shown that peripheral inflammation does not contribute to neuroinflammation in the CNS (You et al., 2011). The peripheral system is separated from the CNS by the blood–brain barrier (BBB), and although most cytokines spans have greater than 15 kDa, they cannot cross the BBB. Although the BBB's permeability could change under pathological conditions, this condition is ephemeral and dose not last long (Henry et al., 2009). In contrast, MDD is a chronic and persistent psychological disorder. Hence, such permeability changes in the BBB seem insufficient to explain depression which is regulated by specific cells in the brain.

Microglia, the innate immune cells that settle in the brain, account for approximately 5%–20% of the total number of adult glial cells (Polazzi and Monti, 2010; von Bartheld et al., 2016). Microglial cells are bone marrow cells derived from the embryonic yolk sac, which migrate to the brain during early

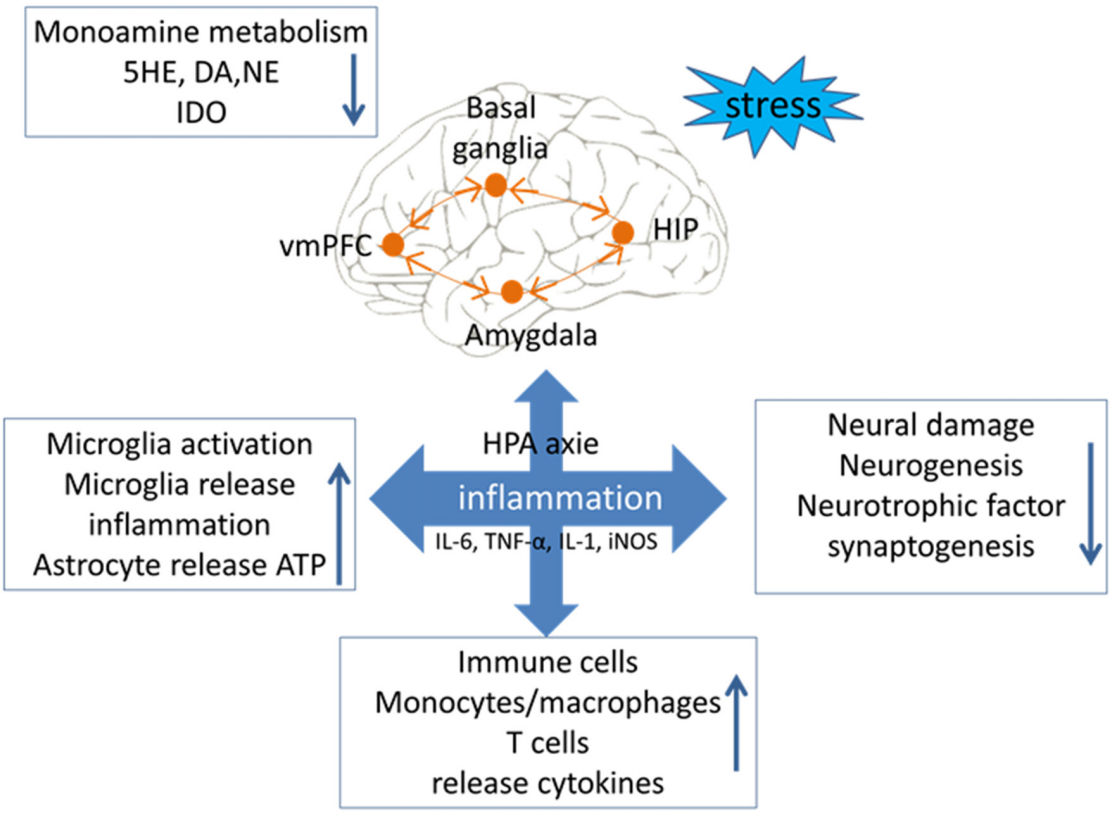

FIGURE 1 | Relationship between inflammation and major depressive disorder (MDD). Stress is an important factor in the occurrence of depression symptoms. There are four main occurrence mechanisms of MDD: (1) stress could lead to disorderly release of neurotransmitters, and then cause an imbalance in the level of neuroinflammatory factors; (2) stress could lead to abnormal intestinal flora and increase the levels of inflammatory factors from the peripheral nervous system and the central nervous system (CNS); (3) stress could lead to excessive activation of microglial cells, causing them to release toxic substances to disrupt the balance of inflammation and anti-inflammation; and (4) stress could lead the immune macrophage to release inflammatory cytokines, which indirectly cause neurological circuit disorders.

development, and they maintain their abundance in the brain by local self-renewal (Kierdorf et al., 2013; Hoeffel et al., 2015). An interruption in CNS homeostasis could induce a cascade of conserved adaptive responses in microglia. They have retractable branches to search and scan the brain for damage and infection. When parts of the brain are found to be damaged or infected, microglial cells trigger an alarm and a signaling cascade by secreting inflammatory signals (Norden et al., 2015). As more microglia receive these signals, more are recruited to the site of the injury, where they secrete more anti-inflammatory cytokines to resolve the inflammation and also secrete neurotrophic factors to repair the damage (Verney et al., 2010). Since microglia are characterized by diversity and plasticity, it becomes very meaningful to study the effect of differently activated microglia on MDD.

Microglial Activation and MDD

Microglial activities were recently linked to MDD's pathological conditions; they have a detrimental effect on neurogenesis by causing neuroinflammation and exacerbating depression (Singhal and Baune, 2017). For example, some models of chronic stresses—such as chronic unpredictable stress, chronic restraint stress, and chronic social defeat stress—can trigger a loss in the number of endogenous hippocampal microglia and cause hippocampal microglial activation (Tong et al., 2017; Wang Y. L. et al., 2018). Many animal studies have shown that changes in microglia structure and function are associated with depressive-like behaviors (Franklin et al., 2018; Wang Y. L. et al., 2018; Wohleb et al., 2018).

Activated microglia have three prominent features: great numbers, an enlarged cell body, and fewer branches. The differently activated phenotypes of microglia are likewise found in the brains of a patient or mouse with depressive-like behaviors (Wang Y. L. et al., 2018). Microglial activation also occurs in MDD patients. Interestingly, autopsies of the anterior cingulate cortex in patients with MDD revealed an activation of microglia and change of inflammation (Steiner et al., 2011), and more activated microglia were found in the ventral prefrontal white matter of patients who had committed suicide after depression (Torres-Platas et al., 2014). In other work, activated microglia appeared in the dorsolateral prefrontal cortex, anterior cingulate cortex and hippocampus of patients with schizophrenia and

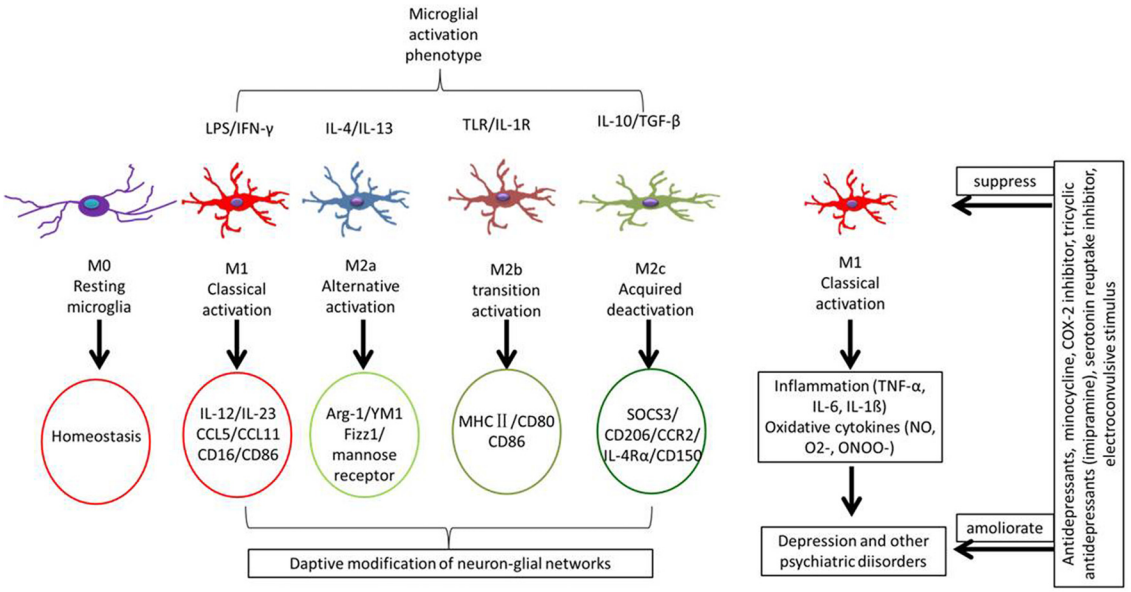

FIGURE 2 | Different microglial phenotypes are related with MDD. Some stimuli induce different types of microglia involving in different functions. Microglial phenotypes are divided into five main states: resting microglia (M0) is mainly to maintain a steady state of the brain's environment under physiological state; classical activated microglia (M1) is with neurotoxic properties and can release inflammatory cytokines; alternative activated microglia (M2a) is involved in repair and regeneration; transitional activated microglia (M2b) is related to immune regulation; and acquired deactivated microglia (M2c) participate in neuroprotection and release some anti-inflammatory cytokines. Under chronic stress, microglial cells are induced to form the M1 type, releasing inflammatory factors that cause neuroinflammatory reactions.

depression (Steiner et al., 2008, 2011). The increased IBA1 gene expression measured in the white matter of depressed suicides may indicate further evidence for increased microglial priming, as this protein is expressed more highly in the "resting" stage of microglial cells (Imai and Kohsaka, 2002). In summary, together these studies suggest that microglia activation may be considered as an important marker of MDD.

Activated Phenotypes of Microglia

Due to their heterogeneity, microglia may be induced into several activation phenotypes to detect pathogenic substances and eliminate cell debris, and they can also contribute to nerve regeneration and tissue reconstruction (Li and Barres, 2018). Microglial phenotypes are divided into M1 (Li et al., 2014) and M2 (Almolda et al., 2015), with the latter divided into M2a, M2b and M2c (Franco and Fernández-Suárez, 2015). M1 and M2 microglia can transform each other depending on their activation pathway (**Figure 2**). Under the action of the IFN-γ cytokine derived from helper T cells (Th1), the resting microglia may turn into the M1 subtype induced by IFN-γ via the classic activation pathway (Prajeeth et al., 2014). Or, conversely, the cytokines IL-4 and IL-13 derived from Type 2 helper T cells (Th2) can induce the transformation of microglia cells into the M2 phenotype through the alternative activation pathway (Ghosh et al., 2016). Crucial participants in this process are interferon regulatory factors (IRFs; Hayakawa et al., 2014), nuclear factor (NF) kappa B (Zhang F. et al., 2017), activator protein 1 (AP1; Wang Y. et al., 2018), and peroxidase (pod) body growth-activated receptor (PPAR)-γ (Pan et al., 2015), which interact with each other to determine the microglial phenotype. The different microglial phenotypes play an important role in regulating the occurrence, development and cessation of inflammatory diseases. Based on the body of evidences, the M1/M2 polarization of microglia contributes significantly to how the production of neuroinflammation is governed in the CNS (**Figure 1**).

In some chronic neurological diseases, microglial cells become activated and gradually change morphology and function. Microglia could enable the sustained release of proinflammatory mediators leading to the development of diverse neurodegenerative disorders via activating some innate immune signaling pathways, such as the NOD-, LRR- and pyrin domain-containing 3 (NLRP3) inflammasome and so on (de Rivero Vaccari et al., 2009; Adamczak et al., 2014; Heneka et al., 2014). We next argue that the mechanism of microglial activation is associated with MDD.

The Mechanism of Microglia Activation Associated With MDD

In clinical depression, how microglial activation occurs is a widely controversial topic that includes several possible mechanisms (**Figure 3**).

(1) Microglial cells respond to stress through neuroinflammation. This "cytokine hypothesis of depression" proposes that inflammatory cytokines play a key role in

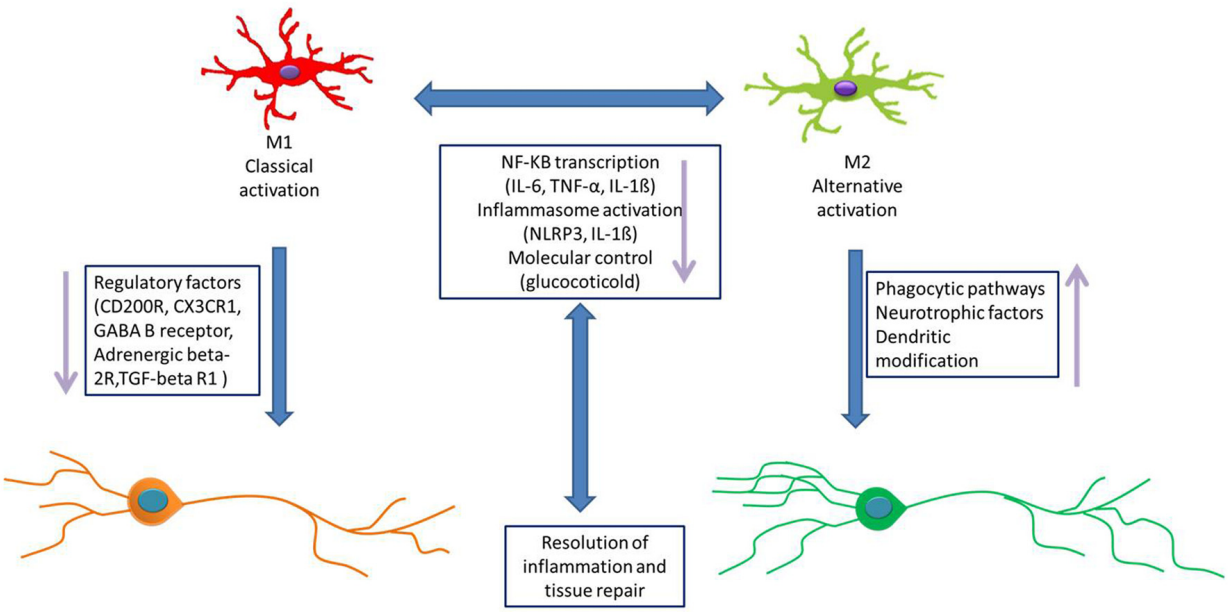

FIGURE 3 | Microglial activation pathway. The activation of microglial cells is affected by many factors. The possible pathways of microglial activation as follows: (1) microglial cells respond to stress through releasing some inflammation, and inflammatory cytokines disrupt the neuronal network, causing MDD. (2) The hypothalamus–pituitary–adrenal (HPA) axis is involved in activated microglia. Intestinal flora could cause changes in the levels of inflammatory factors, which in turn affect the inflammation balance in the CNS and then activate microglia. (3) IL-1ß released from inflammasomes activates microglial cells. Inflammasomes release more inflammatory cytokines, which are amplified by cascade and then activate microglia. (4) Glucocorticoids induce microglia activation. Glucocorticoid-activated microglia respond to a range of immune challenges, including injury, trauma, or infection. (5) The norepinephrine system is also thought to be a stressor of activated microglia. (6) Physiological stress may also trigger the microglia activation directly, by releasing damage-associated molecular patterns (DAMPs) in the brain. (7) Some neurons could directly cause the microglial activation via CX3C receptor 1 (CX3CR1), CD200 and some cytokines.

the crosswalk of the neurochemical, neuroendocrine, and neurotrophic systems of depressive disorder. It is supported by the evidence that the administration of proinflammatory cytokines in both plasma and CSF have been found to influence the progression and severity of MDD in different populations (Young et al., 2014). Some central and peripheral conditions are closely correlated with the increased incidence of MDD, including stroke, stress, and multiple sclerosis (Anisman and Hayley, 2012). Conservative pathogen- and risk-associated molecular patterns are respectively responsible for the infectious or non-infectious inflammatory microglial response, and microglia are activated by inflammatory factors through humoral and neural pathways. Normally, the interaction between peripheral immune cells and microglia are regulated by the choroid plexus and the BBB. Under pathological conditions (such as viral infection, stroke and trauma), the BBB is weakened and immune cells infiltrate into the brain from the outside. Some damage signals directly stimulate microglia to become activated via their binding to specific receptors, causing them to secrete more inflammatory factors, which thus exacerbate the depression symptoms (de Pablos et al., 2014).

(2) The enteric-brain axis is a system involved in the activation of microglia. In depressed patients, antidepressant treatment has been associated with the dysregulation of the HPA axis (Khemissi et al., 2014). Antidepressant effects of SSRI treatment has been found to alleviate HPA axis dysregulation (Young et al., 2004). Additionally, antidepressant treatment resistance is associated with HPA axis dysfunction. However, the underlying mechanisms are poorly understood (Khemissi et al., 2014). A new article points that the P2X7 receptor antagonist reverses microglial activation and neuroendocrine dysregulation of an unpredictable chronic mild stress model in mice (Farooq et al., 2018). Intestinal flora are controlled under normal physiological conditions and can affect the structure, function, and migration of immune cells. Some studies have shown that gut flora disorders can lead to neurological, hormonal and behavioral changes. For example, hyperactivity of the HPA axis has been associated with higher rates of MDD relapse and chronicity. Moreover, the HPA axis changes tend to improve upon resolution of the depressive syndrome (Juruena, 2014). Depression symptoms were associated with greater cortisol levels and a more prolonged activation of the HPA axis and with an impaired from psychosocial stressors (Lopez-Duran et al., 2015). Under certain situations, stress can increases gut permeability, allowing the gut flora or their metabolites to cross the intestinal mucosa and stimulate the immune-brain system, eventually leading to the activation of immune cells (Feng et al., 2018), resulting in microglia activation that is accompanied by depressive-like behaviors (Depino, 2015).

(3) NLRP3 inflammasome activates microglial cells. Inflammatory processes have been implicated in both acute

and chronic stress conditions. The molecular steps leading to IL-1β maturation and a caspase-activating complex take place in an intracellular complex termed the inflammasome (Martinon et al., 2002). NLRP3 (Nucleotide binding and oligomerization domain-like receptor family inflammasome) is a multiprotein complex consisting of NLRP3, pro-caspase-1, and the apoptosis-associated domain (CARD; ASC). There is emerging evidence in animal models that sustained inflammatory responses involving microglia and astrocytes activation contribute to disease progression (Glass et al., 2010). Microglia are the main cell type in the brain responsible for IL-1β and IL-18 secretion. in response to classical inflammasome stimuli (Gustin et al., 2015; Ślusarczyk et al., 2018). Thus microglia-dependent inflammasome activation plays a significant role in the brain and especially in neuroinflammatory condition.

(4) Glucocorticoids induce microglia activation. Most people with MDD showed elevated levels of inflammatory biomarkers. The HPA axis is a major endocrine system that regulates inflammatory responses. Although glucocorticoids are generally anti-inflammatory, they can promote inflammation under certain situations, especially when the brain homeostasis has been disrupted; in this case, glucocorticoids activated microglia respond to a range of immune challenges, including injury, trauma, or infection (Espinosa-Oliva et al., 2011). Glucocorticoid can induce microglia to express the leucine zipper and FK506 binding protein gene 51- itself, mediated by glucocorticoids; hence, these proteins aggravate the stress reaction and depression symptoms. Treatment with corticosterone inhibitor can increase microglial numbers, which further inhibit corticosterone production to eliminate depression symptoms (Nakatani et al., 2012). These results confirm that glucocorticoid can cause the activation of microglia.

(5) The norepinephrine system is also thought to be a stressor of activated microglia. Both social and psychological stress cause the release of norepinephrine, and these signals are released by various immune cells, including microglia. Primary microglia expressed beta(2) adrenergic receptor (AR) and norepinephrine and isoproterenol upregulated the expression of receptor mFPR2, a mouse homolog of human formyl peptide receptor FPR2 that activated beta(2) AR in microglia. Furthermore, the activation of beta(2) AR on microglia induced the expression of an insulin-degrading enzyme and increased the degradation of Aβ42 (Kong et al., 2010). In this way, norepinephrine evidently functions as a link between the neurons and microglia to orchestrate the host response to stress.

(6) Physiological stress may also trigger microglia activation directly by releasing damage-associated molecular patterns (DAMPs) in the brain. The DAMP acts on the toll-like receptor 4 (TLR4) receptor of microglia, producing dangerous signals that are further passed on and cause changes in microglia; specifically, acute stress induces the production of high mobility group box-1 protein (HMGB1) in the DAMP, which enables the microglia to secrete proinflammatory factors, leading to upregulate the gene expression of microglial matrix metal proteins (Kigerl et al., 2018). Stress can also change the expression level of 70 kilodalton heat shock proteins (HSP70) and affect the binding of its molecular partners BAG1, HSP70, and TLR4 receptors, all of which are related to the onset and prevalence of depression (Song et al., 2001).

(7) The activity of neurons causes the activation of microglia. Microglia are involved in synaptic pruning both in development and in the mature CNS. It is now known that, under certain conditions, microglia may adopt a proneurogenic phenotype, which involves the expression of neurotrophins and anti-inflammatory cytokines, such as insulin-like growth factor 1 (IGF-1), brain-derived neurotrophic factor (BDNF), and IL-4 (Ribeiro Xavier et al., 2015; Chen and Trapp, 2016). The physiological functions of microglia are important for maintaining neuronal integrity, network functioning, and neurogenesis in the brain. Stress usually leads to increased neuron activity, and microglial cells may be activated by strong neuronal signals while monitoring environmental changes. Given that the surfaces of microglia have numerous receptors, they can bind to many stress-related neurotransmitters, including glutamate, norepinephrine and serotonin. When faced with stress, threat, anxiety, or pain, we find that many microglial cells are activated and near neurons in the gray matter area of the brain (Hellwig et al., 2016). In addition, chronic mild stress is closely related to the activated microglia and neurons, and pharmacological inhibition of NMDA receptors can inhibit the activation of microglia (Wendt et al., 2016). Clearly then, the activity of neurons interacts with the activation of microglia.

MDD AND NEUROGENESIS

Because of the heterogeneity of MDD, its pathophysiological mechanism and biological basis remain unclear. Decades of research has clearly shown that a variety of neurotransmitters, especially monoamine neurotransmitters and neurotrophic factors, do contribute to MDD (Joca et al., 2015), which has also been linked to glutamate signaling (Cunningham and Watson, 2008). The hypothesis of depression is based on much related research; for example, brain imaging and postmortem studies in MDD patients indicated the apoptosis of mature neurons and a reduced hippocampal volume, and perhaps more interestingly, that the lag time of antidepressant drugs was approximately equivalent to the cycle of neurogenesis (Sahay and Hen, 2008). In addition, stress is a common risk factor for depression, and long-term stressful conditions can inhibit the neurogenesis of nonhuman primates but this is recoverable via antidepressant therapy. In rodents, inhibiting their hippocampal neurogenesis leads to depression, yet antidepressant drugs could promote neurogenesis. TCA-Imipramine, rarely used in neurogenesis studies, has been shown to increase the proliferation and survival of nerve precursor cells (Zhang et al., 2013). In addition, some drugs, although not approved for use in laboratory animals, did show antidepressant effects, such as CRF1 antagonists and V1B antagonists, which increased the proliferation of neural

precursor cells (Henn and Vollmayr, 2004). Nondrug therapy that improves depressive-like behavior also has neurogenic effects. A single electroconvulsive stimulus (ECS), similar to electroconvulsive therapy used for severe depression in clinical practice, can significantly increase the number of newborn neurons that survive (Tang et al., 2016). The stimulation of an electric spasm can also restore to a certain extent the neurogenesis damaged by X-ray irradiation and also restore nerve injuries caused by chronic antidepressant treatments (Santarelli et al., 2003). In addition to influencing both spatial learning and memory, neurogenesis in the hippocampus is also associated with stress-induced depression- and anxiety-like behaviors. An enriched environment can promote the proliferation of nerve precursor cells and alleviate depression and anxiety-like symptoms (Wu et al., 2017). Since different types of antidepressant treatments can increase the proliferation and survival of vital neural precursor cells, this demonstrates that neurogenesis has a positive effect for resisting stress and antidepressant injury, thus suggesting that decreased neurogenesis in the adult hippocampus may be the pathological basis of MDD.

MICROGLIA AND NEUROGENESIS

According to the activation state of microglial cells, they have two potential functions: supporting or damaging neurogenesis in adult brains. The proinflammatory program (termed M1) microglia often release inflammatory mediators that severely result in the injured tissue (Ding et al., 1988), while the anti-inflammatory phenotypes of microglial cells are neuroprotective type in function and promote the survival of new neurons (Gemma and Bachstetter, 2013). In short, the inflammatory phenotypes of microglial cells often impede neurogenesis. Nonetheless, the effects of different microglial phenotypes on hippocampal neurogenesis are complex and slow.

Resting Microglia and Neurogenesis

In a healthy brain, most microglial cells are in a resting state. The morphology of resting microglia is poly-branched with many fine branches and a smaller cytoplasm. These cells use their fine branches to detect infections and damage in their environment. In the hippocampal area, resting microglia actively participate in adult neurogenesis through the process of phagocytosis (Sierra et al., 2010). Yet some studies have shown that phagocytic newborn neurons do not trigger microglial activation, indicating that incompletely activated microglial cells also have phagocytic functions. These findings suggest that resting microglia can also regulate, in part, neurogenesis (Sierra et al., 2014). Resting microglia could affect neurogenesis by regulating the function of the neural stem cells *in vitro*, as well as the proliferation and differentiation of neurons by releasing neurotrophic factors (Wadhwa et al., 2017). For example, a review article has shown that over time, the proportion of nerve cells in the subependymal tissue of mice were reduced when they were cultured separately from activated microglia (Shigemoto-Mogami et al., 2014). Another way that neurogenesis is affected is by the disfiguring of microglial receptors, such as ADP receptor P2Y1 (Stefani et al., 2018), vacuolar sorting protein 35 (VPS35; Appel et al., 2018), and CX3C receptor 1 (CX3CR1; Reshef et al., 2014). Thus, the body of work to date suggests that microglia can enhance neurogenesis by secreting unknown factors or via directing contact with neurons. Moreover, it is interesting to note that microglial cells extracted from young rats promoted significantly more neurogenesis than did those from old rats, indicating that the influence of microglial activity weakens with age (Boehme et al., 2014). Together, the evidence suggests that microglial cells support neurogenesis when not activated, thus giving us a better understanding of their functional role in the brain.

Classical Activation of Microglia on Neurogenesis

There is considerable evidence for the classical activation microglia having a negative effect on neurogenesis in the hippocampus. The bacterial endotoxin LPS can be injected into the CNS or whole body to simulate the inflammatory response in the brain, thereby inducing the classic activation of microglia cells (M1). This activation of microglia by LPS was found to decrease adult neurogenesis, specifically by inhibiting the proliferation or the survival of the new cells (Fujioka and Akema, 2010). LPS with TLR4 molecules induced the microglia activation, and the release of proinflammatory factors, namely IL-1ß, TNFα and IL-6 as well as some other inflammatory molecules (Zhang J. et al., 2017), and an LPS treatment reportedly induced the long-term impairment of hippocampal neurogenesis and memory (Valero et al., 2014). In addition, LPS significantly reduced the number of cells expressing the dual adrenal cortical hormone (DCX), proving that the application of LPS could limit the differentiation of new cells into neurons (Valero et al., 2014). In these studies, the survival of newborn neurons was negatively correlated with the number of microglia activated. In other animal experiments, minocycline, a microglia activity inhibitor, selectively prevented the M1 microglia polarization into a proinflammatory state, providing a basis for understanding the pathogeneses of many diseases accompanied by microglial activation (Kobayashi et al., 2013). Generally, a related report demonstrated that neuroinflammation inhibits neurogenesis in the hippocampus by reducing the differentiation and survival of new neurons (Wang and Jin, 2015). Systemic inflammation, induced by an LPS injection, was sufficient to alter inflammatory status and deregulate the ongoing process of neurogenesis in animals and increased the proliferation of microglia/microglial precursor cells (Smith et al., 2014). Because LPS stimulates M1 microglial activation and this decreased neurogenesis, this strongly suggests that microglial phenotypes are associated with neurogenesis (Zhang J. et al., 2017). Interestingly, over time, aging microglial cells may adopt a potent neurotoxic, proinflammatory "primed" (M1) phenotype when challenged with inflammatory or neurotoxic stimuli that hinder the brain's own restorative potential and inhibit its endogenous neurorepair mechanisms, and microglia interact with neural stem progenitor cells (NSCs). Microglial subtypes are able to

regulate NSCs differently; NSCs from the anti-inflammatory microglial subtype (M2) had better survival and increased migration when kept in a conditioned medium (Osman et al., 2017). This suggests that M2 microglial cells likely contribute to neurogenesis.

Alternative Activation of Microglia on Neurogenesis

The alternative activated microglia (M2) phenotype operates in both neuroprotection and reconstruction of neural networks in the brain. The M2 microglial cells are distinguished by the release anti-inflammatory mediators, such as IL-4, IL-10 and transforming growth factor-(TGF) ß (Almolda et al., 2015; Franco and Fernández-Suárez, 2015). These inflammatory cytokines inhibit the nonimmune cells from releasing proinflammatory factors. M2 microglia consist of three subtypes (M2a, M2b, M2c). M2a contribute to the repair of damaged tissue by expressing anti-inflammatory and neurotrophic factors; M2b constitute the deactivating phenotype and it also expresses anti-inflammatory mediators; M2c is characterized by its phagocytosis function and associated benefits from clearing out cell debris in the brain (Almolda et al., 2015). Moreover, the M2 microglia supernatant could activate the peroxisome proliferator-activated receptor (PPAR)γ signaling pathway to promote neurogenesis and differentiation of NSPCs (Yuan et al., 2017). Newer research is focusing on the effects of herbal medicines on neurogenesis. For example, naringin dihydrochalcone (NDC), a widely used dietary sweetener with strong antioxidant activity, reduced the abundance of activated microglia and inhibited neuroinflammation, which collectively reduced the neuronal damage (Yang et al., 2018). Salvianolic acid B (SalB), with its anti-inflammatory, antioxidant, and neuroprotective effects, significantly lowered the chronic middle stress (CMS)-induced apoptosis and microglia activation in the hippocampus and cortex (Zhang et al., 2016); it also promoted microglial M2-polarization and rescued neurogenesis in stress-exposed mice (Zhang J. et al., 2017). Indeed, there is compelling evidence that anti-inflammatory factors may promote neurogenesis. Positive correlations were found between the serum IFN-γ/IL-4 ratio and the levels of neurotrophic factors and neurogenesis in the hippocampus (Yang et al., 2016). It was recently revealed that microglial cells secreting IL-10 play a supporting role in the differentiation of neurons and the survival of new cells in cell cultures (Qi et al., 2017). Taken together, these results suggest that M2 microglia do promote neurogenesis differentiation.

Microglia can regulate brain circuit connectivity in multiple ways. During embryonic neurogenesis, they regulate the stem cell pool via their secretion of trophic factors and through phagocytosis (Cunningham et al., 2013). Microglia provide trophic support to neurons and endothelial cells, notably by producing BDNF, IGF-1/2 and TGF-ß such that disrupted growth factor production in microglia could interrupt cortical layer formation (Ueno et al., 2013). Microglial cells are inflammatory phenotypes initially associated with brain injury (Toshimitsu et al., 2018). After ischemic injury to the striatum, microglial cells displayed an M2 phenotype. In addition, this injury also caused new cells to accumulate in the subependymal (SVZ) region of the CNS, as many new cells migrated

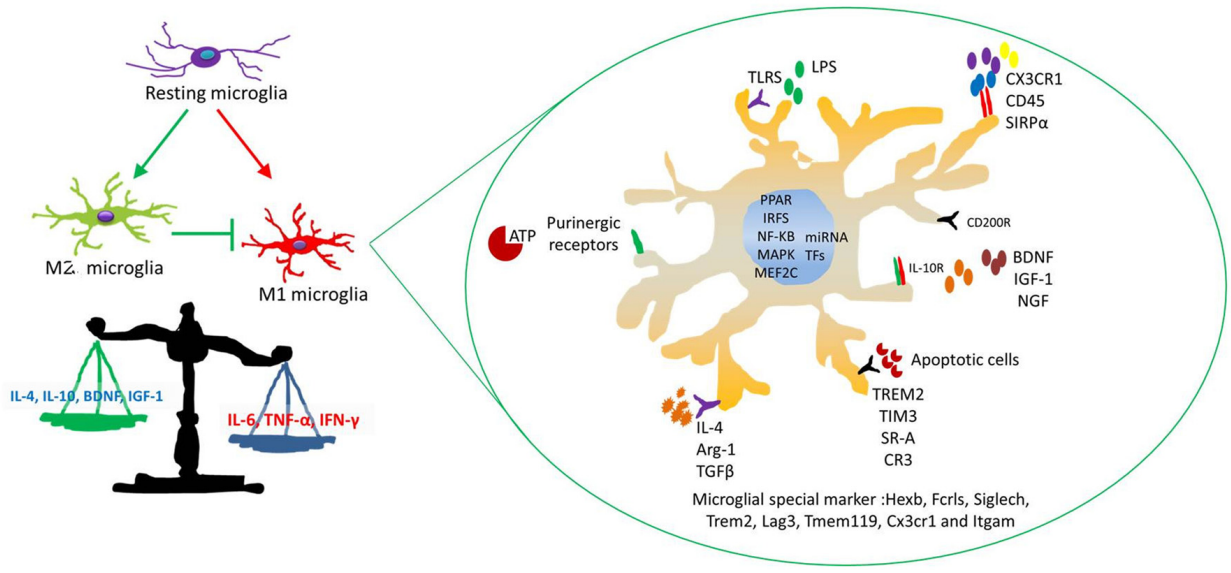

FIGURE 4 | The mechanism of microglial activation. Four major stimuli factors modulate microglial immune activity. These factors are as follows: (a) soluble factors modulate microglial immune responses, such as neurotransmitters and neurotrophic cytokines and so on. (b) Some special receptors are involved in interactions between microglia and neurons. (c) Inflammatory factors and chemokines relate to microglial migration and phagocytosis, such as IL-1ß, IL-10, IL-4 and CCL2, MCP-1 and CXCL1. (d) Some transcription factors (TFs) and microRNAs (miRNAs) affect microglial activation responsed to stress.

into the lesion site in the striatum. Prominent changes to microglia activation patterns mainly occur in the alternative activation of neuroprotective phenotypes. In the stroke model, microglial cells in the SVZ region modulate the expression of IL-1β, IL-6, TNF-α and IL-10 (Wang Q. et al., 2018), contributing to neurogenesis. This would suggest that the M2 microglia in particular contribute to the differentiation and migration of neurons. For this reason, microglial cells are now recognized as "gate-keepers" of a healthy brain's microenvironment, where their disrupted functions adversely affect neurovascular integrity, neuronal homeostasis and network connectivity.

MICROGLIAL PHENOTYPE SWITCHING IS RELATED TO THE TREATMENT OF DEPRESSION

It has become increasingly evident that different internal or external triggers prompt activated microglia to exert their neurotoxicity or neuroprotection. However, which molecules synergistically interact to switch the states of activated microglia and which act in a gene-specific manner to alter later development of an opposing phenotype are not known. Several studies elucidate that *in vitro*, the former microglia phenotype affects the development of the latter phenotype by initially treating with LPS, IL-4, or IL-10, respectively and subsequently, switching the stimulators' order (Gresa-Arribas et al., 2012). On one hand, applying an IL-10 pretreatment before administering LPS prevented the expression of TNF-α, IL-6 and COX2; on the other hand, treatment with LPS before an IL-10 introduction led to the expression of inflammation. Alternatively, while pretreatment with IL-4 before LPS failed to inhibit CD86, COX2, INOS and CD32, treatment with LPS before IL-4 prevented the loss of CD32 but did not decrease the M1 marker (Chhor et al., 2013). These contribute evidence for microglia displaying a morphological switch under different activators.

Evidence is mounting to suggest that PPARγ can inhibit microglial activation, promote M2 polarization and suppress inflammatory cytokines in inflammation-related diseases. Depending on the stimulus encountered, the activation profile of microglia transforms from classical activated (M1) to alternative activated (M2) cells (Cherry et al., 2014). In the case of multiple sclerosis, glatiramer acetate (GA) is a promising molecule capable of altering the inflammatory environment by recruiting Th2 T cells to the CNS, inducing the production of IL-4, which ameliorates depressive-like behaviors (Miki et al., 2018). Inflammatory signals may then act on the neuronal network via their neurotoxic activities or by directly influencing mood regulation. A number of inflammatory cytokines, such as IL-1β, TNF-α and IFN-γ, are known to inhibit serotonin transporter activity and ameliorate depressive-like behaviors (Janssen et al., 2010). Microglial cells can come into close contact with neuronal synapses and enhance neurogenesis, thus contributing to MDD.

THE KEY FACTORS TO MODULATE MICROGLIAL PHENOTYPE

Immune cells are needed to clear endogenous or exogenous factors and repair tissue damage, and most of them are resident myeloid cells-microglia.

Some marker molecules were specially expressed on the microglia in brain regions, such as Cd200r4 and Sirpa (Grabert et al., 2016), while Cx3cr1 was expressed uniformly on the macrophages and microglia (Kim et al., 2011). It is expected that different phenotypes of microglia depend on the communication with neurons. For example, CX3CR1–CX3CL1 signaling may control the microglial phenotype through the release of neuroinflammation; Mef2C and IL-4Rα are highly expressed by microglia in response to TGF-β (Butovsky et al., 2014). Mef2C, as a microglia "off" signal, can alter microglial transcriptome in the presence of type I interferon in aged mouse brain (Deczkowska et al., 2017; **Figure 4**). Altogether, some complex, spatially diverse cytokine is likely to be involved in controlling microglial activity.

Several endogenous molecule stressors shifting the microglia activation phenotype have been identified, and some studies focus on the key microRNAs (miRNAs) and transcription factors (TFs) in microglia (Guedes et al., 2013; Butovsky et al., 2015). MiRNAs regulate gene expression and are major factors in molecular biology. Several studies indicate that miRNAs participate in the regulation of almost all the cellular processes and the changes in their expression are observed in diseases (Bushati and Cohen, 2007). MiRNAs mediate post-transcription to control cell fate, such as cellular activation and proliferation. An increasing number of studies have revealed that MiRNAs provide a genetic switch to activate target genes via regulating TFs (Arora et al., 2013). For example, CEBPα and PU.1 orchestrate microglial development altogether. CEBPα is being considered as the main regulator in hematopoietic stem cell differentiation (Fazi et al., 2005). MiRNAs are related to microglia activation phenotypes (Ponomarev et al., 2013; Porta et al., 2015); resting microglia cells are characterized by low expression levels of miR-155 and high expression of miR-124; M1 microglia increase the expression levels of miR-155 and decrease the level of miR-124; M2 microglia are distinguished by low expression levels of miR-124 and a high expression of miR-155. MiRNAs are also believed to modulate microglial inflammation stations that contribute to neurogenesis (Freilich et al., 2013; Guedes et al., 2013). Therefore, MiRNA-modulated microglial phenotype therapies could contribute to improve depressive-like behaviors.

CONCLUSION

Microglial cells have multiple activation states, namely M1 and M2, that have different effects on modulating neurogenesis in normal and disease conditions. For some, clinical depression is caused by decreasing neurogenesis. Understanding whether the approaches are able to regulate key factors to transform the microglial phenotype for treating MDD is still a great challenge.

Much work remains to be done, but it is possible that a deeper understanding of the interplay between different activations of microglia and adult hippocampal neurogenesis may help to develop future strategies to treat MDD.

SUMMARY

1. The review article elaborately discusses the fact that the activated microglia phenotypes are related to MDD and are helpful for precisely regulating microglia to explore the mechanism of treatment of MDD.
2. The hypothesis of neurogenesis and inflammation, which complement the defects of monoamine hypothesis, gives us a better understanding of the pathogenesis of MDD. Changing the microglial structure and function may link the two hypotheses.
3. The review further elucidates the relationship between inflammation–microglia and neurogenesis–depression symptoms. Such correlations might be of value in the development of a new generation of antidepressants.

AUTHOR CONTRIBUTIONS

LZ collected the literature and wrote the manuscript. JZ drew the pictures and revised the article. ZY approved the manuscript and helped in obtaining financial support.

FUNDING

This work was supported by the National Natural Science Foundation of China (No. 81571174, 81701308), and funded by China Postdoctoral Science Foundation (2017M612934).

REFERENCES

Adamczak, S. E., de Rivero Vaccari, J. P., Dale, G., Brand, F. J. III., Nonner, D., Bullock, M. R., et al. (2014). Pyroptotic neuronal cell death mediated by the AIM2 inflammasome. *J. Cereb. Blood Flow Metab.* 34, 621–629. doi: 10.1038/jcbfm.2013.236

Ajami, B., Bennett, J. L., Krieger, C., Tetzlaff, W., and Rossi, F. M. (2007). Local self-renewal can sustain CNS microglia maintenance and function throughout adult life. *Nat. Neurosci.* 10, 1538–1543. doi: 10.1038/nn2014

Almolda, B., de Labra, C., Barrera, I., Gruart, A., Delgado-Garcia, J. M., Villacampa, N., et al. (2015). Alterations in microglial phenotype and hippocampal neuronal function in transgenic mice with astrocyte-targeted production of interleukin-10. *Brain Behav. Immun.* 45, 80–97. doi: 10.1016/j.bbi.2014.10.015

Anisman, H., and Hayley, S. (2012). Inflammatory factors contribute to depression and its comorbid conditions. *Sci. Signal.* 5:pe45. doi: 10.1126/scisignal.2003579

Appel, J. R., Ye, S., Tang, F., Sun, D., Zhang, H., Mei, L., et al. (2018). Increased microglial activity, impaired adult hippocampal neurogenesis, and depressive-like behavior in microglial VPS35-depleted mice. *J. Neurosci.* 38, 5949–5968. doi: 10.1523/JNEUROSCI.3621-17.2018

Arora, S., Rana, R., Chhabra, A., Jaiswal, A., and Rani, V. (2013). miRNA-transcription factor interactions: a combinatorial regulation of gene expression. *Mol. Genet. Genomics* 288, 77–87. doi: 10.1007/s00438-013-0734-z

Bilbo, S. D., and Schwarz, J. M. (2009). Early-life programming of later-life brain and behavior: a critical role for the immune system. *Front. Behav. Neurosci.* 3:14. doi: 10.3389/neuro.08.014.2009

Boehme, M., Guenther, M., Stahr, A., Liebmann, M., Jaenisch, N., Witte, O. W., et al. (2014). Impact of indomethacin on neuroinflammation and hippocampal neurogenesis in aged mice. *Neurosci. Lett.* 572, 7–12. doi: 10.1016/j.neulet.2014.04.043

Bushati, N., and Cohen, S. M. (2007). microRNA functions. *Annu. Rev. Cell Dev. Biol.* 23, 175–205. doi: 10.1146/annurev.cellbio.23.090506.123406

Butovsky, O., Jedrychowski, M. P., Cialic, R., Krasemann, S., Murugaiyan, G., Fanek, Z., et al. (2015). Targeting miR-155 restores abnormal microglia and attenuates disease in SOD1 mice. *Ann. Neurol.* 77, 75–99. doi: 10.1002/ana.24304

Butovsky, O., Jedrychowski, M. P., Moore, C. S., Cialic, R., Lanser, A. J., Gabriely, G., et al. (2014). Identification of a unique TGF-β-dependent molecular and functional signature in microglia. *Nat. Neurosci.* 17, 131–143. doi: 10.1038/nn.3599

Capuron, L., Fornwalt, F. B., Knight, B. T., Harvey, P. D., Ninan, P. T., and Miller, A. H. (2009). Does cytokine-induced depression differ from idiopathic major depression in medically healthy individuals? *J. Affect. Disord.* 119, 181–185. doi: 10.1016/j.jad.2009.02.017

Casano, A. M., and Peri, F. (2015). Microglia: multitasking specialists of the brain. *Dev. Cell* 32, 469–477. doi: 10.1016/j.devcel.2015.01.018

Chen, Z., and Trapp, B. D. (2016). Microglia and neuroprotection. *J. Neurochem.* 136, 10–17. doi: 10.1111/jnc.13062

Cherry, J. D., Olschowka, J. A., and O'Banion, M. K. (2014). Neuroinflammation and M2 microglia: the good, the bad, and the inflamed. *J. Neuroinflammation* 11:98. doi: 10.1186/1742-2094-11-98

Chhor, V., Le Charpentier, T., Lebon, S., Oré, M. V., Celador, I. L., Josserand, J., et al. (2013). Characterization of phenotype markers and neuronotoxic potential of polarised primary microglia *in vitro*. *Brain Behav. Immun.* 32, 70–85. doi: 10.1016/j.bbi.2013.02.005

Cunningham, C. L., Martínez-Cerdeño, V., and Noctor, S. C. (2013). Microglia regulate the number of neural precursor cells in the developing cerebral cortex. *J. Neurosci.* 33, 4216–4233. doi: 10.1523/JNEUROSCI.3441-12.2013

Cunningham, K. A., and Watson, C. S. (2008). Cell cycle regulation, neurogenesis, and depression. *Proc. Natl. Acad. Sci. U S A* 105, 2259–2260. doi: 10.1073/pnas.0800029105

de Pablos, R. M., Herrera, A. J., Espinosa-Oliva, A. M., Sarmiento, M., Muñoz, M. F., Machado, A., et al. (2014). Chronic stress enhances microglia activation and exacerbates death of nigral dopaminergic neurons under conditions of inflammation. *J. Neuroinflammation* 11:34. doi: 10.1186/1742-2094-11-34

de Rivero Vaccari, J. P., Lotocki, G., Alonso, O. F., Bramlett, H. M., Dietrich, W. D., and Keane, R. W. (2009). Therapeutic neutralization of the NLRP1 inflammasome reduces the innate immune response and improves histopathology after traumatic brain injury. *J. Cereb. Blood Flow Metab.* 29, 1251–1261. doi: 10.1038/jcbfm.2009.46

Deczkowska, A., Matcovitch-Natan, O., Tsitsou-Kampeli, A., Ben-Hamo, S., Dvir-Szternfeld, R., Spinrad, A., et al. (2017). Mef2C restrains microglial inflammatory response and is lost in brain ageing in an IFN-I-dependent manner. *Nat. Commun.* 8:717. doi: 10.1038/s41467-017-00769-0

Depino, A. M. (2015). Early prenatal exposure to LPS results in anxiety- and depression-related behaviors in adulthood. *Neuroscience* 299, 56–65. doi: 10.1016/j.neuroscience.2015.04.065

Ding, A. H., Nathan, C. F., and Stuehr, D. J. (1988). Release of reactive nitrogen intermediates and reactive oxygen intermediates from mouse peritoneal macrophages. Comparison of activating cytokines and evidence for independent production. *J. Immunol.* 141, 2407–2412.

Dowlati, Y., Herrmann, N., Swardfager, W., Liu, H., Sham, L., Reim, E. K., et al. (2010). A meta-analysis of cytokines in major depression. *Biol. Psychiatry* 67, 446–457. doi: 10.1016/j.biopsych.2009.09.033

Espinosa-Oliva, A. M., de Pablos, R. M., Villarán, R. F., Argüelles, S., Venero, J. L., Machado, A., et al. (2011). Stress is critical for LPS-induced activation of microglia and damage in the rat hippocampus. *Neurobiol. Aging* 32, 85–102. doi: 10.1016/j.neurobiolaging.2009.01.012

Farooq, R. K., Tanti, A., Ainouche, S., Roger, S., Belzung, C., and Camus, V. (2018). A P2X7 receptor antagonist reverses behavioural alterations, microglial activation and neuroendocrine dysregulation in an unpredictable chronic mild

stress (UCMS) model of depression in mice. *Psychoneuroendocrinology* 97, 120–130. doi: 10.1016/j.psyneuen.2018.07.016

Farrell, K., Borazjani, A., Damaser, M., and Kothapalli, C. R. (2016). Differential regulation of NSC phenotype and genotype by chronically activated microglia within cocultures. *Integr. Biol. Camb.* 8, 1145–1157. doi: 10.1039/c6ib00126b

Fazi, F., Rosa, A., Fatica, A., Gelmetti, V., De Marchis, M. L., Nervi, C., et al. (2005). A minicircuitry comprised of microRNA-223 and transcription factors NFI-A and C/EBPα regulates human granulopoiesis. *Cell* 123, 819–831. doi: 10.1016/j.cell.2005.09.023

Feng, S., Zou, L., Wang, H., He, R., Liu, K., and Zhu, H. (2018). RhoA/ROCK-2 pathway inhibition and tight junction protein upregulation by catalpol suppresses lipopolysaccaride-induced disruption of blood-brain barrier permeability. *Molecules* 23:E2371. doi: 10.3390/molecules23092371

Ferrini, F., and De Koninck, Y. (2013). Microglia control neuronal network excitability via BDNF signalling. *Neural Plast.* 2013:429815. doi: 10.1155/2013/429815

Franco, R., and Fernández-Suárez, D. (2015). Alternatively activated microglia and macrophages in the central nervous system. *Prog. Neurobiol.* 131, 65–86. doi: 10.1016/j.pneurobio.2015.05.003

Franklin, T. C., Wohleb, E. S., Zhang, Y., Fogaça, M., Hare, B., and Duman, R. S. (2018). Persistent increase in microglial RAGE contributes to chronic stress-induced priming of depressive-like behavior. *Biol. Psychiatry* 83, 50–60. doi: 10.1016/j.biopsych.2017.06.034

Freilich, R. W., Woodbury, M. E., and Ikezu, T. (2013). Integrated expression profiles of mRNA and miRNA in polarized primary murine microglia. *PLoS One* 8:e79416. doi: 10.1371/journal.pone.0079416

Fujioka, H., and Akema, T. (2010). Lipopolysaccharide acutely inhibits proliferation of neural precursor cells in the dentate gyrus in adult rats. *Brain Res.* 1352, 35–42. doi: 10.1016/j.brainres.2010.07.032

Gemma, C., and Bachstetter, A. D. (2013). The role of microglia in adult hippocampal neurogenesis. *Front. Cell. Neurosci.* 7:229. doi: 10.3389/fncel.2013.00229

Ghosh, M., Xu, Y., and Pearse, D. D. (2016). Cyclic AMP is a key regulator of M1 to M2a phenotypic conversion of microglia in the presence of Th2 cytokines. *J. Neuroinflammation* 13:9. doi: 10.1186/s12974-015-0463-9

Ginhoux, F., Greter, M., Leboeuf, M., Nandi, S., See, P., Gokhan, S., et al. (2010). Fate mapping analysis reveals that adult microglia derive from primitive macrophages. *Science* 330, 841–845. doi: 10.1126/science.1194637

Glass, C. K., Saijo, K., Winner, B., Marchetto, M. C., and Gage, F. H. (2010). Mechanisms underlying inflammation in neurodegeneration. *Cell* 140, 918–934. doi: 10.1016/j.cell.2010.02.016

Grabert, K., Michoel, T., Karavolos, M. H., Clohisey, S., Baillie, J. K., Stevens, M. P., et al. (2016). Microglial brain region-dependent diversity and selective regional sensitivities to aging. *Nat. Neurosci.* 19, 504–516. doi: 10.1038/nn.4222

Gresa-Arribas, N., Vieitez, C., Dentesano, G., Serratosa, J., Saura, J., and Solà, C. (2012). Modelling neuroinflammation *in vitro*: a tool to test the potential neuroprotective effect of anti-inflammatory agents. *PLoS One* 7:e45227. doi: 10.1371/journal.pone.0045227

Guedes, J., Cardoso, A. L., and Pedroso de Lima, M. C. (2013). Involvement of microRNA in microglia-mediated immune response. *Clin. Dev. Immunol.* 2013:186872. doi: 10.1155/2013/186872

Gustin, A., Kirchmeyer, M., Koncina, E., Felten, P., Losciuto, S., Heurtaux, T., et al. (2015). NLRP3 inflammasome is expressed and functional in mouse brain microglia but not in astrocytes. *PLoS One* 10:e0130624. doi: 10.1371/journal.pone.0130624

Harry, G. J., and Kraft, A. D. (2008). Neuroinflammation and microglia: considerations and approaches for neurotoxicity assessment. *Expert Opin. Drug Metab. Toxicol.* 4, 1265–1277. doi: 10.1517/17425255.4.10.1265

Hayakawa, K., Okazaki, R., Morioka, K., Nakamura, K., Tanaka, S., and Ogata, T. (2014). Lipopolysaccharide preconditioning facilitates M2 activation of resident microglia after spinal cord injury. *J. Neurosci. Res.* 92, 1647–1658. doi: 10.1002/jnr.23448

Hellwig, S., Brioschi, S., Dieni, S., Frings, L., Masuch, A., Blank, T., et al. (2016). Altered microglia morphology and higher resilience to stress-induced depression-like behavior in CX3CR1-deficient mice. *Brain Behav. Immun.* 55, 126–137. doi: 10.1016/j.bbi.2015.11.008

Heneka, M. T., Kummer, M. P., and Latz, E. (2014). Innate immune activation in neurodegenerative disease. *Nat. Rev. Immunol.* 14, 463–477. doi: 10.1038/nri3705

Henn, F. A., and Vollmayr, B. (2004). Neurogenesis and depression: etiology or epiphenomenon? *Biol. Psychiatry* 56, 146–150. doi: 10.1016/j.biopsych.2004.04.011

Henry, C. J., Huang, Y., Wynne, A. M., and Godbout, J. P. (2009). Peripheral lipopolysaccharide (LPS) challenge promotes microglial hyperactivity in aged mice that is associated with exaggerated induction of both pro-inflammatory IL-1β and anti-inflammatory IL-10 cytokines. *Brain Behav. Immun.* 23, 309–317. doi: 10.1016/j.bbi.2008.09.002

Hoeffel, G., Chen, J., Lavin, Y., Low, D., Almeida, F. F., See, P., et al. (2015). C-Myb^{+} erythro-myeloid progenitor-derived fetal monocytes give rise to adult tissue-resident macrophages. *Immunity* 42, 665–678. doi: 10.1016/j.immuni.2015.03.011

Imai, Y., and Kohsaka, S. (2002). Intracellular signaling in M-CSF-induced microglia activation: role of Iba1. *Glia* 40, 164–174. doi: 10.1002/glia.10149

Janssen, D. G., Caniato, R. N., Verster, J. C., and Baune, B. T. (2010). A psychoneuroimmunological review on cytokines involved in antidepressant treatment response. *Hum. Psychopharmacol.* 25, 201–215. doi: 10.1002/hup.1103

Jo, W. K., Zhang, Y., Emrich, H. M., and Dietrich, D. E. (2015). Glia in the cytokine-mediated onset of depression: fine tuning the immune response. *Front. Cell. Neurosci.* 9:268. doi: 10.3389/fncel.2015.00268

Joca, S. R., Moreira, F. A., and Wegener, G. (2015). Atypical neurotransmitters and the neurobiology of depression. *CNS Neurol. Disord. Drug Targets* 14, 1001–1011. doi: 10.2174/1871527314666150909114804

Juruena, M. F. (2014). Early-life stress and HPA axis trigger recurrent adulthood depression. *Epilepsy Behav.* 38, 148–159. doi: 10.1016/j.yebeh.2013.10.020

Khemissi, W., Farooq, R. K., Le Guisquet, A. M., Sakly, M., and Belzung, C. (2014). Dysregulation of the hypothalamus-pituitary-adrenal axis predicts some aspects of the behavioral response to chronic fluoxetine: association with hippocampal cell proliferation. *Front. Behav. Neurosci.* 8:340. doi: 10.3389/fnbeh.2014.00340

Kierdorf, K., Erny, D., Goldmann, T., Sander, V., Schulz, C., Perdiguero, E. G., et al. (2013). Microglia emerge from erythromyeloid precursors via Pu.1- and Irf8-dependent pathways. *Nat. Neurosci.* 16, 273–280. doi: 10.1038/nn.3318

Kigerl, K. A., Lai, W., Wallace, L. M., Yang, H., and Popovich, P. G. (2018). High mobility group box-1 (HMGB1) is increased in injured mouse spinal cord and can elicit neurotoxic inflammation. *Brain Behav. Immun.* 72, 22–33. doi: 10.1016/j.bbi.2017.11.018

Kim, Y. K., Na, K. S., Shin, K. H., Jung, H. Y., Choi, S. H., and Kim, J. B. (2007). Cytokine imbalance in the pathophysiology of major depressive disorder. *Prog. Neuropsychopharmacol. Biol. Psychiatry* 31, 1044–1053. doi: 10.1016/j.pnpbp.2007.03.004

Kim, K. W., Vallon-Eberhard, A., Zigmond, E., Farache, J., Shezen, E., Shakhar, G., et al. (2011). *In vivo* structure/function and expression analysis of the CX3C chemokine fractalkine. *Blood* 118, e156–e167. doi: 10.1182/blood-2011-04-348946

Kobayashi, K., Imagama, S., Ohgomori, T., Hirano, K., Uchimura, K., Sakamoto, K., et al. (2013). Minocycline selectively inhibits M1 polarization of microglia. *Cell Death Dis.* 4:e525. doi: 10.1038/cddis.2013.54

Kong, Y., Ruan, L., Qian, L., Liu, X., and Le, Y. (2010). Norepinephrine promotes microglia to uptake and degrade amyloid β peptide through upregulation of mouse formyl peptide receptor 2 and induction of insulin-degrading enzyme. *J. Neurosci.* 30, 11848–11857. doi: 10.1523/JNEUROSCI.2985-10.2010

Lehnardt, S. (2010). Innate immunity and neuroinflammation in the CNS: the role of microglia in Toll-like receptor-mediated neuronal injury. *Glia* 58, 253–263. doi: 10.1002/glia.20928

Li, Q., and Barres, B. A. (2018). Microglia and macrophages in brain homeostasis and disease. *Nat. Rev. Immunol.* 18, 225–242. doi: 10.1038/nri.2017.125

Li, Z., Ma, L., Kulesskaya, N., Võikar, V., and Tian, L. (2014). Microglia are polarized to M1 type in high-anxiety inbred mice in response to lipopolysaccharide challenge. *Brain Behav. Immun.* 38, 237–248. doi: 10.1016/j.bbi.2014.02.008

Lopez-Duran, N. L., McGinnis, E., Kuhlman, K., Geiss, E., Vargas, I., and Mayer, S. (2015). HPA-axis stress reactivity in youth depression: evidence

of impaired regulatory processes in depressed boys. *Stress* 18, 545–553. doi: 10.3109/10253890.2015.1053455

Martinon, F., Burns, K., and Tschopp, J. (2002). The inflammasome: a molecular platform triggering activation of inflammatory caspases and processing of proIL-β. *Mol. Cell.* 10, 417–426. doi: 10.1016/S1097-2765(02)00599-3

Mao, R., Zhang, C., Chen, J., Zhao, G., Zhou, R., Wang, F., et al. (2018). Different levels of pro- and anti-inflammatory cytokines in patients with unipolar and bipolar depression. *J. Affect. Disord.* 237, 65–72. doi: 10.1016/j.jad.2018.04.115

Medeiros, I. U., Ruzza, C., Asth, L., Guerrini, R., Romão, P. R., Gavioli, E. C., et al. (2015). Blockade of nociceptin/orphanin FQ receptor signaling reverses LPS-induced depressive-like behavior in mice. *Peptides* 72, 95–103. doi: 10.1016/j.peptides.2015.05.006

Miki, A., Honda, S., Inoue, Y., Yamada, Y., and Nakamura, M. (2018). Foveal depression and related factors in patients with a history of retinopathy of prematurity. *Ophthalmologica* 240, 106–110. doi: 10.1159/000488368

Monje, M. L., Toda, H., and Palmer, T. D. (2003). Inflammatory blockade restores adult hippocampal neurogenesis. *Science* 302, 1760–1765. doi: 10.1126/science.1088417

Nakatani, Y., Amano, T., Tsuji, M., and Takeda, H. (2012). Corticosterone suppresses the proliferation of BV2 microglia cells via glucocorticoid, but not mineralocorticoid receptor. *Life Sci.* 91, 761–770. doi: 10.1016/j.lfs.2012.08.019

Norden, D. M., Muccigrosso, M. M., and Godbout, J. P. (2015). Microglial priming and enhanced reactivity to secondary insult in aging and traumatic CNS injury and neurodegenerative disease. *Neuropharmacology* 96, 29–41. doi: 10.1016/j.neuropharm.2014.10.028

Osman, A. M., Rodhe, J., Shen, X., Dominguez, C. A., Joseph, B., and Blomgren, K. (2017). The secretome of microglia regulate neural stem cell function. *Neuroscience* doi: 10.1016/j.neuroscience.2017.10.034 [Epub ahead of print].

Pan, J., Jin, J. L., Ge, H. M., Yin, K. L., Chen, X., Han, L. J., et al. (2015). Malibatol A regulates microglia M1/M2 polarization in experimental stroke in a PPARγ-dependent manner. *J. Neuroinflammation* 12:51. doi: 10.1186/s12974-015-0270-3

Parnet, P., Kelley, K. W., Bluthé, R. M., and Dantzer, R. (2002). Expression and regulation of interleukin-1 receptors in the brain. Role in cytokines-induced sickness behavior. *J. Neuroimmunol.* 125, 5–14. doi: 10.1016/s0165-5728(02)00022-x

Pocock, J. M., and Kettenmann, H. (2007). Neurotransmitter receptors on microglia. *Trends Neurosci.* 30, 527–535. doi: 10.1016/j.tins.2007.07.007

Polazzi, E., and Monti, B. (2010). Microglia and neuroprotection: from *in vitro* studies to therapeutic applications. *Prog. Neurobiol.* 92, 293–315. doi: 10.1016/j.pneurobio.2010.06.009

Ponomarev, E. D., Veremeyko, T., and Weiner, H. L. (2013). MicroRNAs are universal regulators of differentiation, activation and polarization of microglia and macrophages in normal and diseased CNS. *Glia* 61, 91–103. doi: 10.1002/glia.22363

Porta, C., Riboldi, E., Ippolito, A., and Sica, A. (2015). Molecular and epigenetic basis of macrophage polarized activation. *Semin. Immunol.* 27, 237–248. doi: 10.1016/j.smim.2015.10.003

Powell, T. R., Schalkwyk, L. C., Heffernan, A. L., Breen, G., Lawrence, T., Price, T., et al. (2013). Tumor necrosis factor and its targets in the inflammatory cytokine pathway are identified as putative transcriptomic biomarkers for escitalopram response. *Eur. Neuropsychopharmacol.* 23, 1105–1114. doi: 10.1016/j.euroneuro.2012.09.009

Prajeeth, C. K., Löhr, K., Floess, S., Zimmermann, J., Ulrich, R., Gudi, V., et al. (2014). Effector molecules released by Th1 but not Th17 cells drive an M1 response in microglia. *Brain Behav. Immun.* 37, 248–259. doi: 10.1016/j.bbi.2014.01.001

Qi, F., Zuo, Z., Yang, J., Hu, S., Yang, Y., Yuan, Q., et al. (2017). Combined effect of BCG vaccination and enriched environment promote neurogenesis and spatial cognition via a shift in meningeal macrophage M2 polarization. *J. Neuroinflammation* 14:32. doi: 10.1186/s12974-017-0808-7

Reshef, R., Kreisel, T., Beroukhim Kay, D., and Yirmiya, R. (2014). Microglia and their CX3CR1 signaling are involved in hippocampal- but not olfactory bulb-related memory and neurogenesis. *Brain Behav. Immun.* 41, 239–250. doi: 10.1016/j.bbi.2014.04.009

Ribeiro Xavier, A. L., Kress, B. T., Goldman, S. A., Lacerda de Menezes, J. R., and Nedergaard, M. (2015). A distinct population of microglia supports adult neurogenesis in the subventricular zone. *J. Neurosci.* 35, 11848–11861. doi: 10.1523/JNEUROSCI.1217-15.2015

Sahay, A., and Hen, R. (2008). Hippocampal neurogenesis and depression. *Novartis Found. Symp.* 289, 152–160; discussion 160–154, 193–155. doi: 10.1002/9780470751251.ch12

Santarelli, L., Saxe, M., Gross, C., Surget, A., Battaglia, F., Dulawa, S., et al. (2003). Requirement of hippocampal neurogenesis for the behavioral effects of antidepressants. *Science* 301, 805–809. doi: 10.1126/science.1083328

Sato, K. (2015). Effects of microglia on neurogenesis. *Glia* 63, 1394–1405. doi: 10.1002/glia.22858

Shigemoto-Mogami, Y., Hoshikawa, K., Goldman, J. E., Sekino, Y., and Sato, K. (2014). Microglia enhance neurogenesis and oligodendrogenesis in the early postnatal subventricular zone. *J. Neurosci.* 34, 2231–2243. doi: 10.1523/JNEUROSCI.1619-13.2014

Sierra, A., Beccari, S., Diaz-Aparicio, I., Encinas, J. M., Comeau, S., and Tremblay, M. E. (2014). Surveillance, phagocytosis, and inflammation: how never-resting microglia influence adult hippocampal neurogenesis. *Neural Plast.* 2014:610343. doi: 10.1155/2014/610343

Sierra, A., Encinas, J. M., Deudero, J. J., Chancey, J. H., Enikolopov, G., Overstreet-Wadiche, L. S., et al. (2010). Microglia shape adult hippocampal neurogenesis through apoptosis-coupled phagocytosis. *Cell Stem Cell* 7, 483–495. doi: 10.1016/j.stem.2010.08.014

Singhal, G., and Baune, B. T. (2017). Microglia: an interface between the loss of neuroplasticity and depression. *Front. Cell. Neurosci.* 11:270. doi: 10.3389/fncel.2017.00270

Ślusarczyk, J., Trojan, E., Głombik, K., Piotrowska, A., Budziszewska, B., Kubera, M., et al. (2018). Targeting the NLRP3 inflammasome-related pathways via tianeptine treatment-suppressed microglia polarization to the M1 phenotype in lipopolysaccharide-stimulated cultures. *Int. J. Mol. Sci.* 19:E1965. doi: 10.3390/ijms19071965

Smith, P. L., Hagberg, H., Naylor, A. S., and Mallard, C. (2014). Neonatal peripheral immune challenge activates microglia and inhibits neurogenesis in the developing murine hippocampus. *Dev. Neurosci.* 36, 119–131. doi: 10.1159/000359950

Song, J., Takeda, M., and Morimoto, R. I. (2001). Bag1-Hsp70 mediates a physiological stress signalling pathway that regulates Raf-1/ERK and cell growth. *Nat. Cell Biol.* 3, 276–282. doi: 10.1038/35060068

Stefani, J., Tschesnokowa, O., Parrilla, M., Robaye, B., Boeynaems, J. M., Acker-Palmer, A., et al. (2018). Disruption of the microglial ADP receptor P2Y13 enhances adult hippocampal neurogenesis. *Front. Cell. Neurosci.* 12:134. doi: 10.3389/fncel.2018.00134

Steiner, J., Bielau, H., Brisch, R., Danos, P., Ullrich, O., Mawrin, C., et al. (2008). Immunological aspects in the neurobiology of suicide: elevated microglial density in schizophrenia and depression is associated with suicide. *J. Psychiatr. Res.* 42, 151–157. doi: 10.1016/j.jpsychires.2006.10.013

Steiner, J., Walter, M., Gos, T., Guillemin, G. J., Bernstein, H. G., Sarnyai, Z., et al. (2011). Severe depression is associated with increased microglial quinolinic acid in subregions of the anterior cingulate gyrus: evidence for an immune-modulated glutamatergic neurotransmission? *J. Neuroinflammation* 8:94. doi: 10.1186/1742-2094-8-94

Tang, M. M., Lin, W. J., Pan, Y. Q., Guan, X. T., and Li, Y. C. (2016). Hippocampal neurogenesis dysfunction linked to depressive-like behaviors in a neuroinflammation induced model of depression. *Physiol. Behav.* 161, 166–173. doi: 10.1016/j.physbeh.2016.04.034

Tong, L., Gong, Y., Wang, P., Hu, W., Wang, J., Chen, Z., et al. (2017). Microglia loss contributes to the development of major depression induced by different types of chronic stresses. *Neurochem. Res.* 42, 2698–2711. doi: 10.1007/s11064-017-2270-4

Torres-Platas, S. G., Cruceanu, C., Chen, G. G., Turecki, G., and Mechawar, N. (2014). Evidence for increased microglial priming and macrophage recruitment in the dorsal anterior cingulate white matter of depressed suicides. *Brain Behav. Immun.* 42, 50–59. doi: 10.1016/j.bbi.2014.05.007

Toshimitsu, M., Kamei, Y., Ichinose, M., Seyama, T., Imada, S., Iriyama, T., et al. (2018). Atomoxetine, a selective norepinephrine reuptake inhibitor, improves short-term histological outcomes after hypoxic-ischemic brain injury in the neonatal male rat. *Int. J. Dev. Neurosci.* doi: 10.1016/j.ijdevneu.2018.03.011 [Epub ahead of print].

Tynan, R. J., Weidenhofer, J., Hinwood, M., Cairns, M. J., Day, T. A., and Walker, F. R. (2012). A comparative examination of the anti-inflammatory effects of SSRI and SNRI antidepressants on LPS stimulated microglia. *Brain Behav. Immun.* 26, 469–479. doi: 10.1016/j.bbi.2011.12.011

Ueno, M., Fujita, Y., Tanaka, T., Nakamura, Y., Kikuta, J., Ishii, M., et al. (2013). Layer V cortical neurons require microglial support for survival during postnatal development. *Nat. Neurosci.* 16, 543–551. doi: 10.1038/nn.3358

Valero, J., Mastrella, G., Neiva, I., Sanchez, S., and Malva, J. O. (2014). Long-term effects of an acute and systemic administration of LPS on adult neurogenesis and spatial memory. *Front. Neurosci.* 8:83. doi: 10.3389/fnins.2014.00083

Verney, C., Monier, A., Fallet-Bianco, C., and Gressens, P. (2010). Early microglial colonization of the human forebrain and possible involvement in periventricular white-matter injury of preterm infants. *J. Anat.* 217, 436–448. doi: 10.1111/j.1469-7580.2010.01245.x

von Bartheld, C. S., Bahney, J., and Herculano-Houzel, S. (2016). The search for true numbers of neurons and glial cells in the human brain: a review of 150 years of cell counting. *J. Comp. Neurol.* 524, 3865–3895. doi: 10.1002/cne.24040

Wadhwa, M., Prabhakar, A., Ray, K., Roy, K., Kumari, P., Jha, P. K., et al. (2017). Inhibiting the microglia activation improves the spatial memory and adult neurogenesis in rat hippocampus during 48 h of sleep deprivation. *J. Neuroinflammation* 14:222. doi: 10.1186/s12974-017-0998-z

Wang, Y. L., Han, Q. Q., Gong, W. Q., Pan, D. H., Wang, L. Z., Hu, W., et al. (2018). Microglial activation mediates chronic mild stress-induced depressive- and anxiety-like behavior in adult rats. *J. Neuroinflammation* 15:21. doi: 10.1186/s12974-018-1054-3

Wang, Y., Huang, Y., Xu, Y., Ruan, W., Wang, H., Zhang, Y., et al. (2018). A dual AMPK/Nrf2 activator reduces brain inflammation after stroke by enhancing microglia M2 polarization. *Antioxid. Redox Signal.* 28, 141–163. doi: 10.1089/ars.2017.7003

Wang, B., and Jin, K. (2015). Current perspectives on the link between neuroinflammation and neurogenesis. *Metab. Brain Dis.* 30, 355–365. doi: 10.1007/s11011-014-9523-6

Wang, J., Liu, J., Zhou, R., Ding, X., Zhang, Q., Zhang, C., et al. (2018). Zika virus infected primary microglia impairs NPCs proliferation and differentiation. *Biochem. Biophys. Res. Commun.* 497, 619–625. doi: 10.1016/j.bbrc.2018.02.118

Wang, Q., Lv, C., Sun, Y., Han, X., Wang, S., Mao, Z., et al. (2018). The role of α-lipoic acid in the pathomechanism of acute ischemic stroke. *Cell. Physiol. Biochem.* 48, 42–53. doi: 10.1159/000491661

Wendt, S., Wogram, E., Korvers, L., and Kettenmann, H. (2016). Experimental cortical spreading depression induces NMDA receptor dependent potassium currents in microglia. *J. Neurosci.* 36, 6165–6174. doi: 10.1523/JNEUROSCI.4498-15.2016

Wohleb, E. S., Terwilliger, R., Duman, C. H., and Duman, R. S. (2018). Stress-induced neuronal colony stimulating factor 1 provokes microglia-mediated neuronal remodeling and depressive-like behavior. *Biol. Psychiatry* 83, 38–49. doi: 10.1016/j.biopsych.2017.05.026

Wu, Q., Cai, H., Song, J., and Chang, Q. (2017). The effects of sEH inhibitor on depression-like behavior and neurogenesis in male mice. *J. Neurosci. Res.* 95, 2483–2492. doi: 10.1002/jnr.24080

Yang, J., Qi, F., Gu, H., Zou, J., Yang, Y., Yuan, Q., et al. (2016). Neonatal BCG vaccination of mice improves neurogenesis and behavior in early life. *Brain Res. Bull.* 120, 25–33. doi: 10.1016/j.brainresbull.2015.10.012

Yang, W., Zhou, K., Zhou, Y., An, Y., Hu, T., Lu, J., et al. (2018). Naringin dihydrochalcone ameliorates cognitive deficits and neuropathology in APP/PS1 transgenic mice. *Front. Aging Neurosci.* 10:169. doi: 10.3389/fnagi.2018.00169

Yirmiya, R., Rimmerman, N., and Reshef, R. (2015). Depression as a microglial disease. *Trends Neurosci.* 38, 637–658. doi: 10.1016/j.tins.2015.08.001

You, Z., Luo, C., Zhang, W., Chen, Y., He, J., Zhao, Q., et al. (2011). Pro- and anti-inflammatory cytokines expression in rat's brain and spleen exposed to chronic mild stress: involvement in depression. *Behav. Brain Res.* 225, 135–141. doi: 10.1016/j.bbr.2011.07.006

Young, E. A., Altemus, M., Lopez, J. F., Kocsis, J. H., Schatzberg, A. F., DeBattista, C., et al. (2004). HPA axis activation in major depression and response to fluoxetine: a pilot study. *Psychoneuroendocrinology* 29, 1198–1204. doi: 10.1016/j.psyneuen.2004.02.002

Young, J. J., Bruno, D., and Pomara, N. (2014). A review of the relationship between proinflammatory cytokines and major depressive disorder. *J. Affect. Disord.* 169, 15–20. doi: 10.1016/j.jad.2014.07.032

Yuan, J., Ge, H., Liu, W., Zhu, H., Chen, Y., Zhang, X., et al. (2017). M2 microglia promotes neurogenesis and oligodendrogenesis from neural stem/progenitor cells via the PPARγ signaling pathway. *Oncotarget* 8, 19855–19865. doi: 10.18632/oncotarget.15774

Zhang, J., Groff, R. F., and Dayawansa, S. (2013). Imipramine treatment increases cell proliferation following fluid percussion brain injury in rats. *Neurol. Res.* 35, 247–254. doi: 10.1179/1743132813Y.0000000164

Zhang, J. Q., Wu, X. H., Feng, Y., Xie, X. F., Fan, Y. H., Yan, S., et al. (2016). Salvianolic acid B ameliorates depressive-like behaviors in chronic mild stress-treated mice: involvement of the neuroinflammatory pathway. *Acta Pharmacol. Sin.* 37, 1141–1153. doi: 10.1038/aps.2016.63

Zhang, J., Xie, X., Tang, M., Zhang, J., Zhang, B., Zhao, Q., et al. (2017). Salvianolic acid B promotes microglial M2-polarization and rescues neurogenesis in stress-exposed mice. *Brain Behav. Immun.* 66, 111–124. doi: 10.1016/j.bbi.2017.07.012

Zhang, F., Zhong, R., Li, S., Fu, Z., Cheng, C., Cai, H., et al. (2017). Acute hypoxia induced an imbalanced M1/M2 activation of microglia through NF-kappaB signaling in Alzheimer's disease mice and wild-type littermates. *Front. Aging Neurosci.* 9:282. doi: 10.3389/fnagi.2017.00282

Conflict of Interest Statement: The authors declare that the research was conducted in the absence of any commercial or financial relationships that could be construed as a potential conflict of interest.

frontiers in Cellular Neuroscience

ORIGINAL RESEARCH
published: 23 October 2018
doi: 10.3389/fncel.2018.00375

Clonal Glial Response in a Multiple Sclerosis Mouse Model

Ana Bribian[1], Fernando Pérez-Cerdá[2,3,4], Carlos Matute[2,3,4] and Laura López-Mascaraque[1]**

[1]*Departamento de Neurobiología Molecular, Celular y del Desarrollo, Instituto Cajal-CSIC, Madrid, Spain,* [2]*Centro de Investigación Biomédica en Red de Enfermedades Neurodegenerativas (CIBERNED), Leioa, Spain,* [3]*Achucarro Basque Center for Neuroscience, Leioa, Spain,* [4]*Departamento de Neurociencias, Universidad del País Vasco (UPV)/EHU, Leioa, Spain*

Multiple sclerosis (MS) is an autoimmune disease causing central nervous system (CNS) demyelination and axonal injury. In the last years the importance of astrocytes in MS is rapidly increasing, recognizing astrocytes as highly active players in MS pathogenesis. Usually the role assigned to astrocytes in MS lesions has been the formation of the glial scar, but now their implication during lesion formation and the immune response increasingly recognized. Since astrocytes are a heterogeneous cell population with diverse roles in the CNS, the aim of this study was to analyze the putative clonal response of astrocytes in a demyelinating scenario. To undertake this aim, we used the induced experimental autoimmune encephalomyelitis (EAE) as a murine model for MS in previously electroporated mice with *in vivo* multicolor lineage tracing system, the StarTrack methodology. Our data revealed a variety of morphological changes that were different among distinct clones. In many cases, cells of the same clone responded equally to the injury, while in other cases clonally-related cells responded differently to the injury. Therefore, whereas some clones exhibited a strong morphological alteration, other clones located at similar distances to the lesion were apparently unresponsive. Thus, at present there is no compelling evidences that clonal relationship influences the position or function of astrocytes in the EAE model. Further, the coexistence of different astroglial clonal responses to the bran injury reveals the significance of development to determine the astrocyte features that respond to brain injuries.

Keywords: progenitor, EAE, cortex, lesion, StarTrack, astrocyte, reactive

OPEN ACCESS

Edited by:
Sandra Henriques Vaz, Instituto de Medicina Molecular (IMM), Portugal

Reviewed by:
Andreia Barateiro, Instituto de Investigação do Medicamento, Portugal
Marcos R. Costa, Federal University of Rio Grande do Norte, Brazil

****Correspondence:***
Ana Bribian
abribian@cajal.csic.es
Laura López-Mascaraque
mascaraque@cajal.csic.es

Received: *13 July 2018*
Accepted: *02 October 2018*
Published: *23 October 2018*

Citation:
Bribian A, Pérez-Cerdá F, Matute C and López-Mascaraque L (2018) Clonal Glial Response in a Multiple Sclerosis Mouse Model. Front. Cell. Neurosci. 12:375. doi: 10.3389/fncel.2018.00375

INTRODUCTION

Multiple sclerosis (MS) is a chronic, disabling autoimmune and neurological disorder targeting the white and gray matter of the central nervous system (CNS; Lassmann, 2012; Prins et al., 2015; van Munster et al., 2015). The loss of myelin and oligodendrocytes, axonal loss and glial scar formation in adult brain are the hallmarks for MS. In addition, activated microglia and astrocytes are also involved in the pathogenesis of MS, proliferating during MS progression (Correale, 2014; Correale and Farez, 2015; Ponath et al., 2018).

Current discoveries on the function of astrocytes in the brain in physiological and pathological conditions further highlighted the need to comprehensively evaluate the roles of these cells in all stages of MS (Brosnan and Raine, 2013; Ponath et al., 2018). Apart from the formation of the glial

scar, astrocytes have other significant roles in pathogenesis, including a significant implication in the CNS innate immune response: they are a source of cytotoxic factors and provide support for oligodendrocytes and neurons (Brosnan and Raine, 2013).

Remarkably, reactive astrocytes suffer changes in both phenotype and gene expression in response to the distance to the injury, denoting a high degree of heterogeneity (Mathewson and Berry, 1985; Eddleston and Mucke, 1993; Ridet et al., 1997; Sofroniew, 2009). However, the heterogeneity in astrocytes is not exclusive to reactive cells. In fact, the concept of astrocyte heterogeneity emerged in the late nineteenth century based on morphological differences (Andrizen, 1893). During the last two decades, the development of new immunocytochemical, molecular and genetic techniques allowed researchers to identify differences between astrocytes originated/located in the same or different CNS regions (García-Marqués et al., 2010; Horii-Hayashi et al., 2010; Matyash and Kettenmann, 2010; García-Marqués and López-Mascaraque, 2013, 2017; Tabata, 2015; Bribián et al., 2016). In particular, we developed a multi-color lineage tracing system for astrocytes, the Star Track technology, based on the genomic incorporation of 12 plasmids encoding different fluorescent reporters driven by the GFAP promoter along with the transposase plasmid (García-Marqués and López-Mascaraque, 2013). Star Track provided *in vivo* evidence of the relationship between heterogeneity and lineage in astrocytes (García-Marqués and López-Mascaraque, 2013) as well as how groups of astrocyte clones respond differentially to cortical injury (Martín-López et al., 2013). Taking advantage of this technology, we analyzed the morphological response of clonally-related astrocytes to demyelinating lesions in murine myelin oligodendrocyte glycoprotein (MOG)-induced experimental autoimmune encephalomyelitis (EAE), the most commonly used animal model that resembles immunopathological and neurobiological aspects of MS. The positional identity of astrocyte clones in this brain pathology represents a new approach to unraveling some unknown aspects of pathogenesis of MS. Our data show that most astrocytes are similarly distributed whether or not they share a clonal relationship, while a large diversity of morphological changes were different among different clones.

MATERIALS AND METHODS

Animals

Pregnant C57 mice from Janvier Labs were housed at the Universidad del País Vasco (UPV)-EHU animal facilities in standard cages, maintained under 12 h controlled light-dark cycles with food and water available *ad libitum*. This study was carried out in accordance with the recommendations of the ethical regulations on the use and welfare of experimental animals of the European Union (2010/63/EU) and the Spanish Ministry of Agriculture (RD 1201/2005 and L 32/2007). The protocol was approved by the Bioethical Committee at the UPV-EHU.

We analyzed cortical clones in two groups of mice: (1) nine adult StarTrack-electroporated mice (three sham and six EAE-induced mice); and (2) six adult StarTrack-electroporated animals (two sham and four EAE-induced mice). Sham animals were electroporated, with the exception of the fluid pulse.

StarTrack Mixture

Clonal analysis was performed with the StarTrack approach (García-Marqués and López-Mascaraque, 2013, 2017). Briefly, StarTrack is based on the genomic incorporation of 12 plasmids encoding six different fluorescent reporter proteins, localized cytoplasm or nucleus, under the GFAP promoter. To allow the genomic integration of these constructs, each plasmid incorporates inverted terminal repeat sequences recognized by the piggyBac transposase plasmid. This results in a unique color combination code detecting glial clones derived from single progenitors. This will allow following cell dispersion of the progeny from embryonic mice single progenitor cells and generated an inheritable mark in astrocyte lineages.

In utero Electroporation

Pregnant mice, at embryonic day 14 (E14), were deeply anesthetized by isofluorane inhalation (IsovaH vet, Centauro, 2 ml/L) and maintained at 37°C. After uterine horns were exposed, embryos were visualized by trans-illumination using an optical fiber. Using a glass micropipette, the plasmid mixture (2 ml, 2–5 mg DNA/ml containing 0.1% fast green) was injected into lateral ventricles (LV). Next, by using tweezer-type electrodes, one or two trains of five square pulses (35 V; 50 ms followed by 950 ms intervals) were delivered on each embryo. Uterine horns were placed back into abdominal cavity.

Finally, both abdominal and skin incisions, were sealed with absorbable polyglycolic acid (Surgicryl, Hünningen, BE) and silk (3/0 Lorca-Marin, Murcia, ES) sutures, respectively. Skin was cleaned with povidone-iodine and pregnant mice received a subcutaneous injection of both 5 mg/kg of the antibiotic enrofloxacin (Baytril; Bayer, Kiel, Germany) and 300 mg/kg of the anti-inflammatory/analgesic meloxicam (Metacam; Boehringer Ingelheim). Injected embryos were allowed to develop normally until they were born.

EAE Induction and Treatment

EAE was induced in electroporated C57BL/6 mice by immunization with the immunodominant epitope of MOG (MOG 35–55). Chronic, relapsing EAE was induced successfully induced in male and female animals as previously described (Matute et al., 2007; Pampliega et al., 2011). Although gender differences in susceptibility have been described in mice (Voskuhl and Palaszynski, 2001; Teuscher et al., 2006), we used both males and females in this and previous studies without observing any significant gender difference in the symptoms (Matute et al., 2007; Pampliega et al., 2011; Saab et al., 2016), to minimize the use of animals to comply with institutional regulations. Briefly, C57BL/6 mice, 8-week-old, were immunized with 300 μg of MOG (35–55) (200 μg; Sigma Aldrich) in incomplete Freund's adjuvant supplemented with 8 mg/ml

Mycobacterium tuberculosis H37Ra. Pertussis toxin (500 ng; Sigma) was injected on the day of immunization and again 2 days later.

Motor symptoms were recorded daily and scored as follows from 0 to 8: 0, no detectable changes in muscle tone and motor behavior; 1, flaccid tail; 2, paralyzed tail; 3, impairment or loss of muscle tone in hindlimbs; 4, hindlimb hemiparalysis; 5, complete hindlimb paralysis; 6, complete hindlimb paralysis and loss of muscle tone in forelimbs; 7, tetraplegia; and 8, moribund. Later, mice were fixed by perfusion with 4% paraformaldehyde in phosphate buffer, post-fixed in the same fixation solution, and stored in phosphate-buffered saline (PBS) plus azide at 4°C.

Histology and Immunohistochemistry

Brains were removed and vibratome sectioned in the coronal plane at 50 μm. After several washes in PBS-0.1% Triton (PBST), the sections were pre-incubated for 1 h at RT in 5% normal goat serum. Immunohistochemistry was performed by incubating the sections (overnight, at 4°C) with the following primary antibodies: Tomato Lectin (TL; 1:70, Sigma-Aldrich), and anti-Ki67 (1:500; ThermoScientific) diluted in PBST supplemented with 1% normal goat serum (NGS, Millipore). After washing, slices were incubated with the secondary antibody coupled to Alexa 633 (1:1,000, Invitrogen) in PBST for 2 h at RT.

Image Processing and Data Analyses

The image processing was performed as previously described (García-Marqués and López-Mascaraque, 2013; Figueres-Oñate et al., 2016). Briefly, first the fluorescent labeling was visualized under an epifluorescence microscope (Nikon, Eclipse E600) with the appropriate filter cubes (Semrock): UV-2A (FF01-334/40-25), Cerulean (FF01-405/10), GFP (FF01-473/10), YFP (FF01-520/15), mKO (FF01-540/15), mCherry (FF01-590/20) and Cy5 (FF02-628/40-25). Images were acquired on a Leica TCS-SP5 confocal microscope, capturing the different XFPs in separate channels with the 20× objective. The wavelength of excitation (Ex) and emission (Em) for each XFP were (in nanometers, nm): mT-Sapphire (Ex: 405; Em: 520–535), mCerulean (Ex: 458; Em: 468–480), EGFP (Ex: 488; Em: 498–510), YFP (Ex: 514; Em: 525–535), mKO (Ex: 514; Em: 560–580), mCherry (Ex: 561; Em: 601–620), and Alexa 633 (Ex: 633; Em: 650–760). Confocal laser lines were in-between 25% and 40% in all cases and the maximum projection images were created using confocal (LASAF Leica) and NIH-ImageJ software. Cortical astroglial clones were defined as those cells sharing the same fluorescent marks, based on the fluorescence intensity and specific cellular location of the fluorophores (nucleus or cytoplasm). Those clones were located surrounding the perivascular infiltrates and the enlarged perivascular compartments, identified with TL expression. For the quantifications, we analyzed 10 clones/per animal in three EAE Star-Track electroporated mice. Statistical analysis of the data and graphical representations were performed using R statistical software version 3.5.0 (R Core Team, 2018) and Sigma Plot version 14.0 (Systat Software, San Jose, CA, USA).

RESULTS

Identification of Cortical EAE Lesions

Although in the EAE MOG-induced model the main affectation is located in the spinal cord, EAE experiments in mice demonstrated that, as occurs in human MS, the cerebral cortex is also affected (Procaccini et al., 2015). In fact, neocortical lesions have previously been recognized to be present in MS (Stadelmann et al., 2008). In particular, chronic EAE induced by MOG peptide in mice showed, although with some variability, intracortical MS-like lesions characterized by diffused demyelination, astroglial and microglial activation, oligodendrocyte precursor cells (OPC) proliferation, and a low leukocyte/macrophage infiltrate (Girolamo et al., 2011; Mangiardi et al., 2011; Hasselmann et al., 2017).

Results presented in **Figure 1** correspond to animals previously StarTrack electroporated, both EAE (**Figures 1A,C–F**) and sham mice (**Figure 1B**). We initially performed Tomato-lectin immunohistochemistry, in both MOG-induced (**Figures 1A,C–F**) and sham animals (**Figure 1B**) to visualize the presence of inflammatory infiltrates, microglial cells

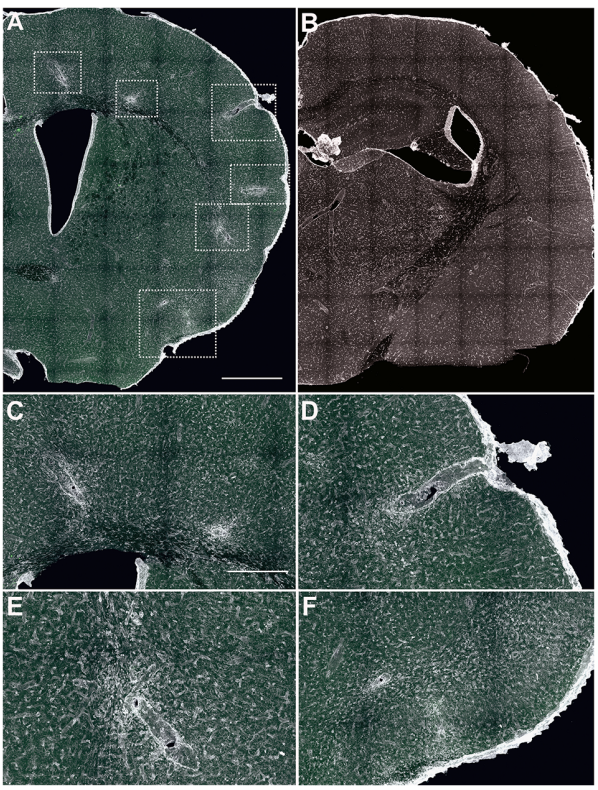

FIGURE 1 | Identification of cortical lesions. **(A,B)** Low magnification images of brain coronal sections labeled with tomato lectin (TL) to label the infiltrates surrounding the lesions. In experimental autoimmune encephalomyelitis (EAE)-induced mice **(A)** cell infiltrates were located along the brain, while in sham animals **(B)**, no lesions or infiltrates were identified. In EAE animals, affected areas (boxed with dotted line) were subcortical white matter **(C,E)**, cortical/subcortical area **(C,D)** and layer I (subpial, **F**). Scale bars: **(A,B)** 400 μm and **(C–F)** 100 μm.

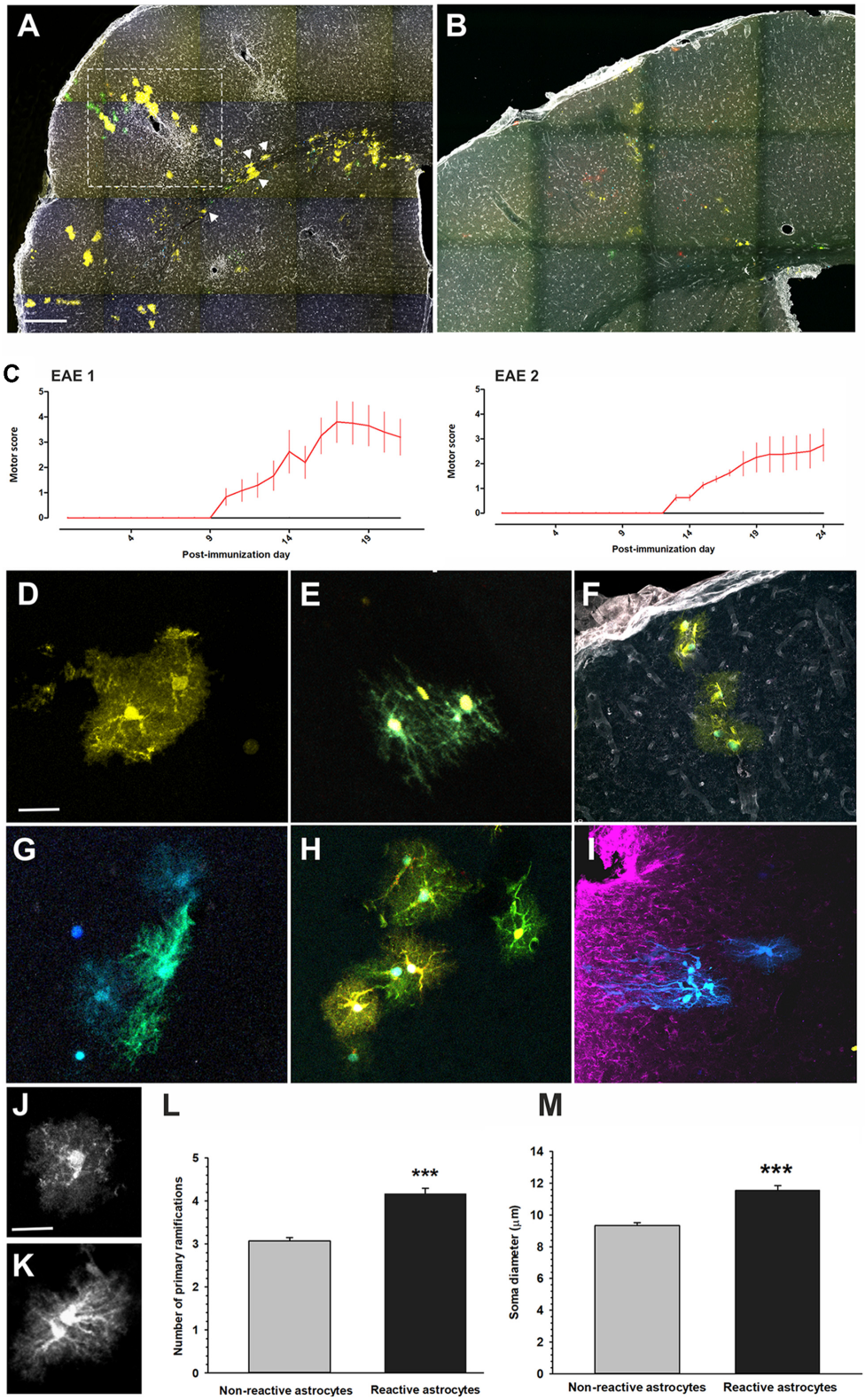

FIGURE 2 | Cortical clonal dispersion in Star Track IUE-adult mice. **(A)** Low magnification image of a coronal cortical brain section of an EAE-induced adult mice *in utero* electroporated at E14. Analysis was restricted to the labeled sibling astrocytes surrounding the cortical lesion (dashed square). The injured area was

(*Continued*)

FIGURE 2 | Continued
determined by the presence of infiltrates close to the enlarge perivascular space (stained with TL, in white). Most clonal groups display protoplasmic morphologies throughout the cortical layers, but some clones of fibrous astrocytes were located in the subcortical white matter (arrowheads). **(B)** Low magnification image of a coronal cortical brain section of a sham adult mice *in utero* electroporated at E14. **(C)** Clinical score of both EAE groups (red) and controls (black) in StarTrack-electroporated mice. **(D)** StarTrack labeled protoplasmic astrocytes in a sham brain. **(E)** StarTrack labeled fibrous sibling astrocytes in a sham brain. **(F)** StarTrack labeled vascular sibling astrocytes in a sham brain. **(G,H)** Hypertrophic astrocytes in an EAE myelin oligodendrocyte glycoprotein (MOG)-injected electroporated mice. **(I)** Hypertrophied astrocytes around the wounded area of an StarTrack electroporated mice lesioned with the model of fine-needle cortical injury (Martín-López et al., 2013). **(J,K)** Image of a typical protoplasmic astrocyte (**J** of a hypertrophied astrocyte **K**). **(L,M)** Graphs show the quantification of the number of primary ramifications **(L)**, and soma diameter **(M)** of non-reactive astrocytes and reactive astrocytes in EAE electroporated mice (***$P < 0.001$). Scale bar: **(A,B)** 200 μm; **(D,G)** 20 μm; **(E)** 30 μm; **(F,I)** 50 μm; **(H)** 40 μm and **(J,K)** 25 μm.

and blood vessels. Affected regions were determined by the presence of perivascular inflammatory infiltrates and larger perivascular compartments located throughout the rostro-caudal axis of cortical gray and white matter (**Figures 1A,C–F**) of MOG-injected animals, similar to our previous results in wildtype mice (Matute et al., 2007; Zabala et al., 2018). No perivascular cuffs were found in sham-electroporated mice brains (**Figure 1B**).

We identified three types of cortical lesions: perivascular intracortical lesions, cortico/subcortical lesions (**Figures 1A,C–E**) and subpial lesions accompanied by meningeal inflammation (**Figure 1F**), which was more evident in those animals with higher clinical score. These data support that the inflammation of meninges is important in the induction and propagation of cortical pathology in MS (Lassmann, 2012). Even some infiltrates were located in the striatum (**Figure 2A**), we focused on the cerebral cortex since most StarTrack labeled cells were located in cortex.

Astrocytes Display Different Morphologies Depending on the Localization of Perivascular Infiltration in EAE-Mice

In utero electroporated mice with the StarTrack mixture were divided in two groups: one EAE induced with MOG35−55 peptide at 8 weeks of age in complete Freund's adjuvant on day 0, and a sham group (**Figures 2A,B**; see "Materials and Methods" section). Both clinical signs and score were monitored up to day 21 and 24, respectively, in each of the two EAE experiments (**Figure 2C**). Even there was some variability in the intensity of the symptoms among mice, the analysis of all tissues was done around the peak of the disease (**Figure 2C**). Mice began to show neurological deficits between days 10–13, reaching a maximum score (hindlimbs symptoms characterized by loss of muscle tone to hemiparalysis) around days 17–22 (**Figure 2C**). Although many types of cells reacted in EAE lesions, we focused on the analysis of StarTrack-labeled astrocytes to identify the astroglial clones. StarkTrack method allowed the analyses of the astrocyte clones heterogeneity, based on their morphology and localization.

To perform the clonal analysis, we selected cortical regions where the StarTrack labeled cells were located close to the EAE affected areas identified by the accumulation of perivascular inflammatory infiltrates and the presence of enlarge perivascular compartments (**Figure 2A**). In electroporated sham animals, the protoplasmic astrocytes located in the gray matter, displayed more primary processes and a higher degree of branching (**Figures 2B,D,J**) compared to fibrous astrocytes with small elongated cell bodies and long processes located in the white matter (**Figure 2E**). Further, vascular clones of astrocytes were also found surrounding blood vessels (**Figure 2F**) in the electroporated sham mice. In EAE–electroporated mice, astrocytes closer to the infiltrate evidenced the typical hypertrophic morphology (**Figures 2A,G,H,K**), characterized by an increment in the number of their cellular processes (**Figure 2L**) and by an enlargement of the cell soma (**Figure 2M**). Remarkably, EAE-reactive astrocytes (**Figures 2A,G,H**) appeared morphologically different than those we previously reported (Martín-López et al., 2013) after fine-needle cortical injury model (**Figure 2I**). In that model, reactive astrocytes displayed an asymmetric hypertrophy with thinner and longer processes pointing out to the injury core (**Figure 2I**), even though both models exhibited enlarged somas than in non-injured brains.

In all the cases, reactive astrocytes were identified by their characteristic reactive morphology (**Figure 3**). Reactive sibling astrocytes were analyzed in serial sections to decipher their morphology and precise clonal cell dispersion, independently of the lesion size. Astroglial clones located close to or within the subcortical white matter were exclusively composed of reactive fibrous astrocytes (**Figures 3A,B**), while those clones within the gray matter lesions were entirely composed of protoplasmic sibling astrocytes (**Figures 3A,E,F**). Astroglial clones related to subpial lesions were composed of a mix of both fibrous and protoplasmic astrocytes (**Figure 3D**). In addition, astrocytes with the same color code of fluorophores composition were assigned as sibling-cells defining the astrocyte clones (**Figures 3E,F**). The vast majority of the astroglial clones were composed by reactive astrocytes (**Figure 3G**). Further, the total number of hypertrophic and non-hypertrophic sibling astrocytes was quantified in relation to the distance from the inflammatory infiltrate (**Figure 3H**), showing a higher number of reactive astrocytes within 100 μm away from the inflammatory infiltrate.

Clonal Analysis of Cortical Astrocytes in EAE-Induced Mice

To decipher how clonally-related cortical astrocytes respond in StarTrack electroporated EAE-induced mice, we performed a clonal analysis of cortical astrocytes surrounding the perivascular inflammatory areas. Astrocytes that were clonally-related displayed the same color-codes (**Figures 3E,F**, **4A–G**).

Most clonally-related cortical astrocytes remained close to an inflammatory area and displayed hypertrophic morphologies, with enlarged cytoplasm and thick cellular processes and soma (**Figures 4A–G**). We analyzed individual clones in the EAE

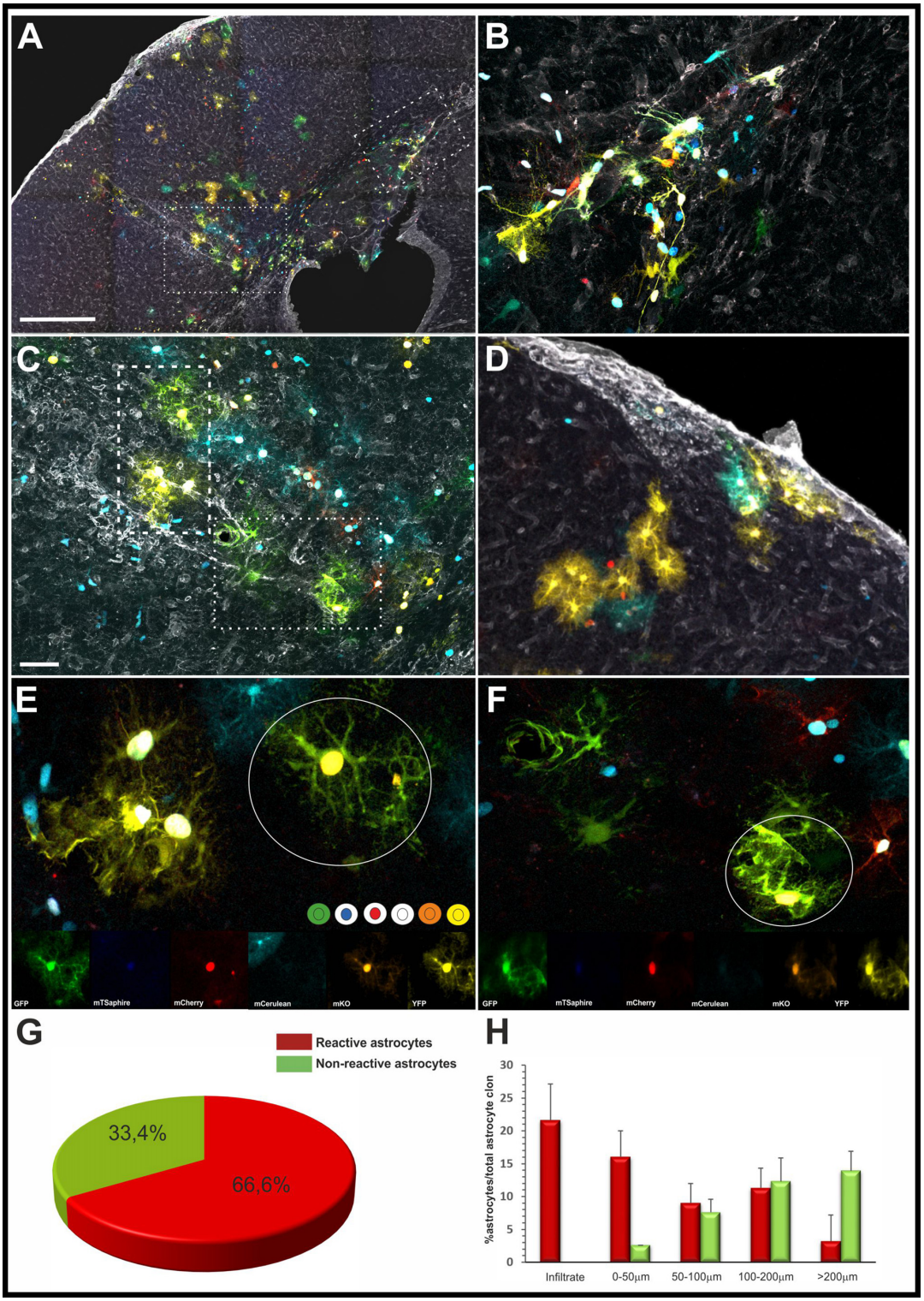

FIGURE 3 | Astrocyte exhibit different reactive morphologies after EAE. **(A)** Low magnification of the clonal labeling in an EAE-StarTrack electroporated mouse. Perivascular inflammation in the subcortical white matter (**B**, dashed square), subcortical/intracortical areas (**C**, dotted square) and pia matter **(D)**. **(B)** Higher magnification of the boxed area in **(A)** shows hypertrophic fibrous astrocytes within the subcortical white matter. **(C)** Higher magnification of the dotted area in **(A)** shows protoplasmic astrocytes radially orientated embracing an enlarge perivascular compartment occupying several cortical layers. **(D)** A subpial infiltrate bordered by both pial and protoplasmic astrocytes clones. **(E,F)** Higher magnification of sibling reactive astrocytes with hypertrophic morphology showing thicker processes

(*Continued*)

FIGURE 3 | Continued
and soma. Qualitative clonal cell analysis based on the color combination and fluorophore cell location (nuclear or cytoplasmic) of clonally related astrocytes in the white circles. **(G)** The graph shows the quantification of the percentage of reactive and non-reactive astrocytes in Star-Track labeled clones. **(H)** Histogram showing the percentage of reactive and reactive astrocyte within the clones depending on their location with the lesion. Scale bar: **(A)** 400 μm; **(B,C)** 150 μm; **(D)** 80 μm; **(E,F)** 25 μm.

electroporated brains showing non-reactive astrocytes were mostly located far apart of the limit of the infiltrate (**Figure 4H**), while hypertrophic astrocytes were mainly located in the core of the infiltrate or really close to it (**Figure 4H**). The cumulative distribution of both populations, reactive and non-reactive astrocytes, is different according to the non-parametric Kolmogorov–Smirnov test ($D = 0{,}528$, $p < 0.0001$). In addition, it is worth to mention that 50% were composed exclusively by hypertrophic astrocytes, 20% by non-reactive astrocytes and 30% correspond to mixed clones (**Figure 4H**, reactive and non-reactive astrocytes in the same clone). Further, the presence of dividing cells was critically related to the lesion, we performed immunohistochemistry for the proliferation marker Ki67. However, not all StarTrack-labeled astrocyte in a specific area were positive for Ki67, just a low proportion of cells surrounding the lesions (33.4 ± 4.5%) was positive for this marker.

Additionally, astrocyte clones with reactive morphologies (**Figure 5**) were located in areas without the presence of clearly identified inflammation or enlarged blood vessels (**Figures 5A,C,E**). Hypertrophied sibling cortical astrocytes (**Figure 5C**) were disposed in columnar disposition with different morphologies across the layers (**Figure 5C**). Within the subcortical white matter, clonally-related astrocytes displayed hypertrophied morphologies with enlarged soma and thicker processes (**Figure 5E**), On the contrary, in sham-StarTrack electroporated animals (**Figures 5B,D,F**) none hypertrophied astrocytes were found across the brain, neither in gray matter (**Figure 5D**) nor in subcortical white matter (**Figure 5F**). These data indicate that the inflammatory environment triggered in the EAE model also affects morphology and behavior of astrocytes in the cerebral cortex.

Since different type of astrocytes develop from specific progenitor cells, we expected that sibling astrocytes responded similarly to the brain damage. Nevertheless, these results revealed different clonal responses. Although the vast majority of the reactive clones acquired hypertrophic morphologies in relation to distance to the injury, others did not modify their morphologies, even at the same distance. We also provide evidence that not all the cells of a clone respond equally, but rather other factors, as distance or localization, are probably involved in their response.

DISCUSSION

Here, we report a heterogeneous behavior of sibling astrocytes in response to cortical damage induced by a demyelinating EAE-induced mice model. Whereas some cortical clones displayed all sibling astrocytes with reactive morphology, other clones, located at equivalent distances, did not display altered cell morphologies. In other cases only those astrocytes of a clone, closer to the core of the perivascular infiltration, showed hypertrophic cytoplasm. Additionally, most astroglial clones acquired hypertrophic morphologies in relation to the injury distance, suggesting a role of the environment in the response of the adjacent astrocytes. Thus, astroglial clones in the EAE model exhibited a varied response with some becoming hypertrophic, while other other clones located similar distances from the lesion were unresponsive as we previously described after a mechanical brain injury (Martín-López et al., 2013).

Astrocytes are the most abundant cell-type of the human brain playing a variety of roles in brain homeostasis and synaptic maturation (Sofroniew and Vinters, 2010; Pekny et al., 2016). After brain damage astrocytes suffer dramatic pathological changes, such as reactive gliosis and glial scar formation, including abnormal hypertrophy and massive proliferation of astrocytes. However, the molecular identity and cues that dictate the structural changes in reactive astrocytes remain unclear (Sofroniew and Vinters, 2010; Liddelow and Barres, 2017). Further, astrocytes must be considered another potential therapeutic target for MS, although few studies focused on the cortical gray matter (Ponath et al., 2017, 2018). However, no study to date addressed the clonal astrocytic response to these lesions.

In this study using MOG-induced EAE model, we showed that astrocytes displayed a reactive morphology displaying thicker cellular processes and soma (Brosnan and Raine, 2013; Correale and Farez, 2015; Eilam et al., 2018). Conversely, in this model hypertrophic astrocytes did not show the asymmetric morphology with cellular processes pointing the core of the lesion, as described after a mechanical brain injury (Martín-López et al., 2013). Likewise, in EAE-model the StarTrack labeled reactive astrocytes were located surrounding enlarged blood vessels and perivascular inflammatory cuffs, while other reactive astrocytes were located away from the perivascular inflammatory infiltrates. In fact, both types of injuries activate a cascade of cellular and molecular events aimed to restore the CNS homeostasis, minimizing the brain damage. While after traumatic injuries astrocytes are involved in the generation of the glial scar (Fawcett and Asher, 1999), in the EAE-induced model, astrocytes actively participate in both lesion development and repair (Brosnan and Raine, 2013; Correale and Farez, 2015; Ponath et al., 2018). In this regard, although reactive astrocytes share common properties, they also display unique cellular and molecular features that are specific to different neuropathologies (Pekny et al., 2016; Ponath et al., 2018). This large astrocyte heterogeneity, in response to injury, validates the importance to design selective strategies to promote CNS repair.

With the StarTrack methodology, which allows to target single embryonic progenitors, we provided the first *in vivo* evidence of the clonal response of astrocytes in a

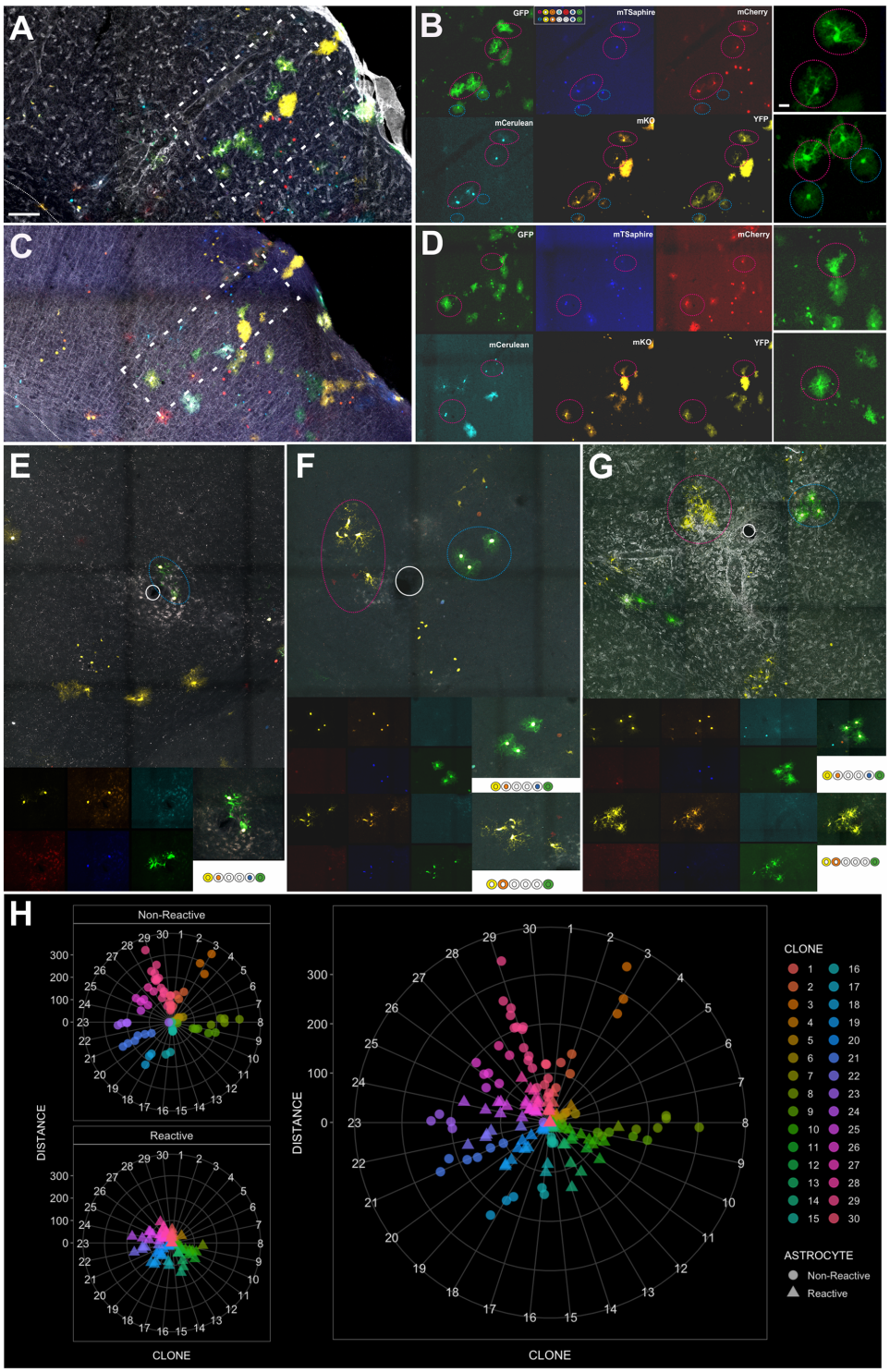

FIGURE 4 | Clonally-related astrocytes targeted by IUE with StarTrack respond to EAE lesions. **(A,C)** Low magnification images of an EAE-electroporated mice. A protoplasmic astrocyte clone (white rectangle) surrounding a perivascular cuff in serial sections. **(B,D)** Qualitative cell analysis based on the color combination and fluorophore cell location (nuclear or cytoplasmic). Different clonal color-codes detailed by the expression of each fluorescent reporters: YFP, mKO, mCerulean, mCherry, mT-Sapphire and GFP. Sibling cells (pink circle), displaying a hypertrophic morphology and located close to the perivascular space. Sibling astrocytes located further (blue circle) displayed the typical protoplasmic morphology. **(E–G)** Clonally-related astrocytes with different morphologies depending on their location from the inflammatory infiltrate and their color-code. Scale bar: **(A,C)** 200 μm; **(B,D)**, inset **(E–G)** 20 μm and **(E–G)** 100 μm. **(H)** Radar plots showing the quantification of reactive and non-reactive astrocytes within 30 individual clones at different distances from the lesion.

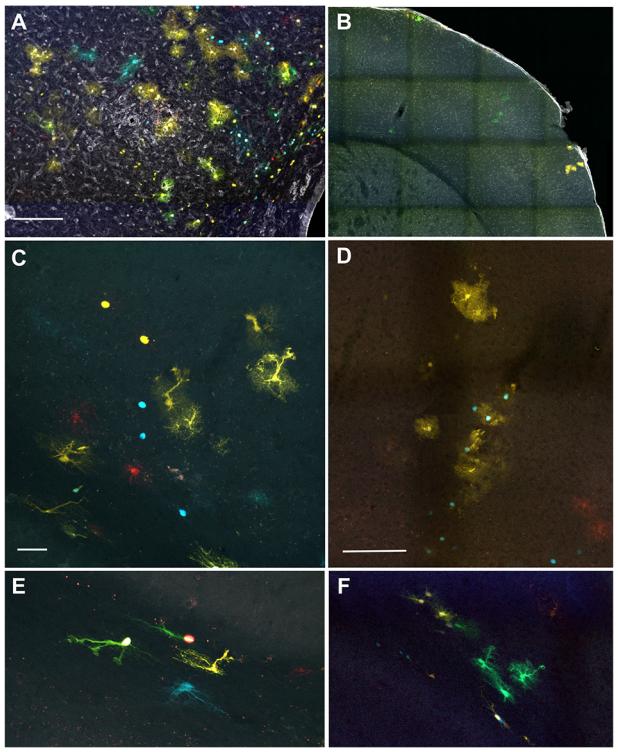

FIGURE 5 | Hypertrophic clonally-related astrocytes are present out from the parenchymal inflammation infiltrates. **(A)** IUE-EAE StarTrack electroporated brain section stained with TL. **(B)** IUE-StarTrack sham electroporated brain section stained with TL. **(C)** Representative clonally-related cortical astrocytes with a reactive morphology arranged in a columnar manner in an IUE-EAE StarTrack electroporated mouse brain. **(D)** Representative clonally-related cortical astrocytes with the typical protoplasmic morphology in a sham StarTrack electroporated mouse. **(E)** Representative clonally-related fibrous astrocytes within a subcortical white matter in an IUE-EAE StarTrack electroporated mouse brain. **(F)** Representative clonally-related fibrous astrocytes in a sham StarTrack electroporated mouse. Scale bar: **(A)** 100 μm; **(B)** 200 μm; **(C,E)** 50 μm and **(D,F)** 100 μm.

demyelinating scenario and their capacity to respond to an injury. Clonally-related astrocytes (sibling astrocytes) responded in a heterogeneous manner to the perivascular inflammatory cortical environment of EAE induced animals. Whereas in some clones all sibling cells exhibited the typical hypertrophic morphology of reactive astrocytes, other clones, located at similar distances, did not exhibit altered cell morphologies. In addition, several astrocyte clones with hypertrophic morphologies were located away from the perivascular/parenchymal inflammatory infiltrates. This suggest that EAE induction could generate a widespread neural inflammation that affects all the cortical astrocytes. These results resembled very closely those previously described in a traumatic brain injury model (Martín-López et al., 2013).

Further, astrocytes contribute to the innate immune response in MS, playing a critical role in both oligodendrocyte damage and axonal degeneration (Sofroniew and Vinters, 2010; Correale and Farez, 2015). In fact, reactive astrocytes are categorized as types A1 or A2 (in analogy to the "M1" and "M2" phenotype categories for macrophages) according to their transcriptome profiles and their role in inflammation/immune response (Liddelow and Barres, 2017). A1-type astrocytes, induced by inflammation, are abundant in MS and other neurodegenerative diseases, including Alzheimer/Parkinson diseases, whereas A2-type astrocytes, induced by ischemia, express neurotrophic factors (Liddelow and Barres, 2017; Liddelow et al., 2017). It is likely that, distinct astrocytic phenotypes concur during different phases of a pathological process: first, reactive astrocytes produce pro-inflammatory cytokines combined with hypertrophy and proliferation; and, in a second phase, they promote anti-inflammatory functions and neurodegeneration (Colombo and Farina, 2016). Actually, in MS lesions the reactive astrocytes drive inflammatory and neurotoxic responses, reduce inflammation and promote neuroprotection and lesion repair (Correale and Farez, 2015; Ponath et al., 2018). Furthermore, astrocytes contributed to the development of MS lesions and by extension to the progression of the disease, which highlights their critical role as early and active players in lesion pathology (Ponath et al., 2018). These data are in agreement with our results, even we just analyzed the astrocyte response in the peak score of the acute EAE phase, when probably just a subpopulation of astrocyte clones is reactive. Further clonal analyses at other stages of the disease (onset, remission) would reveal whether different lineages or cell clones are activated depending on the progression of the disease.

Our results also show that in some cases there is a distinct response of sibling cells to the inflammation. This could be related to the distance to the perivascular infiltrate or perivascular compartment, but it also could be due to the gradual expression of molecules within the lesion. There are many molecules and genes that are known to be expressed in MS lesions that affect the remyelination and also the progression of the lesion (Clemente et al., 2011; Piaton et al., 2011; Zeis et al., 2018). Several diffusible molecules could be implicated in this process, including basic fibroblast growth factor (bFGF), anosmin 1 or class 3 semaphorins (Clemente et al., 2011; Piaton et al., 2011). It is possible that, these molecules could affect those astrocytes located close to the lesion, in addition to other molecular cues secreted by both the inflammatory infiltrates and astrocytes (Legroux and Arbour, 2016).

The variability in the clonal response to brain damage clearly indicates that the heterogeneity of reactive astrocytes could be probably determined early in CNS development, but also by environmental cues present in the injured brain. Nevertheless, our findings showed a high heterogeneity in the astroglial response to inflammation that could be influenced by the signals received from the environment, their location respect to the affected brain area and factors during development. In fact, astroglial clonal response provides *in vivo* evidence of how brain development leaves a fingerprint of heterogeneity in astrocyte roles during the course of MS lesions. Further, these responses to brain injury could contribute to the inflammatory response, promoting lesion repair. Additionally, the presence of intrinsic factors, determined during the embryonic development and related to the cell lineage, could affect the astrocyte response. All these evidences should be taken into account for the further design of strategies and treatments for neurological diseases.

AUTHOR CONTRIBUTIONS

AB, LL-M and CM conceived and designed the experiments. AB performed electroporations and analyzed clonal data. FP-C and CM performed the EAE and tissue processing. AB and LL-M wrote the article, all authors revised and approved the manuscript.

FUNDING

This work was supported by Ministerio de Economía y Competitividad (MINECO; BFU2016-75207-R and SAF2016-75292-R), CIBERNED and Basque Government. We also aknowledge a partial support of the publication fee by the CSIC Open Access Publication Support initiative through its Unit of Information Resources for Research (URICI).

ACKNOWLEDGMENTS

We are grateful to UPV-EHU animal facilities and Image and microscope facilities from Instituto Cajal-CSIC and Achucarro Basque Center for their excellent technical assistance. We are also grateful to Lluis Fortes Marco for his help with the radial plots representations and Sonsoles Barriola for her technical help.

REFERENCES

Andrizen, W. L. (1893). The neuroglia elements in the human brain. *Br. Med. J.* 2, 227–230. doi: 10.1136/bmj.2.1700.227

Bribián, A., Figueres-Oñate, M., Martín-López, E., and López-Mascaraque, L. (2016). Decoding astrocyte heterogeneity: new tools for clonal analysis. *Neuroscience* 323, 10–19. doi: 10.1016/j.neuroscience.2015.04.036

Brosnan, C. F., and Raine, C. S. (2013). The astrocyte in multiple sclerosis revisited. *Glia* 61, 453–465. doi: 10.1002/glia.22443

Clemente, D., Ortega, M. C., Arenzana, F. J., and de Castro, F. (2011). FGF-2 and anosmin-1 are selectively expressed in different types of multiple sclerosis lesions. *J. Neurosci.* 31, 14899–14909. doi: 10.1523/JNEUROSCI.1158-11.2011

Colombo, E., and Farina, C. (2016). Astrocytes: key regulators of neuroinflammation. *Trends Immunol.* 37, 608–620. doi: 10.1016/j.it.2016.06.006

Correale, J. (2014). The role of microglial activation in disease progression. *Mult. Scler.* 20, 1288–1295. doi: 10.1177/1352458514533230

Correale, J., and Farez, M. F. (2015). The role of astrocytes in multiple sclerosis progression. *Front. Neurol.* 6:180. doi: 10.3389/fneur.2015.00180

Eddleston, M., and Mucke, L. (1993). Molecular profile of reactive astrocytes—implications for their role in neurologic disease. *Neuroscience* 54, 15–36. doi: 10.1016/0306-4522(93)90380-x

Eilam, R., Segal, M., Malach, R., Sela, M., Arnon, R., and Aharoni, R. (2018). Astrocyte disruption of neurovascular communication is linked to cortical damage in an animal model of multiple sclerosis. *Glia* 66, 1098–1117. doi: 10.1002/glia.23304

Fawcett, J. W., and Asher, R. A. (1999). The glial scar and central nervous system repair. *Brain Res. Bull.* 49, 377–391. doi: 10.1016/s0361-9230(99)00072-6

Figueres-Oñate, M., García-Marqués, J., and López-Mascaraque, L. (2016). UbC-StarTrack, a clonal method to target the entire progeny of individual progenitors. *Sci. Rep.* 6:33896. doi: 10.1038/srep33896

García-Marqués, J., De Carlos, J. A., Greer, C. A., and López-Mascaraque, L. (2010). Different astroglia permissivity controls the migration of olfactory bulb interneuron precursors. *Glia* 58, 218–230. doi: 10.1002/glia.20918

García-Marqués, J., and López-Mascaraque, L. (2013). Clonal identity determines astrocyte cortical heterogeneity. *Cereb. Cortex* 23, 1463–1472. doi: 10.1093/cercor/bhs134

García-Marqués, J., and López-Mascaraque, L. (2017). Clonal mapping of astrocytes in the olfactory bulb and rostral migratory stream. *Cereb. Cortex* 27, 2195–2209. doi: 10.1093/cercor/bhw071

Girolamo, F., Ferrara, G., Strippoli, M., Rizzi, M., Errede, M., Trojano, M., et al. (2011). Cerebral cortex demyelination and oligodendrocyte precursor response to experimental autoimmune encephalomyelitis. *Neurobiol. Dis.* 43, 678–689. doi: 10.1016/j.nbd.2011.05.021

Hasselmann, J. P. C., Karim, H., Khalaj, A. J., Ghosh, S., and Tiwari-Woodruff, S. K. (2017). Consistent induction of chronic experimental autoimmune encephalomyelitis in C57BL/6 mice for the longitudinal study of pathology and repair. *J. Neurosci. Methods* 284, 71–84. doi: 10.1016/j.jneumeth.2017.04.003

Horii-Hayashi, N., Tatsumi, K., Matsusue, Y., Okuda, H., Okuda, A., Hayashi, M., et al. (2010). Chondroitin sulfate demarcates astrocytic territories in the mammalian cerebral cortex. *Neurosci. Lett.* 483, 67–72. doi: 10.1016/j.neulet.2010.07.064

Lassmann, H. (2012). Cortical lesions in multiple sclerosis: inflammation versus neurodegeneration. *Brain* 135, 2904–2905. doi: 10.1093/brain/aws260

Legroux, L., and Arbour, N. (2016). Multiple sclerosis and T lymphocytes: an entangled story T lymphocytes: key cells of the adaptive immune responses. *J. Neuroimmune Pharmacol.* 10, 528–546. doi: 10.1007/s11481-015-9614-0

Liddelow, S. A., and Barres, B. A. (2017). Reactive astrocytes: production, function, and therapeutic potential. *Immunity* 46, 957–967. doi: 10.1016/j.immuni.2017.06.006

Liddelow, S. A., Guttenplan, K. A., Clarke, L. E., Bennett, F. C., Bohlen, C. J., Schirmer, L., et al. (2017). Neurotoxic reactinve astroctes are induced by activated microglia. *Nature* 541, 481–487. doi: 10.1038/nature21029

Mangiardi, M., Crawford, D. K., Xia, X., Du, S., Simon-Freeman, R., Voskuhl, R. R., et al. (2011). An animal model of cortical and callosal pathology in multiple sclerosis. *Brain Pathol.* 21, 263–278. doi: 10.1111/j.1750-3639.2010.00444.x

Martín-López, E., García-Marques, J., Núñez-Llaves, R., and López-Mascaraque, L. (2013). Clonal astrocytic response to cortical injury. *PLoS One* 8:e74039. doi: 10.1371/journal.pone.0074039

Mathewson, A. J., and Berry, M. (1985). Observations on the astrocyte response to a cerebral stab wound in adult rats. *Brain Res.* 327, 61–69. doi: 10.1016/0006-8993(85)91499-4

Matute, C., Torre, I., Pérez-Cerdá, F., Pérez-Samartín, A., Alberdi, E., Etxebarria, E., et al. (2007). $P2X_7$ receptor blockade prevents ATP excitotoxicity in oligodendrocytes and ameliorates experimental autoimmune encephalomyelitis. *J. Neurosci.* 27, 9525–9533. doi: 10.1523/JNEUROSCI.0579-07.2007

Matyash, V., and Kettenmann, H. (2010). Heterogeneity in astrocyte morphology and physiology. *Brain Res. Rev.* 63, 2–10. doi: 10.1016/j.brainresrev.2009.12.001

Pampliega, O., Domercq, M., Soria, F. N., Villoslada, P., Rodríguez-antigüedad, A., and Matute, C. (2011). Increased expression of cystine/glutamate antiporter in multiple sclerosis. *J. Neuroinflammation* 8:63. doi: 10.1186/1742-2094-8-63

Pekny, M., Pekna, M., Messing, A., Steinhäuser, C., Lee, J. M., Parpura, V., et al. (2016). Astrocytes: a central element in neurological diseases. *Acta Neuropathol.* 131, 323–345. doi: 10.1007/s00401-015-1513-1

Piaton, G., Aigrot, M. S., Williams, A., Moyon, S., Tepavcevic, V., Moutkine, I., et al. (2011). Class 3 semaphorins influence oligodendrocyte precursor recruitment and remyelination in adult central nervous system. *Brain* 134, 1156–1167. doi: 10.1093/brain/awr022

Ponath, G., Park, C., and Pitt, D. (2018). The role of astrocytes in multiple sclerosis. *Front. Immunol.* 9:217. doi: 10.3389/fimmu.2018.00217

Ponath, G., Ramanan, S., Mubarak, M., Housley, W., Lee, S., Sahinkaya, F. R., et al. (2017). Myelin phagocytosis by astrocytes after myelin damage promotes lesion pathology. *Brain* 140, 399–413. doi: 10.1093/brain/aww298

Prins, M., Schul, E., Geurts, J., van der Valk, P., Drukarch, B., and van Dam, A. M. (2015). Pathological differences between white and grey matter multiple sclerosis lesions. *Ann. N Y Acad. Sci.* 1351, 99–113. doi: 10.1111/nyas.12841

Procaccini, C., De Rosa, V., Pucino, V., Formisano, L., and Matarese, G. (2015). Animal models of multiple sclerosis. *Eur. J. Pharmacol.* 759, 182–191. doi: 10.1016/j.ejphar.2015.03.042

R Core Team. (2018). *R: A Language and Environment for Statistical Computing. Vienna: R Foundation for Statistical Computing*. Available online at: www.R-project.org

Ridet, J. L., Malhotra, S. K., Privat, A., and Gage, F. H. (1997). Reactive astrocytes: cellular and molecular cues to biological function. *Trends Neurosci.* 20, 570–577. doi: 10.1016/s0166-2236(97)01139-9

Saab, A. S., Tzvetavona, I. D., Trevisiol, A., Baltan, S., Dibaj, P., Kusch, K., et al. (2016). Oligodendroglial NMDA receptors regulate glucose import and axonal energy metabolism. *Neuron* 91, 119–132. doi: 10.1016/j.neuron.2016.05.016

Sofroniew, M. V. (2009). Molecular dissection of reactive astrogliosis and glial scar formation. *Trends Neurosci.* 32, 638–647. doi: 10.1016/j.tins.2009.08.002

Sofroniew, M. V., and Vinters, H. V. (2010). Astrocytes: biology and pathology. *Acta Neuropathol.* 119, 7–35. doi: 10.1007/s00401-009-0619-8

Stadelmann, C., Albert, M., Wegner, C., and Brück, W. (2008). Cortical pathology in multiple sclerosis. *Curr. Opin. Neurol.* 21, 229–234. doi: 10.1097/01.wco.0000318863.65635.9a

Tabata, H. (2015). Diverse subtypes of astrocytes and their development during corticogenesis. *Front Neurosci.* 9:114. doi: 10.3389/fnins.2015.00114

Teuscher, C., Noubade, R., Spach, K., Mcelvany, B., Bunn, J. Y., Fillmore, P. D., et al. (2006). Evidence that the Y chromosome influences autoimmune disease in male and female mice. *Proc. Natl. Acad. Sci. U S A* 103, 8024–8029. doi: 10.1073/pnas.0600536103

van Munster, C. E. P., Jonkman, L. E., Weinstein, H. C., Uitdehaag, B. M., and Geurts, J. J. (2015). Gray matter damage in multiple sclerosis: impact on clinical symptoms. *Neuroscience* 303, 446–461. doi: 10.1016/j.neuroscience.2015.07.006

Voskuhl, R. R., and Palaszynski, K. (2001). Neuroscientist sex hormones in experimental autoimmune encephalomyelitis: implications for multiple sclerosis. *Neuroscientist* 7, 258–270. doi: 10.1177/107385840100700310

Zabala, A., Vazquez-villoldo, N., Rissiek, B., Gejo, J., Martin, A., Palomino, A., et al. (2018). P2X4 receptor controls microglia activation and favors remyelination in autoimmune encephalitis. *EMBO Mol. Med.* 10:e8743. doi: 10.15252/emmm.201708743

Zeis, T., Howell, O. W., Reynolds, R., and Schaeren-Wiemers, N. (2018). Molecular pathology of Multiple Sclerosis lesions reveals a heterogeneous expression pattern of genes involved in oligodendrogliogenesis. *Exp. Neurol.* 305, 76–88. doi: 10.1016/j.expneurol.2018.03.012

Conflict of Interest Statement: The authors declare that the research was conducted in the absence of any commercial or financial relationships that could be construed as a potential conflict of interest.

frontiers in Cellular Neuroscience

ORIGINAL RESEARCH
published: 12 November 2018
doi: 10.3389/fncel.2018.00410

Evidence of Müller Glia Conversion Into Retina Ganglion Cells Using Neurogenin2

Roberta Pereira de Melo Guimarães[1,2,3†], Bruna Soares Landeira[1†], Diego Marques Coelho[1,4], Daiane Cristina Ferreira Golbert[1], Mariana S. Silveira[2], Rafael Linden[2], Ricardo A. de Melo Reis[3] and Marcos R. Costa[1]*

[1] Brain Institute, Federal University of Rio Grande do Norte, Natal, Brazil, [2] Lab Neurogenesis, Institute of Biophysics Carlos Chagas Filho, Federal University of Rio de Janeiro, Rio de Janeiro, Brazil, [3] Lab Neurochemistry, Institute of Biophysics Carlos Chagas Filho, Federal University of Rio de Janeiro, Rio de Janeiro, Brazil, [4] Bioinformatics Multidisciplinary Environment, IMD, Federal University of Rio Grande do Norte, Rio de Janeiro, Brazil

Degenerative retinopathies are the leading causes of irreversible visual impairment in the elderly, affecting hundreds of millions of patients. Müller glia cells (MGC), the main type of glia found in the vertebrate retina, can resume proliferation in the rodent adult injured retina but contribute weakly to tissue repair when compared to zebrafish retina. However, postnatal and adult mouse MGC can be genetically reprogrammed through the expression of the transcription factor (TF) Achaete-scute homolog 1 (ASCL1) into induced neurons (iNs), displaying key hallmarks of photoreceptors, bipolar and amacrine cells, which may contribute to regenerate the damaged retina. Here, we show that the TF neurogenin 2 (NEUROG2) is also sufficient to lineage-reprogram postnatal mouse MGC into iNs. The efficiency of MGC lineage conversion by NEUROG2 is similar to that observed after expression of ASCL1 and both TFs induce the generation of functionally active iNs. Treatment of MGC cultures with EGF and FGF2 prior to Neurog2 or Ascl1 expression enhances reprogramming efficiencies, what can be at least partially explained by an increase in the frequency of MGCs expressing sex determining region Y (SRY)-box 2 (SOX2). Transduction of either Neurog2 or Ascl1 led to the upregulation of key retina neuronal genes in MGC-derived iNs, but only NEUROG2 induced a consistent increase in the expression of putative retinal ganglion cell (RGC) genes. Moreover, *in vivo* electroporation of Neurog2 in late progenitors from the neonatal rat retina, which are transcriptionally similar to MGCs, also induced a shift in the generation of retinal cell subtypes, favoring neuronal differentiation at the expense of MGCs and resuming the generation of RGCs. Altogether, our data indicate that NEUROG2 induces lineage conversion of postnatal rodent MGCs into RGC-like iNs *in vitro* and resumes the generation of this neuronal type from late progenitors of the retina *in vivo*.

Keywords: retina, müller glia cells, induced neurons, lineage-reprogramming, neurogenin2, Ascl1, retina ganglion cells

OPEN ACCESS

Edited by:
Sandra Henriques Vaz, Instituto de Medicina Molecular (IMM), Portugal

Reviewed by:
Antje Grosche, Ludwig-Maximilians-Universität München, Germany
Xiao-Feng Zhao, University of Michigan, United States

***Correspondence:**
Marcos R. Costa
mrcosta@neuro.ufrn.br

† These authors have contributed equally to this work

Received: *24 August 2018*
Accepted: *22 October 2018*
Published: *12 November 2018*

Citation:
Guimarães RPdM, Landeira BS, Marques-Coelho D, Golbert DCF, Silveira MS, Linden R, de Melo Reis RA and Costa MR (2018) Evidence of Müller Glia Conversion Into Retina Ganglion Cells Using Neurogenin2. Front. Cell. Neurosci. 12:410. doi: 10.3389/fncel.2018.00410

INTRODUCTION

The retina is a unique tissue with highly organized architecture, known to be one of the most energetically demanding systems in the nervous system (Wong-Riley, 2010). Due to oxidative stress, trauma, or genetic mutations, gradual and irreversible cell death affects specific neuronal types in the retina (Athanasiou et al., 2013). For instance, retinal ganglion cells (RGCs) and their axons degenerate in glaucoma, a neurodegenerative disease associated with increased intraocular pressure, eventually leading to blindness (Kimura et al., 2017). In the last 5 years almost 65 million people worldwide were diagnosed with glaucoma (Gill et al., 2016; Liang et al., 2017), which is the leading cause of visual impairment in developed countries (WHO). Still, despite the social and economic burden of such disease, therapeutic approaches are limited. Recent progress in cell-based therapy may, nonetheless, provide novel means to restore vision in glaucoma patients (Abu-Hassan et al., 2015; Chamling et al., 2016).

Cell lineage-reprogramming techniques, which allow the direct conversion of a non-neuronal cell into neurons, offer a powerful strategy to regenerate neuronal cells in the injured retina. In fact, expression of the bHLH neurogenic transcription factor (TF) Achaete-scute homolog 1 (ASCL1) *in vitro* induced the reprogramming of mouse Müller glia cells (MGC) into bipolar cells and, to a lesser extent, amacrine cells (Pollak et al., 2013). Following NMDA-mediated injury in postnatal mouse retina, ASCL1 expression reprogrammed MGCs into neurons expressing markers of bipolar cells, amacrine cells and photoreceptors (Ueki et al., 2015). Notably, when combined with the inhibitor of histone deacetylases trichostatin A, expression of ASCL1 elicited the conversion of some MGC into bipolar (∼18%) and amacrine (∼3%) cells in the injured adult retina (Jorstad et al., 2017). These findings demonstrate that regenerative effects of transgenic expression of ASCL1 in the adult mouse Müller glia are more limited as compared to the regenerative response observed in non-mammalian vertebrates (Wilken and Reh, 2016). Moreover, ASCL1 expression is not sufficient to reprogram MGCs into RGCs either *in vitro* or *in vivo* (Pollak et al., 2013; Ueki et al., 2015; Jorstad et al., 2017).

During development, expression of ASCL1 defines a subset of retinal progenitor cells (RPCs) that generate all neuronal types in the retina, except RGCs (Brzezinski et al., 2011). In contrast, expression of the bHLH TF Neurogenin 2 (NEUROG2) defines a separate set of RPCs, co-expressing the POU Class 4 Homeobox 1 and 2 (Pou4f1/Brn3a and Pou4f2/Brn3b) and contributing to the generation of RGCs (Hufnagel et al., 2010; Brzezinski et al., 2011). Interestingly, knocking down the expression of Pou4f2/Brn3b in MGCs cultured in conditions to induce stem cell-like properties hampers the differentiation into RGCs (Singhal et al., 2012; Song et al., 2013; Wu et al., 2016).

Here we report that forced expression of NEUROG2 is sufficient to convert postnatal rodent MGC into a neurogenic state. Either ASCL1 or NEUROG2 elicited induced neurons (iNs) that express genes of bipolar, horizontal and amacrine cells, as well as photoreceptors. However, only forced expression of NEUROG2 led to the generation of iNs expressing hallmarks of RGCs. We also show that treatment with epidermal growth factor (EGF) and basic fibroblast growth factor (FGF-2) during the expansion of MGCs affects lineage-conversion efficiencies and iN-fate specification. Finally, we provide evidence for an instructive role of NEUROG2 in the specification of RGC fate in late retinal progenitors that are not competent to generate this cell type *in vivo* (Young, 1985; Turner et al., 1990; Rapaport et al., 2004; He et al., 2012). Collectively, our results indicate that NEUROG2 can regulate the specification program of both late retinal progenitors and MGC to generate RGCs, and, therefore, might be an interesting candidate for gene-based therapies to treat retinal degenerations.

MATERIALS AND METHODS

Animals

C57BL/6 mice were obtained from the Biotério Setorial do Instituto do Cérebro (BISIC). All experiments were approved by and carried out in accordance with the guidelines of the Institutional Animal Care and Use Committee of the Federal University of Rio Grande do Norte (license number #048/2014).

Müller Glial Cell (MGC) Culture

MGCs were purified from postnatal day (P)7-9 mice according to previously described protocols (de Melo Reis et al., 2008). Briefly, retinas were dissected out and chemically dissociated with TrypLE (Life Technologies) for 10 min at 37°C. Isolated cells were counted using a Neubeuer chamber and plated onto T75 culture flasks with DMEM F12 (Gibco) plus 10% fetal bovine serum (Gibco), 3.5 mM glucose (Sigma), 4.5g/L GlutaMax (Gibco), 100 U/mL penicillin/streptomycin (Gibco), either with or without 10 ng/mL of epidermal growth factor (EGF, Gibco) and 10 ng/mL of fibroblast growth factor 2 (FGF2, Gibco). Half of the medium was changed once a week during the period of MGCs expansion.

Plasmids

Plasmids contain the internal chicken β-actin promoter fused with a cytomegalovirus enhancer (pCAG), the coding sequence for either Ascl1 or Neurog2, an internal ribosomal entry site (I) and coding sequences for either DsRed or GFP (pCAG-Ascl1-I-DsRed, pCAG-Neurog2-I-DsRed and pCAG-Neurog2-I-GFP). Control plasmids encode only DsRed or GFP (pCAG-I-DsRed or pCAG-I-GFP).

Plasmid stocks were prepared in *Escherichia coli* and purified using an endotoxin-free Maxiprep plasmid kit (Invitrogen). DNA concentration was adjusted to 1 μg/μL in endotoxin free TE buffer, and plasmids were stored at −20°C.

Nucleofection

After confluence, MGCs were chemically detached from T75 culture flasks with TrypLE enzyme at 37°C, and ∼3 × 10^5 cells were mixed with P3 solution (Lonza) and 1 μg of plasmids encoding for either NEUROGENIN2 (pCAG-Neurog2-IRES-DsRed) or ASCL1 (pCAG-Ascl1-IRES-DsRed) or only reporter protein DSRED (pCAG-IRES-DsRed). These solutions were placed in a special cuvette and electroporated using Nucleofector

4D (Lonza) with the P3 primary cell program. Next, 8×10^4 cells were plated onto glass-coverslips (100013-Knittel) previously coated with laminin (L2020–SIGMA) and Poly-D lysine (Sigma) containing pre-warmed DMEM F12, 10% fetal bovine serum, 3.5 mM glucose, 4.5g/L GlutaMax and 100U/mL penicillin/streptomycin. After 24h, medium was replaced with differentiation medium containing DMEM F12, 3.5 mM glucose, 4.5 g/l GlutaMax, 100 U/ml penicillin/streptomycin and 2% B27 (Gibco).

In vivo Electroporation

In vivo electroporation was performed as previously described (Matsuda and Cepko, 2004, 2007). Briefly, P0 Lister hooded rats were anesthetized by placing on ice. One microliter of DNA mix (6.5 μg/μL) containing 0.1% Fast Green dye (Sigma) prepared in HBSS saline was injected into the subretinal space with a Hamilton syringe equipped with a 33G blunt end needle. Five 99 V pulses were administered for 50 ms at 950 ms intervals, using a forceps-type electrode (Nepagene, CUY650P7) with Neurgel (Spes Medica). The electrodes were oriented such that the positive pole electrode was placed over the injected eye and the negative pole electrode was placed over non-injected eye to ensure that the electrical field is oriented correctly to drive the injected DNA solution from the subretinal space into progenitors. Fast Green in the DNA mix is an injection tracer, which facilitates observation of the spread of the injection solution into the subretinal space (de Melo and Blackshaw, 2018). In addition, the efficiency of electroporation was verified 10 days after electroporation when GFP positive cells were observed in freshly dissected retinas. Retinas were then fixed by immersion in 4% paraformaldehyde in PBS for 16 h. Serial transversal sections of cryoprotected material (10 μm) were mounted on either Poly-L-lysine (300 μg/mL) or silane (6%, Sigma)-treated microscope slides.

Immunocytochemistry

Cell cultures were fixed in 4% paraformaldehyde (PFA) in PBS for 15 min at room temperature. The cells were incubated overnight at 4°C, with primary antibodies diluted in PBS, 0.5% Triton X-100 and 5% goat serum, washed and incubated for 2 h at room temperature, with species-specific secondary antibodies conjugated to Alexa fluorophores. To stain the nuclei, cells were incubated for 5 min with 0.1 μg/mL DAPI (4'6'-diamino-2-phenylindone) in PBS 0.1 M. Coverslips were mounted onto glass slides with Aqua Poly/Mount mounting medium (Polysciences, Warrington, PA). Primary antibodies and respective dilutions were: chicken anti-Green Fluorescent Protein (Aves Labs, cat#GFP-1020, 1:1000), rabbit anti-Red Fluorescent Protein (Rockland, cat#600-401-379, 1:1000), mouse anti-microtubule associated protein (Sigma, cat#M1406, 1:500), mouse anti-β_{III}-TUBULIN (TUBB3; Biolegend, cat#MMS-435P, 1:1000), rabbit anti-RBPMS (PhosphoSolutions, cat#1830; 1:100), mouse anti-SYNAPSIN 1 (Synaptic Systems, cat#106001, 1:2000), mouse anti-PARVALBUMIN (SIGMA, cat#p3088, 1:1000), mouse anti-CRALBP (ABCAM, cat# ab15051, 1:500), rabbit anti-GFAP (DakoCytomation, cat#z0334, 1:4000) rabbit anti-SOX2 (ABCAM, cat# ab97959, 1:500), rat anti-BrdU (ABCAM, cat# ab6326 1:500), rabbit anti-phospho-histone 3 (Millipore, cat#06-570, 1:1000), mouse anti-PAX6 (Millipore, cat#MAB5552, 1:500) and mouse anti-NESTIN (Millipore, cat#mab353, 1:200 millipore).

Calcium Imaging

Calcium imaging was done on MGC cultures at 2–3 weeks post-nucleofection, using Oregon green 488 BAPTA-1 (Invitrogen, 10μM). Imaging was performed in a physiological solution containing 140 mM NaCl, 5 mM KCl, 2 mM $MgCl_2$, 2 mM $CaCl_2$, 10 mM HEPES, 10 mM glucose, and 6 mM sucrose, and pH 7.35. Images were acquired every 10 ms with virtually no intervals using a scientific CMOS camera (Andor). The microscope was controlled by Micro-Manager software together with the image processor ImageJ. Changes in fluorescence were measured for individual cells using the time series analyzer plugin v3.0 in ImageJ v1.37. The average of the first ten time-lapse images for each region of interest (ROI) was defined as initial fluorescence (F_0), and the variation of fluorescence (ΔF) in each frame (n) was calculated as F_n-F_0/F_0.

Quantitative RT-PCR

MGC cultures were harvested at 13 days after nucleofection, and mRNA was isolated from all cells, including non-transfected MGCs. RNA was extracted using RNeasy Mini Kit (QIAGEN, CA, USA), which includes a genomic DNA elimination step, and the purity and quantity of total RNA was estimated using a ND8000 spectrophotometer (Thermo Scientific NanoDrop Products, DE, EUA). Extractions were carried out of cells from each group (Control, Neurog2 or Ascl1), detached chemically with TrypLE and washed with nuclease free PBS, following the manufacturer's protocol. The first-strand cDNA was synthetized using the High-Capacity cDNA Reverse Transcription Kit (Applied Biosystems, NY, USA) in accordance with the manufacturer's instructions, using 900 ng of extracted RNA per sample. Conditions for each cycle of amplification were as follows: 10 min at 25°C; 120 min at 37°C, 5 min at 85°C. The final cDNA products were amplified using RT2 Real-Timer SyBR Green/ROX PCR Mix (QIAGEN, CA, USA) in 25 μL of a reaction mixture pipetted into each well of a 96-well in a Mouse RT2 Profiler Custom PCR Array. The array was designed to simultaneously examine mRNA levels of 18 genes commonly expressed in retina cell types (RLBP1, GLUL, NRL, RHO, RCVRN, PDE6G, PROX1, LHX1, VSX2, SLC32A1, TH, CHAT, SLC17A6, POU4F1, CALB2, RBFOX3, SYN1, and PVALB) and 2 housekeeping genes (GAPDH and RPL19), following the manufacturer's protocol. Real-time PCR was performed using a two-step cycling program, with an initial single cycle of 95°C for 10 min, followed by 40 cycles of 95°C for 15 s, then 60°C for 1 min, in an ABI ViiA 7 Real-Time PCR System (Applied Biosystems, NY, USA) with Sequence Detector System software v1.2. The ramp rate was adjusted to 1°C/s following manufacturer's instruction. A first derivative dissociation curve was built (95°C for 1 min, 65°C for 2 min, then ramped from 65°C to 95°C at a rate of 2°C/min). The formation of a single peak at temperatures higher than 80°C confirmed the presence of a single PCR product in the reaction mixture.

For data analysis the $2^{(-\Delta\Delta Ct)}$ method (Livak and Schmittgen, 2001) was implemented using normalized threshold cycle (Ct) values provided by two independent experiments of nucleofection. Furthermore, we applied experiments using mRNA pool of two independent transfection experiments and used the Ct data to perform normalization and follow the $2^{(-\Delta\Delta Ct)}$ method (Livak and Schmittgen, 2001), considering the sensitivity, specificity, and reproducibility expected of real-time PCR using RT^2 Profiler PCR Array System from QIAGEN. Endogenous gene control used in the normalization was the average of the mouse GAPDH and RPL19. A positive value indicates gene up-regulation and a negative value indicates gene down-regulation.

To confirm that genes upregulated in MGCs could indicate the acquisition of a retinal neuron-like phenotype in MGC-derived iNs, we performed the same analysis using cerebellum astroglia cell cultures 13 days after nucleofection with either Neurog2 or Ascl1 (Chouchane et al., 2017).

Bioinformatics

Dataset raw count table and published metadata were obtained from GSE63472 accession code. A modified Seurat pipeline was used to re-analyze single-cell RNAseq data. First, we excluded from our analysis genes that were not expressed in at least 10 cells. Next, we selected cells expressing 500 to 5,000 genes, and <5% of mitochondrial genes (n = 21,494 cells). Metadata variables as number of genes and percentage of mitochondrial expression were also used to regress out some unnecessary clustering bias. Based on *PCElbowPlot*, we used 30 PC's in *FindClusters* (resolution = 2) and *RunTSNE* Seurat's functions. After that, using old assigned clusters and markers found by *FindAllMarkers* function (Macosko et al., 2015), new assigned clusters were labeled. Retinal cell types (n = 21,176 cells) were classified according to the levels of expression of genes in Müller glia cells, astrocytes, amacrine cells, bipolar cells, horizontal cells, cones, rod cells, and ganglion cells (Macosko et al., 2015). Cones and rod cells were merged in a single-group (Photoreceptors).

Quantifications

To characterize MGC cultures we examined 20 fields at 40× magnification for CRALBP and GFAP, and 20 fields at 20× magnification for Nestin, Pax6, and PH3 proteins. To quantify the reprogramming process, cells were examined for colocalization of DSRED and TUBB3 immunoreactivity at 13 days post nucleofection (dpn), in 20 fields at 20x magnification, and the same was done for MAP2 protein. For all protocols of quantification, we counted immunoreactive cells in 3 independent experiments.

To estimate a neuronal polarization index, we divided the neurons into 4 quadrants and measured the axial distribution of neuronal processes. Nineteen neurons were analyzed for the condition MGC with EGF/FGF + Neurog2, 31 neurons for MGC without + Neurog2, 26 neurons for MGC with EGF/FGF + Ascl1 and 21 neurons for MGC without EGF/FGF + Ascl1.

Distribution of GFP+ cells in the P10 rat retinas following *in vivo* electroporation at P0 in Lister-hooded pups was examined in 26 sections from 5 control-electroporated retinas and 27 sections from 5 Neurog2-electroporated retinas. The outer nuclear layer (ONL), inner nuclear layer (INL), and ganglion cell layer (GCL) were identified using DAPI counter-staining. MGCs were identified by their radial morphology and expression of CRALBP.

Statistical Analysis

All statistical data are presented as the mean ± standard error of the mean (SEM) of at least three independent experiments. Statistically significant differences were assessed using unpaired t-test, one-way or two-way analysis of variance (ANOVA). Confidence interval is 95%.

RESULTS

Properties of Cells Expanded in the Presence or Absence of EGF/FGF2

Enrichment of MGCs was done according to a previously described method (Hicks and Courtois, 1990). Using this method we (de Melo Reis et al., 2008) and others (Das et al., 2006) have shown that virtually all cells after 2–3 weeks in culture express the MGC markers vimentin, glutamine synthetase (GS), cellular retinaldehyde-binding protein (CRALBP). Based on the previously reported use of selected growth factors to expand astroglial populations for lineage reprogramming into iNs (Berninger et al., 2007; Heinrich et al., 2010; Chouchane et al., 2017), we cultured cells either with or without EGF/FGF2. After expansion, virtually all cells in cultures obtained using both protocols expressed the MGC protein CRALBP (**Figures 1A,B**). A high percentage of cells also expressed glial acid fibrillary protein (GFAP), which is upregulated in MGC cultures (Das et al., 2006). No significant difference was observed between the two expansion conditions (**Figures 1A,B**).

MGCs and late-progenitors in the retina share the expression of several proteins, including NESTIN, sex determining region Y (SRY)-box 2 (SOX2) and Paired box 6 [PAX6; (Karl et al., 2008; Lin et al., 2009; Bhatia et al., 2011)], what has led to the suggestion that MGCs may have neural stem cell-like properties (Das et al., 2006; Lawrence et al., 2007; Nickerson et al., 2008; Giannelli et al., 2011). Accordingly, we found that more than 97% of cells expressed NESTIN and this percentage was slightly increased in the presence of EGF/FGF2 (**Figures 1C,D**; 97.02 ± 0.95% vs. 99.05 ± 0.32%, p = 0.0466, unpaired t-test. N = 3 independent experiments). Similarly, expression of SOX2 was also higher among MGCs expanded in the presence of EGF/FGF2 (**Figure 1D**; 78.71 ± 3.21% vs. 98.20 ± 0.48%, $p < 0.0001$, unpaired t-test. $N = 3$ independent experiments). In contrast, the proportion of MGCs expressing PAX6 was higher in the absence of EGF/FGF2 (**Figures 1C,D**; 34.87 ± 2.60% vs. 27.20 ± 1.58%, $p = 0.013$, unpaired t-test. $N = 3$ independent experiments).

To examine the proliferative potential of enriched MGCs, we added the thymidine analog BrdU to the cultures at day 20. The percentage of MGCs labeled with BrdU (BrdU+) after 36 h of incubation was slightly higher with, rather than without EGF/FGF2 (**Figures 1C,D**; 65.54 ± 2.97% vs. 75.41 ± 3.94%, p = 0.047, unpaired t-test. N = 3 independent experiments). However, the percentage of phospho-histone labeled (PH3+) mitotic MGCs was similar in both conditions (**Figure 1D**; 8.40

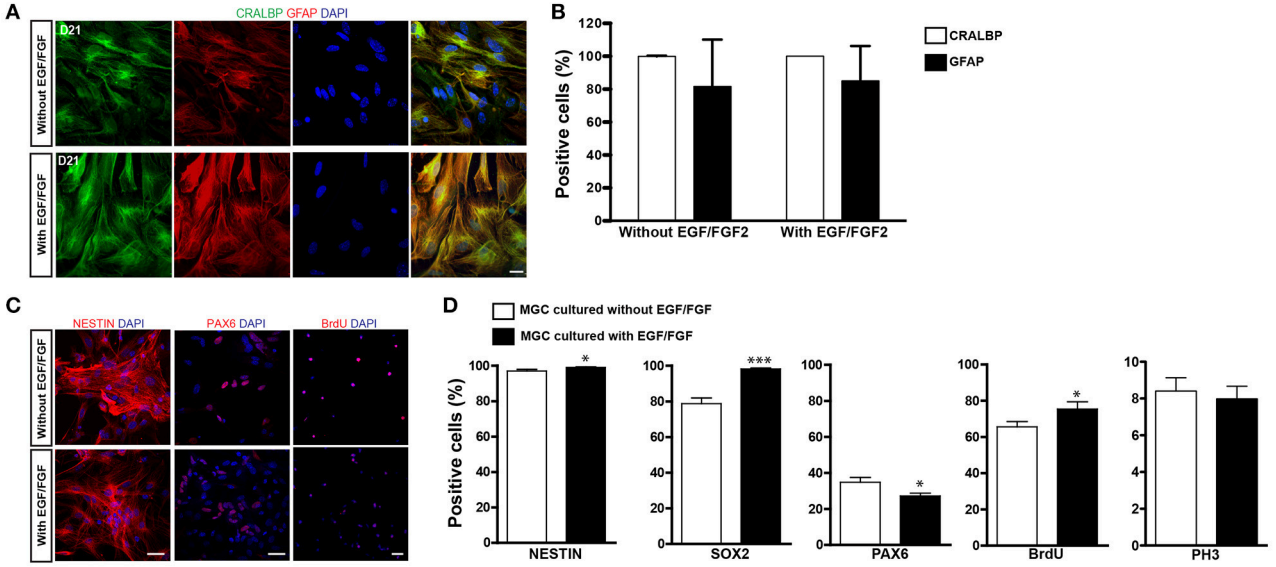

FIGURE 1 | Characterization of MGC cultures expanded with or without EGF/FGF2. **(A)** Representative photomicrographs of MGC cultures showing the expression of CRALBP (green) and GFAP (red) 21 days after expansion in the absence (top) or presence (bottom) of EGF/FGF2. **(B)** Frequencies of CRALBP and GFAP positive cells in enriched MGC cultures. **(C)** Immunolabeling for NESTIN, PAX6, and BRDU (red) in MGCs expanded in the absence (top) or presence (bottom) of EGF/FGF2. **(D)** Frequencies of MGCs immunolabeled for NESTIN, SOX2, PAX6, BrdU, and PH3 prior to lineage reprogramming (*$p < 0.05$; ***$p < 0.001$; Unpaired *t*-test). Scale bars: 20 μm.

± 0.72% vs. 7.98 ± 0.69%, $p = 0.70$, unpaired *t*-test. $N = 3$ independent experiments), which could be explained by a selective lengthening of the S-phase upon EGF/FGF2 treatment. Collectively, these observations support the interpretation that cells enriched in our cultures are presumptive MGCs that retain some properties observed in late-progenitors of the developing retina. However, we never observed spontaneous neurogenesis in these cultures, suggesting that a potential progenitor state of presumptive MGCs in culture is associated with a glial-fate restriction.

Expression of Either NEUROG2 or ASCL1 Is Sufficient to Convert MGCs Into iNs

Next, we tested whether the expression of NEUROG2 may reprogram enriched MGCs into iNs, as compared with ASCL1 as previously described (Pollak et al., 2013). Expanded MGCs were harvested and transfected with control-I-GFP, Neurog2-I-GFP (**Figure 2B**), Neurog2-I-DsRed (**Figures 2D,F**) or Ascl1-I-DsRed plasmids (**Figures 3A,C**), and maintained for 13 days (1 day in growth medium + 12 days in differentiation medium; **Figure 2A**). At the end of this period, cells transfected with control plasmids maintained both their typical glial morphology and the content of the glia-specific protein GFAP (**Figure 2C**). In contrast, a substantial fraction of NEUROG2-containing cells underwent robust morphological changes, characterized by reduction of the cell body and extension of thin and long primary processes (usually 2 or 3) with small ramifications, similar to the morphology of neuronal cells in culture (**Figures 2B,D,F**). Accordingly, these cells also contained the neuron-specific proteins TUBB3 (**Figure 2D**) and microtubule associated protein 2 (MAP2) (**Figure 2F**), indicating that NEUROG2 led to conversion of cultured MGCs into iNs. The frequency of iNs was significantly higher in cultures containing MGCs expanded in the presence, as compared with the absence of EGF and FGF2 (71.0 ± 4.1 vs. 26.4 ± 5.1%; $p < 0.001$; Tukey's multiple comparison test; **Figure 2E**), suggesting that these growth factors facilitate reprogramming. Additionally, about 90% of iNs also expressed MAP2 (**Figures 2F,G**) independently of mitogenic factors during enrichment, further suggesting the acquisition of a neuronal phenotype.

Lentiviral-mediated expression of ASCL1 reportedly induced the conversion of about 30% of cultured MGCs into neuronal-like cells (Pollak et al., 2013). In our model, nucleofection of ASCL1 led more than half of cultured MGCs to convert into iNs (**Figures 3A,B**). The proportion of iNs was higher among MGCs previously expanded in the presence, rather than in the absence of EGF and FGF2 (68.1 ± 4.9 vs. 53.7 ± 5.5%; $p < 0.05$; Tukey's multiple comparison test; **Figure 3B**), and 97% of iNs also expressed MAP2 (**Figure 3D**). Collectively, our data indicate that the expression of either NEUROG2 or ASCL1 is sufficient to lineage-reprogram MGCs into iNs, as well as that previous exposure of MGCs to EGF and FGF2 facilitates reprogramming.

Functional and Morphological Differentiation of MGC-Derived iNs

To evaluate whether iNs derived from lineage reprogrammed cultured MGCs develop features of mature functional neurons, we performed calcium imaging using a genetically encoded calcium indicator (GCAMP5) and a fluorescent dye (Oregon green BAPTA-1). MGC cultures nucleofected with either Ascl1

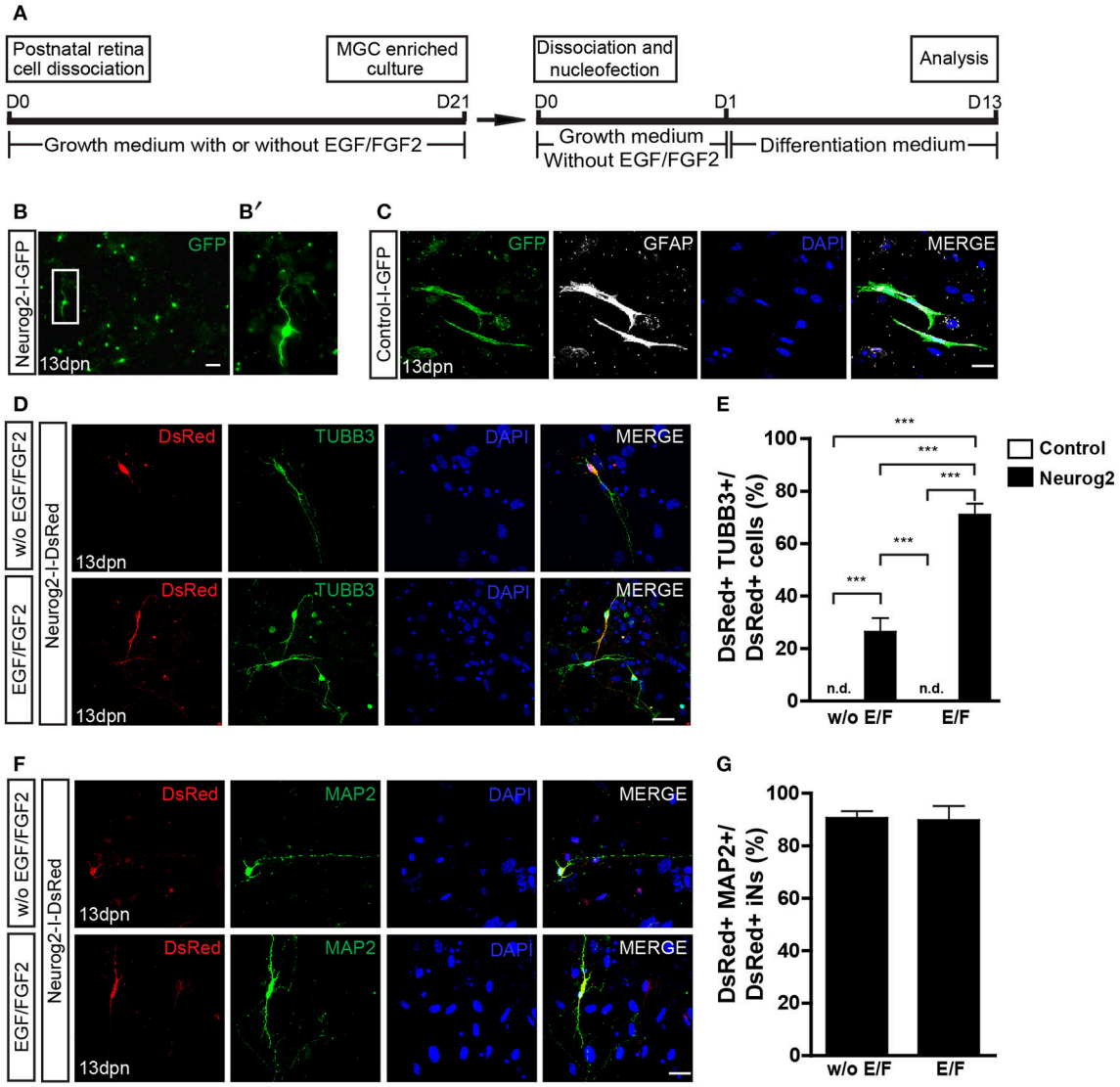

FIGURE 2 | Expression of NEUROG2 converts MGCs into iNs. **(A)** Experimental design. Note that EGF/FGF2 are used only during MGC expansion. **(B–B')** Overview of MGC cultures 13 days post nucleofection (dpn) with Neurog2-I-GFP showing the presence of GFP+ cells (green) adopting a neuronal-like morphology (white inset, magnified in **B'**). **(C)** Representative photomicrographs of MGC cultures at 13 dpn with control-I-GFP, showing GFP+ cells (green) that maintain glial morphology and contain GFAP (white). **(D)** Immunolabeling of the neuronal protein β_{III}-TUBULIN (TUBB3, green) in DsRed (red) cells at 13 dpn with Neurog2-I-DsRed in MGCs cultures expanded either without (top) or with (bottom) EGF/FGF2. **(E)** Frequencies of DsRed+/TUBB3+ iNs amongst total DsRed+ cells at 13 dpn (***$p < 0.001$; Tukey's multiple comparison test). **(F)** Immunolableing for the neuronal protein MAP2 (green) in DsRed (red) cells at 13 dpn with Neurog2-I-DsRed in MGCs expanded either without or with EGF/FGF2. **(G)** Frequencies of DsRed+MAP2+ iNs amongst all DsRed+ iNs. Photomicrographs in **(C,D,F)** are single confocal Z stacks. Nuclei are stained with DAPI (blue). Scale bars: 20 μm.

or Neurog2 expression plasmids were maintained for 15 days, and then treated with Oregon green BAPTA (see Materials and Methods). Fast fluctuations of intracellular calcium levels leading to sudden fluorescence changes, likely produced by an abrupt aperture of voltage-gated calcium channels mediated by synaptic activity (Bonifazi et al., 2009; Yang and Yuste, 2017), were detected in more than half of iNs (Neurog2 with EGF/FGF2: 12/20; Neurog2 without EGF/FGF2: 13/18; and Ascl1 with EGF/FGF2: 11/20; Ascl1 without EGF/FGF: 12/19) (**Figure 4** and **Supplementary Videos**). In contrast, non-transfected MGCs showed slow calcium fluctuations (**Figure 4**).

We also examined the morphology of MGC-derived iNs in the various experimental groups (**Figure S1**). Expression of either Neurog2 or Ascl1 leads to the generation of diverse iNs (**Figures S1A,B**). Notwithstanding, whereas three-quarters of Neurog2-converted iNs were either unipolar or bipolar, Ascl1-converted iNs had approximately equal proportions of either multipolar or uni/bipolar morphologies (**Figure S1C**). These

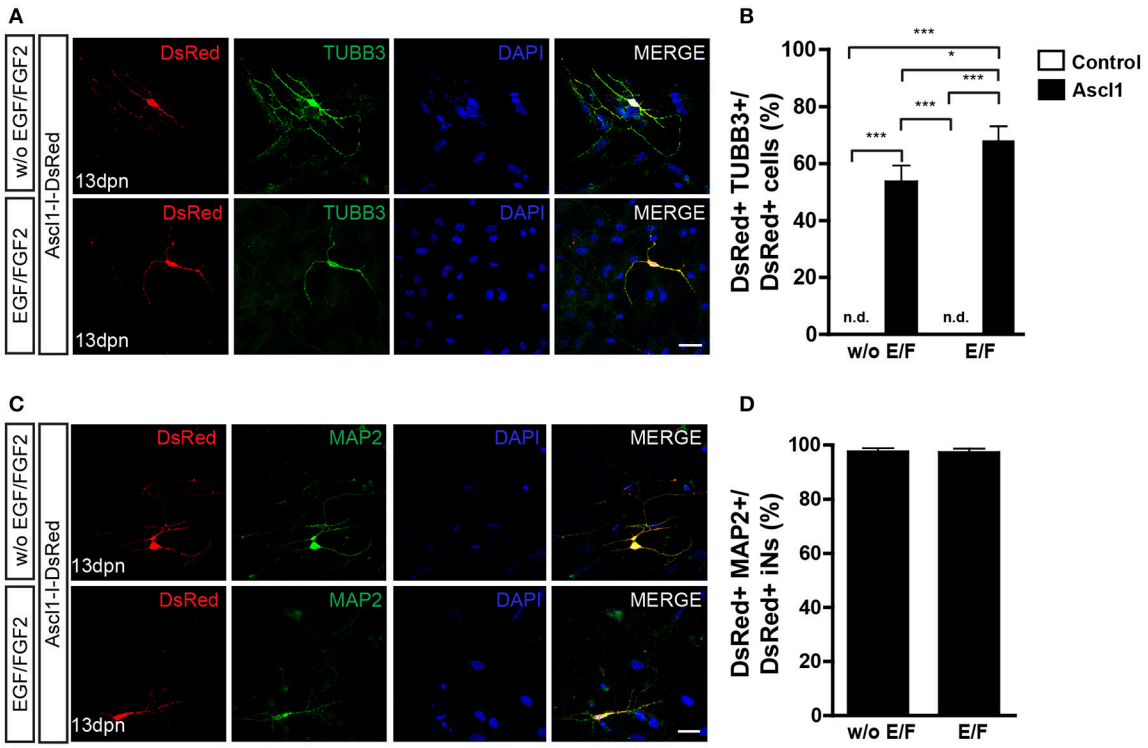

FIGURE 3 | Expression of ASCL1 converts MGCs into iNs. **(A)** Representative photomicrographs of MGC cultures expanded without or with EGF/FGF2 at 13 dpn with Ascl1-I-DsRed, showing DsRed+ cells (red) immunolabeled for β_{III}-TUBULIN (TUBB3, green) **(B)** Frequencies of DsRed+/TUBB3+ iNs amongst total DsRed+ cells at 13 dpn (*$p < 0.05$; ***$p < 0.001$; Tukey's multiple comparison test). **(C)** Immunolabeling of the neuronal protein MAP2 (green) in DsRed (red) cells at 13 dpn with Ascl1-I-DsRed in MGCs expanded without or with EGF/FGF2. **(D)** Frequencies of DsRed+MAP2+ iNs amongst all DsRed+ iNs. Photomicrographs in **(A,C)** are single confocal Z stacks. Nuclei are stained with DAPI (blue). Scale bars: 20 μm.

observations suggest that Neurog2 and Ascl1 iNs may acquire distinct phenotypes.

MGC-Derived iNs Express Key Genes of Retinal Neurons

It has been suggested that the origin of reprogrammed astroglial cell lineages affects the phenotype of induced neurons (Chouchane et al., 2017). We tested whether MGC-derived iNs show hallmarks of bona fide retina neurons, after lineage conversion induced by either ASCL1 or NEUROG2 (**Figure 5**). First, we took advantage of single-cell transcriptomes available in the literature (Macosko et al., 2015) to identify molecular signatures of the major retinal cell types (**Figure 5A** and **Figure S2**). Based on single-cell RNA sequence of adult mouse retina cells (Macosko et al., 2015), we defined a small set of transcripts with enriched expression in MGCs (RLBP1 and GLUL), astrocytes (GFAP), photoreceptors (NRL, RHO, RCVRN ,and PDE6G), horizontal cells (PROX1 and LHX1), bipolar cells (VSX2), amacrine cells (PAX6, SLC32A1, GAD1, GAD2, TH, and CHAT) and RGCs (RBPMS, SLC17A6, POU4F1, CALB2, RBFOX3, SYN1, TUBB3, and PVALB). Next, we used qRT-PCR to compare the expression of these molecular markers in MGC cultures expanded in the presence or absence of EGF/FGF2, and nucleofected with either Neurog2 or Ascl1 (**Figures 5B,C**). Despite the small number of iNs amongst the total population of MGCs (∼1–2%), we detected an increase in the expression of several genes commonly expressed by retina neurons in MGC cultures nucleofected with Neurog2 or Ascl1 (**Figures 5B, C**), but not among cerebellum astroglial cells nucleofected with the same plasmids (**Figure S3**), which are known to adopt mostly a GABAergic iN phenotype (Chouchane et al., 2017). Interestingly, differences were observed among cells converted through each of the two expansion protocols. While MGC-derived iNs, induced by expression of either ASCL1 and NEUROG2 grown in the absence of EGF/FGF2 upregulated key genes of photoreceptors, genes of amacrine cells were expressed only in iNs derived from MGCs expanded in the presence of growth factors. In contrast, increased levels of genes commonly expressed by horizontal and bipolar cells were detected in all experimental conditions. Surprisingly, we also found that many genes commonly expressed by RGCs were upregulated in MGC-derived iNs, in particular the specific RGC genes SLC17A6 and POU4F1 (Quina et al., 2005; Martersteck et al., 2017), but the same was not observed in cerebellar astroglia-derived iNs (**Figure S3**). This effect was much more robust after expression of NEUROG2 (**Figure 5B**), independently of the expansion protocol. Altogether, the transcriptome panel suggests that either Neurog2 or Ascl1 may induce distinct, but

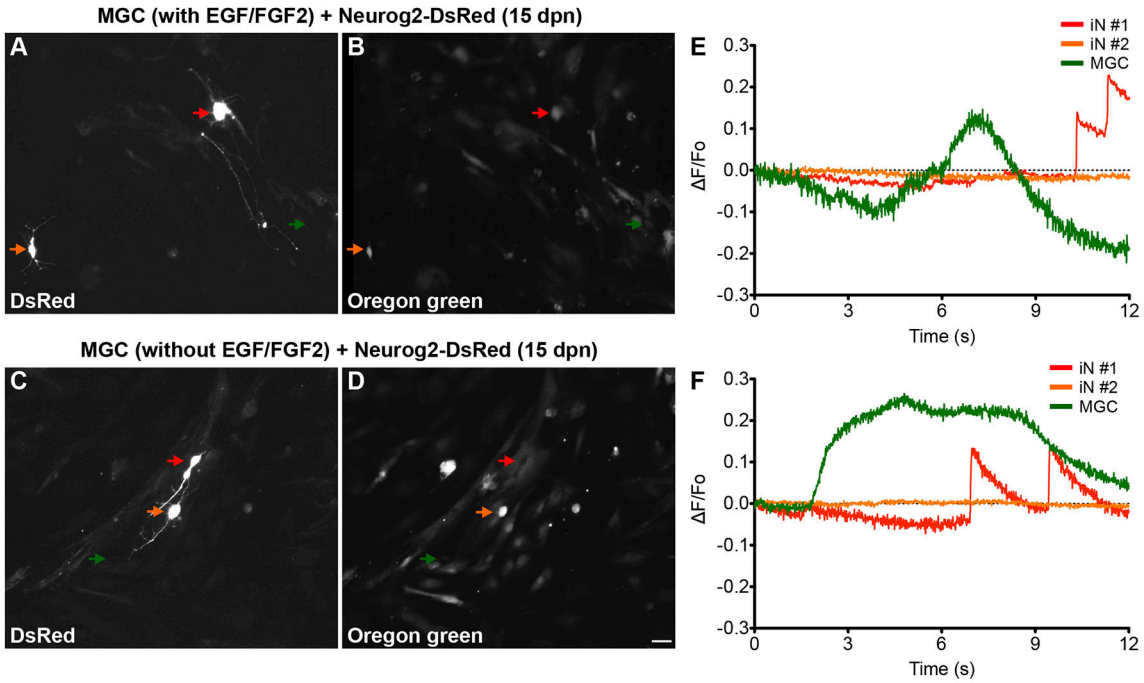

FIGURE 4 | MGC-derived iNs display fast calcium transients. **(A–D)** Photomicrographs show examples of MGC-derived iNs at 13 days dpn with Neurog2-I-DsRed expressing DsRed **(A,C)**, and labeled with Oregon Green Bapta **(B,D)**. Red and orange arrows point to DsRed+ MGC-derived iNs, whereas green arrows point to non-transfected MGCs randomly selected within the same fields of observation. Top **(A,B)** and bottom **(C,D)** images were obtained from MGCs expanded in the presence of absence of EGF/FGF2, respectively. **(E,F)** Representative traces of calcium-transients in cells indicated by colored arrows in **(A,E)** and **(C,F)**. Calcium responses were calculated as the change in fluorescence (ΔF) over the initial fluorescence (F_0). Note that only iNs indicated by the red arrows displayed fast calcium-transients as indicated by rapid variations in the fluorescence (raising interval between 10 – 30 ms). In contrast, non-transfected MGCs (green arrows) have only slow calcium-transients as indicated by gradual changes in fluorescence levels (raising interval > 1s), suggestive of metabotropic responses. DsRed+ cells indicated by the orange arrows did not show any significant fluctuation in fluorescence levels during the period of observation. Scale bar: 20 μm.

partly overlapping retina neuronal phenotypes in MGC-derived iNs, but Neurog2 seems to induce a more complete RGC-like phenotype.

Neurog2-Induced RGC-Like Phenotypes

To further test for the acquisition of RGC features by MGC-derived iNs, we immunolabeled markers of retina neurons in individual iNs (**Figure 6**). NEUROG2-converted neurons contained RNA Binding Protein mRNA Processing Factor (RBPMS; **Figures 6A–C**), a selective marker of RGCs in the mammalian retina (Rodriguez et al., 2014), as well as TUBB3 (**Figures 2**, **6D–F**), PARV (**Figures 6G–I**) and SYN1 (**Figures 6J–L**), all of which are enriched in RGCs *in vivo* (**Figure 5A**). These findings, together with the qRT-PCR data, support the interpretation that NEUROG2 is sufficient to induce a RGC-like phenotype in MGC-derived iNs.

Overexpression of NEUROG2 Resumes RGC Generation in the Neonatal Retina *in vivo*

Finally, we tested whether the expression of NEUROG2 in late retinal progenitors induces *de novo* generation of RGCs. To that effect, sub-retinal injections of either pCAG-I-GFP or pCAG-Neurog2-I-GFP plasmids were followed by electroporation in P0 rats (**Figure 7**). Late progenitors are transcriptionally similar to MGCs and also have restricted neurogenic potential (Cepko, 1999; Blackshaw et al., 2004; Ooto et al., 2004; Jadhav et al., 2009; Nelson et al., 2011; He et al., 2012; Karl and Reh, 2012; Loffler et al., 2015). Both late progenitors and MGCs are not competent to generate RGCs in the rodent retina. As previously described (Matsuda and Cepko, 2004), 10 days after *in vivo* electroporation the vast majority (∼80%) of GFP+ cells in control-electroporated retinas settled in the outer nuclear layer (ONL) and differentiated into rod cells, while the remaining cells located mostly in the inner nuclear layer (INL) and differentiated into bipolar, MGCs or amacrine cells (**Figures 7A,E**). Also consistent with the literature (Matsuda and Cepko, 2004), a negligible number of GFP+ cells was found in the ganglion cell layer (GCL) of control-electroporated animals (2 cells in one animal out of 1,254 GFP+ cells counted from 5 animals—26 × 250 μm sections), whereas a significant proportion of cells in all animals displayed radial morphologies and expressed CRALBP (**Figure S4**), indicating the acquisition of a MGC phenotype (10.71 ± 0.69 %, $n = 5$ animals, 1,487 GFP+ cells). In sharp contrast, in retinas electroporated with pCAG-Neurog2-I-GFP plasmid, we failed to detect any cell with a radial morphology or expression of CRALBP (1,340

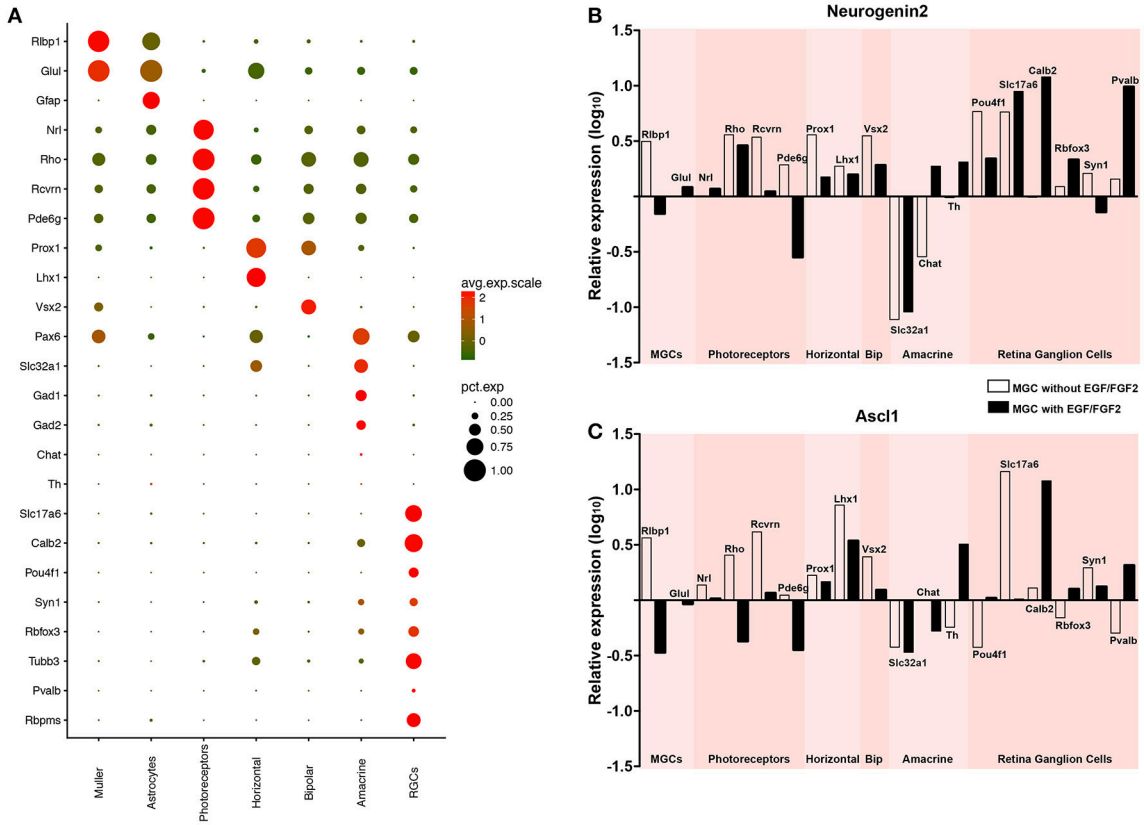

FIGURE 5 | Expression of either NEUROG2 or ASCL1 induces upregulation of key retina neuron genes in MGC-derived iNs. **(A)** Expression levels of selected genes used to identify different classes of retina neurons using scRNAseq data available in the literature (Macosko et al., 2015) (see also **Figure S2**). Dot sizes and colors (green-low to red-high) represent the percentage of cells expressing the gene and its average scaled expression, respectively. Observe that the expression of Slc17a6 and Pou4f1 are specific for a high percentage of cells assigned as RGCs. **(B,C)** Graphics showing the relative expression levels (log_{10}) of genes enriched in Müller glia (Rlbp1, Glul), photoreceptors (Rho, Rcvrn, Pde6g), horizontal (Prox1, Lhx1), bipolar (Vsx2), amacrine (Slc32a1, Chat, Th) and retina ganglion cells (Pou4f1, Slc17a6, Calb2, Rbfox3, Syn1, Pvalb, Rbpms), as shown in **(A)**, in MGC cultures nucleofected with either Neurog2 **(B)** or Ascl1 **(C)**. White and black bars indicate that MGC were expanded in the absence or presence of EGF/FGF2, respectively, prior to the expression of Neurog2 or Ascl1.

GFP+ cells analyzed from 5 animals). About 65.5% of GFP+ cells settled in the ONL and 33% in the INL, but a significant fraction (17 cells in 5 animals out of 1340 GFP+ cells counted from 5 animals−27 × 250 μm sections) of cells was found in the GCL (**Figures 7C–I**). Quantification of the number of GFP+ cells in 250 μm of 27 sections of 5 retinas showed that the mean number of GFP+ cells in the GCL was significantly increased in Neurog2-electroporated animals as compared to controls, suggesting that NEUROG2 expression resumed the generation of RGCs (**Figure 7F**). Accordingly, we also found that GFP+ cells in the GCL expressed classical markers of RGCs, such as RBPMS (**Figures 7 G–I**) and TUBB3 (**Figure S5**) and extended thin axonal processes that reached the optic nerve (**Figure 7J**). Some GFP-expressing cells within the GCL also extended processes toward the inner plexiform layer, consistent with the morphology of RGCs (**Figures 7G, 8**). Moreover, GFP+ cells within the GCL also displayed varied patterns of dendrite stratification (**Figure 8**), consistent with distinct RGC morphologies in the rodent retina (Sanes and Masland, 2015). Altogether, these data support the hypothesis that the expression of NEUROG2 endows late retinal progenitors with the potential to generate RGCs, while it inhibits the differentiation of MGCs *in vivo*.

DISCUSSION

Here we show that cells isolated in culture and expressing several hallmarks of Müller cells, the main type of glia found in the vertebrate retina, can be reprogrammed into neurons when transduced with plasmids encoding either of the basic Helix loop Helix (bHLH) transcription factors Neurog2 or Ascl1. Cell–lineage reprogramming is affected by treatment with EGF and FGF2 during MGC enrichment, and led to the expression of typical neuronal markers, MAP-2 and TUBB3. Induced neurons expressed clusters of genes consistent with the profile of retinal cells, suggesting that distinct retinal neuron phenotypes are elicited in MGC-derived iNs. Notably, only iNs generated after expression of NEUROG2 upregulated a set of genes compatible with the acquisition of a possible RGC identity. A role for NEUROG2 in the induction of RGC fate was also

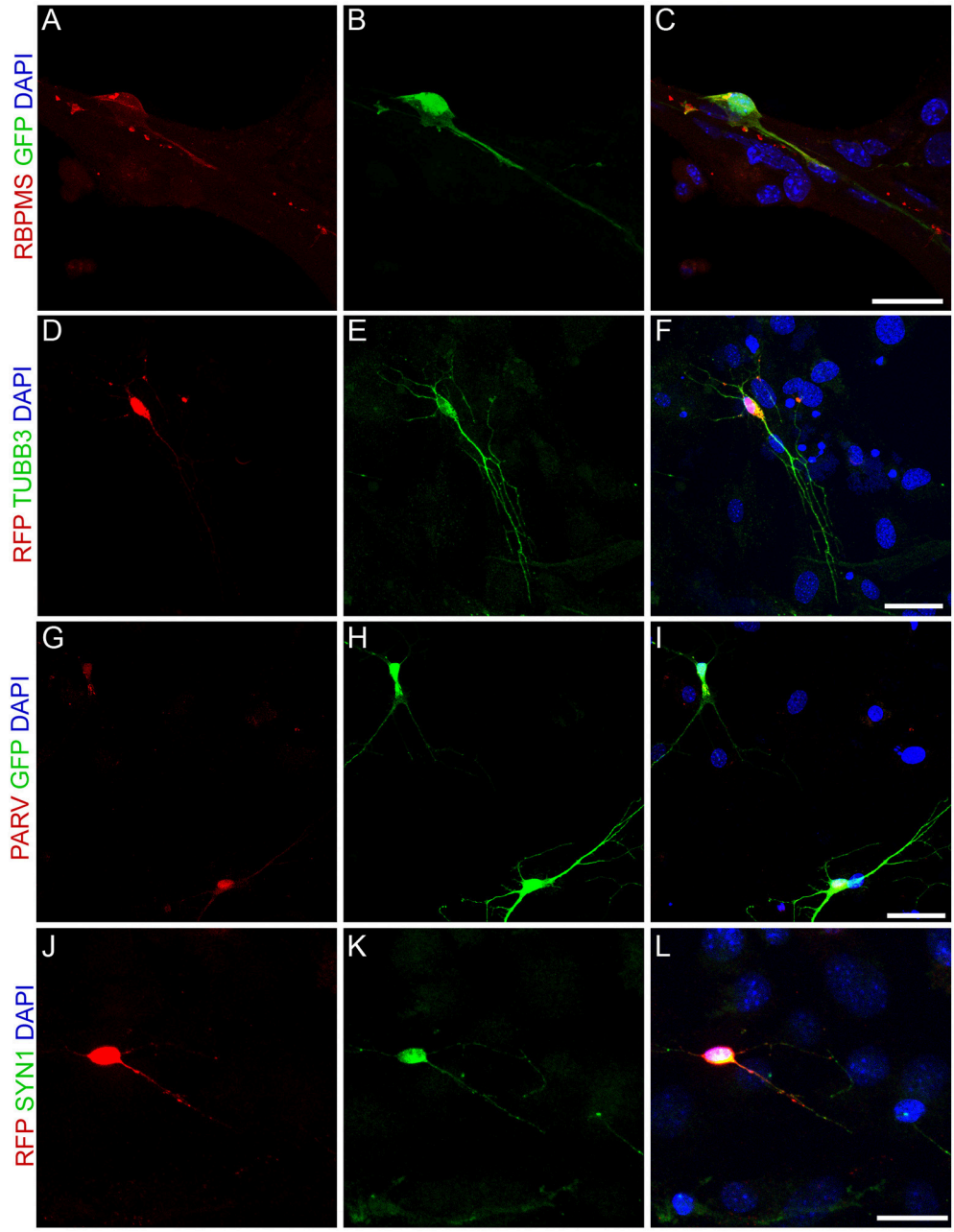

FIGURE 6 | Expression of NEUROG2 induces the acquisition of RGC-like phenotypes in MGC-derived iNs. **(A–L)** Immunolabeling of the RGC proteins RBPMS (red, **A–C**), β_{III}-TUBULIN (green, **D–F**), PARV (red, **G–I**) and SYN1 (green, **J–L**) in MGC converted into iNs at 15 days post-nucleofection with either Neurog2-I-GFP (green, **A–C** and **G–I**) or Neurog2-I-DsRed (red, **D-F** and **J-L**). Scale bars: 20 μm.

observed in late progenitors of the neonatal mouse retina *in vivo*, suggesting that Neurog2 is a good candidate for gene therapies aiming at the regeneration of RGCs in the adult injured retina.

Lineage reprogramming of astroglial cells into neurons has been heralded as a possible treatment for degenerative or traumatic brain disorders, and recent studies showed evidence of conversion of glial cells into functional neurons with high efficiency in the murine brain, induced by virally delivered transcription factors (Torper and Gotz, 2017). Astroglial cells isolated from the postnatal rodent cerebral cortex (Berninger et al., 2007; Heinrich et al., 2010) and cerebellum (Chouchane et al., 2017), as well as retinal MGCs (Singhal et al., 2012; Pollak et al., 2013; Song et al., 2013; Ueki et al., 2015; Wu et al., 2016; Jorstad et al., 2017) have been reprogrammed into neurons.

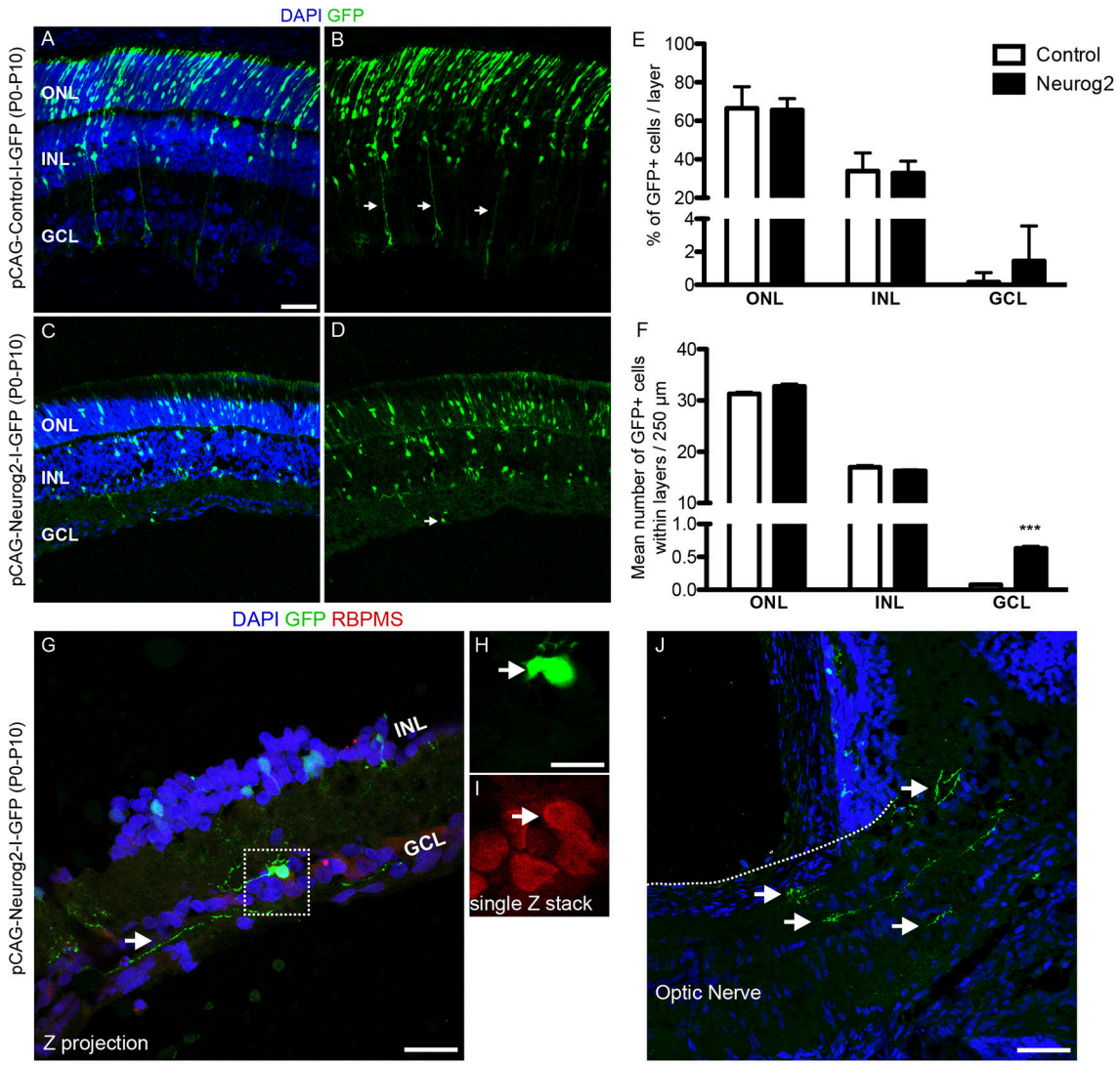

FIGURE 7 | Forced-expression of NEUROG2 resumes the generation of RGCs in the developing retina *in vivo*. **(A–D)** Representative images of P10 rat retinas after electroporation with control-I-GFP **(A,B)** and Neurog2-I-GFP **(C,D)** plasmids at P0. Note the presence of GFP+ radial fibers typical of MGCs (arrows in **B**) and the complete absence of GFP+ cells in the GCL in controls. Observe also the decrease of GFP+ cells in the ONL and the presence of GFP+ cells in the GCL of Neurog2-electroporated retina (arrow in **D**). **(E)** Frequencies of GFP+ cells in the ONL, INL e GCL of the retina of control- and Neurog2-electroporated animals. **(F)** Mean numbers of GFP+ cells within the ONL, INL or GCL per 250 µm longitudinal section (***$p < 0.001$; Two-way ANOVA, Bonferroni *post-hoc* test). **(G–I)** Expression of RBPMS (red) in GFP+ cells (green) within the GCL of Neurog2-electroporated retinas. White arrow points to the axon-like process of the GFP+ cell observed within the GCL. Dashed box **(G)** is amplified in H and I to show the co-localization of GFP and RBPMS in a single confocal Z-stack. **(J)** Axon-like GFP+ processes (arrows) reaching the optic nerve in a Neurog2-electroporated retina. Nuclei are stained with DAPI (blue). Scale bars: **A-D** and **J**: 50 µm; **G**: 25 µm; **H-I**: 12,5 µm.

Lentiviral gene transfer of the proneural factor Ascl1 partially reprogrammed P11/12 Müller glial cells *in vitro* into retinal progenitors 3 weeks after infection (Pollak et al., 2013), a process facilitated by microRNA miR-124-9-9* (Wohl and Reh, 2016). Combination of Ascl1 and miR-124-9-9* led to a peak of 50–60% reprogrammed iNs, whereas Ascl1 alone reached 30–35% (Wohl and Reh, 2016). The latter is lower than what we found following expression of Ascl1, which may be due to the earlier age of the mice from which cells were isolated in our study (P7-9). Indeed, in our hands, MGCs isolated from P21 retina failed to reprogram into iNs upon expression of either ASCL1 or NEUROG2 (data not shown), similar to what has been described for astroglia isolated from the adult mouse cerebral cortex (Heinrich et al., 2010) or even for astroglia isolated from the postnatal cerebral cortex or cerebellum, and maintained in differentiation conditions for several days before ASCL1 or NEUROG2 expression (Masserdotti et al., 2015; Chouchane et al., 2017). This resistance to lineage conversion in astrocytes isolated at late developmental stages is likely explained by the epigenetic changes occurring in these cells during differentiation from an

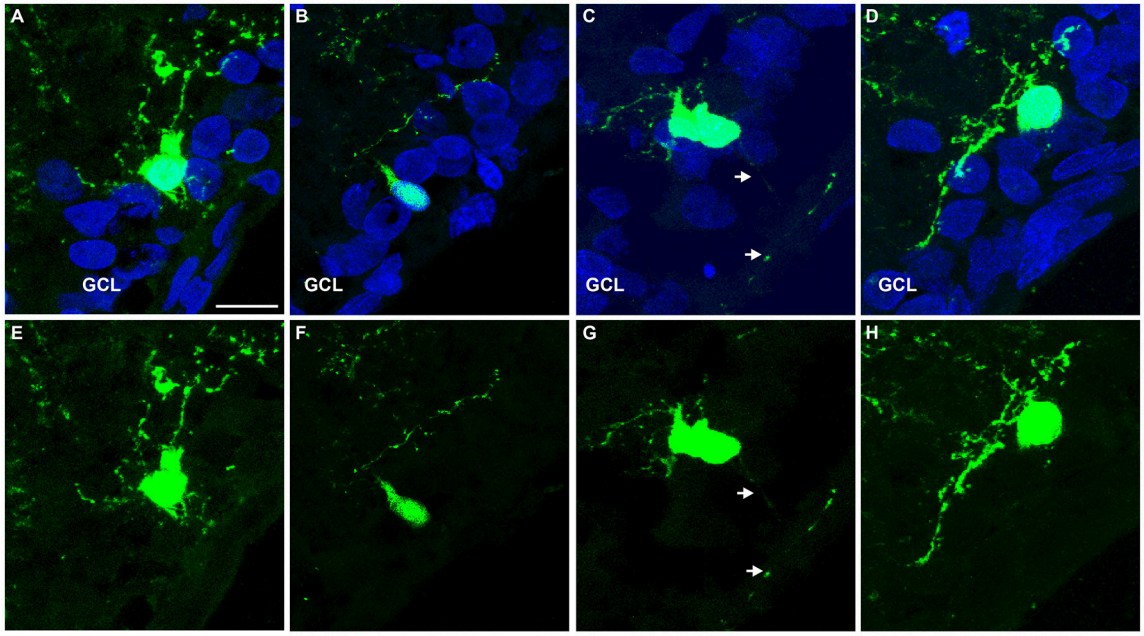

FIGURE 8 | Representative examples of GFP+ cells within the GCL of Neurog2-electroporated retinas. **(A–H)** Images show GFP+ cells (green) within the GCL of P10 rats after electroporation with Neurog2-I-GFP at P0. Nuclei are stained with DAPI (blue, **A–D**). Note the distinct positions and dendrite stratifications of GFP+ cells **(E-H)**, resembling *bona fide* subtypes of rodent RGCs (Sanes and Masland, 2015). Scale bar: 25 μm.

immature to mature state (Masserdotti et al., 2015). According to this interpretation, ASCL1-mediated lineage reprogramming of MGCs into iNs in adult mouse retina requires co-treatment with histone deacetylase-inhibitors (Jorstad et al., 2017).

Our data also showed that the presence of mitogenic factors EGF and FGF2 during MGC expansion substantially increased the efficiency of conversion into iNs, suggesting that exposure to those growth factors endows MGCs with higher plasticity. It has been shown that FGF2 induces methylation of Lysine 4 and suppresses methylation of Lysine 9 of histone H3 at the signal transducer and activator of transcription (STAT) binding site (Song and Ghosh, 2004), whereas EGF affects chromatin architecture at the regulatory element of cyclin D1, through a process involving Cre-binding protein (CBP), Histone deacetylase 1 (HDAC1) and Suv39h1 histone/chromatin remodeling complex (Lee et al., 2012). It is conceivable that such effects of EGF/FGF2 upon MGCs may facilitate the binding of NEUROG2 and ASCL1 to their target genes and, therefore, increases the efficiency of conversion. The effect was more pronounced for NEUROG2 than ASCL1; the latter has a known role in the remodeling of the chromatin landscape by itself, which increases its own accessibility to target genes (Raposo et al., 2015). In addition, expression of ASCL1 in NMDA-injured retinas of adult mice was sufficient to lineage reprogram only about 20% of MGCs into Otx2+ neurons, but this effect was enhanced by 2-fold in animals receiving concomitant treatment with trichostatin-A, a potent inhibitor of histone deacetylase (Jorstad et al., 2017).

Alternative explanations for the effects of EGF/FGF2 upon MGC-lineage conversion into iNs are rooted on the roles of these growth factors in cell proliferation (Todd et al., 2015) and survival (Rolf et al., 2003; Nickerson et al., 2011), dedifferentiation and possibly reprogramming, reviewed in Hamon et al. (2016). Recent work in the adult mouse retina demonstrates that genetic lineage reprogramming of MGCs into photoreceptors *in vivo* requires previous activation of cell proliferation trough activation of the beta-catenin pathway (Yao et al., 2018). Here, we observed a larger fraction of NESTIN+, SOX2+, and BrdU+ cells in MGC cultures grown in the presence of EGF/FGF2, suggesting an increase in cell proliferation. However, this effect was much smaller than that observed in lineage-reprogramming efficiencies, indicating that the increased number of iNs observed in cultures treated with EGF/FGF2 cannot be exclusively explained by an increase in MGC proliferation. Thus, the explanation that reprogramming is facilitated by EGF/FGF2 through effects upon chromatin structure remains a likely explanation, although further studies are needed to support this hypothesis.

A critical question in cell reprogramming is whether iNs acquire either single or multiple neuronal phenotypes (Amamoto and Arlotta, 2014; Heinrich et al., 2015). Recent work in our laboratory has shown that the origin of astroglial cells, either from cerebral cortex or cerebellum, affects the phenotype of iNs lineage-converted by either ASCL1 or NEUROG2 (Chouchane et al., 2017). Notably, most iNs generated from astroglia from either cerebellum or neocortex showed central hallmarks of neurons commonly observed in those regions, suggesting that a "molecular memory" in the astroglial cells contributes to the acquisition of specific neuronal phenotypes in iNs (Chouchane and Costa, 2018).

This notion is supported by our current finding that MGC-derived iNs upregulate several genes expressed in retinal neurons. Consistent with previous work (Pollak et al., 2013; Wohl and Reh, 2016; Jorstad et al., 2017), we found that ASCL1-converted MGCs generated iNs which express genes of horizontal and bipolar cells, but few genes commonly observed in photoreceptors, amacrine cells and RGCs, suggesting that these phenotypes are rare and/or incomplete in the converted cells. In contrast, expression of NEUROG2 converted MGCs into iNs accompanied by up-regulation of several genes of photoreceptors, amacrine cells and RGCs. Importantly, the latter phenotype is supported by the expression of two RGC-specific genes, namely Pou4f1 and Scl17a6 (Quina et al., 2005; Martersteck et al., 2017), as well as four other genes highly enriched in RGCs (Syn1, Parv, Calb2 and Tubb3). Immunolabeling confirmed the increased content of three of these markers (TUBB3, SYNAPSIN 1, PARVALBUMIN). Moreover, expression of the selective RGC marker RBPMS (Rodriguez et al., 2014) in MGC nucleofected with Neurog2 further suggests the acquisition of a RGC-like phenotype in iNs. These observations are particularly important, because previous attempts to lineage reprogram MGCs into iNs, both *in vitro* and *in vivo*, have failed to generate iNs with RGC-like phenotypes (Pollak et al., 2013; Wohl and Reh, 2016; Jorstad et al., 2017). Future experiments should address whether the expression of NEUROG2 in MGCs in the intact or injured adult retina are sufficient to lineage convert these cells into RGCs. Nevertheless, our observations in post-natal retinas indicate that NEUROG2 has an important instructive role for the RGC phenotype *in vivo*.

Altogether, our study corroborates previous evidence of the potential of MGC to reprogram into iNs following expression of ASCL1 (Pollak et al., 2013; Wohl and Reh, 2016; Jorstad et al., 2017), and provides compelling evidence that NEUROG2 expression is also sufficient to convert MGCs into iNs expressing several features of RGCs. Our results may thus contribute to develop new strategies of gene therapy aiming at the regeneration of retinal neurons in patients with glaucoma and other neurodegenerative retinopathies.

AUTHOR CONTRIBUTIONS

All authors reviewed the manuscript. RG and BL contributed to design and perform the experiments, analyzed the data, discussed the results, and prepare figures of the manuscript. DG. performed qPCR experiments. DC analyzed single cell RNAseq data. MS conceived electroporation experiments, discussed the results, and contributed to the manuscript. RdMR and RL co-supervised RG's thesis, and contributed to the manuscript. MC provided financial support, directed the project, conceived the experiments, analyzed data, discussed the results, and wrote the manuscript.

ACKNOWLEDGMENTS

We would like to thank Viviane Valença and Pedro Lucas França for their contribution with *in vivo* electroporation experiments. This work was supported by Conselho Nacional de Desenvolvimento Científico e Tecnológico (CNPq), Coordenação de Aperfeiçoamento de Pessoal de Nível Superior (CAPES), Fundação de Amparo à pesquisa do Rio de Janeiro (FAPERJ) and Instituto Nacional de Neurociência Translacional (INNT).

SUPPLEMENTARY MATERIAL

The Supplementary Material for this article can be found online at: https://www.frontiersin.org/articles/10.3389/fncel.2018.00410/full#supplementary-material

Figure S1 | Polarized morphologies are more common in Neurog2- than Ascl1-iNs. **(A)** Morphologies of iNs derived from MGCs nucleofected with either *Neurog2* or *Ascl1*. **(B)** Cartesian plot representing the orientations of primary dendrites in iNs generated in different conditions (Neurog2 without GF = 31 iNs; Neurog2 with GF = 19 iNs; Ascl1 without GF = 21 iNs; Ascl1 with GF = 26 iNs). **(C)** Frequencies of iNs showing unipolar, bipolar, or multipolar morphologies according to the TF used (Neurog2= 50 iNs; Asc1= 47 iNs). Observe the higher number of uni/bipolar among Neurog2-induced neurons ($p < 0.05$; Chi-square test).

Figure S2 | Identification of major retina cell types using single-cell transcriptomes. **(A)** Clustering of 21,176 single-cell expression profiles into 39 retinal cell populations using available dataset (Macosko et al., 2015). The plot shows a two-dimensional representation (tSNE) of global gene expression relationships among 21,176 cells. **(B)** Annotation of the same cells into the 7 major retinal cell types, according to the expression of cell-type specific genes. **(C)** List of some differently expressed genes used to classify the 7 major retina cell types and also used to identify the phenotypes of iNs in this study (RT-qPCR and immunocytochemistry).

Figure S3 | Gene expression in cerebellar astroglia cells nucleofected with Neurog2 or Asc1. Graphic showing the relative expression levels (log_{10}) of genes used to identify presumptive retina cell phenotypes (**Figure 5**) cerebellar astroglia cell cultures nucleofected with either Neurog2 (white bars) or Ascl1 (black bars). Observe that genes commonly observed in cerebellar neurons (Prox1, Vsx2, Slc32a1, Chat, Rbfox3, and Syn1) are upregulated, whereas genes whose expression is restricted to retinal neurons (Nrl, Rho, Pou4f1, Slc17a6) are not up regulated in cerebellar astroglia-derived iNs.

Figure S4 | Expression of CRALBP in MGCs generated in the postnatal retina electroporated with control-I-GFP. **(A–C)** Coronal section of a P10 rat retina after electroporation with Control-I-GFP at P0, immunolabeled for GFP (green) and CRALBP (red). Images are single confocal Z-stacks and show the co-localization of GFP and CRALB in MGC fibers (arrows). Scale bar: 25 μm.

Figure S5 | Expression of β_{III}-TUBULIN in RGCs generated in the postnatal retina following Neurog2-electroporation. **(A)** Coronal section of a P10 rat retina after electroporation with Neurog2-I-GFP at P0, immunolabeled for GFP (green) and β_{III}-TUBULIN (TUBB3, red). Nuclei are stained with DAPI (blue). Image is a Z-projection of 8 confocal Z-stacks. Dashed box delimits a GFP+ cell within the ganglion cell layer (GCL). **(B,C)** Magnification of the dashed box in A showing the co-localization of GFP and β_{III}-TUBULIN in a single confocal Z-stack. Scale bars: **A**: 50 μm; **B,C**: 25 μm.

Supplementary Video 1 | MGC expanded in the presence of EGF/FGF2 and lineage reprogrammed into iNs by NEUROG2 show fast calcium transients. Movie shows 600 frames taken with 10 ms exposure time and no interval. Observe the fast fluorescence intensity increase in the MGC-derived iN indicated by a red arrow in **Figures 4A,B.** MGCs in the same field show slow oscillations in fluorescence.

Supplementary Video 2 | MGC expanded in the absence of EGF/FGF2 and lineage reprogrammed into iNs by NEUROG2 show fast calcium transients. Movie shows 600 frames taken with 10 ms exposure time and no interval. Observe the fast fluorescence intensity increase in the MGC-derived iN indicated by a red arrow in **Figures 4C**,**D**. MGCs in the same field show slow oscillations in fluorescence.

REFERENCES

Abu-Hassan, D. W., Li, X., Ryan, E. I., Acott, T. S., and Kelley, M. J. (2015). Induced pluripotent stem cells restore function in a human cell loss model of open-angle glaucoma. *Stem Cells* 33, 751–761. doi: 10.1002/stem.1885

Amamoto, R., and Arlotta, P. (2014). Development-inspired reprogramming of the mammalian central nervous system. *Science* 343:1239882. doi: 10.1126/science.1239882

Athanasiou, D., Aguila, M., Bevilacqua, D., Novoselov, S. S., Parfitt, D. A., and Cheetham, M. E. (2013). The cell stress machinery and retinal degeneration. *FEBS Lett*. 587, 2008–2017. doi: 10.1016/j.febslet.2013.05.020

Berninger, B., Costa, M. R., Koch, U., Schroeder, T., Sutor, B., Grothe, B., et al. (2007). Functional properties of neurons derived from *in vitro* reprogrammed postnatal astroglia. *J Neurosci* 27, 8654–8664. doi: 10.1523/JNEUROSCI.1615-07.2007

Bhatia, B., Singhal, S., Tadman, D. N., Khaw, P. T., and Limb, G. A. (2011). SOX2 is required for adult human muller stem cell survival and maintenance of progenicity *in vitro*. *Invest. Ophthalmol. Vis. Sci*. 52, 136–145. doi: 10.1167/iovs.10-5208

Blackshaw, S., Harpavat, S., Trimarchi, J., Cai, L., Huang, H., Kuo, W. P., et al. (2004). Genomic analysis of mouse retinal development. *PLoS Biol*. 2:E247. doi: 10.1371/journal.pbio.0020247

Bonifazi, P., Goldin, M., Picardo, M. A., Jorquera, I., Cattani, A., Bianconi, G., et al. (2009). GABAergic hub neurons orchestrate synchrony in developing hippocampal networks. *Science* 326, 1419–1424. doi: 10.1126/science.1175509

Brzezinski, J. A. T., Kim, E. J., Johnson, J. E., and Reh, T. A. (2011). Ascl1 expression defines a subpopulation of lineage-restricted progenitors in the mammalian retina. *Development* 138, 3519–3531. doi: 10.1242/dev.064006

Cepko, C. L. (1999). The roles of intrinsic and extrinsic cues and bHLH genes in the determination of retinal cell fates. *Curr. Opin. Neurobiol*. 9, 37–46. doi: 10.1016/S0959-4388(99)80005-1

Chamling, X., Sluch, V. M., and Zack, D. J. (2016). The potential of human stem cells for the study and treatment of glaucoma. *Invest. Ophthalmol. Vis. Sci*. 57, ORSFi1-6. doi: 10.1167/iovs.15-18590

Chouchane, M., and Costa, M. R. (2018). Instructing neuronal identity during CNS development and astroglial-lineage reprogramming: roles of NEUROG2 and ASCL1. *Brain Res*. doi: 10.1016/j.brainres.2018.02.045. [Epub ahead of print].

Chouchane, M., Melo De Farias, A. R., Moura, D. M. S., Hilscher, M. M., Schroeder, T., Leao, R. N., et al. (2017). Lineage reprogramming of astroglial cells from different origins into distinct neuronal subtypes. *Stem Cell Rep*. 9, 162–176. doi: 10.1016/j.stemcr.2017.05.009

Das, A. V., Mallya, K. B., Zhao, X., Ahmad, F., Bhattacharya, S., Thoreson, W. B., et al. (2006). Neural stem cell properties of Muller glia in the mammalian retina: regulation by Notch and Wnt signaling. *Dev. Biol*. 299, 283–302. doi: 10.1016/j.ydbio.2006.07.029

de Melo Reis, R. A., Cabral-Da-Silva, M., De Mello, F. G., and Taylor, J. S. (2008). Muller glia factors induce survival and neuritogenesis of peripheral and central neurons. *Brain Res*. 1205, 1–11. doi: 10.1016/j.brainres.2008.02.035

de Melo, J., and Blackshaw, S. (2018). *In vivo* electroporation of developing mouse retina. *Methods Mol. Biol*. 1715, 101–111. doi: 10.1007/978-1-4939-7522-8_8

Giannelli, S. G., Demontis, G. C., Pertile, G., Rama, P., and Broccoli, V. (2011). Adult human Muller glia cells are a highly efficient source of rod photoreceptors. *Stem Cells* 29, 344–356. doi: 10.1002/stem.579

Gill, K. P., Hung, S. S., Sharov, A., Lo, C. Y., Needham, K., Lidgerwood, G. E., et al. (2016). Enriched retinal ganglion cells derived from human embryonic stem cells. *Sci. Rep*. 6:30552. doi: 10.1038/srep30552

Hamon, A., Roger, J. E., Yang, X. J., and Perron, M. (2016). Muller glial cell-dependent regeneration of the neural retina: an overview across vertebrate model systems. *Dev. Dyn*. 245, 727–738. doi: 10.1002/dvdy.24375

He, J., Zhang, G., Almeida, A. D., Cayouette, M., Simons, B. D., and Harris, W. A. (2012). How variable clones build an invariant retina. *Neuron* 75, 786–798. doi: 10.1016/j.neuron.2012.06.033

Heinrich, C., Blum, R., Gascon, S., Masserdotti, G., Tripathi, P., Sanchez, R., et al. (2010). Directing astroglia from the cerebral cortex into subtype specific functional neurons. *PLoS Biol*. 8:e1000373. doi: 10.1371/journal.pbio.1000373

Heinrich, C., Spagnoli, F. M., and Berninger, B. (2015). *In vivo* reprogramming for tissue repair. *Nat. Cell Biol*. 17, 204–211. doi: 10.1038/ncb3108

Hicks, D., and Courtois, Y. (1990). The growth and behaviour of rat retinal Muller cells *in vitro*. 1. An improved method for isolation and culture. *Exp. Eye Res*. 51, 119–129. doi: 10.1016/0014-4835(90)90063-Z

Hufnagel, R. B., Le, T. T., Riesenberg, A. L., and Brown, N. L. (2010). Neurog2 controls the leading edge of neurogenesis in the mammalian retina. *Dev. Biol*. 340, 490–503. doi: 10.1016/j.ydbio.2010.02.002

Jadhav, A. P., Roesch, K., and Cepko, C. L. (2009). Development and neurogenic potential of Muller glial cells in the vertebrate retina. *Prog. Retin. Eye Res*. 28, 249–262. doi: 10.1016/j.preteyeres.2009.05.002

Jorstad, N. L., Wilken, M. S., Grimes, W. N., Wohl, S. G., Vandenbosch, L. S., Yoshimatsu, T., et al. (2017). Stimulation of functional neuronal regeneration from Muller glia in adult mice. *Nature* 548, 103–107. doi: 10.1038/nature23283

Karl, M. O., Hayes, S., Nelson, B. R., Tan, K., Buckingham, B., and Reh, T. A. (2008). Stimulation of neural regeneration in the mouse retina. *Proc. Natl. Acad. Sci. U.S.A.* 105, 19508–19513. doi: 10.1073/pnas.0807453105

Karl, M. O., and Reh, T. A. (2012). Studying the generation of regenerated retinal neuron from Muller glia in the mouse eye. *Methods Mol. Biol*. 884, 213–227. doi: 10.1007/978-1-61779-848-1_15

Kimura, A., Namekata, K., Guo, X., Noro, T., Harada, C., and Harada, T. (2017). Targeting oxidative stress for treatment of glaucoma and optic neuritis. *Oxid. Med. Cell Longev*. 2017:2817252. doi: 10.1155/2017/2817252

Lawrence, J. M., Singhal, S., Bhatia, B., Keegan, D. J., Reh, T. A., Luthert, P. J., et al. (2007). MIO-M1 cells and similar muller glial cell lines derived from adult human retina exhibit neural stem cell characteristics. *Stem Cells* 25, 2033–2043. doi: 10.1634/stemcells.2006-0724

Lee, J. H., Choy, M. L., and Marks, P. A. (2012). Mechanisms of resistance to histone deacetylase inhibitors. *Adv. Cancer Res*. 116, 39–86. doi: 10.1016/B978-0-12-394387-3.00002-1

Liang, Y. B., Zhang, Y., Musch, D. C., and Congdon, N. (2017). Proposing new indicators for glaucoma healthcare service. *Eye Vis*. 4:6. doi: 10.1186/s40662-017-0071-0

Lin, Y. P., Ouchi, Y., Satoh, S., and Watanabe, S. (2009). Sox2 plays a role in the induction of amacrine and Muller glial cells in mouse retinal progenitor cells. *Invest. Ophthalmol. Vis. Sci*. 50, 68–74. doi: 10.1167/iovs.07-1619

Livak, K. J., and Schmittgen, T. D. (2001). Analysis of relative gene expression data using real-time quantitative PCR and the 2(-Delta Delta C(T)) Method. *Methods* 25, 402–408. doi: 10.1006/meth.2001.1262

Loffler, K., Schafer, P., Volkner, M., Holdt, T., and Karl, M. O. (2015). Age-dependent Muller glia neurogenic competence in the mouse retina. *Glia* 63, 1809–1824. doi: 10.1002/glia.22846

Macosko, E. Z., Basu, A., Satija, R., Nemesh, J., Shekhar, K., Goldman, M., et al. (2015). Highly parallel genome-wide expression profiling of individual cells using nanoliter droplets. *Cell* 161, 1202–1214. doi: 10.1016/j.cell.2015.05.002

Martersteck, E. M., Hirokawa, K. E., Evarts, M., Bernard, A., Duan, X., Li, Y., et al. (2017). Diverse central projection patterns of retinal ganglion cells. *Cell Rep*. 18, 2058–2072. doi: 10.1016/j.celrep.2017.01.075

Masserdotti, G., Gillotin, S., Sutor, B., Drechsel, D., Irmler, M., Jorgensen, H. F., et al. (2015). Transcriptional mechanisms of proneural factors and REST in regulating neuronal reprogramming of astrocytes. *Cell Stem Cell* 17, 74–88. doi: 10.1016/j.stem.2015.05.014

Matsuda, T., and Cepko, C. L. (2004). Electroporation and RNA interference in the rodent retina *in vivo* and *in vitro*. *Proc. Natl. Acad. Sci. U.S.A.* 101, 16–22. doi: 10.1073/pnas.2235688100

Matsuda, T., and Cepko, C. L. (2007). Controlled expression of transgenes introduced by *in vivo* electroporation. *Proc. Natl. Acad. Sci. U.S.A*. 104, 1027–1032. doi: 10.1073/pnas.0610155104

Nelson, B. R., Ueki, Y., Reardon, S., Karl, M. O., Georgi, S., Hartman, B. H., et al. (2011). Genome-wide analysis of Muller glial differentiation reveals a requirement for Notch signaling in postmitotic cells to maintain the glial fate. *PLoS ONE* 6:e22817. doi: 10.1371/journal.pone.0022817

Nickerson, P. E., Da Silva, N., Myers, T., Stevens, K., and Clarke, D. B. (2008). Neural progenitor potential in cultured Muller glia: effects of passaging and exogenous growth factor exposure. *Brain Res*. 1230, 1–12. doi: 10.1016/j.brainres.2008.03.095

Nickerson, P. E., Mcleod, M. C., Myers, T., and Clarke, D. B. (2011). Effects of epidermal growth factor and erythropoietin on Muller glial activation and phenotypic plasticity in the adult mammalian retina. *J. Neurosci. Res*. 89, 1018–1030. doi: 10.1002/jnr.22629

Ooto, S., Akagi, T., Kageyama, R., Akita, J., Mandai, M., Honda, Y., et al. (2004). Potential for neural regeneration after neurotoxic injury in the adult mammalian retina. *Proc. Natl. Acad. Sci. U.S.A.* 101, 13654–13659. doi: 10.1073/pnas.0402129101

Pollak, J., Wilken, M. S., Ueki, Y., Cox, K. E., Sullivan, J. M., Taylor, R. J., et al. (2013). ASCL1 reprograms mouse Muller glia into neurogenic retinal progenitors. *Development* 140, 2619–2631. doi: 10.1242/dev.091355

Quina, L. A., Pak, W., Lanier, J., Banwait, P., Gratwick, K., Liu, Y., et al. (2005). Brn3a-expressing retinal ganglion cells project specifically to thalamocortical and collicular visual pathways. *J. Neurosci.* 25, 11595–11604. doi: 10.1523/JNEUROSCI.2837-05.2005

Rapaport, D. H., Wong, L. L., Wood, E. D., Yasumura, D., and Lavail, M. M. (2004). Timing and topography of cell genesis in the rat retina. *J. Comp. Neurol.* 474, 304–324. doi: 10.1002/cne.20134

Raposo, A. A., Vasconcelos, F. F., Drechsel, D., Marie, C., Johnston, C., Dolle, D., et al. (2015). Ascl1 coordinately regulates gene expression and the chromatin landscape during neurogenesis. *Cell Rep.* 10, 1544–1556. doi: 10.1016/j.celrep.2015.02.025

Rodriguez, A. R., De Sevilla Muller, L. P., and Brecha, N. C. (2014). The RNA binding protein RBPMS is a selective marker of ganglion cells in the mammalian retina. *J. Comp. Neurol.* 522, 1411–1443. doi: 10.1002/cne.23521

Rolf, B., Lang, D., Hillenbrand, R., Richter, M., Schachner, M., and Bartsch, U. (2003). Altered expression of CHL1 by glial cells in response to optic nerve injury and intravitreal application of fibroblast growth factor-2. *J. Neurosci. Res.* 71, 835–843. doi: 10.1002/jnr.10533

Sanes, J. R., and Masland, R. H. (2015). The types of retinal ganglion cells: current status and implications for neuronal classification. *Annu. Rev. Neurosci.* 38, 221–246. doi: 10.1146/annurev-neuro-071714-034120

Singhal, S., Bhatia, B., Jayaram, H., Becker, S., Jones, M. F., Cottrill, P. B., et al. (2012). Human Muller glia with stem cell characteristics differentiate into retinal ganglion cell (RGC) precursors *in vitro* and partially restore RGC function *in vivo* following transplantation. *Stem Cells Transl. Med.* 1, 188–199. doi: 10.5966/sctm.2011-0005

Song, M. R., and Ghosh, A. (2004). FGF2-induced chromatin remodeling regulates CNTF-mediated gene expression and astrocyte differentiation. *Nat. Neurosci.* 7, 229–235. doi: 10.1038/nn1192

Song, W. T., Zhang, X. Y., and Xia, X. B. (2013). Atoh7 promotes the differentiation of retinal stem cells derived from Muller cells into retinal ganglion cells by inhibiting Notch signaling. *Stem Cell Res. Ther.* 4:94. doi: 10.1186/scrt305

Todd, L., Volkov, L. I., Zelinka, C., Squires, N., and Fischer, A. J. (2015). Heparin-binding EGF-like growth factor (HB-EGF) stimulates the proliferation of Muller glia-derived progenitor cells in avian and murine retinas. *Mol. Cell Neurosci.* 69, 54–64. doi: 10.1016/j.mcn.2015.10.004

Torper, O., and Gotz, M. (2017). Brain repair from intrinsic cell sources: Turning reactive glia into neurons. *Prog. Brain. Res.* 230, 69–97. doi: 10.1016/bs.pbr.2016.12.010

Turner, D. L., Snyder, E. Y., and Cepko, C. L. (1990). Lineage-independent determination of cell type in the embryonic mouse retina. *Neuron* 4, 833–845. doi: 10.1016/0896-6273(90)90136-4

Ueki, Y., Wilken, M. S., Cox, K. E., Chipman, L., Jorstad, N., Sternhagen, K., et al. (2015). Transgenic expression of the proneural transcription factor Ascl1 in Muller glia stimulates retinal regeneration in young mice. *Proc. Natl. Acad. Sci. U.S.A.* 112, 13717–13722. doi: 10.1073/pnas.1510595112

Wilken, M. S., and Reh, T. A. (2016). Retinal regeneration in birds and mice. *Curr. Opin. Genet. Dev.* 40, 57–64. doi: 10.1016/j.gde.2016.05.028

Wohl, S. G., and Reh, T. A. (2016). miR-124-9-9* potentiates Ascl1-induced reprogramming of cultured Muller glia. *Glia* 64, 743–762. doi: 10.1002/glia.22958

Wong-Riley, M. T. (2010). Energy metabolism of the visual system. *Eye Brain* 2, 99–116. doi: 10.2147/EB.S9078

Wu, Z. K., Cao, L., Zhang, X. Y., Song, W. T., and Xia, X. B. (2016). Promotion on the differentiation of retinal Muller cells into retinal ganglion cells by Brn-3b. *Int. J. Ophthalmol.* 9, 948–954. doi: 10.18240/ijo.2016.07.03

Yang, W., and Yuste, R. (2017). *In vivo* imaging of neural activity. *Nat. Methods* 14, 349–359. doi: 10.1038/nmeth.4230

Yao, K., Qiu, S., Wang, Y. V., Park, S. J. H., Mohns, E. J., Mehta, B., et al. (2018). Restoration of vision after *de novo* genesis of rod photoreceptors in mammalian retinas. *Nature* 560, 484–488. doi: 10.1038/s41586-018-0425-3

Young, R. W. (1985). Cell differentiation in the retina of the mouse. *Anat. Rec.* 212, 199–205. doi: 10.1002/ar.1092120215

Conflict of Interest Statement: The authors declare that the research was conducted in the absence of any commercial or financial relationships that could be construed as a potential conflict of interest.

frontiers in Cellular Neuroscience

ORIGINAL RESEARCH
published: 28 November 2018
doi: 10.3389/fncel.2018.00441

Brain-Derived Neurotrophic Factor (BDNF) Role in Cannabinoid-Mediated Neurogenesis

*Filipa Fiel Ferreira[1,2†], Filipa F. Ribeiro[1,2†], Rui S. Rodrigues[1,2†], Ana Maria Sebastião[1,2] and Sara Xapelli[1,2]**

[1] Instituto de Farmacologia e Neurociências, Faculdade de Medicina, Universidade de Lisboa, Lisbon, Portugal, [2] Instituto de Medicina Molecular João Lobo Antunes, Faculdade de Medicina, Universidade de Lisboa, Lisbon, Portugal

The adult mammalian brain can produce new neurons in a process called adult neurogenesis, which occurs mainly in the subventricular zone (SVZ) and in the hippocampal dentate gyrus (DG). Brain-derived neurotrophic factor (BDNF) signaling and cannabinoid type 1 and 2 receptors (CB1R and CB2R) have been shown to independently modulate neurogenesis, but how they may interact is unknown. We now used SVZ and DG neurosphere cultures from early (P1-3) postnatal rats to study the CB1R and CB2R crosstalk with BDNF in modulating neurogenesis. BDNF promoted an increase in SVZ and DG stemness and cell proliferation, an effect blocked by a CB2R selective antagonist. CB2R selective activation promoted an increase in DG multipotency, which was inhibited by the presence of a BDNF scavenger. CB1R activation induced an increase in SVZ and DG cell proliferation, being both effects dependent on BDNF. Furthermore, SVZ and DG neuronal differentiation was facilitated by CB1R and/or CB2R activation and this effect was blocked by sequestering endogenous BDNF. Conversely, BDNF promoted neuronal differentiation, an effect abrogated in SVZ cells by CB1R or CB2R blockade while in DG cells was inhibited by CB2R blockade. We conclude that endogenous BDNF is crucial for the cannabinoid-mediated effects on SVZ and DG neurogenesis. On the other hand, cannabinoid receptor signaling is also determinant for BDNF actions upon neurogenesis. These findings provide support for an interaction between BDNF and endocannabinoid signaling to control neurogenesis at distinct levels, further contributing to highlight novel mechanisms in the emerging field of brain repair.

Keywords: postnatal neurogenesis, subventricular zone, dentate gyrus, cannabinoid receptors, brain-derived neurotrophic factor

OPEN ACCESS

Edited by:
Josef Bischofberger, Universität Basel, Switzerland

Reviewed by:
Alex Dranovsky, Columbia University, United States
Jorge Matias-Guiu, Complutense University of Madrid, Spain

****Correspondence:***
Sara Xapelli
sxapelli@medicina.ulisboa.pt

†Shared authorship

Received: *31 July 2018*
Accepted: *05 November 2018*
Published: *28 November 2018*

Citation:
Ferreira F, Ribeiro FF, Rodrigues RS, Sebastião AM and Xapelli S (2018) Brain-Derived Neurotrophic Factor (BDNF) Role in Cannabinoid- Mediated Neurogenesis. Front. Cell. Neurosci. 12:441. doi: 10.3389/fncel.2018.00441

INTRODUCTION

Constitutive neurogenesis occurs in the adult mammalian brain where NSPC are able to differentiate into three neural lineages, neurons, astrocytes and oligodendrocytes (Gage, 2000; Gross, 2000). These multipotent cells exhibit properties of self-renewal and cell proliferation that allow the maintenance of their own pool (Ma et al., 2009). Neurogenesis occurs mainly in two brain areas, the subventricular zone (SVZ) and the subgranular zone (SGZ) within the DG of

Abbreviations: Δ^9-THC, Δ^9-tetrahydrocannabinol; BDNF, brain-derived neurotrophic factor; CB1R, cannabinoid receptor type 1; CB2R, cannabinoid receptor type 2; CNS, central nervous system; DG, dentate gyrus; EGF, epidermal growth factor; FGF-2, fibroblast growth factor-2; NSPC, neural stem/progenitor cells; SGZ, subgranular zone; SVZ, subventricular zone.

the hippocampus. These regions are packed with NSPC that originate neuroblasts which migrate toward their final destinations, where they differentiate into mature neurons and are integrated into the neuronal circuitry (Lledo et al., 2006; Zhao et al., 2008; Ming and Song, 2011).

Adult neurogenesis and the neurogenic niches are highly regulated by several factors (intrinsic and extrinsic factors) that control the NSPC rates of proliferation, lineage differentiation, migration, maturation and survival (Ming and Song, 2011). Knowing and understanding the actions of these factors will further contribute to develop new therapeutic strategies useful for brain repair and regeneration. However, there is still a lack of knowledge regarding the key factors that regulate each step of postnatal neurogenesis.

The role of neurotrophins and, in particular, brain-derived neurotrophic factor (BDNF) in adult neurogenesis has been the subject of many studies (Henry et al., 2007; Chan et al., 2008; Vilar and Mira, 2016). BDNF is expressed in both SVZ and SGZ neurogenic niches (Galvão et al., 2008; Li et al., 2008) but its precise role in adult neurogenesis is still not consensual. In fact, some studies suggest that BDNF is important to positively regulate DG cell proliferation and survival (Chan et al., 2008; Li et al., 2008) while others report no BDNF-induced changes in DG neurogenesis (Choi et al., 2009). In SVZ, most studies depict that BDNF does not promote any significant changes in cell proliferation and survival (Henry et al., 2007; Galvão et al., 2008), despite having a role in the migration of SVZ-derived cells (Snapyan et al., 2009; Bagley and Belluscio, 2010). Despite the available contradictory data, BDNF, through TrkB signaling, was shown to have an essential role in the regulation of dendritic complexity as well as synaptic formation, maturation and plasticity of newborn neurons (Chan et al., 2008; Gao et al., 2009; Wang et al., 2015).

Besides expressing BDNF, NSPC present in the neurogenic niches were shown to express all the elements of the endocannabinoid system (Aguado et al., 2005; Arévalo-Martín et al., 2007), including the main cannabinoid receptors type 1 (CB1R) and type 2 (CB2R) receptors (Rodrigues et al., 2017). They are both present in the CNS, although CB2R expression is relatively higher in the immune system (Galve-Roperh et al., 2007). In recent years, the role of cannabinoids in neurogenesis has been of particular interest given their multiplicity of neuromodulatory functions (Mechoulam and Parker, 2013). Cannabinoid receptors modulate adult neurogenesis by acting at distinct neurogenic phases (Prenderville et al., 2015). Importantly, activation of type 1 (Xapelli et al., 2013) or type 2 cannabinoid receptors (Palazuelos et al., 2006) by selective agonists was found to regulate cell proliferation, neuronal differentiation and maturation (Rodrigues et al., 2017).

Several studies have provided molecular and functional evidence for a crosstalk between BDNF and endocannabinoid signaling (Maison et al., 2009; Zhao et al., 2015). Synergism between BDNF and CB1R has been observed both *in vitro* and *in vivo* (De Chiara et al., 2010; Galve-Roperh et al., 2013). In particular, BDNF was shown to regulate striatal CB1R actions (De Chiara et al., 2010). Moreover, evidence for BDNF-TrkB signaling interplay with CB1R has been shown to trigger endocannabinoid release at cortical excitatory synapses (Yeh et al., 2017). Importantly, genetic deletion of CB1R was shown to promote a decrease in BDNF expression (Aso et al., 2008) while induction of BDNF expression contributed to the protective effect of CB1R activity against excitotoxicity (Marsicano, 2003; Khaspekov et al., 2004). Moreover, CB1R activity can enhance TrkB signaling partly by activating MAP kinase/ERK kinase pathways (Derkinderen et al., 2003) but also by directly transactivating the TrkB receptors (Berghuis et al., 2005). Δ^9-THC, the principal active component of cannabis, was shown to promote upregulation of BDNF expression (Butovsky et al., 2005) whereas increased levels of BDNF were shown to rescue the cognitive deficits promoted by Δ^9-THC administration (Segal-Gavish et al., 2017). Interestingly, clinical data suggests that acute and chronic intermittent exposure to Δ^9-THC alters BDNF serum levels in humans (D'Souza et al., 2009).

Given the evidence that BDNF and cannabinoid signaling can affect neurogenesis as well as the fact that BDNF may interact with cannabinoid receptors, we hypothesized that cannabinoid receptors could act together with BDNF signaling to fine-tune neurogenesis. We show for the first time that endogenous BDNF is crucial for the cannabinoid-mediated effects on SVZ and DG neurogenesis to happen. Moreover, we demonstrate that CB2R has a preponderant role in regulating some of the BDNF actions on neurogenesis. Taken together, our results suggest an important crosstalk between BDNF and cannabinoid signaling to modulate postnatal neurogenesis.

MATERIALS AND METHODS

Ethics

All experiments were performed in accordance with the European Community (86/609/EEC; 2010/63/EU; 2012/707/EU) and Portuguese (DL 113/2013) legislation for the protection of animals used for scientific purposes. The protocol was approved by the "iMM's institutional Animal Welfare Body – ORBEA-iMM and the National competent authority – DGAV (Direcção Geral de Alimentação e Veterinária)." The work was performed with biological material obtained from rat pups and subsequently maintained *in vitro*. The pups were handled according to standard and humanitarian procedures to reduce animal suffering.

SVZ and DG Cell Cultures

SVZ and DG neurospheres were prepared from early postnatal (P1-3) Sprague-Dawley rats. SVZ and DG fragments were dissected out from 450 μm-thick coronal brain slices, digested with 0.05% Trypsin-EDTA (Life Technologies, Carlsbad, CA, United States) in Hank's balanced saline solution (HBSS, Life Technologies), and mechanically dissociated with a P1000 pipette. The originated cell suspension was then diluted in serum-free medium (SFM), composed of Dulbecco's modified Eagle's medium/Ham's F-12 medium with glutaMAX (DMEM+GlutaMAX, Life Technologies) supplemented with 100 U/mL penicillin and 100 μg/mL streptomycin (Pen/Strep; Life Technologies), 1% B27 (Life Technologies) and growth

factors (for SVZ cells: 20 ng/mL epidermal growth factor (EGF; Life Technologies); for DG cells: 20 ng/mL epidermal growth factor (EGF; Life Technologies) and 10 ng/mL fibroblast growth factor-2 (FGF-2; Life Technologies) (proliferative conditions). SVZ cells were then plated on uncoated Petri dishes and allowed to develop for 6 days, whereas DG cells were allowed to develop for 10 days, both in a 95% air-5% CO2 humified atmosphere at 37°C. Six-day-old SVZ neurospheres and 10-day-old DG neurospheres were adhered for 24 h onto glass coverslips coated with 0.1 mg/mL poly-D-lysine (PDL, Sigma-Aldrich, St. Louis, MO, United States) in SFM devoid of growth factors (differentiative conditions). Two days after plating, the medium was renewed with or without (control) a range of pharmacological treatments (see **Table 1**).

Pharmacological Treatments

To investigate the crosstalk between CB1R, CB2R and BDNF on cell-fate, cell proliferation and neuronal differentiation CB1R selective agonist (ACEA, 1 μM), CB2R selective agonist (HU-308, 1 μM), non-selective cannabinoid receptor agonist WIN55,212-2 (1 μM) or BDNF (30 ng/mL) were incubated in SVZ and DG cell cultures. Moreover, selective antagonists for CB1R (AM251, 1 μM) and CB2Rs (AM630, 1 μM) or scavenger for BDNF (TrkB-Fc, 2 μg/mL) were used (**Table 1**). TrkB-Fc chimera consists of an extracellular domain of human TrkB fused to the C-terminal Fc region of human IgG1 used to bind to BDNF, therefore, removing available BDNF in the media. The ligand concentrations used in the studies were selected from previous published work (Rodrigues et al., 2017).

To study cell-fate, a Sox2 cell-pair assay was performed as described by Xapelli et al. (2013), where dissociated SVZ and DG cell suspensions obtained during the cell culture procedure were plated on poly-D-lysine coated glass coverslips at a density of 12800 cells/cm^2 and 19200 cells/cm^2, respectively. After seeding, SVZ and DG cells were grown, respectively, in SFM supplemented with 10 ng/mL EGF (low EGF) and in SFM supplemented with 10 ng/mL EGF and 5 ng/mL FGF-2 (low EGF/FGF-2). Moreover, plated cells were treated for 24 h with the drugs that modulate CB1R and CB2R and, BDNF (**Table 1**).

To study cell proliferation, plated neurospheres in differentiative conditions were allowed to develop for 48h in the absence (control) or presence with the aforementioned drugs (**Table 1**).

Neuronal differentiation was assessed by allowing neurospheres to develop for 7 days in the absence (control) or presence of the drugs (**Table 1**).

Whenever cultures needed to be co-treated with a combination of drugs, treatment with selective antagonists for CB1Rs and CB2Rs or TrkB-Fc was performed 30 min prior to the treatment with the CB1R or CB2R selective agonists or BDNF.

Cell Commitment Study (Cell-Pair Assay)

Dissociated SVZ or DG cells that were treated for 24 h with the drugs were fixed in phosphate-buffered saline (PBS) containing

TABLE 1 | Pharmacological treatments used.

Drug	Chemical name	Concentration used	Catalog number	K_i value, nM (according to Pertwee, 2008)	Company
WIN55,212-2 [(R)-(+)-[2,3-Dihydro-5-methyl-3-(4-morpholinylmethyl)pyrrolo[1,2,3-de]-1,4-benzoxazin-6-yl]-1-naphthalenylmethanone]	Cannabinoid receptor CB_1 or CB_2 non-selective agonist	1 μM	1038	1.89–123 for CB1R or 0.28–16.2 for CB2R	Tocris, Bristol (United Kingdom)
ACEA [*N*-(2-Chloroethyl)-5*Z*,8*Z*,11*Z*,14*Z*-eicosatetraenamide]	Cannabinoid CB_1 receptor selective agonist	1 μM	1319	1.4 for CB1R	
HU-308 [4-[4-(1,1-Dimethylheptyl)-2,6-dimethoxyphenyl]-6,6-dimethylbicyclo[3.1.1]hept-2-ene-2-methanol]	Cannabinoid CB_2 receptor selective agonist	1 μM	3088	22.7 for CB2R	
AM251 [*N*-(Piperidin-1-yl)-5-(4-iodophenyl)-1-(2,4-dichlorophenyl)-4-methyl-1*H*-pyrazole-3-carboxamide]	Cannabinoid CB_1 receptor selective antagonist	1 μM	1117	7.49 for CB1R	
AM630 [6-Iodo-2-methyl-1-[2-(4-morpholinyl)ethyl]-1*H*-indol-3-yl](4-methoxyphenyl)methanone]	Cannabinoid CB_2 receptor selective antagonist	1 μM	1120	31.2 for CB2R	
BDNF	TrkB ligand	30 ng/mL	–	0.99 for TrkB (according to Hempstead et al., 1991)	Kind gift from Regeneron Pharmaceuticals (Tarrytown, NY, United States)
TrkB-Fc	BDNF scavenger	2 μg/mL	688-TK	NA	R&D Systems (Minneapolis, MN, United States)

TABLE 2 | Antibodies used for immunocytochemistry.

Antigen	Company	Catalog number	Host	Dilution
Primary antibodies				
Sox2 (a marker of neural stem cells with the ability to self-renew)	Santa Cruz Biotechnology (Dallas, TX, United States)	sc-17320	Goat	1:100
BrdU (5-bromo-2′-deoxyuridine)	AbD Serotec, Bio-Rad Laboratories (Oxford, United Kingdom)	OBT00306	Rat	1:200
Neuronal Nuclei (NeuN) (mature neuronal marker)	Cell Signaling Technology (Danvers, MA, United States)	12943	Rabbit	1:200
Secondary antibodies				
Anti-Goat Alexa Fluor® 568	Thermo Fisher Scientific (Rockford, IL, United States)	A-11057	Donkey	1:200
Anti-Rat Alexa Fluor® 488	Thermo Fisher Scientific (Rockford, IL, United States)	A-21208	Donkey	1:200
Anti-Rabbit Alexa Fluor® 568	Thermo Fisher Scientific (Rockford, IL, United States)	A-10042	Donkey	1:200

4% paraformaldehyde (PFA) for 30 min and the stained for Sox2 (**Table 2**), a marker of NSPC with the ability to self-renewal. Cell pairs resulting from the division of a single NSPC were counted and categorized in 3 groups according to their Sox 2 expression: in both daughter cells (Sox2 +/+ cell pairs), in only one of the daughter cell (Sox2 +/− cell pairs) and no expression (Sox2 −/− cell pairs). Sox2 expression in the daughter cells characterizes the response of cells to the pharmacological treatment applied, ultimately reflecting the cell-fate of the pool of NSPC, namely expansion (symmetrical self-renewal), maintenance (asymmetrical self-renewal) or extinction (symmetrical commitment) (Xapelli et al., 2013).

Cell Proliferation Study

To investigate the effect of the different pharmacological treatments on cell proliferation, SVZ and DG cells were exposed to 10 μM 5-bromo-2′-deoxyuridine (BrdU) (Sigma-Aldrich), a synthetic thymidine analog able to substitute thymidine in the DNA double chain synthesis occurring in dividing cells, for the last 4 h of each specific pharmacological treatment (48 h). Then, SVZ and DG cells were fixed in 4% PFA for 30 min and rinsed with PBS at room temperature (RT). Subsequently, BrdU was unmasked by permeabilizing cells in PBS 1% Triton X-100 at RT for 30 min and DNA was denaturated in 1 M HCl for 40 min at 37°C. Following incubation in PBS with 0.5% Triton X-100 and 3% bovine serum albumin (BSA) to block non-specific binding sites, cells were incubated overnight with the anti-rat BrdU antibody (**Table 2**). After an additional rinse in PBS, nuclei counterstaining and mounting were performed as described previously.

Cell Differentiation Study

SVZ and DG neurosphere-derived cells treated for 7 days with the drugs were fixed for 30 min in 4% PFA in PBS, permeabilized and blocked for non-specific binding sites for 1h30 with 0.5% Triton X-100 (Sigma-Aldrich) and 6% BSA in PBS. Cells were then incubated overnight at 4°C with the antibody anti-neuronal nuclei (NeuN), a marker of mature neurons (**Table 2**) in 0.1% Triton X-100 and BSA 0.3% (w/v) in PBS, and then for 1 h at RT with the appropriate secondary antibody (**Table 2**) in PBS. Nuclei were stained with Hoechst 33342 (6 μg/mL in PBS, Life Technologies). The final preparations were mounted using Mowiol fluorescent medium.

Microscopy

Fluorescence images were captured using an AxioCamMR3 monochrome digital camera (Carl Zeiss Inc., Göttingen, Germany) mounted on an Axiovert 200 inverted widefield fluorescence microscope (Carl Zeiss Inc.), with a 40x objective. Images were recorded using the software AxioVision 4 (Carl Zeiss Inc.). The pixel size in the object space was 0.25 μm and the captured image size was 1388 × 1040 pixels. Images were stored and analyzed in an uncompressed 8-bit Tiff format.

Statistical Analysis

In all experiments, measurements were performed at the border of SVZ and DG neurospheres, where migrating cells form a pseudo-monolayer of cells. In every independent experiment, each condition was measured in triplicate, i.e., in three different coverslips. Percentages of Sox2 cell pairs were obtained from counting 60 cell pairs for each condition obtained from 5-9 independent cultures. Percentages of BrdU and NeuN immunoreactive cells were calculated from cell counts in five independent microscopic fields per coverslip with a 40x objective (approximately 200–400 cells per field).

All experiments were analyzed in a double-blind fashion and obtained data was normalized to each corresponding control. Data are expressed as mean ± standard error of the mean (SEM). Statistical significance was determined using one-way analysis of variance followed by Bonferroni's-multiple comparison test, with $P < 0.05$ considered to represent statistical significance.

RESULTS

Neurospheres were used as a model to study postnatal neurogenesis dynamics. They consist of spheroid clones of NSPCs that express both Sox2 and Nestin (markers expressed by self-renewing neural precursor cells) and that are able to differentiate into neurons, expressing immature neuronal markers, such as doublecortin and βIII tubulin and mature neuronal markers, such as NeuN (Rodrigues et al., 2017).

Furthermore, during neuronal differentiation, these cells start to express phenotypic markers such as vesicular GABA transporter (VGAT, marker for GABAergic neurons) and tyrosine hydroxylase (TH, marker for dopaminergic neurons) in the case of SVZ-derived neurons and VGAT and Vesicular Glutamate transporter 1 (VGlut1, marker for glutamatergic neurons) in the case of DG-derived neurons (Rodrigues et al., 2017). Importantly, SVZ and DG neurospheres were shown to express both CB1R and CB2R throughout the process of differentiation at DIV 1 and DIV 7 as well as in adult tissue (Rodrigues et al., 2017).

BDNF-CB2R Interaction Regulates Self-Renewal in SVZ Cell Cultures

To investigate the ability of BDNF and cannabinoid receptor ligands to modulate the cell-fate of SVZ cells, a Sox2 cell-pair assay was performed in SVZ cells plated for 24 h in medium supplemented or not (control) with receptor ligands (**Figure 1A**). Cell pairs resulting from the division of a single NSPC were counted and categorized in 3 groups according to their Sox 2 expression: Sox2+/+ cell pairs indicative of pool expansion through symmetrical self-renewal, Sox2+/− cell pairs, indicative of pool maintenance through asymmetrical self-renewal and Sox2−/− cell pairs, indicative of pool extinction through symmetrical commitment. In SVZ cells, neither selective agonists for CB1R (ACEA, 1 μM) or CB2R (HU-308, 1 μM), nor the non-selective cannabinoid receptor agonist, WIN 55,212-2 (1 μM), modified the percentages of either Sox2+/+ cell pairs (**Figure 1B**).

SVZ cells treated with BDNF (30 ng/mL) showed a significant increase in the percentages of Sox2+/+ cell pairs (66.2 ± 1.78% [95% CI: 62.1–70.3%]; $n = 9$, $p < 0.001$ vs. control) with a concomitant decrease in the percentage of Sox2−/− cell pairs (29.4 ± 2.33% [95% CI: 24.1–34.8%]; $n = 9$, $p < 0.001$ vs. control) (**Figures 1C,D**), indicating that BDNF is promoting self-renewal of SVZ cells. We next evaluated whether the action of BDNF depends on cannabinoid receptors. SVZ cells were treated with either the CB1R antagonist, AM251 (1 μM), or the CB2R antagonist, AM630 (1 μM), 30 min prior to BDNF treatment and then grown for 24 h in the presence of BDNF (30 ng/mL). The presence of the CB1R antagonist did not block the BDNF-induced effect on SVZ cell-fate (**Figure 1C**). Remarkably, the increase in the percentage of Sox2+/+ SVZ cell pairs promoted by BDNF treatment was blocked by the presence of the CB2R selective antagonist, AM630 (1 μM) (50.1 ± 7.18% [95% CI: 30.1–70.0%]; $n = 5$, $p < 0.05$ vs. BDNF alone). Similarly, CB2R blockage abolished BDNF-mediated decrease in the percentage of Sox2−/− cell pairs (44.7 ± 6.14%, [95% CI: 27.6–61.7%]; $n = 5$, $p < 0.05$ vs. BDNF alone) (**Figure 1D**), showing a preponderant role of CB2R in modulating the BDNF actions upon SVZ cell fate. Treatment with selective receptor antagonists alone did not alter SVZ cell-fate (**Figures 1C,D**).

Altogether, the above data indicate that CB2R modulation interferes with BDNF signaling in regulating SVZ cell-fate.

CB1R-Induced SVZ Cell Proliferation Is Dependent on Endogenous BDNF

Next it was investigated whether CB1R/CB2R activation and BDNF could modulate SVZ cell proliferation. For that SVZ cells were treated with selective ligands for 48 h and BrdU was added during the last 4h of the culture to label SVZ cells that went through S-phase. After fixation, incorporated BrdU was immunolabeled and the percentage of positive nuclei was determined (**Figure 2A**).

As previously described by our group (Rodrigues et al., 2017), treatment of SVZ cells with CB1R agonist ACEA (1 μM) promoted a substantial increase in the number of BrdU-positive cells when compared to control cultures (control: 100.5 ± 0.53% [95% CI: 99.4–101.7%]; ACEA 1 μM: 134.3 ± 6.96% [95% CI: 119.5–149.2%]; $n = 16$, $p < 0.001$) whereas treatment with CB2R agonist HU-308 (1 μM) and cannabinoid non-selective receptor agonist WIN 55,212-2 (1 μM) induced no significant alterations in the number of BrdU-positive cells when compared to control cultures (**Figures 2B,D**).

We next sought to investigate the combined actions of BDNF and cannabinoid receptor activation on SVZ cell proliferation. We observed that incubation with exogenous BDNF promoted a significant increase in the number of SVZ BrdU-positive cells (BDNF 30 ng/mL: 146.9 ± 9.17% [95% CI: 127.6–166.2%]; $n = 19$, $p < 0.001$) and that this increase was maintained when co-incubating with cannabinoid non-selective receptor agonist WIN 55,212-2 (BDNF 30 ng/mL+WIN 55,212-2 1 μM: 121.9 ± 10.9% [95% CI: 74.8–168.8%]; $n = 3$), although incubation with WIN 55,212-2 *per se* did not affect SVZ cell proliferation (**Figures 2C,D**).

To evaluate the influence of endogenous BDNF on cannabinoid-mediated SVZ cell proliferation, we used a BDNF scavenger (TrkB-Fc chimera, 2 μg/mL). The incubation with the scavenger alone caused a significant decrease in the percentage of BrdU-positive cells (TrkB-Fc 2 μg/mL: 67.6 ± 3.85% [95% CI: 51.1–84.3%]; $n = 3$, $p < 0.05$ vs. control) (**Figure 2E**), indicating a preponderant role of endogenous BDNF upon cell proliferation. The presence of the scavenger abolished the enhancement in BrdU-positive cells caused by CB1R agonist, ACEA (1 μM) (**Figure 2E**), indicating not only that SVZ cell proliferation is modulated by CB1R but that this modulation is dependent on endogenous BDNF.

Interestingly, in the presence of the selective CB1R or CB2R antagonists (AM251 and AM630, respectively) the increase in cell proliferation mediated by BDNF was not changed ($p > 0.05$ vs. BDNF, **Figure 2F**). These data suggest that BDNF plays a crucial role in regulating SVZ cell proliferation and that endogenous BDNF availability is required for CB1R actions upon this process. However, the effect mediated by BDNF in SVZ cell proliferation is not dependent on CB1R or CB2R.

BDNF Crosstalk With Cannabinoid Receptors Modulates Neuronal Differentiation at SVZ

To evaluate the effects on SVZ neuronal differentiation, SVZ cells were treated with the test drugs in serum-free medium

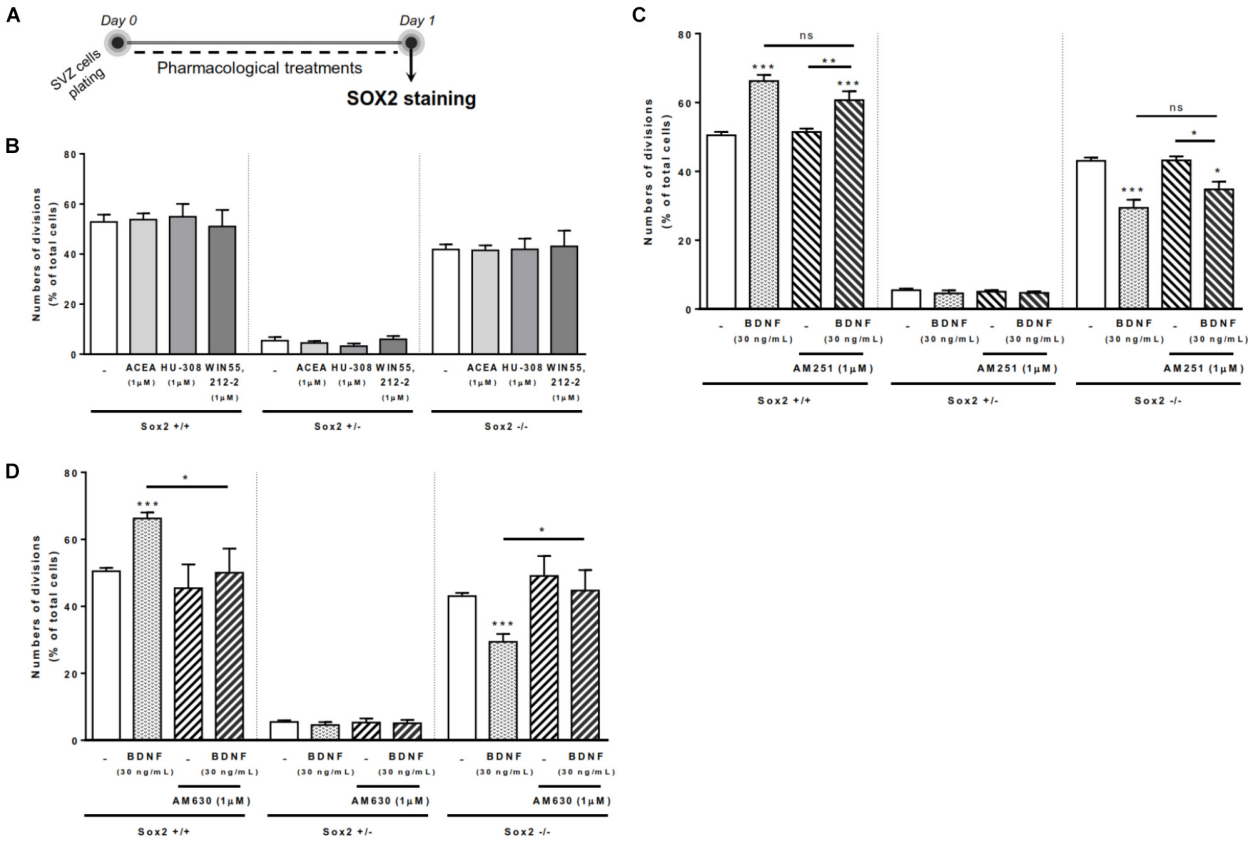

FIGURE 1 | BDNF-CB2R interaction regulates SVZ self-renewal. BDNF treatment promoted an increase in self-renewing capacity of SVZ cells which was blocked by CB2R antagonism, albeit cannabinoid receptor activation had no effect. **(A)** Schematic representation of the experimental protocol used to study cell-fate. Day 0 represents the day of cultures where the SVZ cell suspension was treated with the drugs for 24 h. **(B–D)** Bar graphs depict the percentage of Sox2+/+, Sox2+/–, Sox2–/– cell pairs expressed as percentage of total cells per culture. Data are expressed as mean ± SEM. $n = 3$–9. $^{*}p < 0.05$, $^{**}p < 0.01$ and $^{***}p < 0.001$ using Dunnett's multiple comparison test. ns, non-significant.

devoid of growth factors for 7 days (**Figure 3A**). As previously reported (Rodrigues et al., 2017), treatment of SVZ cells with selective agonists for CB1R and/or CB2R as well as treatment with non-selective cannabinoid receptor agonist, WIN 55,212-2, induced a significant increase in the number of NeuN-positive cells when compared to control cultures (**Figures 3B–D**). While testing the action of exogenous BDNF, we observed a significant increase in the percentage of NeuN-positive cells upon incubation with BDNF (163.0 ± 11.78% [95% CI: 138.4–187.6%]; $n = 20$, $p < 0.001$ vs. control) (**Figures 3C,D**). This effect persisted when cultures were co-incubated with BDNF together with non-selective cannabinoid agonist WIN 55,212-2 (147.1 ± 11.02% [95% CI: 121.7–172.5%]; $n = 9$, $p < 0.05$ vs. control) (**Figures 3C**).

Remarkably, in the presence of the BDNF scavenger (TrkB-Fc) none of the cannabinoid receptor agonists affected the percentage of NeuN-positive cells ($p < 0.001$ vs. agonists alone, **Figures 3E–G**). BDNF chimera scavenger (TrkB-Fc) alone was devoid of effect ($p > 0.05$ vs. control) (**Figures 3E–G**). These data indicate that endogenous BDNF is necessary for the actions of CB1R and CB2R upon SVZ neuronal differentiation.

Interestingly, the effect promoted by BDNF on SVZ neuronal differentiation was blocked when cells were co-incubated with either the CB1R selective antagonist AM251 (BDNF 30 ng/mL+AM251 1 μM: 113.3 ± 10.6% [95% CI: 89.2–137.4%]; $n = 10$, $p < 0.01$ vs. BDNF) (**Figure 3H**) or with the CB2R selective antagonist AM630 (BDNF 30 ng/mL+AM630 1 μM: 101.5 ± 10.8% [95% CI: 67.1–135.9%]; $n = 4$, $p < 0.01$ vs. BDNF) (**Figure 3H**). No significant alterations were found when incubating cultures with selective antagonists alone (**Figure 3H**).

Altogether the above results indicate that the effect of BDNF on SVZ neuronal differentiation is dependent on both CB1R and CB2R, while the effect of CB1R and CB2R is dependent on endogenous BDNF.

BDNF-CB2R Interaction Regulates Self-Renewal in DG Cell Cultures

Since effects in SVZ may differ from effects on DG, both neurogenic niches having different functions (Bond et al., 2015), we repeated the above-mentioned experiments, but using DG cell cultures (**Figure 4A**). We firstly observed that although CB1R selective activation promoted no significant changes in the percentages of either Sox2+/+ or Sox2−/−

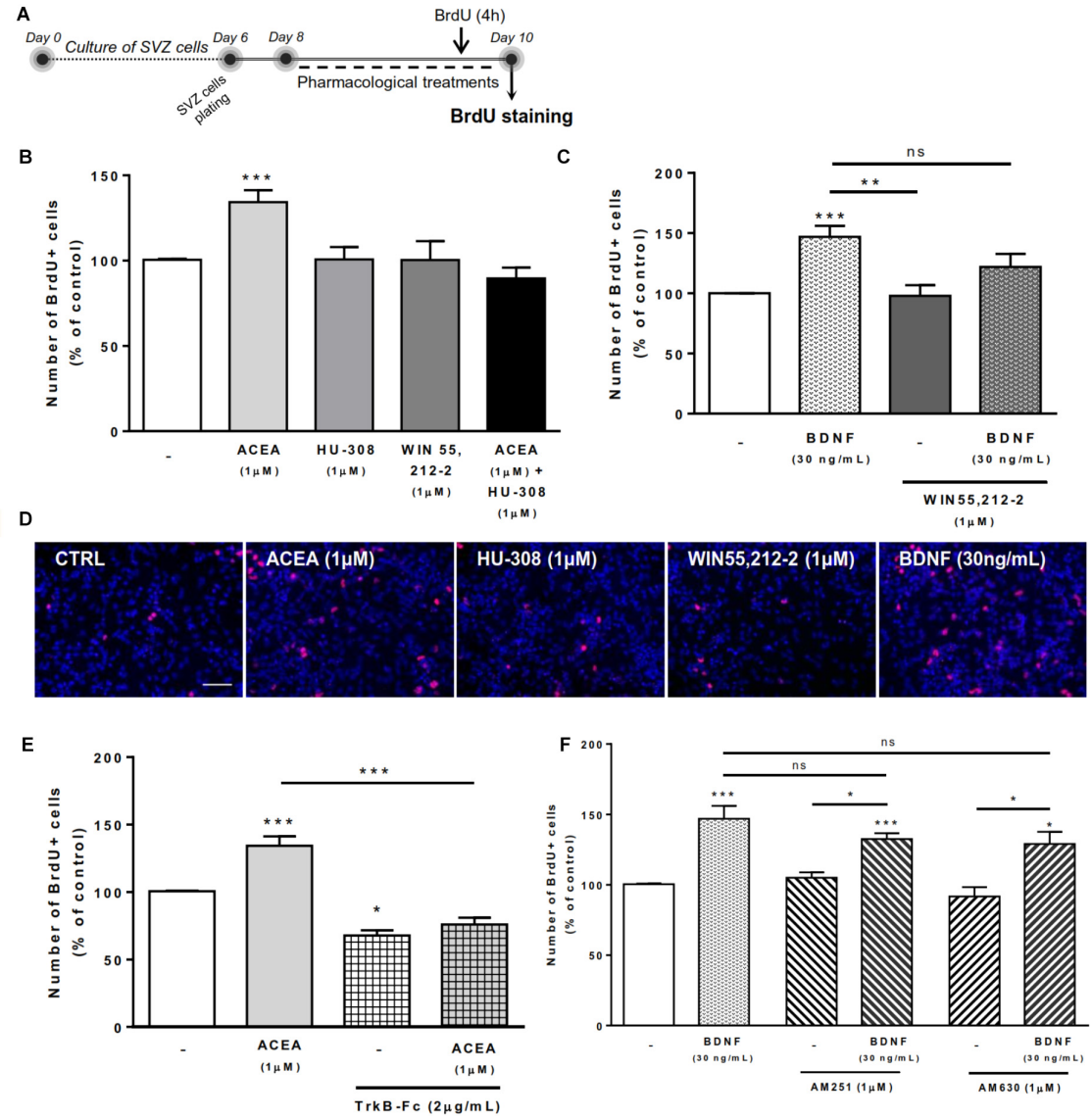

FIGURE 2 | CB1R-induced SVZ proliferation is dependent on endogenous BDNF. SVZ proliferation was increased by CB1R activation and treatment with BDNF. BDNF was required for CB1R-mediated effect to occur. Conversely, BDNF-mediated effect was independent of CB1R or CB2R modulation. **(A)** Schematic representation of the experimental protocol. Day 0 represents the day of cultures; at Day 6 SVZ neurospheres were plated for 48 h and at Day 8 cells were exposed to pharmacological treatments for further 48 h (Day 10). **(B,C,E,F)** Bar graphs depict the number of BrdU-positive cells. Values were normalized to the control mean for each experiment and are represented as mean ± SEM. Control was set to 100%. n = 3-19. $^{*}p < 0.05$ and $^{***}p < 0.001$ using Dunnett's multiple comparison test. ns, non-significant. **(D)** Representative fluorescent digital images of cells immunopositive for BrdU (in red) and Hoechst 33342 staining (blue nuclei). Scale bar = 50 μm.

cell pairs, CB2R selective activation with HU-308 or non-selective cannabinoid activation with WIN 55,212-2 induced a significant increase in the percentage of Sox2+/+ cell pairs (control: 53.70 ± 1.212% [95% CI: 50.5–56.8%]; HU-308 1 μM: 65.17 ± 1.35% [95% CI: 61.4–68.9%]; WIN 55,212-2 1 μM: 62.94 ± 2.02% [95% CI: 57.3–68.5%]; n = 3–5, $p < 0.001$) (**Figure 4B**), with a concomitant decrease in the percentage of Sox2−/− cell pairs (control: 45.35 ± 0.86% [95% CI: 42.9–47.7%]; HU-308 1 μM: 33.82 ± 1.23% [95% CI: 30.3–37.2%]; WIN 55,212-2 1 μM: 33.28 ± 2.31% [95% CI: 26.8–39.7%]; n = 3–5, $p < 0.001$ vs. control) (**Figure 4B**). This suggests modulation of DG cell-fate by CB2R selective activation, which was further tested by co-incubation with selective antagonists for CB1R and CB2R. Corroborating the involvement of CB2R, we observed that the effect mediated by CB2R selective agonist or by the non-selective CB1R/CB2R agonist in DG self-renewal was blocked by co-incubation with a CB2R selective antagonist, AM630 (1 μM), but not with a CB1R selective antagonist, AM251 (1 μM) (**Supplementary Figure S1**).

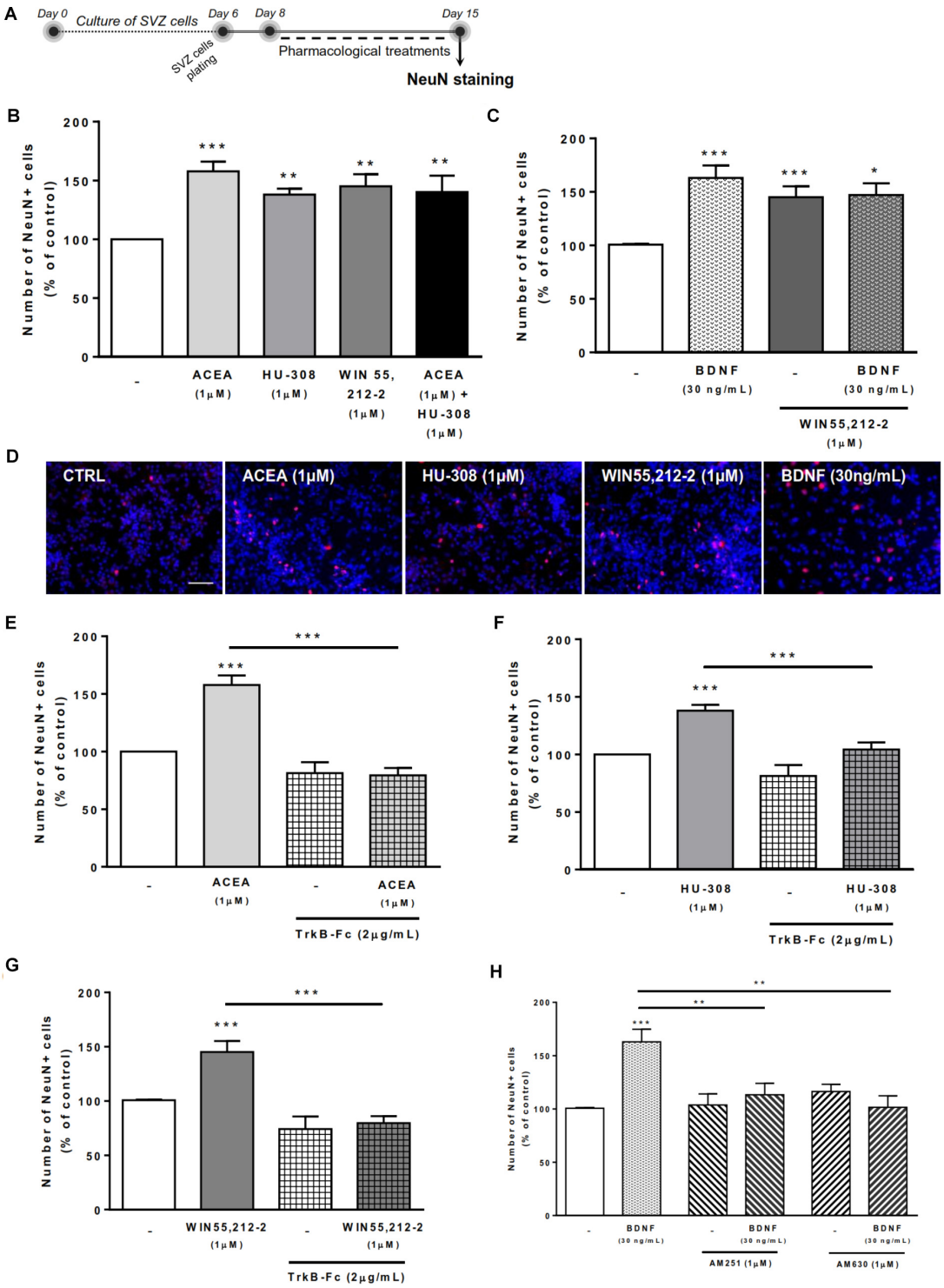

FIGURE 3 | Cannabinoid receptor crosstalk with BDNF modulates SVZ neuronal differentiation. Cannabinoid receptor activation promoted SVZ neuronal differentiation, an effect dependent on the presence of endogenous BDNF. Similarly, BDNF effect upon SVZ neuronal differentiation was abolished by CB1R or CB2R antagonism. **(A)** Schematic representation of the experimental protocol. Day 0 represents the day of cultures; at Day 6 SVZ neurospheres were plated for 48h and at Day 8 cells were exposed to pharmacological treatments for further 7 days (Day 15). **(B,C,E–H)** Bar graphs depict the number of NeuN-positive cells. Values were normalized to the control mean for each experiment and are represented as mean ± SEM. Control was set to 100%. $n = 5$–24. $^{*}p < 0.05$ and $^{***}p < 0.001$ using Dunnett's multiple comparison test. **(D)** Representative fluorescent digital images of cells immunopositive for NeuN (in red) and Hoechst 33342 staining (blue nuclei). Scale bar = 50 μm.

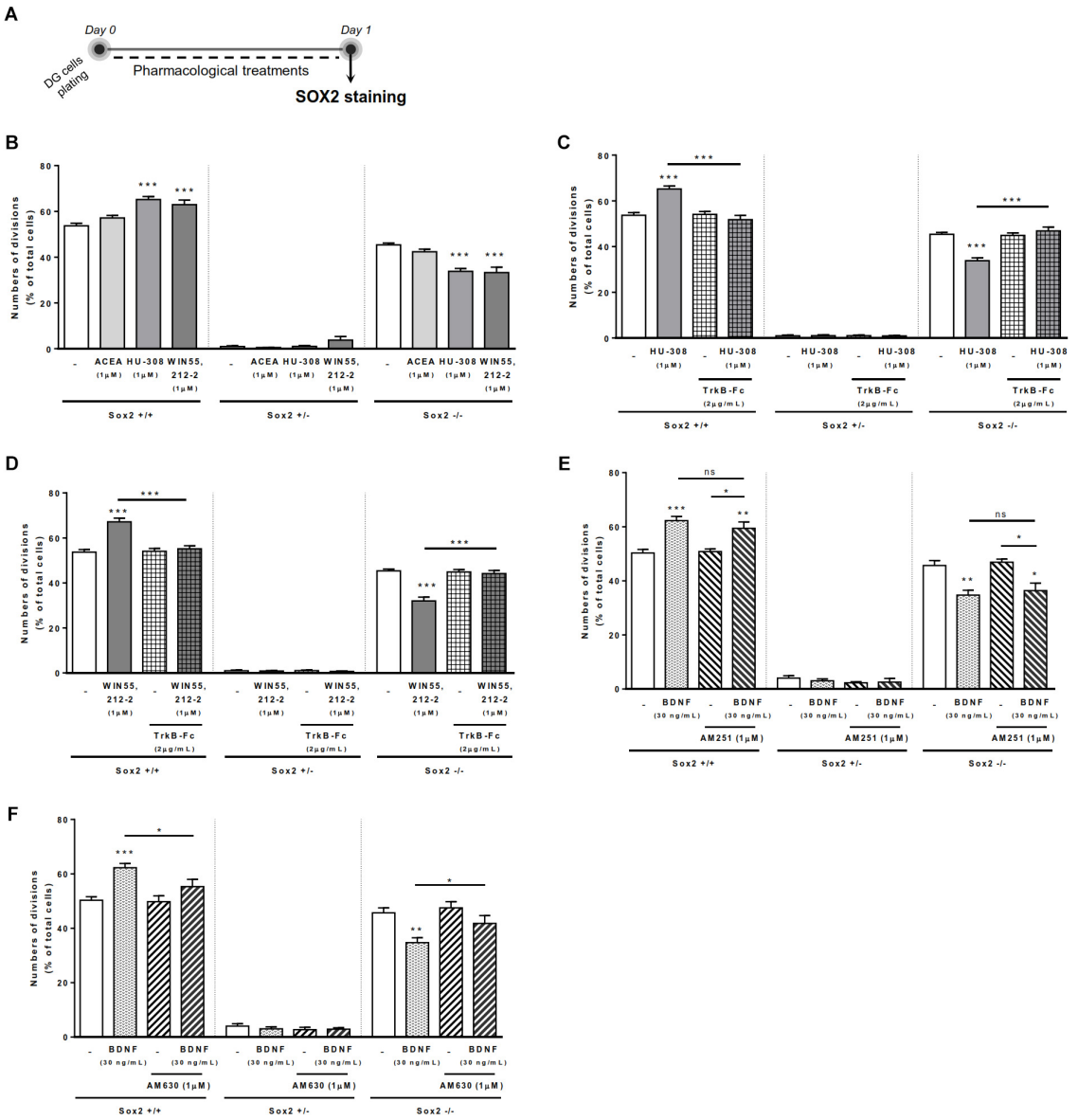

FIGURE 4 | BDNF-CB2R crosstalk regulates DG self-renewal. CB2R selective and non-selective activation increased DG self-renewal capacity, an effect abrogated by endogenous BDNF removal. Conversely, BDNF-mediated increase in DG self-renewal was dependent on CB2R, but not CB1R, modulation. **(A)** Schematic representation of the experimental protocol used to study cell-fate. Day 0 represents the day of cultures where the DG cell suspension was treated with the drugs for 24 h. **(B–F)** Bar graphs depict the percentage of Sox2+/+, Sox2+/–, Sox2–/– cell pairs expressed as percentage of total cells per culture. Data are expressed as mean ± SEM. $n = 3$–7. *$p < 0.05$, **$p < 0.01$, and ***$p < 0.001$ using Dunnett's multiple comparison test. ns, non-significant.

The presence of the BDNF scavenger, TrkB-Fc (2 μg/mL), abrogated both the increase in the percentage of Sox2+/+ cell pairs, and the concomitant decrease of Sox2−/− cell pairs, induced by either the CB2R selective agonist, HU-308 (1 μM; **Figure 4C**) or the CB1R/CB2R agonist, WIN 55,212-2 (1 μM; **Figure 4D**). This data clearly indicates that endogenous BDNF is important for CB2R-mediated control of DG cell-fate.

Exogenously added BDNF (30 ng/ml) increased the percentage of Sox2+/+ cell pairs (control: 50.31 ± 1.28% [95% CI: 47.17–53.45%]; BDNF 30 ng/mL: 62.25 ± 1.58% [95% CI: 58.38–66.12%]; $n = 7$, $p < 0.001$), and concomitantly decreased in the percentage of Sox2−/− cell pairs (control: 45.66 ± 1.85% [95% CI: 41.12–50.21%]; BDNF 30 ng/mL: 34.70 ± 1.79% [95% CI: 30.31–39.09%]; $n = 7$, $p < 0.001$) (**Figures 4E,F**). Remarkably, the action of BDNF on DG cell-fate was blocked by co-incubation with the CB2R selective antagonist AM630 (**Figure 4F**), but not by the CB1R selective antagonist AM251 (**Figure 4E**). No significant changes were found when incubating cultures with the selective receptor antagonists alone (**Figures 4E,F**). Overall, these data suggest that both BDNF and

CB2R have a leading role in modulating DG cell-fate and that they reciprocally regulate each other actions.

BDNF-CB2R Interaction Regulates Cell Proliferation in DG Cell Cultures

To assess the effects on DG cell proliferation, as we did before for SVZ cell proliferation, DG cells were treated with selective ligands for 48 h, incorporated BrdU was immunolabeled and positive nuclei percentage was determined (**Figure 5A**).

We could confirm (Rodrigues et al., 2017) that CB1R or CB2R selective activation with ACEA (1 μM) and HU-308 (1 μM), respectively, did not promote DG cell proliferation (**Figures 5B,D**). Interestingly, upon co-incubation with both selective cannabinoid receptor agonists (ACEA+HU-308) or with non-selective cannabinoid receptor agonist WIN 55,212-2 (1 μM), there was a significant increase in the number of BrdU-positive cells (ACEA 1 μM+HU-308 1 μM: 161.4 ± 31.85% [95% CI: 79.5–243.3%]; WIN 55,212-2 1 μM: 155.4 ± 8.89% [95% CI: 136.5–174.3%]; n = 13–17, $p < 0.01$ and $p < 0.001$ vs. control, respectively) (**Figures 5B–D**). These findings suggest that there is the need of a positive interaction between CB1R and CB2R for cannabinoids to affect cell proliferation at the DG.

Concerning the influence of exogenous BDNF, we observed a significant increase in the percentage of BrdU-positive cells upon incubation with BDNF (30 ng/mL; 160.4 ± 10.90% [95% CI: 137.0–183.8%]; n = 15, $p < 0.001$ vs. control) (**Figures 5C,D**) which persisted when co-incubation with the non-selective cannabinoid receptor agonist was performed (BDNF 30 ng/mL + WIN 55,212-2 1 μM: 145.2 ± 15.02% [95% CI: 103.5–186.9%]; n = 5, $p < 0.05$ vs. control) (**Figure 5C**).

Importantly, endogenous BDNF withdrawal from the media with TrkB-Fc blocked the WIN 55,212-2-mediated increase in BrdU-positive cells (WIN 55,212-2 1 μM + TrkB-Fc 2 μg/mL: 120.5 ± 9.21% [95% CI: 96.8–144.2%]; n = 6, $p < 0.05$ vs. WIN 55,212-2 alone) (**Figure 5E**) indicating that BDNF plays an important role on cannabinoid receptor-mediated DG cell proliferation. Interestingly, and similarly to what happens with DG cell-fate, the use of a CB2R selective antagonist was able to block the BDNF-mediated effect on DG cell proliferation (BDNF 30 ng/mL + AM630 1 μM: 107.3 ± 16.80% [95% CI: 53.8–160.8%]; n = 4, $p < 0.05$ vs. BDNF alone) (**Figure 5F**) while CB1R blockade did not affect the increase in BrdU-positive cells promoted by BDNF (BDNF 30 ng/mL+AM251 1 μM: 174.6 ± 17.84% [95% CI: 132.4–216.8%]; n = 8, $p < 0.05$ vs. BDNF alone) (**Figure 5F**). This suggests that CB2R plays an important role in modulating BDNF actions on DG cell proliferation, and that this action is independent of CB1R.

BDNF Crosstalk With Cannabinoid Receptor Activation Modulates DG Neuronal Differentiation

Treatment of DG cells with all cannabinoid receptor agonists for CB1R and/or CB2R (**Figure 6A**) promoted a significant increase in the number of NeuN-positive cells when compared to control cultures (ACEA 1 μM: 170.4 ± 11.95% [95% CI: 143.4–197.5%]; HU-308 1 μM: 161.4 ± 11.42% [95% CI: 135.0–187.7%]; ACEA 1 μM+ HU-308 1 μM: 160.1 ± 26.07% [95% CI: 93.08–227.1%]; WIN 55,212-2 1 μM: 198.80 ± 16.74% [95 CI: 163.6–234%]; n = 9–19, $p < 0.05$, $p < 0.01$ or $p < 0.001$ vs. control) (**Figures 6B–D**), corroborating our previous data on the effects of cannabinoids on DG neuronal differentiation (Rodrigues et al., 2017).

We then investigated the role of exogenous BDNF administration in modulating DG neuronal differentiation. BDNF was shown to promote a significant increase in the number of NeuN-positive cells (173.0 ± 15.42% [95% CI: 140.1–205.9%]; n = 16, $p < 0.001$ vs. control) (**Figures 6C,D**), an effect that was maintained after co-treatment with non-selective cannabinoid receptor agonist (BDNF 30 ng/mL + WIN 55,212-2 1 μM: 205.9 ± 37.41% [95% CI: 114.4–297.4%]; n = 7, $p < 0.001$ vs. control).

Endogenous BDNF seems to be necessary for the actions cannabinoids upon DG neuronal differentiation, since the enhancement caused by CB1R or CB2R agonists in the percentage of NeuN-positive cells was prevented by co-incubation with the BDNF scavenger (**Figures 6E–G**).

Finally, we have observed that the effect promoted by BDNF on DG neuronal differentiation was blocked when cells were co-incubated with the CB2R selective antagonist AM630 (BDNF 30 ng/mL+AM630 1 μM: 84.3 ± 14.7% [95% CI: 20.8–147.8%]; n = 3, $p < 0.05$ vs. BDNF alone) (**Figure 6H**) but not with the CB1R selective antagonist AM251 (**Figure 6H**), indicating that CB2R is preponderant to modulate the action of BDNF on DG neuronal differentiation.

DISCUSSION

The present work reveals a yet not described interaction between BDNF and cannabinoid receptors (CB1R and CB2R) responsible to modulate several aspects of SVZ and DG postnatal neurogenesis. BDNF was shown to be an important modulator of SVZ and DG postnatal neurogenesis, its actions being under control of cannabinoid receptors. The relevance of each cannabinoid receptor to control the action of BDNF upon neurogenesis is different in the two neurogenic niches. While CB2R has a preponderant role in modulating BDNF actions on DG, BDNF-mediated SVZ postnatal neurogenesis is modulated by both CB1R and CB2R. A constant and clear finding in both neurogenic niches is that BDNF is required for cannabinoid actions to occur. It thus appears that a reciprocal cross-talk between cannabinoids and BDNF exist to modulate postnatal neurogenesis.

BDNF is a neurotrophin important in the regulation of several neuronal processes such as neuronal branching, dendrite formation and synaptic plasticity (Dijkhuizen and Ghosh, 2005; Gómez-Palacio-Schjetnan and Escobar, 2013). In line with this evidence, several studies have shed light on the actions of BDNF in the survival and differentiation of newborn neurons (Benraiss

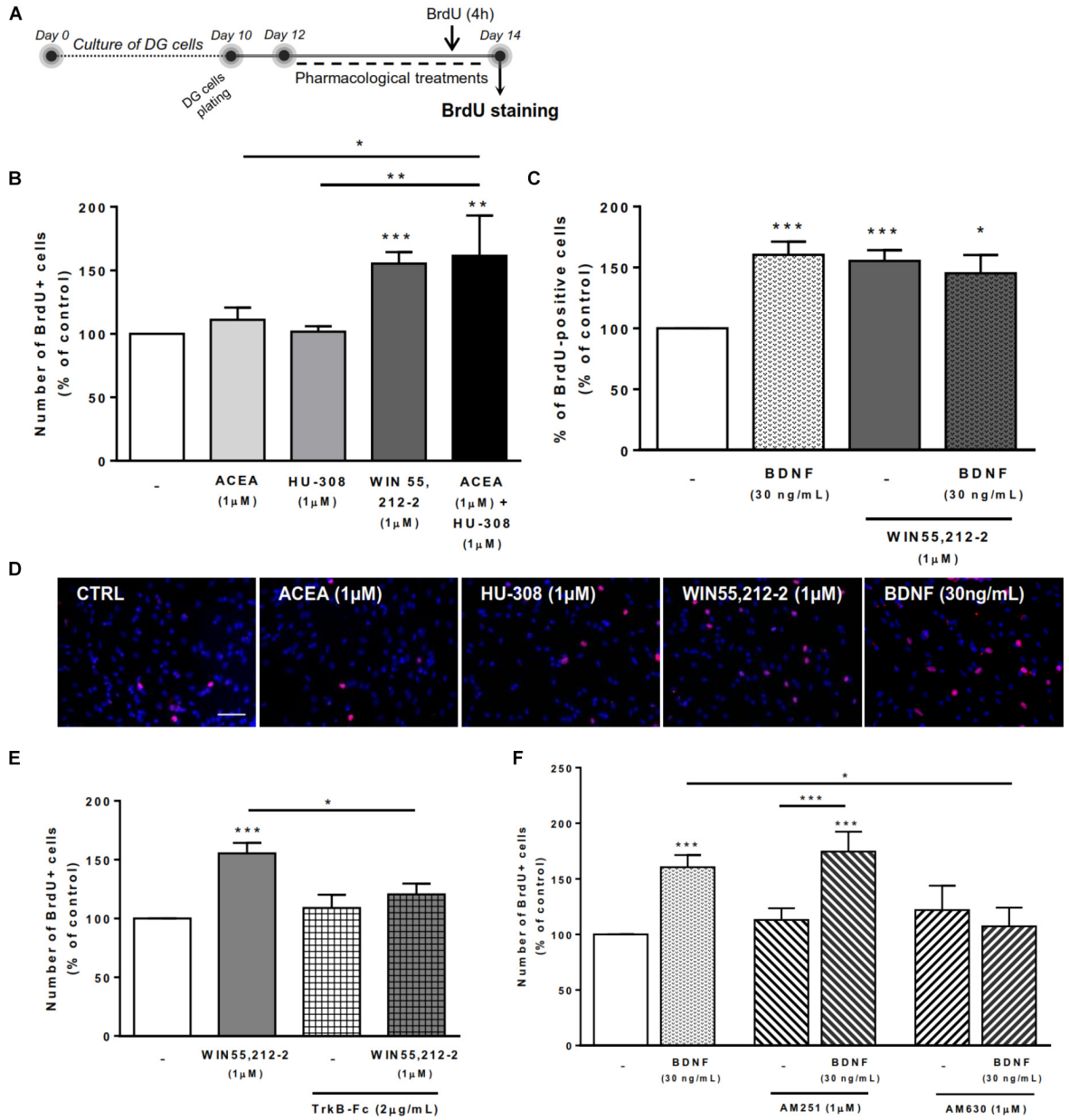

FIGURE 5 | BDNF-CB2R interaction modulates DG cell proliferation. CB1R activation together with CB2R activation promoted DG cell proliferation, an effect dependent on the presence of BDNF. CB2R, but not CB1R, blockage abrogated BDNF-mediated increase in DG cell proliferation. **(A)** Schematic representation of the experimental protocol. Day 0 represents the day of cultures; at Day 10 DG neurospheres were plated for 48 h and at Day 12 cells were exposed to pharmacological treatments for further 48 h (Day 14). **(B,C,E,F)** Bar graphs depict the percentage of BrdU-positive cells. Values were normalized to the control mean for each experiment and are represented as mean ± SEM. Control was set to 100%. $n = 6$–17. $^{*}p < 0.05$ and $^{***}p < 0.001$ using Dunnett's multiple comparison test. **(D)** Representative fluorescent digital images of cells immunopositive for BrdU (in red) and Hoechst 33342 staining (blue nuclei). Scale bar = 50 μm.

et al., 2001; Henry et al., 2007; Chan et al., 2008; Snapyan et al., 2009). Our findings now demonstrate that BDNF is able to affect early steps of postnatal neurogenesis, such as cell-fate, cell proliferation and neuronal differentiation of SVZ and DG cultures. We observed that BDNF promoted self-renewal of SVZ- and DG-derived cells as observed by an increase in self-renewal divisions, i.e., an increase in the percentage of Sox2+/+ cell-pairs. BDNF-CBR crosstalk has been reported to control several processes at the synaptic level (Zhao and Levine, 2014; Zhong et al., 2015) and we now extended these findings toward very early stages of postnatal neurogenesis. Interestingly, the increase in the SVZ and DG pool of stem/progenitor cells mediated by BDNF was fully abolished in the presence of CB2R antagonist but not CB1R antagonist. An exception is the influence of BDNF upon SVZ cell proliferation, which is not affected by CB1R or CB2R selective antagonism. In what

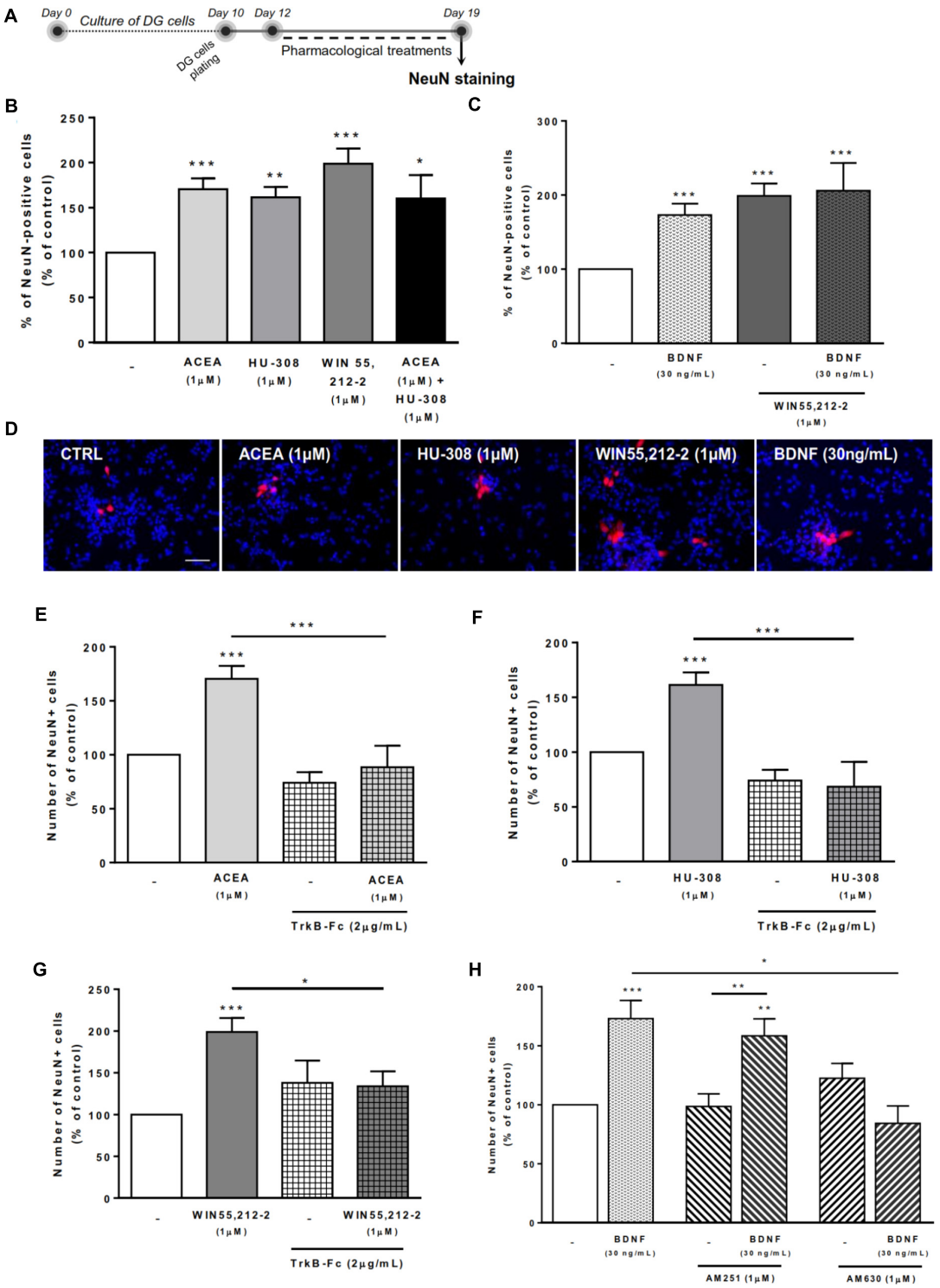

FIGURE 6 | BDNF crosstalk with cannabinoid receptors tightly regulates DG neuronal differentiation. DG neuronal differentiation was increased upon cannabinoid receptor activation. BDNF was required for cannabinoid receptor-mediated effect on DG neuronal differentiation. CB2R, but not CB1R, antagonism blocked the effect promoted by BDNF upon SVZ neuronal differentiation. **(A)** Schematic representation of the experimental protocol. Day 0 represents the day of cultures; at Day 10 DG neurospheres were plated for 48 h and at Day 12 cells were exposed to pharmacological treatments for further 7 days (Day 19). **(B,C,E–H)** Bar graphs depict the percentage of NeuN-positive cells. Values were normalized to the control mean for each experiment and are represented as mean ± SEM. Control was set to 100%. $n = 6–19$. $^{*}p < 0.05$ and $^{***}p < 0.001$ using Dunnett's multiple comparison test. **(D)** Representative fluorescent digital images of cells immunopositive for NeuN (in red) and Hoechst 33342 staining (blue nuclei). Scale bar = 50 μm.

concerns neuronal differentiation, both CB1R and CB2R are required for BDNF actions on SVZ whereas at the DG, only CB2R seem to affect BDNF-promoted neuronal differentiation. Overall, cannabinoid receptor blockade appears to influence more BDNF-induced actions upon early stages of DG neurogenesis in comparison to SVZ, highlighting the fact that cannabinoids distinctly modulate the effects promoted by BDNF in SVZ and DG neurogenesis.

It was previously known that the endocannabinoid system and cannabinoid receptors are important modulators of several stages of neurogenesis (Palazuelos et al., 2012; Xapelli et al., 2013; Prenderville et al., 2015; Rodrigues et al., 2017). In accordance with our previous data, SVZ and DG cells were differently affected by the same cannabinoid pharmacological treatments (Rodrigues et al., 2017). Considering cell fate, we observed that selective activation of CB2R activation promotes self-renewal of DG cells, but not of SVZ cells. This is consistent with several pieces of evidence showing a regulation of cell fate promoted by the activation of several signaling pathways [such as mitogen-activated protein kinase (MAPK) family (ERK, JNK and p38) and the phosphoinositide-3 kinase (PI3K)/AKT pathways] triggered by CBR activation (Molina-Holgado et al., 2007; Gomez et al., 2010; Soltys et al., 2010; Compagnucci et al., 2013).

On the other hand, our results reveal, for the first time, a role of cannabinoid receptors (CB1R and CB2R) in regulating DG cell commitment.

Considering cell proliferation, it is promoted by CB1R but not CB2 at SVZ, while at DG cell proliferation was only induced by co-activation of CB1R and CB2R. These results are in accordance with previous reports that have shown an increase in SVZ cell proliferation promoted by CB1R selective activation (Trazzi et al., 2010; Xapelli et al., 2013) and an increase in DG cell proliferation triggered by CB1R/CB2R non-selective activation (Aguado et al., 2005; Rodrigues et al., 2017). Importantly, while we also detected an effect with the non-selective CB1R/CB2R agonists, none of the selective agonists when applied in the absence of the other agonist were effective to promote cell proliferation in the DG, highlighting the need of caution while interpreting negative results with each of those agonists separately.

Regarding neuronal differentiation, our data indicate that in SVZ and DG neurogenic niches both subtypes of cannabinoid receptors are able to promote neuronal differentiation. These data are in accordance with previous reports in which cannabinoid receptor activation enhanced neuronal differentiation of NSPC by CB1R- (Compagnucci et al., 2013) or CB2R-dependent (Avraham et al., 2014) mechanisms.

The most important finding in the present work is that most of the cannabinoid-induced effects upon cell proliferation and neuronal differentiation depend on the presence of BDNF, suggesting the existence of a BDNF-endocannabinoid feedback loop responsible for regulating these processes. Previous reports have shed light on the existence of a putative interaction between BDNF and cannabinoid receptors (Howlett et al., 2010), but none focused upon neurogenesis. De Chiara et al. (2010) have identified a novel mechanism by which BDNF mediates the regulation of striatal CB1R function. Moreover, others have suggested that BDNF can regulate neuronal sensitivity to endocannabinoids through a positive feedback loop important for the regulation of neuronal survival (Maison et al., 2009). Evidence also shows the involvement of BDNF in the actions mediated by cannabinoids against excitotoxicity (Khaspekov et al., 2004), in synaptic transmission and plasticity (Klug and van den Buuse, 2013; Zhao et al., 2015; Yeh et al., 2017) and in several behavioral outputs (Aso et al., 2008; Bennett et al., 2017). Previous animal studies have shown that acute (Derkinderen et al., 2003) and chronic (Butovsky et al., 2005) Δ^9-THC (major psychoactive constituent of cannabis; CB1R and CB2R agonist) administration is associated with an increase in BDNF gene expression. Moreover, it was shown that overexpression of BDNF is able to rescue cognitive deficits promoted by Δ^9-THC administration in a mouse model of schizophrenia (Segal-Gavish et al., 2017). In human studies it was found that Δ^9-THC increased serum BDNF levels in healthy controls, but not in chronic cannabis users (D'Souza et al., 2009). In fact, cyclic AMP response element-binding protein (CREB) may be the common linking element because it is an important regulator of BDNF-induced gene expression (Finkbeiner et al., 1997), and has been reported to control several steps of the neurogenic process in the adult hippocampus (Nakagawa et al., 2002) and SVZ (Giachino et al., 2005). Consistently, cannabinoids have been shown to induce CREB phosphorylation (Isokawa, 2009) and also to promote changes in BDNF and CREB gene expression (Grigorenko et al., 2002). In addition, the work done by Berghuis et al. (2005) showed that endocannabinoids stimulate TrkB receptor phosphorylation during interneuron morphogenesis. Most importantly, in the same study, the authors observed by co-immunoprecipitation the formation of heteromeric complexes in PC12 cells expressing TrkB receptors and CB1R (Berghuis et al., 2005). Our study brings new and relevant information on the interaction between cannabinoid receptors and BDNF in controlling SVZ and DG neurogenesis, and clearly highlights that this interaction is reciprocal. In fact, neurogenesis promoted by cannabinoid receptor activation depends on the presence of endogenous BDNF, while the effects mediated by BDNF upon neurogenesis are directly regulated by modulation of CB1R or CB2R.

Although our study is based on an *in vitro* approach, the neurosphere assay, it represents a highly relevant model. *In vitro* systems of NSPC allow an easier access and better control of experimental variables as well as a thorough analysis of mechanisms happening at cellular and molecular level providing useful information to be further validated *in vivo* (Singec et al., 2006). Moreover, the heterogeneous composition of the NSPC grown in neurospheres is extremely relevant because it holds some of the features, such as close contact with neighboring cells (newly generated neuroblasts, astrocytes and oligodendrocytes), that resemble those of the physiological niche (Casarosa et al., 2014). These well-established advantages (Aguado et al., 2007; Agasse et al., 2008; Azari et al., 2010) are the reason why we have used this *in vitro* approach to study the intrinsic properties of NSPC and to understand the interaction between BDNF and cannabinoids in modulating neurogenesis. It is, however, important to mention that the mechanisms

governing the regulation of neurosphere dynamics might be different from the ones regulating *in vivo* adult neurogenesis (Casarosa et al., 2014). Indeed, further *in vivo* studies will be required to comprehensively understand the role of BDNF in regulating the actions of cannabinoid receptors on postnatal neurogenesis.

Taken together, our data highlight a novel level of complexity for the regulatory mechanisms involved in NSPC dynamics, which involve the interplay of multiple signaling cues, and where BDNF and cannabinoids may play a relevant role. Further *in vitro* studies are required to detail the molecular mechanisms involved, as well as *in vivo* studies to determine the functional consequences of the BDNF/cannabinoid crosstalk to control neurogenesis. Nevertheless, our study provides evidence for the need of integrative strategies whenever focusing on NSPC for brain repair.

AUTHOR CONTRIBUTIONS

FF, FR, and RR: conception and design of the work, acquisition, analysis and interpretation of data for the work; drafting and revising critically the work for important intellectual content and final approval of the version to be published. AS: conception and design of the work; interpretation of data for the work; revising critically the work for important intellectual content and final approval of the version to be published. SX: conception and design of the work, acquisition, analysis and interpretation of data for the work; drafting and revising critically the work for important intellectual content and final approval of the version to be published.

ACKNOWLEDGMENTS

This work was supported by Fundação para a Ciência e Tecnologia (FCT) Portugal (PTDC/DTP-FTO/3346/2014). RR (SFRH/BD/129710/2017) and FR (SFRH/BD/74662/2010) were in receipt of a fellowship from FCT. AS thanks the H2020 Twinning Action from EU (SynaNet 692340). SX is an iFCT researcher (IF/01227/2015). BDNF was kindly given by Regeneron. Funded by LISBOA-01-0145-FEDER-007391, project co-funded by FEDER, through POR Lisboa 2020 – Programa Operacional Regional de Lisboa, PORTUGAL 2020, and Fundação para a Ciência e a Tecnologia.

SUPPLEMENTARY MATERIAL

The Supplementary Material for this article can be found online at: https://www.frontiersin.org/articles/10.3389/fncel.2018.00441/full#supplementary-material

FIGURE S1 | CB2R modulation regulates DG cell-fate. Non-selective cannabinoid receptor activation or selective CB2R activation increased DG self-renewing capacity and these effects were dependent on CB2R. **(A–D)** Bar graphs depict the percentage of Sox2+/+, Sox2+/−, Sox2−/− cell pairs expressed as percentage of total cells per culture. Data are expressed as mean ± SEM. $n = 5–7$. $^{*}p < 0.05$, $^{**}p < 0.01$ and $^{***}p < 0.001$ using Dunnett's multiple comparison test.

REFERENCES

Agasse, F., Bernardino, L., Silva, B., Ferreira, R., Grade, S., and Malva, J. O. (2008). Response to histamine allows the functional identification of neuronal progenitors, neurons, astrocytes, and immature cells in subventricular zone cell cultures. *Rejuvenation Res.* 11, 187–200. doi: 10.1089/rej.2007.0600

Aguado, T., Monory, K., Palazuelos, J., Stella, N., Cravatt, B., Lutz, B., et al. (2005). The endocannabinoid system drives neural progenitor proliferation. *FASEB J.* 19, 1704–1706. doi: 10.1096/fj.05-3995fje

Aguado, T., Romero, E., Monory, K., Palazuelos, J., Sendtner, M., Marsicano, G., et al. (2007). The CB1 cannabinoid receptor mediates excitotoxicity-induced neural progenitor proliferation and neurogenesis. *J. Biol. Chem.* 282, 23892–23898. doi: 10.1074/jbc.M700678200

Arévalo-Martín, Á., García-Ovejero, D., Rubio-Araiz, A., Gómez, O., Molina-Holgado, F., and Molina-Holgado, E. (2007). Cannabinoids modulate Olig2 and polysialylated neural cell adhesion molecule expression in the subventricular zone of post-natal rats through cannabinoid receptor 1 and cannabinoid receptor 2. *Eur. J. Neurosci.* 26, 1548–1559. doi: 10.1111/j.1460-9568.2007.05782.x

Aso, E., Ozaita, A., Valdizán, E. M., Ledent, C., Pazos, Á., Maldonado, R., et al. (2008). BDNF impairment in the hippocampus is related to enhanced despair behavior in CB1 knockout mice. *J. Neurochem.* 105, 565–572. doi: 10.1111/j.1471-4159.2007.05149.x

Avraham, H. K., Jiang, S., Fu, Y., Rockenstein, E., Makriyannis, A., Zvonok, A., et al. (2014). The cannabinoid CB2 receptor agonist AM1241 enhances neurogenesis in GFAP/Gp120 transgenic mice displaying deficits in neurogenesis. *Br. J. Pharmacol.* 171, 468–479. doi: 10.1111/bph.12478

Azari, H., Rahman, M., Sharififar, S., and Reynolds, B. A. (2010). Isolation and expansion of the adult mouse neural stem cells using the neurosphere assay. *J. Vis. Exp.* 45:2393. doi: 10.3791/2393

Bagley, J. A., and Belluscio, L. (2010). Dynamic imaging reveals that brain-derived neurotrophic factor can independently regulate motility and direction of neuroblasts within the rostral migratory stream. *Neuroscience* 169, 1449–1461. doi: 10.1016/j.neuroscience.2010.05.075

Bennett, M. R., Arnold, J., Hatton, S. N., and Lagopoulos, J. (2017). Regulation of fear extinction by long-term depression: the roles of endocannabinoids and brain derived neurotrophic factor. *Behav. Brain Res.* 319, 148–164. doi: 10.1016/j.bbr.2016.11.029

Benraiss, A., Chmielnicki, E., Lerner, K., Roh, D., and Goldman, S. (2001). Adenoviral brain-derived neurotrophic factor induces both neostriatal and olfactory neuronal recruitment from endogenous progenitor cells in the adult forebrain. *J. Neurosci.* 21, 6718–6731.

Berghuis, P., Dobszay, M. B., Wang, X., Spano, S., Ledda, F., Sousa, K. M., et al. (2005). Endocannabinoids regulate interneuron migration and morphogenesis by transactivating the TrkB receptor. *Proc. Natl. Acad. Sci. U.S.A.* 102, 19115–19120. doi: 10.1073/pnas.0509494102

Bond, A. M., Ming, G. L., and Song, H. (2015). Adult mammalian neural stem cells and neurogenesis: five decades later. *Cell Stem Cell* 17, 385–395. doi: 10.1016/j.stem.2015.09.003

Butovsky, E., Juknat, A., Goncharov, I., Elbaz, J., Eilam, R., Zangen, A., et al. (2005). In vivo up-regulation of brain-derived neurotrophic factor in specific brain areas by chronic exposure to Delta9-tetrahydrocannabinol. *J. Neurochem.* 93, 802–811. doi: 10.1111/j.1471-4159.2005.03074.x

Casarosa, S., Zasso, J., and Conti, L. (2014). "Systems for ex-vivo isolation and culturing of neural stem cells," in *Neural Stem Cells - New Perspectives*, ed. L. Bonfanti (London: InTech), 1–27. doi: 10.5772/56573

Chan, J. P., Cordeira, J., Calderon, G. A., Iyer, L. K., and Rios, M. (2008). Depletion of central BDNF in mice impedes terminal differentiation of new granule neurons in the adult hippocampus. *Mol. Cell. Neurosci.* 39, 372–383. doi: 10.1016/j.mcn.2008.07.017

Choi, S. H., Li, Y., Parada, L. F., and Sisodia, S. S. (2009). Regulation of hippocampal progenitor cell survival, proliferation and dendritic development by BDNF. *Mol. Neurodegener.* 4:52. doi: 10.1186/1750-1326-4-52

Compagnucci, C., Di Siena, S., Bustamante, M. B., Di Giacomo, D., Di Tommaso, M., Maccarrone, M., et al. (2013). Type-1 (CB1) cannabinoid receptor promotes neuronal differentiation and maturation of neural stem cells. *PLoS One* 8:e54271. doi: 10.1371/journal.pone.0054271

De Chiara, V., Angelucci, F., Rossi, S., Musella, A., Cavasinni, F., Cantarella, C., et al. (2010). Brain-derived neurotrophic factor controls cannabinoid CB1 receptor function in the striatum. *J. Neurosci.* 30, 8127–8137. doi: 10.1523/JNEUROSCI.1683-10.2010

Derkinderen, P., Valjent, E., Toutant, M., Corvol, J.-C., Enslen, H., Ledent, C., et al. (2003). Regulation of extracellular signal-regulated kinase by cannabinoids in hippocampus. *J. Neurosci.* 23, 2371–2382.

Dijkhuizen, P. A., and Ghosh, A. (2005). BDNF regulates primary dendrite formation in cortical neurons via the PI3-kinase and MAP kinase signaling pathways. *J. Neurobiol.* 62, 278–288. doi: 10.1002/neu.20100

D'Souza, D. C., Pittman, B., Perry, E., and Simen, A. (2009). Preliminary evidence of cannabinoid effects on brain-derived neurotrophic factor (BDNF) levels in humans. *Psychopharmacology* 202, 569–578. doi: 10.1007/s00213-008-1333-2

Finkbeiner, S., Tavazoie, S. F., Maloratsky, A., Jacobs, K. M., Harris, K. M., and Greenberg, M. E. (1997). CREB: a major mediator of neuronal neurotrophin responses. *Neuron* 19, 1031–1047.

Gage, F. H. (2000). Mammalian neural stem cells. *Science* 287, 1433–1438. doi: 10.1126/science.287.5457.1433

Galvão, R., Garcea-Verdugo, J., and Alvarez-Buylla, A. (2008). Brain-derived neurotrophic factor signaling does not stimulate subventricular zone neurogenesis in adult mice and rats. *J. Neurosci.* 28, 13368–13383. doi: 10.1523/JNEUROSCI.2918-08.2008.Brain-Derived

Galve-Roperh, I., Aguado, T., Palazuelos, J., and Guzmán, M. (2007). The endocannabinoid system and neurogenesis in health and disease. *Neuroscientist* 13, 109–114. doi: 10.1177/1073858406296407

Galve-Roperh, I., Chiurchiù, V., Díaz-Alonso, J., Bari, M., Guzmán, M., and Maccarrone, M. (2013). Cannabinoid receptor signaling in progenitor/stem cell proliferation and differentiation. *Prog. Lipid Res.* 52, 633–650. doi: 10.1016/j.plipres.2013.05.004

Gao, X., Smith, G. M., and Chen, J. (2009). Impaired dendritic development and synaptic formation of postnatal-born dentate gyrus granular neurons in the absence of brain-derived neurotrophic factor signaling. *Exp. Neurol.* 215, 178–190. doi: 10.1016/j.expneurol.2008.10.009

Giachino, C., De Marchis, S., Giampietro, C., Parlato, R., Perroteau, I., Schütz, G., et al. (2005). cAMP response element-binding protein regulates differentiation and survival of newborn neurons in the olfactory bulb. *J. Neurosci.* 25, 10105–10118. doi: 10.1523/JNEUROSCI.3512-05.2005

Gomez, O., Arevalo-Martin, A., Garcia-Ovejero, D., Ortega-Gutierrez, S., Cisneros, J. A., Almazan, G., et al. (2010). The constitutive production of the endocannabinoid 2-arachidonoylglycerol participates in oligodendrocyte differentiation. *Glia* 58, 1913–1927. doi: 10.1002/glia.21061

Gómez-Palacio-Schjetnan, A., and Escobar, M. L. (2013). Neurotrophins and synaptic plasticity. *Curr. Top. Behav. Neurosci.* 15, 117–136. doi: 10.1007/7854_2012_231

Grigorenko, E., Kittler, J., Clayton, C., Wallace, D., Zhuang, S. Y., Bridges, D., et al. (2002). Assessment of cannabinoid induced gene changes: tolerance and neuroprotection. *Chem. Phys. Lipids* 121, 257–266. doi: 10.1016/S0009-3084(02)00161-5

Gross, C. G. (2000). Neurogenesis in the adult brain: death of a dogma. *Nat. Rev. Neurosci.* 1, 67–73. doi: 10.1038/35036235

Hempstead, B. L., Martin-Zanca, D., Kaplan, D. R., Parada, L. F., and Chao, M. V. (1991). High-affinity NGF binding requires coexpression of the trk proto-oncogene and the low-affinity NGF receptor. *Nature* 350, 678–683.

Henry, R. A., Hughes, S. M., and Connor, B. (2007). AAV-mediated delivery of BDNF augments neurogenesis in the normal and quinolinic acid-lesioned adult rat brain. *Eur. J. Neurosci.* 25, 3513–3525. doi: 10.1111/j.1460-9568.2007.05625.x

Howlett, A. C., Blume, L. C., and Dalton, G. D. (2010). CB(1) cannabinoid receptors and their associated proteins. *Curr. Med. Chem.* 17, 1382–1393. doi: 10.2174/092986710790980023

Isokawa, M. (2009). Time-dependent induction of CREB phosphorylation in the hippocampus by the endogenous cannabinoid. *Neurosci. Lett.* 457, 53–57. doi: 10.1016/j.jacc.2007.01.076.White

Khaspekov, L. G., Verca, M. S. B., Frumkina, L. E., Hermann, H., Marsicano, G., and Lutz, B. (2004). Involvement of brain-derived neurotrophic factor in cannabinoid receptor-dependent protection against excitotoxicity. *Eur. J. Neurosci.* 19, 1691–1698. doi: 10.1111/j.1460-9568.2004.03285.x

Klug, M., and van den Buuse, M. (2013). An investigation into "two hit" effects of BDNF deficiency and young-adult cannabinoid receptor stimulation on prepulse inhibition regulation and memory in mice. *Front. Behav. Neurosci.* 7:149. doi: 10.3389/fnbeh.2013.00149

Li, Y., Luikart, B. W., Birnbaum, S., Chen, J., Kwon, C., Steven, G., et al. (2008). TrkB regulates hippocampal neurogenesis and governs sensitivity to antidepressive treatment. *Neuron* 59, 399–412. doi: 10.1016/j.neuron.2008.06.023.TrkB

Lledo, P.-M., Alonso, M., and Grubb, M. S. (2006). Adult neurogenesis and functional plasticity in neuronal circuits. *Nat. Rev. Neurosci.* 7, 179–193. doi: 10.1038/nrn1867

Ma, D. K., Bonaguidi, M. A., Ming, G.-L., and Song, H. (2009). Adult neural stem cells in the mammalian central nervous system. *Cell Res.* 19, 672–682. doi: 10.1038/cr.2009.56

Maison, P., Walker, D. J., Walsh, F. S., Williams, G., and Doherty, P. (2009). BDNF regulates neuronal sensitivity to endocannabinoids. *Neurosci. Lett.* 467, 90–94. doi: 10.1016/j.neulet.2009.10.011

Marsicano, G. (2003). CB1 cannabinoid receptors and on-demand defense against excitotoxicity. *Science* 302, 84–88. doi: 10.1126/science.1088208

Mechoulam, R., and Parker, L. A. (2013). The endocannabinoid system and the brain. *Annu. Rev. Psychol.* 64, 21–47. doi: 10.1146/annurev-psych-113011-143739

Ming, G.-L., and Song, H. (2011). Adult neurogenesis in the mammalian brain: significant answers and significant questions. *Neuron* 70, 687–702. doi: 10.1016/j.neuron.2011.05.001

Molina-Holgado, F., Rubio-Araiz, A., García-Ovejero, D., Williams, R. J., Moore, J. D., Arévalo-Martín, A., et al. (2007). CB2 cannabinoid receptors promote mouse neural stem cell proliferation. *Eur. J. Neurosci.* 25, 629–634. doi: 10.1111/j.1460-9568.2007.05322.x

Nakagawa, S., Kim, J.-E., Lee, R., Malberg, J. E., Chen, J., Steffen, C., et al. (2002). Regulation of neurogenesis in adult mouse hippocampus by cAMP and the cAMP response element-binding protein. *J. Neurosci.* 22, 3673–3682.

Palazuelos, J., Aguado, T., Egia, A., Mechoulam, R., Guzmán, M., and Galve-Roperh, I. (2006). Non-psychoactive CB2 cannabinoid agonists stimulate neural progenitor proliferation. *FASEB J.* 20, 2405–2407. doi: 10.1096/fj.06-6164fje

Palazuelos, J., Ortega, Z., Díaz-Alonso, J., Guzmán, M., and Galve-Roperh, I. (2012). CB2 cannabinoid receptors promote neural progenitor cell proliferation via mTORC1 signaling. *J. Biol. Chem.* 287, 1198–1209. doi: 10.1074/jbc.M111.291294

Pertwee, R. G. (2008). Ligands that target cannabinoid receptors in the brain: from THC to anandamide and beyond. *Addict. Biol.* 13, 147–159. doi: 10.1111/j.1369-1600.2008.00108.x

Prenderville, J. A., Kelly, Á. M., and Downer, E. J. (2015). The role of cannabinoids in adult neurogenesis. *Br. J. Pharmacol.* 172, 3950–3963. doi: 10.1111/bph.13186

Rodrigues, R. S., Ribeiro, F. F., Ferreira, F., Vaz, S. H., Sebastião, A. M., and Xapelli, S. (2017). Interaction between cannabinoid type 1 and type 2 receptors in the modulation of subventricular zone and dentate gyrus neurogenesis. *Front. Pharmacol.* 8:516. doi: 10.3389/fphar.2017.00516

Segal-Gavish, H., Gazit, N., Barhum, Y., Ben-Zur, T., Taler, M., Hornfeld, S. H., et al. (2017). BDNF overexpression prevents cognitive deficit elicited by adolescent cannabis exposure and host susceptibility interaction. *Hum. Mol. Genet.* 26, 2462–2471. doi: 10.1093/hmg/ddx139

Singec, I., Knoth, R., Meyer, R. P., Maciaczyk, J., Volk, B., Nikkhah, G., et al. (2006). Defining the actual sensitivity and specificity of the neurosphere assay in stem cell biology. *Nat. Methods* 3, 801–806. doi: 10.1038/nmeth926

Snapyan, M., Lemasson, M., Brill, M. S., Blais, M., Massouh, M., Ninkovic, J., et al. (2009). Vasculature guides migrating neuronal precursors in the adult mammalian forebrain via brain-derived neurotrophic factor signaling. *J. Neurosci.* 29, 4172–4188. doi: 10.1523/JNEUROSCI.4956-08.2009

Soltys, J., Yushak, M., and Mao-Draayer, Y. (2010). Regulation of neural progenitor cell fate by anandamide. *Biochem. Biophys. Res. Commun.* 400, 21–26. doi: 10.1016/j.bbrc.2010.07.129

Trazzi, S., Steger, M., Mitrugno, V. M., Bartesaghi, R., and Ciani, E. (2010). CB1 cannabinoid receptors increase neuronal precursor proliferation through AKT/glycogen synthase kinase-3beta/beta-catenin signaling. *J. Biol. Chem.* 285, 10098–10109. doi: 10.1074/jbc.M109.043711

Vilar, M., and Mira, H. (2016). Regulation of neurogenesis by neurotrophins during adulthood: expected and unexpected roles. *Front. Neurosci.* 10:26. doi: 10.3389/fnins.2016.00026

Wang, L., Chang, X., She, L., Xu, D., Huang, W., and Poo, M.-M. (2015). Autocrine action of BDNF on dendrite development of adult-born hippocampal neurons. *J. Neurosci.* 35, 8384–8393. doi: 10.1523/JNEUROSCI.4682-14.2015

Xapelli, S., Agasse, F., Sardà-Arroyo, L., Bernardino, L., Santos, T., Ribeiro, F. F., et al. (2013). Activation of type 1 cannabinoid receptor (CB1R) promotes neurogenesis in murine subventricular zone cell cultures. *PLoS One* 8:e63529. doi: 10.1371/journal.pone.0063529

Yeh, M. L., Selvam, R., and Levine, E. S. (2017). BDNF-induced endocannabinoid release modulates neocortical glutamatergic neurotransmission. *Synapse* 71:e21962. doi: 10.1002/syn.21962

Zhao, C., Deng, W., and Gage, F. H. (2008). Mechanisms and functional implications of adult neurogenesis. *Cell* 132, 645–660. doi: 10.1016/j.cell.2008.01.033

Zhao, L., and Levine, E. S. (2014). BDNF-endocannabinoid interactions at neocortical inhibitory synapses require phospholipase C signaling. *J. Neurophysiol.* 111, 1008–1015. doi: 10.1152/jn.00554.2013

Zhao, L., Yeh, M. L., and Levine, E. S. (2015). Role for endogenous BDNF in endocannabinoid-mediated long-term depression at neocortical inhibitory synapses. *eNeuro* 2:ENEURO.0029-14.2015. doi: 10.1523/ENEURO.0029-14.2015

Zhong, P., Liu, Y., Hu, Y., Wang, T., Zhao, Y.-P., and Liu, Q.-S. (2015). BDNF interacts with endocannabinoids to regulate cocaine-induced synaptic plasticity in mouse midbrain dopamine neurons. *J. Neurosci.* 35, 4469–4481. doi: 10.1523/JNEUROSCI.2924-14.2015

Conflict of Interest Statement: The authors declare that the research was conducted in the absence of any commercial or financial relationships that could be construed as a potential conflict of interest.

frontiers in Cellular Neuroscience

ORIGINAL RESEARCH
published: 07 December 2018
doi: 10.3389/fncel.2018.00478

Methyl 3,4-Dihydroxybenzoate Induces Neural Stem Cells to Differentiate Into Cholinergic Neurons *in vitro*

Jun-Ping Pan[1,2†], Yang Hu[1,3†], Jia-Hui Wang[1†], Yi-Rong Xin[1], Jun-Xing Jiang[1], Ke-Qi Chen[1], Cheng-You Yang[4], Qin Gao[1], Fei Xiao[1,3], Li Yan[5*] and Huan-Min Luo[1,3*]*

[1] Department of Pharmacology, College of Basic Medicine, Jinan University, Guangzhou, China, [2] Department of Neurosurgery, Guangzhou Women and Children's Medical Center, Guangzhou, China, [3] Institute of Brain Sciences, Jinan University, Guangzhou, China, [4] Department of Neurosurgery, The First Affiliated Hospital of Jinan University, Guangzhou, China, [5] Guangzhou Quality R&D Center of Traditional Chinese Medicine, Guangdong Key Laboratory of Plant Resources, School of Life Sciences, Sun Yat-sen University, Guangzhou, China

OPEN ACCESS

Edited by:
Carlos P. Fitzsimons,
University of Amsterdam, Netherlands

Reviewed by:
Hermona Soreq,
The Hebrew University of Jerusalem, Israel
Sara Xapelli,
Universidade de Lisboa, Portugal

***Correspondence:**
Fei Xiao
xiaofei@jnu.edu.cn
Li Yan
yanli@mail.sysu.edu.cn
Huan-Min Luo
tlhm@jnu.edu.cn

† These authors have contributed equally to this work as first authors

Received: 23 June 2018
Accepted: 22 November 2018
Published: 07 December 2018

Citation:
Pan J-P, Hu Y, Wang J-H, Xin Y-R, Jiang J-X, Chen K-Q, Yang C-Y, Gao Q, Xiao F, Yan L and Luo H-M (2018) Methyl 3,4-Dihydroxybenzoate Induces Neural Stem Cells to Differentiate Into Cholinergic Neurons in vitro. Front. Cell. Neurosci. 12:478. doi: 10.3389/fncel.2018.00478

Neural stem cells (NSCs) have been shown as a potential source for replacing degenerated neurons in neurodegenerative diseases. However, the therapeutic potential of these cells is limited by the lack of effective methodologies for controlling their differentiation. Inducing endogenous pools of NSCs by small molecule can be considered as a potential approach of generating the desired cell types in large numbers. Here, we reported the characterization of a small molecule (Methyl 3,4-dihydroxybenzoate; MDHB) that selectively induces hippocampal NSCs to differentiate into cholinergic motor neurons which expressed synapsin 1 (SYN1) and postsynaptic density protein 95 (PSD-95). Studies on the mechanisms revealed that MDHB induced the hippocampal NSCs differentiation into cholinergic motor neurons by inhibiting AKT phosphorylation and activating autophosphorylation of GSK3β at tyrosine 216. Furthermore, we found that MDHB enhanced β-catenin degradation and abolished its entering into the nucleus. Collectively, this report provides the strong evidence that MDHB promotes NSCs differentiation into cholinergic motor neurons by enhancing gene *Isl1* expression and inhibiting cell cycle progression. It may provide a basis for pharmacological effects of MDHB directed on NSCs.

Keywords: methyl 3,4-dihydroxybenzoate, neural stem cells, differentiate, cholinergic neurons, GSK3β, cell cycle, *Isl1*

INTRODUCTION

Neural stem cells (NSCs) have the ability of self-renewal and to differentiate into multiple specialized neural cell types, such as neurons, astrocytes and oligodendrocytes, thus serving as the common source of these fundamental components of the CNS (Gage, 2000). Consequently, NSCs can furnish an unlimited source of cells for cell transplantation therapy to supplement degenerating cells (Ager et al., 2015; Reidling et al., 2018). Facing this potential, some defects, such as the uncontrollability of stem cell differentiation pathway and immune rejection for stem cell therapy, can be surmounted. At present, NSCs have been proved to exist not only in the embryonic

mammal nervous system, but also in the nervous system of most adult mammals (Goncalves et al., 2016). In adulthood, the main neurogenic niches are the sub-granular zone (SGZ) of hippocampal dentate gyrus (DG) as well as the sub-ventricular zone (SVZ), both of which continuously generate newborn neurons with potential functions their contribution to behavior, and their relevance to disease (Zhao et al., 2008).

Glycogen synthase kinase 3s are serine/threonine kinases in receptor tyrosine kinase. Wnt/Frizzled signaling pathway is originally confirmed as important regulatory enzymes in glucose metabolism (Hur and Zhou, 2010; Mussmann et al., 2014). There are two subtypes(GSK3α and GSK3β) encoded by different genes, which are overall 85% homologous to each other, with 95% identity in the kinase domains. Kim et al. (2009) showed that the phosphorylation levels of β-catenin, target of GSK3β, are increased at later stages in development when stem cell proliferation is declining and cholinergic neuronal differentiation predominates (Ming and Song, 2009). Degradation of β-catenin by activation of GSK3β will inhibit cell proliferation and increase cell differentiation. These finding demonstrate that the activation of GSK3β increases cell differentiation (Kuwabara et al., 2009).

Cholinergic neurons are located in extensive regions of the CNS, which regulates complicated behaviors (Hangya et al., 2015). The cholinergic neurotransmission system adjusts the effects of several key factors that are strongly expressed in all cholinergic neurons, termed cholinergic pathway genes (Saunders et al., 2015). Understanding the gene regulatory mechanisms that monitor the expression of cholinergic pathway genes in different groups of cholinergic neurons will provide crucial insights into the process of cholinergic fate specification in CNS diseases (Cho et al., 2014). Previous studies found that seven regulators controlled the identity of cholinergic neuron types. Three LIM homeobox genes (*lim-4/Lhx6/8, lim-11/Lhx1, and ceh-14/Lhx3/4*) and two Prox-type homeobox genes (*unc3/EBF, unc-42/Prd*) control cholinergic identity of cholinergic neuron types, including sensory neurons, interneurons and motor neurons in *Caenorhabditis elegans*. Pitx-type homeobox gene (*unc-30/Pitx)* control the identity of the PVP interneurons (in conjunction with *lin-11*) and POU homeobox gene (*unc-86*/*Brn3*) controls cholinergic identity of the URX, RIH and male-specific CEM neurons (Duerr et al., 2008). lim-7 (*Isl1*), a specific cholinergic identity in the spinal cord and forebrain in the *C. elegans*, has a function as a cholinergic fate determinant in vertebrate CNS (Cho et al., 2014; Zhang et al., 2018).

Methyl 3,4-dihydroxybenzoate (MDHB, C8H8O4), with a molecular weight of 168.15 (CAS), is a small molecular compound extracted from the traditional herbs. Previous researches have described that MDHB has the effect of antioxidant (Cai et al., 2016). In addition, studies in our laboratory have shown that MDHB could accelerate the neurite outgrowth of primary cortical neurons *in vitro* by inducing brain-derived neurotrophic factor (BDNF) expression (Zhang Z. et al., 2015), protect the primary cortical neurons against Aβ(25-35)-induced apoptosis by mitochondria pathway (Zhou et al., 2013), as well as prolong the lifespan of *C. elegans* (Zhang et al., 2014).

In this study, we found that MDHB can specifically induce neuronal differentiation *in vitro* and promote excitatory cholinergic motor neuron differentiation. Additionally, MDHB can increase the activity of tyrosine-phosphorylated GSK3β, and then the activated GSK3β promotes phosphorylation of β-catenin, resulting in the degradation of β-catenin. Subsequently, cell cycle and *Tacc3* gene controlled neuronal differentiation can be inhibited. *Isl1* gene controlled cholinergic neuronal differentiation will be up-regulated. In summary, we showed that the expression of neuronal differentiation transforming acidic coiled-coil 3 (*Tacc3*) gene and cell cycle are inhibited and cholinergic neuronal differentiation gene *Isl1* are up-regulated by MDHB.

MATERIALS AND METHODS

Animals and Ethics Statement

This study was carried out in accordance with the recommendations of the Animal Research Committee of the School of Medicine of Jinan University (Approval Number: 20170607002). The protocol was approved by the Animal Research Committee of the School of Medicine of Jinan University.

Isolation and *in vitro* Culture of NSCs

Rat NSCs were derived and cultured as described previously by others (Rietze and Reynolds, 2006). Briefly, the hippocampi of several postnatal rats were chopped, mechanical digested by 0.25% trypsin (Gibco) in a humidified 5% CO_2 incubator at 37°C for 10 min and triturated. The cell suspension was added into an equal volume of DMEM/F12 (Gibco) supplemented with 10%fetal bovine serum (Lonsera) and 0.1 mg/ml DNase I (Sigma), afterward filtered through a 70 μm microfiltration membrane and centrifuged for 5 min. The cells cultured in DMEM/F12 containing 10 ng/mL basic fibroblast growth factor (Proteintech), 20 ng/mL EGF (Proteintech), 1%penicillin and streptomycin (Sigma) and 2% B27 (Gibco) without vitamin A were seeded in 6 well plate in a humidified 5% CO2 incubator at 37°C. Within 3–5 days, the cells grew into free floating neurospheres which were then gathered by centrifugation and passaged after mechanical, dissociation by pipetting.

NSCs Differentiation

For NSCs differentiation, neurospheres (passage 2–3) were dissociated into a NSC by stem cell digestive enzyme (Gibco) and NSCs were seeded in 0.0125 mg/ml poly-D-lysine (PDL, Sigma) and 10 ng/ml laminin (Sigma)-coated glass cover slips at the density of 35,000 cells/cm^2 directly in DMEM/F12 supplemented with 1%FBS (Gibco) and 1%penicillin and streptomycin. When cells were completely adherent in the plate after 2 h, DMEM/F12 containing 1%FBS was replaced by rat NSCs differentiation medium (NeuroCult Differentiation Kit, Catalog #05700). The cultures were then treated with MDHB (0, 8, 16, and 32 μM) which was dissolved in DMSO (Sigma). The culture treated with MDHB was changed every second day.

Immunofluorescence Staining

Treated cells were fixed with 4% paraformaldehyde (PFA) for 45 min at room temperature, washed with phosphate-buffered saline (PBS, pH7.6) and blocked with super blocking solution containing 0.5% goat serum, 1%fish serum, 0.5% donkey serum and 0.5% bovine serum in 0.3% Triton X-100 PBS at room temperature for 60 min. Subsequently cells were incubated with primary antibodies at 4°C for 16 h overnight. The primary antibodies were mouse anti-Nestin (1:100, Millipore), mouse anti-neuron-specific class III beta-tubulin (Tuj-1, 1:1000, Sigma), mouse anti-microtubule-associated protein 2 (MAP2, 1:500, Sigma), and rabbit anti-glial fibrillary acidic protein (GFAP, 1:1000, Abcam), rabbit anti-PSD95 (1:500, Abcam), Mouse anti-CAMKII (1:500, Abcam), rabbit anti-Ki67 (1:500, Abcam), mouse anti-ChAT (1:500, Sigma), mouse anti- VGluT1 (1:500, Millipore), mouse anti-TPH (1:500, Millipore), rabbit anti-Gad67 (1:500, Sigma), rabbit anti-TH (Millipore), goat anti-Isl1 (1:500, Abcam), chicken anti-MAP2 (1:2000, Sigma), rabbit anti-Tbr1 (1:500, Sigma), rabbit anti-Prox1(1:500, Abcam), rat anti-Ctip2 (1:500, Millipore), mouse anti-Cux1(1:500, Sigma), rabbit anti-NeuN (1:1000, Abcam). The cells were washed three times with 0.3% PBST and incubated with Alexa Fluor 488, CY3, 647-conjugated secondary antibody (1:1000, Earthox) at room temperature for1h. To visualize nuclei, cells were counterstained with 1 ng/ml 4′,6-diamidino-2-phenylindole (DAPI, 1 ng/ml, Sigma) for 5 min. Finally, all images were captured with a confocal microscope (Zeiss, LSM700) and then processed via Image J software (NIH, Bethesda, MD, United States). The number of Nestin, Tuj-1, MAP2, GFAP, Nestin, ChAT, NeuN, Cux1, Ctip2, Tbr1 and Prox1 positive cells and cell nuclei were counted in each of seven random fields per well.

Western Blot Analysis

Cells differentiate for 5 days in differentiation medium in the presence of MDHB and then collected. Cells were washed with pre-cooling phosphate-buffered saline (pH7.6) added with the lysis buffer, and then they were homogenized via ultrasonication and centrifuged at 12000 *g* for 10 min at 4°C. The protein concentration in the supernatant was detected by a BCA assay kit (Beyotime Institute of Biotechnology). Then the supernatants were blended with loading buffer in a ratio of 1:1 and boiled for 5 min at 100°C, and then subjected to SDS page (12% and 10% acrylamide gels, 120 V, 1.5 h). The separated proteins were transferred to poly-vinyli dene fluoride (PVDF) membranes (100 V, 85 min) and blocked with 5% skimmed milk dissolved in 0.05%TBST. After three times rinsing in 0.05%TBST, the proteins were incubated with primary antibodies overnight at 4°C. The membrane was exposed to either HRP- rabbit or mouse secondary antibody for 1 h at room temperature. The fluorescent signal of the blots was collected by ALLIANCE 4.7 apparatus and quantified with the Quantity One software. The expressions of β-III-tubulin, GFAP, AKT (CST), p-AKT (CST), GSK3β (CST), p-ser9-GSK3β (CST), p-try-GSK3β (Thermofisher) andβ-catenin (CST) were determined via calculating their density ratio to the GAPDH band.

Cell Collection and mRNA Preparation

Cells were collected after differentiating for 5d in differentiation medium in the presence of MDHB. Total RNA was isolated using Trizol Reagent (Invitrogen), in combination with RNAase-free DNAase to eliminate the potential DNA contamination (TAKARA). The concentration and purity of RNA were measured by Nanodrop 2000C Spectrophotometer.

Transcriptome Analysis of MDHB-Induced Differentiation

The RNA-seq technique was used to analyze the gene expression profiling in MDHB-induced NSCs differentiation (SRA accession:PRJNA505930). The cDNA fragments were purified using a QIAquick PCR extraction kit following the manufacturer's protocol. Next, the cDNA fragments were enriched by PCR to construct the final cDNA, which was sequenced by Illumina sequencing platform (IlluminaHiSeq^{TM} 2500).

Gene Expression Validation by qRT-PCR

Reverse transcription was performed into cDNA using the PrimeScript TMRT reagent Kit with gDNA Eraser following the manufacturer's protocol. Real-time PCR was performed with a SYBR® Premix Ex TaqTM II detection System. The primer sequences are shown as follows (**Table 1**):

TABLE 1 | The primer sequences.

Gene	Primer sequence
Cdkn1a-Forward	5-GGGATGCATCTATCTTGTGATATG-3
Cdkn1a-Reverse	5-GCGAAGTCAAAGTTCCACCG-3
Cdc20-Forward	5-TGGAGAAAGTGGCTGGGTTC-3
Cdc20-Reverse	5-ATGCGAATGTGTCGGTCACT-3
Tacc3-Forward	5-GTCTGGCTCCGGAAATCCAA-3
Tacc3-Reverse	5-CACCATAGGCTCGGCAGGAA-3
Actin-Forward	5-CACCCGCGAGTACAACCTTC-3
Actin-Reverse	5-CCCATACCCACCATCACACC-3
Isl1-Forward	5-GACATGATGGTGGTTTACAGGC-3
Isl1-Reverse	5-GCTGTTGGGTGTATCTGGGAG-3
Lhx8-Forward	5-CAGTTCGCTCAGGACAACAA-3
Lhx8-Reverse	5-AGCCATTTCTTCCAACATGG-3
Lhx3-Forward	5-AGAGCGCCTACAACACTTCG-3
Lhx3-Reverse	5-GGCCAGCGTCTTTCTTCAGT-3

Statistical Analysis

The data are expressed as mean ± SEM. Statistical analyses were performed by using a Test or ANOVA followed by Boferonni's test, using the Prism software (GraphPad, San Diego, CA, United States). A value of $P < 0.05$ was considered as significantly different from the control.

RESULTS

Neural Stem Cells, Culture and Identification

To extract primary hippocampal NSCs, neurospheres were passaged *in vitro* (Reynolds and Rietze, 2005). Experimental materials were prepared from the second or the third generation of NSCs. The third generation of NSCs (**Figure 1B**) were most suspended neurospheres. Nestin and DAPI were used to stain single neural stem cell (**Figure 1C**) from digested neurospheres by immunofluorescence (**Figure 1A**). Analysis showed that the purity of the primary cells were most NSCs (**Figure 1D**), and DCX (neurons marker) and GFAP (astrocytes marker) were immunonegative of primary NSCs (**Figures 1E,F**).

MDHB Promotes the Differentiation of NSCs Into Neurons

To determine the effects of different concentrations of MDHB on neuronal differentiation of NSCs, neurospheres were dissociated into a single NSC, which was treated in the presence of the following concentrations: 0 μM MDHB, 8 μM MDHB, 16 μM MDHB, 32 μMMDHB. After 5 days, we observed that the cell bodies of different concentrations of MDHB groups had neuronal morphological features (**Figures 2A–D**). The expressions of Tuj1 (immature neuron) and GFAP (astrocyte) were detected by western blot (**Figures 2E,J,K**). The results revealed that MDHB increased the expression of Tuj1 and inhibited the expression of GFAP in the differentiation of NSCs. Neuronal marker Tuj1 and astrocyte marker GFAP were used to identify cells (Ray et al., 2018) (**Figures 2F–I**). The DMSO group had more GFAP positive cells, while MDHB treated group (8, 16, and 32 μM) had more Tuj1 positive cells. Above results indicated that MDHB enhanced the differentiation of NSCs into neurons (**Figure 2J**) and inhibited NSCs differentiation into astrocytes (**Figure 2K**).

MDHB-Induced Immature Neurons Form Mature Neurons

Next, we examined whether immature neurons in MDHB-induced differentiation can form mature neurons. After 9 days using different doses of MDHB presenting on NSCs, cells were stained with MAP2 and NeuN marker which are specific markers of mature neurons (**Figures 3A–F**). The result showed

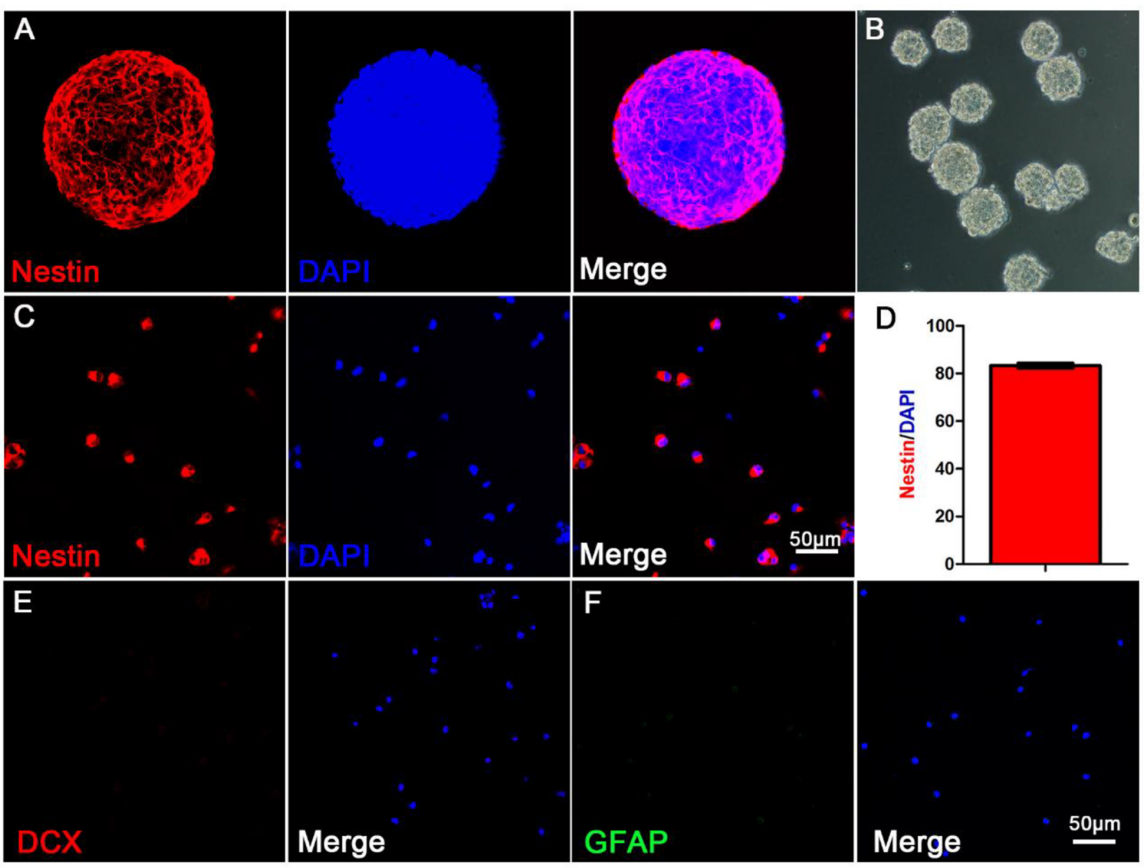

FIGURE 1 | The morphological and purity identification of primary neurospheres and neural stem cells. **(A)** Nestin and DAPI fluorescent staining of primary neurospheres composed of neural stem cells; **(B)** The morphological status of primary neurospheres *in vitro*; **(C)** Nestin and DAPI fluorescent staining of scattered primary NSCs; **(D)** The purity statistics of primary NSCs; **(E)** DCX and DAPI staining of scattered primary NSCs; **(F)** GFAP and DAPI staining of scattered primary NSCs.

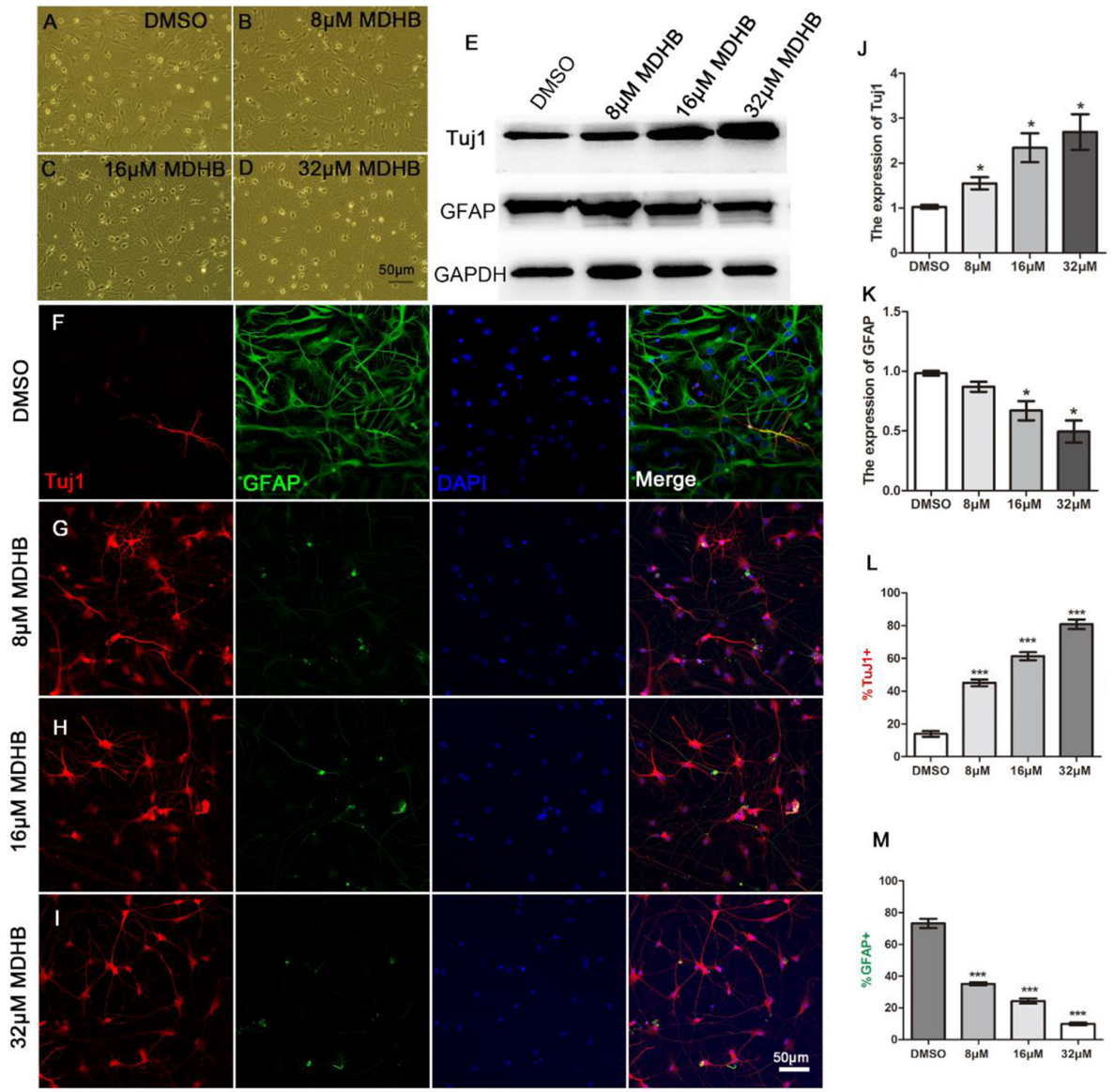

FIGURE 2 | MDHB promotes NSCs differentiation into neurons. **(A)** The solvent control group (DMSO); **(B–D)** Low dose (8 μM MDHB), middle dose (16 μM MDHB), and high dose (32 μM MDHB) groups. **(E)** Western blot analysis for Tuj1 (immature neuron) and GFAP (astrocyte) on differentiation of NSCs. **(F–I)** After 5 days of NSCs differentiation induced by MDHB, new cells were fluorescently stained, the cells with neuronal marker Tuj1 were dyed red; with glial marker GFAP dyed green; and all cell nuclei with nuclear marker DAPI were dyed blue. **(J,K)** Quantification of protein blots is shown, GAPDH serves as protein loading control. **(L)** The statistical results of neurons differentiated by MDHB-induced NSCs. **(M)** The statistical results of astrocytes differentiated by MDHB-induced NSCs (*$P < 0.05$, ***$P < 0.001$, compared with DMSO group, $n = 3$).

that MAP2 positive cells were significantly increased in a MDHB dose-dependent way, and NeuN positive cells were also promoted by MDHB-induced NSCs differentiation. Thus, MDHB can promote NSCs differentiation into mature neurons (**Figures 3G,H**).

MDHB Promotes the Differentiation of NSCs Into Cholinergic Neurons

Here, we investigated neuronal subtypes based on neurotransmitters they contain. We first found that the majority of MDHB-induced neurons were immunopositive for cholinergic neurons marker ChAT (**Figure 4A**) and motor neurons marker Isl1 (**Figure 4F**). A small fraction of the converted neurons was immunopositive for glutamatergic neurons marker VGluT1 (**Figure 4E**). On the other hand, the MDHB-induced neurons were immunonegative for GABAergic neurons marker GAD67 (**Figure 4B**), dopaminergic neurons marker TH (**Figure 4C**), and serotonergic (5-HT) neurons marker TPH (**Figure 4D**). The quantitative analyses of the neuronal subtypes were shown in **Figure 4F** (n = 3 batches).

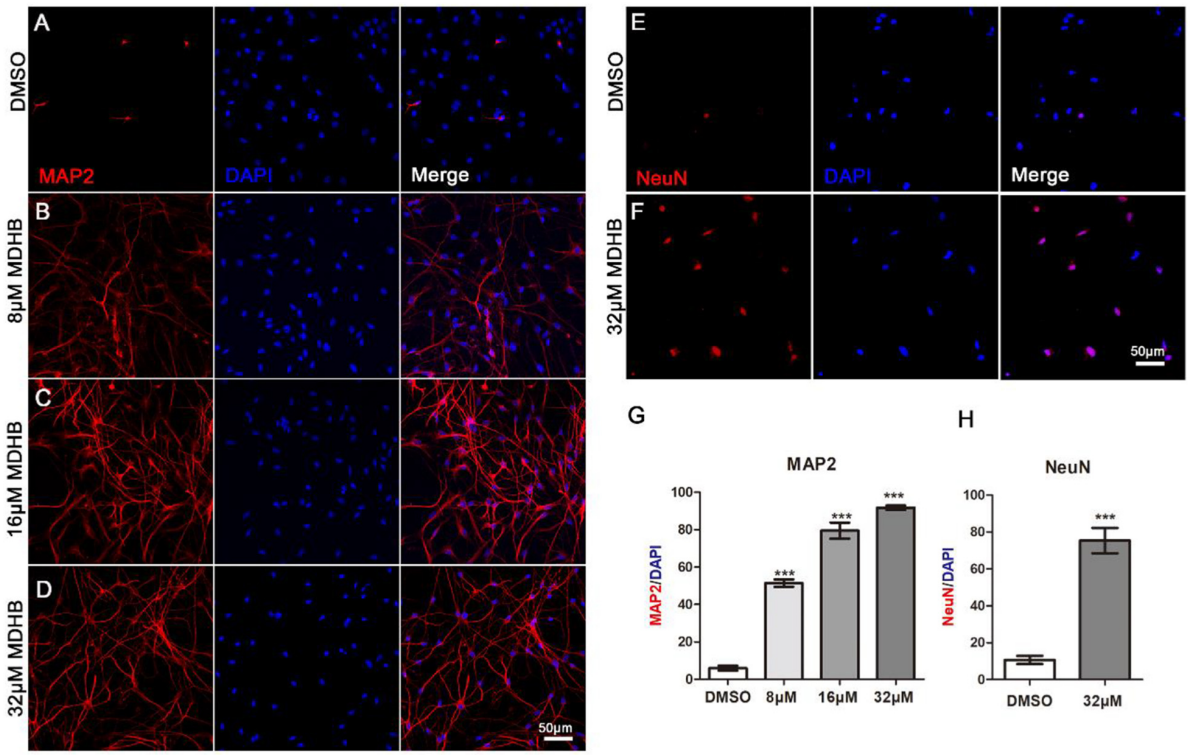

FIGURE 3 | MDHB-induced immature neurons form mature neurons. **(A–F)** After 9 days of NSCs differentiation induced by MDHB, the new cells were fluorescently stained, the cells with MAP2 and NeuN were dyed red and the cell nuclei with DAPI was dyed blue; **(G,H)** the statistical results of mature neurons differentiated by MDHB-induced NSCs (***$P < 0.001$, compared with DMSO group, $n = 3$).

These results suggested that the cholinergic motor neurons were the major subtype of MDHB-induced neurons.

To characterize the neuronal properties after small molecule-induced differentiation, we examined neuronal markers expressed from anterior to posterior nervous system. We found that the MDHB-induced neurons were- immunonegative for superficial layer neuronal marker Cux1 (**Figure 4J**), but positive for deep layer neuronal markers Ctip2 (**Figure 4I**). The MDHB-induced neurons were also immunonegative for cortical neuronal marker Tbr1 (**Figure 4H**), as well as hippocampal neuronal marker Prox1 (**Figure 4G**). **Figures 4K,L** showed the quantitative results. Therefore, our MDHB-induced neurons were mainly hippocampal neurons (**Figures 4K,L**).

The Expression of Synaptic Proteins in MDHB-Induced Neurons

We next investigated whether MDHB-induced neurons have synapse formation. Synapsin I exists in the nerve terminal of axons, mainly in the membranes of synaptic vesicles. The encoded protein acts as a substrate for several different protein kinases, and phosphorylation can play a role in the regulation of proteins in the nerve terminal. PSD-95 is a member of the membrane-associated guanylate kinase (MAGUK) family, and it plays an important role in synaptic plasticity and the stabilization of synaptic changes (Perche et al., 2018; Whalley, 2018). Calcium/calmodulin-dependent protein kinase II (CaMKII)-the main protein of the postsynaptic density-is a Ca^{2+}/calmodulin-activated dodecameric enzyme (Lisman et al., 2002). The expression of synaptic proteins in neurons was identified by cellular immunofluorescence. The Figure showed that Synapsin I (SYN1) (**Figures 5E,F**) and postsynaptic density protein 95 (PSD-95) (**Figures 5A–D**) significantly expressed. It indicated that these neurons could form neural network.

Effect of MDHB on AKT, GSK3β and β-catenin

To understand the molecular mechanisms of MDHB-induced differentiation of NSCs into cholinergic neurons (**Figures 6A,B**). Western blot results revealed that the phosphorylation level of AKT protein was down-regulated in the MDHB group (**Figure 6C**), and the total AKT protein expression was unchanged (**Figure 6D**), MDHB activated phosphorylation of GSK3β at tyrosine 216 (Y216) (**Figure 6F**). The phosphorylation level of serine at position 9 was unchanged (**Figure 6G**) and the transcription factor β-catenin was down-regulated (**Figure 6E**). As shown above, the mechanism of MDHB promoted differentiation of NSCs into cholinergic neurons may perform by increasing. The activity of GSK3β (**Figure 6H**) and inhibiting the activity of PI3K.

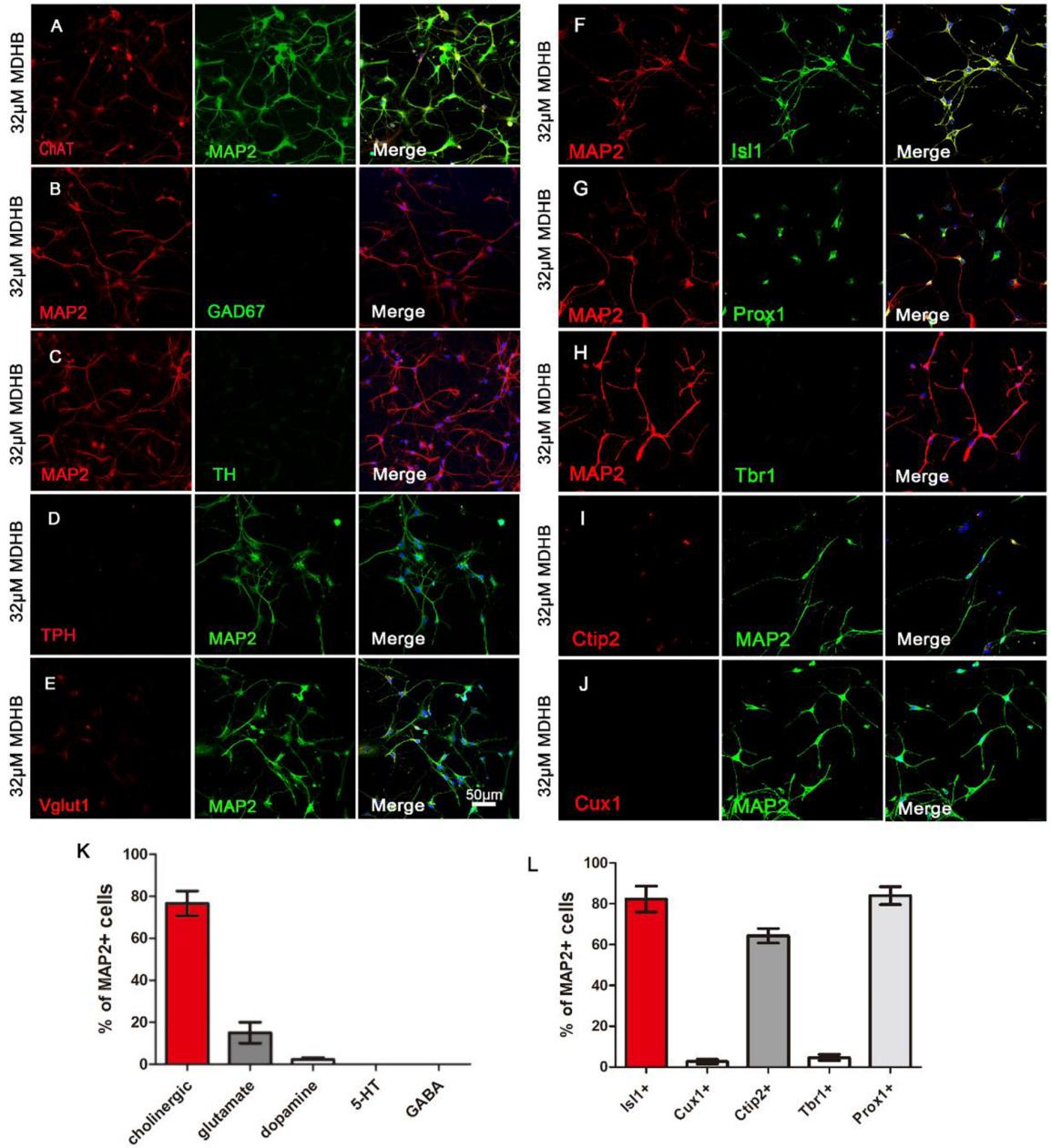

FIGURE 4 | The types analysis of MDHB-induced neurons. **(A)** The cholinergic neurons with ChAT and MAP2 were respectively dyed red and green; **(B)** the GABAergic neurons with MAP2 and Gad67 were respectively dyed red and green; **(C)** the dopaminergic neurons with MAP2 and TH were respectively dyed red and green; **(D)** the serotonergic (5-HT) neurons with TPH and MAP2 were respectively dyed red and green; **(E)** the glutamatergic neurons with Vglut1 and MAP2 were respectively dyed red and green; **(F)** MDHB-induced neurons were also immunopositive for motor neuron marker Isl1; **(G,H)** Immunostaining with neuron markers revealed that MDHB-induced neurons were negative for general cortical neuron marker Tbr1, but positive for hippocampal neuron marker Prox1 **(G)**; **(I,J)** Immunostaining with neuron markers revealed that MDHB-induced neurons were negative for superficial layer marker Cux1 **(J)**, but positive for deep layer marker Ctip2 **(I)**. **(K,L)** The statistical results showed that MDHB promoted NSCs differentiation into hippocampal cholinergic neurons.

MDHB Inhibits Cell Cycle and Increases the Expression of Cholinergic Neuronal Gene *Isl1*

The transcription factor β-catenin was down-regulated, which is critical for the control of NSCs' cell cycle in multiple regions of the developing CNS. We further performed immunostaining to examine the cell cycle protein expression changes during induced NSCs differentiation process. MDHB was utilized to treat NSCs in 24, 48, and 72 h for differentiation. The data showed that the expression of Ki67 in MDHB group was less in 24, 48, and 72 h (**Figures 7A–G**). Compared

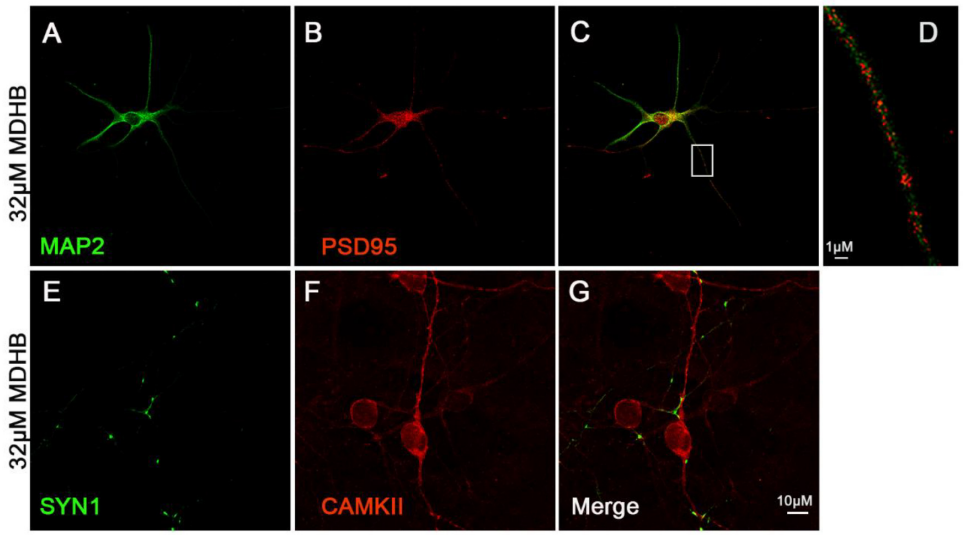

FIGURE 5 | The expression of synaptic protein in MDHB –induced neurons. **(A–D)** MDHB –induced neurons has the expression of postsynaptic dense protein (PSD95); **(E–G)** MDHB –induced neurons has the expression of Synapsin I (SYN1).

with the DMSO group, the expression of *Tacc3 in* neuronal differentiation and *Cdc20* in cell cycle were decreased, and the expression of *Cdkn1a* in cell cycle and *Isl1* in cholinergic pathway was up-regulated. *Lhx3* and *Lhx8* had not change. Our data indicated that MDHB induced NSCs differentiation by regulating cell cycle-related gene and cholinergic neuron-related gene.

DISCUSSION

Since the neuronal differentiation of NSCs is an intricate process, it is not surprising that many substances have been involved in the regulation action (Gauthier-Fisher et al., 2009; Ming and Song, 2009; Akizu et al., 2010; Luo et al., 2010; Park et al., 2016; Vasconcelos et al., 2016). However, little is known about the small molecules in NSCs. The small molecules controlling the direction of NSCs differentiation would be a critical advance in neurodegeneration and CNS repair. Here, we described a novel small molecule -named MDHB that modulates cholinergic neuronal differentiation of NSCs. We found that MDHB promotes the differentiation of NSCs into neurons and inhibits NSCs differentiation into astrocytes. The major subtypes of MDHB-induced neurons are cholinergic neurons.

NSCs refer to a type of cell population that exists in CNS and has the latent energy to differentiate into neurons, astrocytes, and oligodendrocytes, and they can proliferate to replenish lost brain cells (Mosher et al., 2012; Aharonowiz et al., 2018). Mouse NSCs were successfully isolated and established in 1992. Subsequently, NSC lines of human and other organisms were successively established(Kim et al., 2008; Chicheportiche et al., 2018). We performed Nestin and DAPI fluorescent staining of NSCs, which is widely used as a specific marker of NSCs (Crook and Tomaskovic-Crook, 2017; Jin et al., 2017). The results demonstrated that the high purity of NSCs in the cultured primary cells.

These results indicated that MDHB (8, 16, and 32 μM) promotes NSCs differentiation into immature neurons and overrides NSCs differentiation into astrocytes. In this study, the effect of MDHB on the differentiation of NSCs was observed. The whole cell exhibited obviously neuronal morphological characteristics. Tuj1 is a neuron-specific marker which has been widely used for the identification of immature neurons, GFAP is an astrocytes marker which is generally used for identification of glial cells(Park et al., 2017). These results indicated that MDHB (8, 16, and 32 μM) promotes differentiation of NSCs into immature neurons while inhibiting their differentiation into astrocytes (**Figure 2**). MAP2 is the skeleton protein of neurons and plays a vital role in the stability and function in maintaining microtubules. It widely distributes in mature neuronal dendrites and is used as a marker to measure the growth of neuronal processes (Gumy et al., 2017). NeuN is also a mature neuronal marker in the neuronal nucleus. Through mature neuronal immunofluorescence staining, we found that the expressions of MAP2 and NeuN in MDHB groups are significantly higher than the DMSO group in a dose-dependent manner. It indicated that MDHB can promote not only NSCs differentiation into immature neurons, but the development into mature neurons.

Neurons have a wide variety of classifications, which include basis on the structure of neurons, the function of neurons and neurotransmitters releasing (Zeng and Sanes, 2017). At present, according to the neurotransmitters, they are classified into the following categories: cholinergic neurons, dopaminergic neurons, GABAergic neurons, serotonergic (5-HT) neurons, glutamatergic neurons and so on (Dvoryanchikov et al., 2017). Neurons released different neurotransmitters have distinct

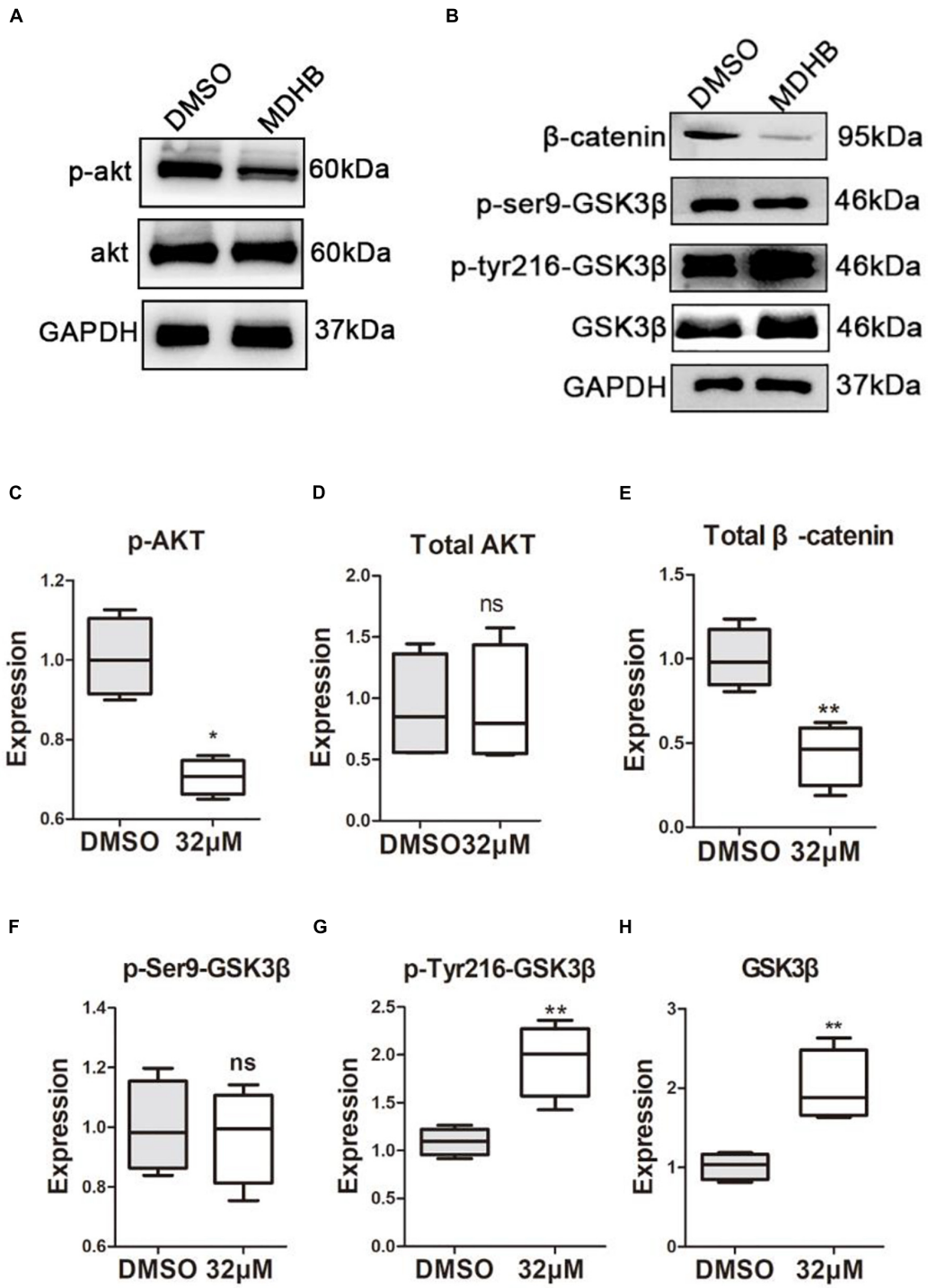

FIGURE 6 | The effect of MDHB on AKT, GSK3β and β-catenin. MDHB inhibited phosphorylation of AKT in the differentiation of neural stem cells, activated phosphorylation of GSK3β at tyrosine 216 (Y216), and downregulated transcription factor β-catenin. **(A,B)** Western blot analyses of proteins extracted from MDHB-treated neural stem cell in differentiation, **(C–H)** quantification of protein blots is shown, GAPDH serves as protein loading control. Each point represents the mean relative protein level of each group (*$P < 0.05$, compared with DMSO group, **$P < 0.01$, compared with DMSO group, $n = 4$).

functions in the CNS (Haim and Rowitch, 2017; Zhou et al., 2017). According to the localization that they place in brain, they can be classified into superficial layer neurons, deep layer neurons and so on (Zeng and Sanes, 2017). Previous research showed that the main hippocampal neurons were Glutamatergic and GABAergic (Lei et al., 2016). Although the cholinergic

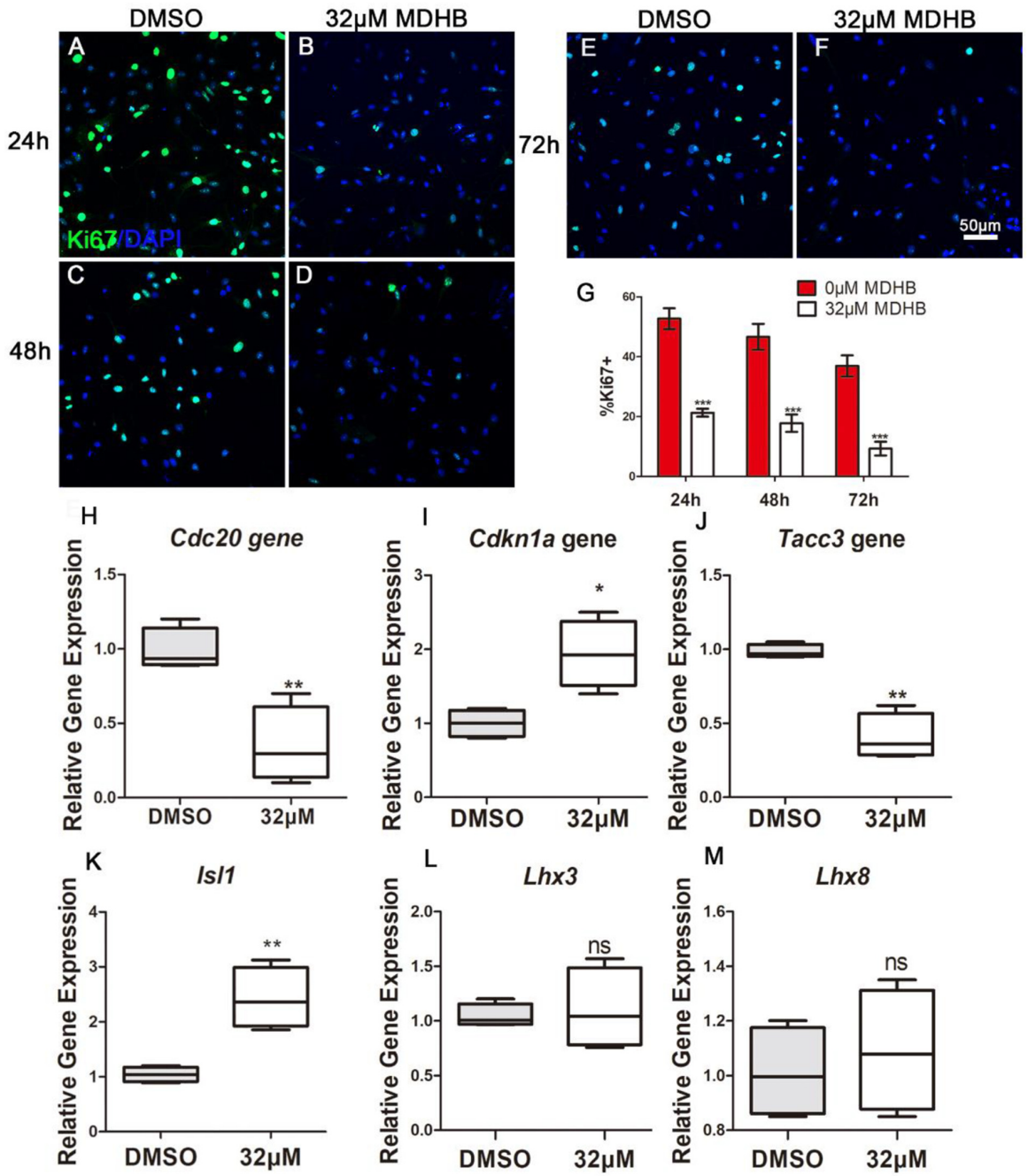

FIGURE 7 | MDHB promotes the differentiation of NSCs into cholinergic neurons by inhibiting cell cycle and increasing cholinergic pathway gene *Isl1*. **(A)** The effect of DMSO on differentiation of NSCs for 24 h; **(B)** the effect of MDHB on differentiation of NSCs for 24 h; **(C)** the effect of DMSO on differentiation of NSCs for 48 h; **(D)** The effect of MDHB on differentiation of NSCs for 48 h; **(E)** the effect of DMSO on differentiation of NSCs for 72 h; **(F)** The effect of MDHB on differentiation of NSCs for 72 h; **(G)** the statistical results of Ki67 staining for different time point. **(H)** The relative expression levels of *Tacc3* gene; **(I)** the relative expression levels of *Cdc20* gene; **(J)** the relative expression levels of *Cdkn1a* gene; **(K)** the relative expression levels of *Isl1* gene; **(L)** the relative expression levels of *Lhx3* gene; **(M)** the relative expression levels of *Lhx8* gene (*$P < 0.05$, compared with DMSO group; **$P < 0.01$, compared with DMSO group; ***$P < 0.001$ compared with DMSO group, green = ki67, blue = DAPI).

neuron is not the main type in the hippocampus, they still play a major function in the hippocampus. Our results demonstrated that ChAT was the marker of cholinergic neurons, while Prox1 and Ctip2 were the markers of hippocampal and deep layer neurons respectively (Zhang L. et al., 2015). Recent study showed that single cholinergic neuron can extend into multiple

areas. Most target areas of individual cholinergic neuron are interconnected, such as the olfactory bulb connecting to the piriform and entorhinal cortex, while the subregions of the hippocampal complex connecting with the striatum, isocortex, and hypothalamus (Li et al., 2018). Interestingly, our research has demonstrated that most of MDHB-induced neurons were cholinergic neurons. But this also prompt that it is precisely because MDHB can differentiate NSCs into cholinergic neurons, thus acting as a therapeutic effect for memory disorder. In the near future, we will need to further verify the function of this part of cholinergic neurons. Due to the potential limitations of our experimental conditions, we were unable to identify the exact type of the differentiated cells using multiple experimental methods, which could not totally exclude the possibility of other cell types. So it is worthy of further research in this direction. A semiautonomous circuit of striatal GABAergic interneurons is responsible for transmitting behaviorally relevant cholinergic signals to spiny projection neurons (Faust et al., 2016). Cholinergic neuron play a major role in motor and learning functions of the striatum. At recent studies, the cholinergic neurons have also been a main focus of research in aging and neural degradation, specifically as it relates to Alzheimer's Disease (Tabet, 2006). Through the observation and analysis of the staining of presynaptic membrane protein SYN1 and PSD95, the results showed that the differentiated neurons expressed SYN1 and PSD95 (**Figure 5**), suggesting the possibility of synapse formation and the potential to form neural networks. The experiments revealed that MDHB can promote NSCs differentiation into hippocampal cholinergic neurons, and the differentiated neurons may form a neural network.

Previous research showed that Wnt pathway promotes neuronal differentiation (Hirabayashi et al., 2004). In the classical WNT pathway, inhibition of GSK3βleads to the accumulation of β-catenin, which enters the cell nucleus, causing transcription of the *TCF4* gene (Hirabayashi et al., 2004). GSK3β is also regulated by the PI3K/AKT signaling pathway. Activated by AKT (Jiang et al., 2016), inhibits GSK3β activity, In contrast, inactivating AKT, activates GSK3β activity. PI3K/AKT signaling pathway regulate NSCs differentiation into motor neurons in adult. In this study, we found that MDHB regulates the fate of NSCs by regulating cell cycle, possibly inhibiting AKT phosphorylation and activating GSK3β activity, which lead to β-catenin degradation and abolishment of entering the nucleus. Subsequently, it will regulate cell cycle-related gene expression and cholinergic signal pathway. Recent studies have found that transforming coiled coil acid repeat protein 3 (TACC3) can regulate ARNT2 transcription factor to determine neural cell fate (Wurdak et al., 2010). Knocking out the *TACC3* gene can promote the differentiation of NSCs into neurons (Xie et al., 2007). Cell division cyclin 20 is a basic regulator of cell division, and it have an important function to activate late-promotion complex (APC/C), which is a large 11-13 subunit complex that initiates staining (Paul et al., 2017; Omrani et al., 2018). The body separates and enters later stages, it also targets the destruction of S and M phase (S/M) cyclins, inactivates

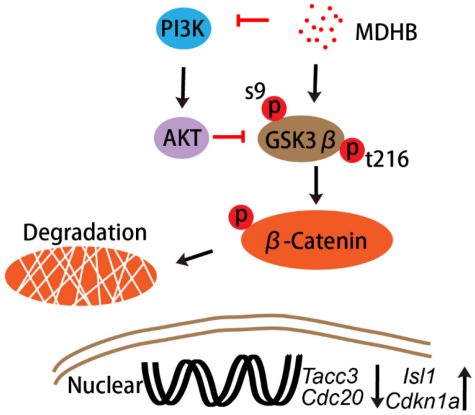

FIGURE 8 | The signal transduction pathway in MDHB-induced cholinergic neurons differentiation.

S/M cyclin-dependent kinases (Cdks) and quits cells from mitosis (Lee et al., 2018). The LIM homeodomain transcription factor Islet1 (*Isl1*) is expressed in multiple organs and plays essential roles during embryogenesis. Isl1 is required for the survival and specification of motor neurons, *Isl1* orchestrates the process to generate cholinergic neurons in the spinal cord and forebrain. In this experiment, the expressions of *Cdc20* and *TACC3* are decreased and the expressions of *Cdkn1a* and *Isl1*gene are up-regulated after NSCs was exposed to MDHB (**Figure 7**).

In this study, we showed that MDHB may induce NSCs to differentiate into cholinergic neurons by regulating cell cycle-associated proteins and cholinergic signal pathway (**Supplementary Figure S1**). Ki67 is a nuclear protein associated with cellular proliferation (Calzolari et al., 2015). The results were consistent with the transcriptome levels. Western blot was used to detect the proteins which included the phosphorylation of AKT and total AKT in the PI3K pathway at the fifth day of NSCs differentiation. We found that MDHB inhibited the phosphorylation of AKT, but the total amount of AKT was not affected. Subsequently, the classical WNT pathway protein was verified, and the data that MDHB regulates phosphorylation of GSK3β at tyrosine 216 (Y216), but does not cause phosphorylation of GSK3β at serine 9 (S9). MDHB activates GSK3β and cause β-catenin degradation which leads to the inability to enter the nucleus and initiate the expression of cholinergic-related genes and cell cycle-related genes. At the transcriptome level, it was also found that the expressions of *Cdc20* and *Tacc3* were decreased and *Cdkn1a and cholinergic* genes was upregulated. The qPCR assay of *Isl1, Cdc20*, *Tacc3*, and *Cdkn1a* revealed that *Cdc20* and *Tacc3* were down-regulated, Isl1 expression was also increased by immunofluorescence. In this process, β-catenin may control the expression of the *Isl1* and *Tacc3*. In summary, MDHB may promote NSCs differentiation into cholinergic neurons by inhibiting the proteins in the PI3K signaling pathway and activating the proteins in GSK3β signaling pathway to regulate the expression of cholinergic gene (**Figure 8**). The differentiation-inducing agents such as MDHB may lead

to new therapeutics that act by enhancing the contribution of newborn neurons to neurodegeneration and CNS repair.

AUTHOR CONTRIBUTIONS

H-ML conceived and designed the study. J-PP performed the experiments, analyzed the data and wrote the manuscript. J-PP and YH analysis was performed using the OmicShare tools, a free online platform for data analysis (http://www.omicshare.com/tools). YH, FX, LY, and Y-RX assisted in performing the research. LY, J-HW, J-XJ, K-QC, C-YY, and QG provided language help and assisted in analyzing data.

FUNDING

This research was funded by grants from the National Natural Science Foundation of China (No. 81473296), and the Guangdong Provincial Department of Science and Technology, China (No. 2012B050300018).

SUPPLEMENTARY MATERIAL

The Supplementary Material for this article can be found online at: https://www.frontiersin.org/articles/10.3389/fncel.2018.00478/full#supplementary-material

REFERENCES

Ager, R. R., Davis, J. L., Agazaryan, A., Benavente, F., Poon, W. W., LaFerla, F. M., et al. (2015). Human neural stem cells improve cognition and promote synaptic growth in two complementary transgenic models of Alzheimer's disease and neuronal loss. *Hippocampus* 25, 813–826. doi: 10.1002/hipo.22405

Aharonowiz, M., Einstein, O., Reubinoff, B., and Ben-Hur, T. (2018). Human stem cell-derived neural precursors for treatment of autoimmune diseases of the central nervous system. U.S. Patent No. US20110189135A1.

Akizu, N., Estaras, C., Guerrero, L., Marti, E., and Martinez-Balbas, M. A. (2010). H3K27me3 regulates BMP activity in developing spinal cord. *Development* 137, 2915–2925. doi: 10.1242/dev.049395

Cai, L., Wang, L.-F., Pan, J.-P., Mi, X.-N., Zhang, Z., Geng, H.-J., et al. (2016). Neuroprotective effects of Methyl 3, 4-dihydroxybenzoate against TBHP-induced oxidative damage in SH-SY5Y cells. *Molecules* 21:1071. doi: 10.3390/molecules21081071

Calzolari, F., Michel, J., Baumgart, E. V., Theis, F., Götz, M., and Ninkovic, J. (2015). Fast clonal expansion and limited neural stem cell self-renewal in the adult subependymal zone. *Nat. Neurosci.* 18:490. doi: 10.1038/nn.3963

Chicheportiche, A., Ruat, M., Boussin, F. D., and Daynac, M. (2018). Isolation of neural stem and progenitor cells from the adult brain and live imaging of their cell cycle with the FUCCI system. *Methods Mol. Biol.* 1686, 69–78. doi: 10.1007/978-1-4939-7371-2_5

Cho, H.-H., Cargnin, F., Kim, Y., Lee, B., Kwon, R.-J., Nam, H., et al. (2014). Isl1 directly controls a cholinergic neuronal identity in the developing forebrain and spinal cord by forming cell type-specific complexes. *PLoS Genet.* 10:e1004280. doi: 10.1371/journal.pgen.1004280

Crook, J. M., and Tomaskovic-Crook, E. (2017). Culturing and cryobanking human neural stem cells. *Stem Cell Bank.* 1590, 199–206. doi: 10.1007/978-1-4939-6921-0_15

Duerr, J. S., Han, H. P., Fields, S. D., and Rand, J. B. (2008). Identification of major classes of cholinergic neurons in the nematode *Caenorhabditis elegans*. *J. Comp. Neurol.* 506, 398–408. doi: 10.1002/cne.21551

Dvoryanchikov, G., Hernandez, D., Roebber, J. K., Hill, D. L., Roper, S. D., and Chaudhari, N. (2017). Transcriptomes and neurotransmitter profiles of classes of gustatory and somatosensory neurons in the geniculate ganglion. *Nat. Commun.* 8:760. doi: 10.1038/s41467-017-01095-1

Faust, T. W., Assous, M., Tepper, J. M., and Koós, T. (2016). Neostriatal GABAergic interneurons mediate cholinergic inhibition of spiny projection neurons. *J. Neurosci.* 36, 9505–9511. doi: 10.1523/JNEUROSCI.0466-16.2016

Gage, F. H. (2000). Mammalian neural stem cells. *Science* 287, 1433–1438. doi: 10.1126/science.287.5457.1433

Gauthier-Fisher, A., Lin, D. C., Greeve, M., Kaplan, D. R., Rottapel, R., and Miller, F. D. (2009). Lfc and Tctex-1 regulate the genesis of neurons from cortical precursor cells. *Nat. Neurosci.* 12, 735–744. doi: 10.1038/nn.2339

Goncalves, J. T., Schafer, S. T., and Gage, F. H. (2016). Adult neurogenesis in the hippocampus: from stem cells to behavior. *Cell* 167, 897–914. doi: 10.1016/j.cell.2016.10.021

Gumy, L. F., Katrukha, E. A., Grigoriev, I., Jaarsma, D., Kapitein, L. C., Akhmanova, A., et al. (2017). MAP2 defines a pre-axonal filtering zone to regulate KIF1-versus KIF5-dependent cargo transport in sensory neurons. *Neuron* 94, 347.e7–362.e7. doi: 10.1016/j.neuron.2017.03.046

Haim, L. B., and Rowitch, D. H. (2017). Functional diversity of astrocytes in neural circuit regulation. *Nat. Rev. Neurosci.* 18:31. doi: 10.1038/nrn.2016.159

Hangya, B., Ranade, S. P., Lorenc, M., and Kepecs, A. (2015). Central cholinergic neurons are rapidly recruited by reinforcement feedback. *Cell* 162, 1155–1168. doi: 10.1016/j.cell.2015.07.057

Hirabayashi, Y., Itoh, Y., Tabata, H., Nakajima, K., Akiyama, T., Masuyama, N., et al. (2004). The Wnt/beta-catenin pathway directs neuronal differentiation of cortical neural precursor cells. *Development* 131, 2791–2801. doi: 10.1242/dev.01165

Hur, E. M., and Zhou, F. Q. (2010). GSK3 signalling in neural development. *Nat. Rev. Neurosci.* 11, 539–551. doi: 10.1038/nrn2870

Jiang, H., Xiao, J., Kang, B., Zhu, X., Xin, N., and Wang, Z. (2016). PI3K/SGK1/GSK3β signaling pathway is involved in inhibition of autophagy in neonatal rat cardiomyocytes exposed to hypoxia/reoxygenation by hydrogen sulfide. *Exp. Cell Res.* 345, 134–140. doi: 10.1016/j.yexcr.2015.07.005

Jin, X., Yu, Z. F., Chen, F., Lu, G. X., Ding, X. Y., Xie, L. J., et al. (2017). Neuronal nitric oxide synthase in neural stem cells induces neuronal fate commitment via the inhibition of histone deacetylase 2. *Front. Cell Neurosci.* 11:66. doi: 10.3389/fncel.2017.00066

Kim, J. B., Zaehres, H., Wu, G., Gentile, L., Ko, K., Sebastiano, V., et al. (2008). Pluripotent stem cells induced from adult neural stem cells by reprogramming with two factors. *Nature* 454:646. doi: 10.1038/nature07061

Kim, W. Y., Wang, X., Wu, Y., Doble, B. W., Patel, S., Woodgett, J. R., et al. (2009). GSK-3 is a master regulator of neural progenitor homeostasis. *Nat. Neurosci.* 12, 1390–1397. doi: 10.1038/nn.2408

Kuwabara, T., Hsieh, J., Muotri, A., Yeo, G., Warashina, M., Lie, D. C., et al. (2009). Wnt-mediated activation of NeuroD1 and retro-elements during adult neurogenesis. *Nat. Neurosci.* 12, 1097–1105. doi: 10.1038/nn.2360

Lee, S., Liu, P., Teinturier, R., Jakob, J., Tschaffon, M., Tasdogan, A., et al. (2018). Deletion of Menin in craniofacial osteogenic cells in mice elicits development of mandibular ossifying fibroma. *Oncogene* 37:616. doi: 10.1038/onc.2017.364

Lei, M., Xu, H., Li, Z., Wang, Z., O'Malley, T. T., Zhang, D., et al. (2016). Soluble Aβ oligomers impair hippocampal LTP by disrupting glutamatergic/GABAergic balance. *Neurobiol. Dis.* 85, 111–121. doi: 10.1016/j.nbd.2015.10.019

Li, X., Yu, B., Sun, Q., Zhang, Y., Ren, M., Zhang, X., et al. (2018). Generation of a whole-brain atlas for the cholinergic system and mesoscopic projectome analysis of basal forebrain cholinergic neurons. *Proc. Natl. Acad. Sci. U.S.A.* 115, 415–420. doi: 10.1073/pnas.1703601115

Lisman, J., Schulman, H., and Cline, H. (2002). The molecular basis of CaMKII function in synaptic and behavioural memory. *Nat. Rev. Neurosci.* 3:175. doi: 10.1038/nrn753

Luo, Y., Shan, G., Guo, W., Smrt, R. D., Johnson, E. B., Li, X., et al. (2010). Fragile x mental retardation protein regulates proliferation and differentiation of adult neural stem/progenitor cells. *PLoS Genet.* 6:e1000898. doi: 10.1371/journal.pgen.1000898

Ming, G. L., and Song, H. (2009). DISC1 partners with GSK3beta in neurogenesis. *Cell* 136, 990–992. doi: 10.1016/j.cell.2009.03.005

Mosher, K. I., Andres, R. H., Fukuhara, T., Bieri, G., Hasegawa-Moriyama, M., He, Y., et al. (2012). Neural progenitor cells regulate microglia functions and activity. *Nat. Neurosci.* 15, 1485. doi: 10.1038/nn.3233

Mussmann, C., Hubner, R., Trilck, M., Rolfs, A., and Frech, M. J. (2014). HES5 is a key mediator of Wnt-3a-induced neuronal differentiation. *Stem Cells Dev.* 23, 1328–1339. doi: 10.1089/scd.2013.0557

Omrani, M. R., Yaqubi, M., and Mohammadnia, A. (2018). Transcription factors in regulatory and protein subnetworks during generation of neural stem cells and neurons from direct reprogramming of non-fibroblastic cell sources. *Neuroscience* 380, 63–77. doi: 10.1016/j.neuroscience.2018.03.033

Park, J. C., Jeong, W. J., Kim, M. Y., Min, D., and Choi, K. Y. (2016). Retinoic-acid-mediated HRas stabilization induces neuronal differentiation of neural stem cells during brain development. *J. Cell Sci.* 129, 2997–3007. doi: 10.1242/jcs.184366

Park, S.-Y., Yoon, S. N., Kang, M.-J., Lee, Y., Jung, S. J., and Han, J.-S. (2017). Hippocalcin promotes neuronal differentiation and inhibits astrocytic differentiation in neural stem cells. *Stem Cell Rep.* 8, 95–111. doi: 10.1016/j.stemcr.2016.11.009

Paul, D., Ghorai, S., Dinesh, U., Shetty, P., Chattopadhyay, S., and Santra, M. K. (2017). Cdc20 directs proteasome-mediated degradation of the tumor suppressor SMAR1 in higher grades of cancer through the anaphase promoting complex. *Cell Death Dis.* 8:e2882. doi: 10.1038/cddis.2017.270

Perche, O., Felgerolle, C., Ardourel, M., Bazinet, A., Pâris, A., Rossignol, R., et al. (2018). Early retinal defects in Fmr1-/y Mice: toward a critical role of visual Dys-sensitivity in the fragile X syndrome phenotype? *Front. Cell. Neurosci.* 12:96. doi: 10.3389/fncel.2018.00096

Ray, S., Corenblum, M., Anandhan, A., Reed, A., Ortiz, F., Zhang, D., et al. (2018). A role for Nrf2 expression in defining the aging of hippocampal neural stem cells. *Cell Transplant.* 27, 589–606. doi: 10.1177/0963689718774030

Reidling, J. C., Relaño-Ginés, A., Holley, S. M., Ochaba, J., Moore, C., Fury, B., et al. (2018). Human neural stem cell transplantation rescues functional deficits in R6/2 and Q140 huntington's disease mice. *Stem Cell Rep.* 10, 58–72. doi: 10.1016/j.stemcr.2017.11.005

Reynolds, B. A., and Rietze, R. L. (2005). Neural stem cells and neurospheres—re-evaluating the relationship. *Nat. Methods* 2:333. doi: 10.1038/nmeth758

Rietze, R. L., and Reynolds, B. A. (2006). Neural stem cell isolation and characterization. *Methods Enzymol.* 19, 3–23. doi: 10.1016/S0076-6879(06)19001-1

Saunders, A., Granger, A. J., and Sabatini, B. L. (2015). Corelease of acetylcholine and GABA from cholinergic forebrain neurons. *eLife* 4:e06412. doi: 10.7554/eLife.06412

Tabet, N. (2006). Acetylcholinesterase inhibitors for Alzheimer's disease: anti-inflammatories in acetylcholine clothing! *Age Ageing* 35, 336–338. doi: 10.1093/ageing/afl027

Vasconcelos, F. F., Sessa, A., Laranjeira, C., Raposo, A., Teixeira, V., Hagey, D. W., et al. (2016). MyT1 Counteracts the neural progenitor program to promote vertebrate neurogenesis. *Cell Rep.* 17, 469–483. doi: 10.1016/j.celrep.2016.09.024

Whalley, K. (2018). Synaptic building blocks. *Nat. Rev. Neurosci.* 19, 388–389. doi: 10.1038/s41583-018-0018-z

Wurdak, H., Zhu, S., Min, K. H., Aimone, L., Lairson, L. L., Watson, J., et al. (2010). A small molecule accelerates neuronal differentiation in the adult rat. *Proc. Natl. Acad. Sci. U.S.A.* 107, 16542–16547. doi: 10.1073/pnas.1010300107

Xie, Z., Moy, L. Y., Sanada, K., Zhou, Y., Buchman, J. J., and Tsai, L.-H. (2007). Cep120 and TACCs control interkinetic nuclear migration and the neural progenitor pool. *Neuron* 56, 79–93. doi: 10.1016/j.neuron.2007.08.026

Zeng, H., and Sanes, J. R. (2017). Neuronal cell-type classification: challenges, opportunities and the path forward. *Nat. Rev. Neurosci.* 18:530. doi: 10.1038/nrn.2017.85

Zhang, L., Yin, J.-C., Yeh, H., Ma, N.-X., Lee, G., Chen, X. A., et al. (2015). Small molecules efficiently reprogram human astroglial cells into functional neurons. *Cell Stem Cells* 17, 735–747. doi: 10.1016/j.stem.2015.09.012

Zhang, Q., Huang, R., Ye, Y., Guo, X., Lu, J., Zhu, F., et al. (2018). Temporal requirements for ISL1 in sympathetic neuron proliferation, differentiation, and diversification. *Cell Death Dis.* 9:247. doi: 10.1038/s41419-018-0283-9

Zhang, W., Cai, L., Geng, H. J., Su, C. F., Yan, L., Wang, J. H., et al. (2014). Methyl 3,4-dihydroxybenzoate extends the lifespan of Caenorhabditis elegans, partly via W06A7.4 gene. *Exp. Gerontol.* 60, 108–116. doi: 10.1016/j.exger.2014.10.007

Zhang, Z., Cai, L., Zhou, X., Su, C., Xiao, F., Gao, Q., et al. (2015). Methyl 3, 4-dihydroxybenzoate promote rat cortical neurons survival and neurite outgrowth through the adenosine A2a receptor/PI3K/Akt signaling pathway. *NeuroReport* 26, 367–373. doi: 10.1097/WNR.0000000000000358

Zhao, C., Deng, W., and Gage, F. H. (2008). Mechanisms and functional implications of adult neurogenesis. *Cell* 132, 645–660. doi: 10.1016/j.cell.2008.01.033

Zhou, Q., Zhou, P., Wang, A. L., Wu, D., Zhao, M., Südhof, T. C., et al. (2017). The primed SNARE–complexin–synaptotagmin complex for neuronal exocytosis. *Nature* 548:420. doi: 10.1038/nature23484

Zhou, X. W., Zhang, Z., Su, C. F., Lv, R. H., Zhou, X., Cai, L., et al. (2013). Methyl 3, 4-dihydroxybenzoate protects primary cortical neurons against Aβ25–35-induced neurotoxicity through mitochondria pathway. *J. Neurosci. Res.* 91, 1215–1225. doi: 10.1002/jnr.23235

Conflict of Interest Statement: The authors declare that the research was conducted in the absence of any commercial or financial relationships that could be construed as a potential conflict of interest.

frontiers in Cellular Neuroscience

MINI REVIEW
published: 12 February 2019
doi: 10.3389/fncel.2019.00044

Astrocytes in Neuropathologies Affecting the Frontal Cortex

*Ulla-Kaisa Peteri, Mikael Niukkanen and Maija L. Castrén**

Department of Physiology, Faculty of Medicine, University of Helsinki, Helsinki, Finland

To an increasing extent, astrocytes are connected with various neuropathologies. Astrocytes comprise of a heterogeneous population of cells with region- and species-specific properties. The frontal cortex exhibits high levels of plasticity that is required for high cognitive functions and memory making this region especially susceptible to damage. Aberrations in the frontal cortex are involved with several cognitive disorders, including Alzheimer's disease, Huntington's disease and frontotemporal dementia. Human induced pluripotent stem cells (iPSCs) provide an alternative for disease modeling and offer possibilities for studies to investigate pathological mechanisms in a cell type-specific manner. Patient-specific iPSC-derived astrocytes have been shown to recapitulate several disease phenotypes. Addressing astrocyte heterogeneity may provide an improved understanding of the mechanisms underlying neurodegenerative diseases.

Keywords: astrocyte, frontal cortex, Alzheimer's disease, Huntington's disease, frontotemporal dementia, neurodegeneration, induced pluripotent stem cells

OPEN ACCESS

Edited by:
Sara Xapelli,
Universidade de Lisboa, Portugal

Reviewed by:
João Filipe Oliveira,
University of Minho, Portugal
Karen Muller Smith,
University of Louisiana at Lafayette, United States

***Correspondence:**
Maija L. Castrén
Maija.Castren@helsinki.fi

Received: *31 October 2018*
Accepted: *28 January 2019*
Published: *12 February 2019*

Citation:
Peteri U-K, Niukkanen M and Castrén ML (2019) Astrocytes in Neuropathologies Affecting the Frontal Cortex. Front. Cell. Neurosci. 13:44. doi: 10.3389/fncel.2019.00044

INTRODUCTION

Astrocytes are implicated as active mediators of synaptic activity, synaptogenesis and neurogenesis and are crucial in maintaining extracellular homeostasis and controlling blood-brain barrier permeability (Zhao et al., 2015; Allen and Lyons, 2018; Marina et al., 2018). Considering their versatile role in regulating brain function, it is no surprise that astrocyte malfunctions have been connected to various neurodegenerative disorders (Phatnani and Maniatis, 2015). Astrocytes are known as a morphologically and functionally diverse population of cells that differ both between distinct brain regions as well as within specific areas (Vasile et al., 2017). This diversity is reflected in their pathological features observed in psychiatric disorders (Rajkowska et al., 2002; Wallingford et al., 2017). Drugs used to treat mood disorders affect astrocytes as well and antidepressant effect on neurons is considered to be partially due to induction of astrocytic release of trophic factors (Marathe et al., 2018). Combined astrocyte and neuron-mediated effects also influence responses of antipsychotics (Khan et al., 2001). However, typical and atypical antipsychotics may display differential effects on the gliotransmitter release and the inflammatory response of astrocytes

Abbreviations: 5-HT, 5-hydroxytryptamine receptor; Aβ, amyloid β; AD, Alzheimer's disease; APOE, apolipoprotein E; APP, amyloid precursor protein; BDNF, brain-derived neurotrophic factor; BG, Bergmann glia; cAMP, cyclic adenosine monophosphate; CTE, chronic traumatic encephalopathy; C1q, complement component 1q; EAAT, excitatory amino acid transporter; FAD, familial Alzheimer's disease; FTD, frontotemporal dementia; GFAP, glial fibrillary acidic protein; GLAST, glutamate aspartate transporter; GLT-1, glutamate transporter 1; HD, Huntington's disease; Htt, huntingtin; Il-1α, interleukin 1α; iPSC, induced pluripotent stem cell; JAK/STAT3, Janus kinase/signal transducers and activators of transcription 3; ROS, reactive oxygen species; SAD, sporadic Alzheimer's disease; TNFα, tumor necrosis factor α; TDP-34, transactive response DNA-binding protein 34; TrkB, tyrosine-related kinase B; VEGF-A, vascular endothelial growth factor A.

(Tanahashi et al., 2012; Bobermin et al., 2018). Understanding the function of astrocytes is therefore crucial for disease modeling and for developing treatments. Heterogeneity of the cell population and species-specific differences pose a challenge in the study of astrocytes. A method developed by Takahashi et al. (2007) allows the reprogramming of somatic cells into iPSCs, which can be used to generate patient-specific cells of a desired type (Takahashi et al., 2007). In this review, we describe how iPSC-derived astrocytes have been used to model neurodegenerative disorders involving frontal lobe malfunctions.

ASTROCYTE HETEROGENEITY IN THE BRAIN

The generation of cortical glia is initiated once neurogenesis has been completed. The temporal patterning is based on a positive feedback signal from new-born neurons (Molofsky and Deneen, 2015; Takouda et al., 2017). Astrocyte progenitors migrate radially, obtaining their region specific properties upon maturation and this process continues postnatally (Colombo et al., 1997; Tsai et al., 2012). Several genes enriched in neuronal progenitors are also expressed in astrocytes, suggesting that astrocytes retain some proliferative potential even in the mature brain (Cahoy et al., 2008). However, only a distinct subset of astrocytes show neurogenic potential (Ghashghaei et al., 2007; Bardehle et al., 2013).

Mature astrocytes can be distinguished based on their morphology and functional properties. In the human cortex, astrocytes are morphologically categorized into four subtypes; interlaminar, protoplasmic, varicose projections and fibrous astroglia, located in the layers I and II, III and IV, V and VI and in the white matter, respectively (Vasile et al., 2017). The brain also contains other, both morphologically and functionally, distinct astrocytes such as elongated radial glia-like tanycytes and unipolar BG with several radially ascending processes. Tanycytes specialized in the regulation of neuroendocrine functions are located in the hypothalamus (Prevot et al., 2018) while BG modulate the efficacy of the synaptic transmission of Purkinje cells in the cerebellum (De Zeeuw and Hoogland, 2015).

Some astrocyte subtypes found in the human cortex are not represented in the rodent brain. Furthermore, human cortical astrocytes exceed their mouse counterparts both in complexity and size, and propagate calcium signals several times faster (Oberheim et al., 2009). Although human and mouse astrocytes share similar properties related to their effects on synapse formation, they differ in their function and transcriptional profiles (Zhang et al., 2016). Species-specific functional differences in glial cells are supported by improved learning and memory in chimeric animals following engrafting human glia into mouse brain (Han et al., 2013).

A higher relative number of astrocytes in the human frontal cortex, compared to that of many other species including other primates, is thought to be due to the high metabolomic cost of maintaining a bigger brain size (Bass et al., 1971; Sherwood et al., 2006). One of the key mechanism's astrocytes apply to provide energy to neurons is via the astrocyte-neuron lactate shuttle. This metabolomic coupling is known to be crucial for memory formation (Alberini et al., 2018). Astrocytes respond to neuronal activity with spatially and temporally regulated Ca^{2+} fluctuations that shape neuronal activity via the regulation of the gliotransmitter release (Semyanov, 2019). Molecular and functional variations in astrocytes are considered to contribute to differences in distinct neural circuit signaling (Chai et al., 2017; Morel et al., 2017; Xin and Bonci, 2018). Another central role of astrocytes is the regulation of neurotransmitter uptake including glutamate via excitatory amino acid transporters 1 and 2 (EAAT1, EAAT2, respectively) in humans, or glutamate/aspartate transporter (GLAST) and glutamate transporter-1 (GLT-1) in rodents (Roberts et al., 2014; Meunier et al., 2017). Regulation of the extracellular neurotransmitter levels is affected in a number of neuropsychiatric disorders (John et al., 2012).

ASTROCYTES AS MEDIATORS OF PATHOLOGIES AFFECTING THE FRONTAL CORTEX

The frontal cortex is responsible for higher executive functions such as cognition and working memory (Fuster, 2002). The expression of genes involved in processes mediating synaptic plasticity, memory and learning is, respectively, enriched in a human and primate frontal cortex (Sjostedt et al., 2015; Garcia-Cabezas et al., 2017). A high level of flexibility is necessary for learning and memory functions but may also lead to increased structural vulnerability, which may explain why aberrations in the frontal cortex are connected to several neuropathologies (John et al., 2012; Feresten et al., 2013; Torres-Platas et al., 2016).

Astrocytes contribute to the regulation of neuronal activity that is altered in several frontal cortex pathologies (Braun et al., 2009; Cao et al., 2013; Lima et al., 2014; Bull et al., 2015; Ebrahimi et al., 2016; Beamer et al., 2017). A common feature for brain diseases is the activation of astrocytes into an inflammatory, reactive state (Chanaday and Roth, 2016). White matter astrocytes in the frontal cortex appear to be especially vulnerable to ischemic stroke, leading to disrupted gliovascular interactions caused by astrogliosis (Chen et al., 2016). Astrogliosis in the frontal cortex, upon aging, is also linked to mood disorders (Miguel-Hidalgo et al., 2000; Narita et al., 2006). Neurodegenerative disorders have overlapping characteristics suggesting common underlying pathological mechanisms. For instance, CTE caused by repeated head injuries, displays a similar accumulation of neurofibrillary tangles to that in AD but can be differentiated from AD by astrocytic tangles that are considered a hallmark of CTE (Turner et al., 2016; Hsu et al., 2018). Below, examples of neurodegenerative disorders with fronto-temporal pathologies and studies employing iPSC-derived astrocytes are described.

Alzheimer's Disease

Alzheimer's disease is a progressive neurodegenerative disease that manifests through cognitive impairment, motor abnormalities and behavioral changes. AD pathology is

hallmarked by the accumulation of insoluble amyloid-β (Aβ) plaques, amyloid deposits in the blood vessel walls and aggregation of the microtubule protein tau, within neurons. The abnormalities seen in AD usually occur first in the frontotemporal region then spread progressively to other areas of the neocortex (Masters et al., 2015).

The contribution of astrocytes in AD pathology comprises of both the loss of neuroprotective features as well as the acquirement of pathological properties. Initially, astrocytes uptake and degrade Aβ and have a neuroprotective role. However, disease progression often leads to impaired astrocytic Aβ clearance and induces toxic gain-of-functions that contribute to disease progression (Garwood et al., 2017). Neural plaques adjacent to GFAP expressing astrocytes are known to induce hypertrophy and there is also evidence showing that astrocyte reactivity may precede plaque formation (Teneka et al., 2005; Olabarria et al., 2010; Rodrieguez-Veitez et al., 2015). Morphological aberrances in AD astrocytes that compromise vascular coverage are detrimental to neurovascular regulation, while disrupted potassium (K^+) mediated neurovascular coupling, due to downregulation of K^+ channels Kir4.1 and BK_{Ca}, result in abnormal regional cerebral blood flow (Acosta et al., 2017).

Aβ has been shown to alter the expression of metabotropic glutamate receptor 5 (mGluR5) and nicotinic acetylcholine receptors (nAchRs) in astrocytes, which leads to changes in Ca^{2+} homeostasis and signaling (Haughey and Mattson, 2003; Xiu et al., 2005; Lim et al., 2013). Excitotoxicity is a common characteristic of AD and astrocytes contribute to excessive glutamate signaling. Insufficient clearance of glutamate is connected to the reduced expression of glutamate transporters and their aberrant trafficking, which has been linked to altered cholesterol synthesis (Masliah et al., 1996; Tian et al., 2010; Merlini et al., 2011; Talantova et al., 2013). Furthermore, the release of glutamate has been shown to be enhanced in AD astrocytes (Talantova et al., 2013).

Reactivity is a common feature of AD astrocytes. Aβ induces the astrocytic release of pro-inflammatory mediators and, in turn, pro-inflammatory signals stimulate astrocytic Aβ production leading to a positive feedback loop between astrocyte Aβ response and production (Gonzáles-Reyes et al., 2017). S100β-positive astrocytes are connected to AD pathology and they are reduced following immunization against Aβ (Neus Bosch et al., 2015). S100β expressed by astrocytes is important for the regulation of neuronal oscillations associated with cognitive flexibility and depressive behavior (Stroth and Svenningsson, 2015; Brockett et al., 2018).

Glucose hypometabolism can precede clinical symptoms of AD (Mosconi et al., 2006). There is evidence that carriers of apolipoprotein Eε4 (APOEε4) allele, with an increased risk for AD, have lower levels of glucose metabolism in various brain regions, including the prefrontal cortex, before the manifestation of clinical symptoms (Reiman et al., 2004). Dementia in AD is related to altered lactate processing. Under normal circumstances lactate-producing enzymes are down-regulated with age and an increase in the expression of these enzymes improve memory in wild type mice but leads to memory deficits in AD mice (Harris et al., 2016). Astrocyte defects in AD have been described extensively in a recent review (Acosta et al., 2017).

Huntington's Disease

Huntington's disease (HD) is characterized by motor dysfunction, cognitive impairment and neuropsychiatric features. HD is an inherited neurological disorder caused by CAG trinucleotide repeat expansion in the gene encoding Htt. The expansion gives rise to a mutated form of Htt (mHtt) with an abnormally long polyglutamine sequence which leads to the formation of mHtt aggregates (Bates et al., 2015). Clearance of aggregates is more efficient from astrocytes than from neurons, rendering astrocytes more resistant to mHtt accumulation (Zhao et al., 2016; Jansen et al., 2017; Zhao T. et al., 2017). Eventual accumulation of mHtt into astrocytes results in altered glutamate homeostasis and, sub-sequentially, neuronal excitotoxicity (Shin et al., 2005; Bradford et al., 2009). In addition to the enhanced release of glutamate, the presence of mHtt in astrocytes decreases the expression of glutamate transporters in an age-dependent manner (Lievens et al., 2001; Estrada-Sanchez et al., 2009; Faideau et al., 2010; Lee et al., 2013). However, excitotoxicity in HD neurons has also been reported without defects in the glutamate clearance (Parsons et al., 2016).

Huntington's disease astrocytes possess an altered K^+ signaling due to the decreased expression of Kir4.1 (Tong et al., 2014; Zhang et al., 2018). Restoration of Kir4.1 function can ameliorate impaired GLT1-mediated homeostasis and, sub-sequentially astrocyte Ca^{2+} signaling, implying a causative effect of Kir4.1 dysfunction on these mechanisms (Tong et al., 2014; Jiang et al., 2016). Kir4.1 defects precede the appearance of reactive astrocytes, indicating that inflammation is a secondary effect of HD pathology possibly induced by neurotoxicity (Tong et al., 2014).

Both reactive astrocytes and microglia have been implicated in the pathogenesis of HD (Khakh et al., 2017). Microglia promote the reactivity of astrocytes via the secretion of pro-inflammatory factors such as Il-1α, TNFα, and C1q (Liddelow et al., 2017). Reactive astrocytes have an impaired ability for synaptic maintenance and decreased phagocytic capacity (Bradford et al., 2009; Haim et al., 2015). Additionally, they promote degeneration of a subset of neurons and mature oligodendrocytes (Liddelow et al., 2017). Activation of the JAK/STAT3 pathway appears to be a common pathological feature of HD and AD. Astrocyte specific inhibition of this pathway, in animal models, reduces the reactive astrocyte phenotype (Haim et al., 2015). Interestingly, some studies have shown that reactive astrocytes can also have a neuroprotective role in HD (Haim et al., 2015; Liddelow et al., 2017).

Accumulation of mHtt disrupts exosome secretion from astrocytes (Hong et al., 2017). This can be connected to the reduced BDNF release from astrocytes (Hong et al., 2016). BDNF signaling is associated with HD pathogenesis and restoration of BDNF release from astrocytes has been shown to have neuroprotective effects (Giralt et al., 2010; Hong et al., 2016; Reick et al., 2016). However, there is also evidence that at early stages of HD, TrkB signaling is altered due to an indirect effect of p75 neurotrophic receptor ($p75^{NTR}$) activity, indicating that signaling

defects may precede aberrant secretion of BDNF, a ligand of both TrkB and $p75^{NTR}$ (Plotkin et al., 2014).

Frontotemporal Dementia

Frontotemporal dementia (FTD) is an umbrella term for neurodegenerative diseases affecting the frontal or temporal lobes. Behavioral changes and deficits in executive functioning and language characterize FTD (Bang et al., 2015). The role of astrocytes in FTD is not fully understood. However, FTD pathology is known to involve astrogliosis that occurs at an early stage of the disease progression and precedes neuronal loss (Su et al., 2000; Kersaitis et al., 2004). Astrocytic degeneration is marked by the expression of apoptotic markers, such as caspase-3, and morphological changes (Su et al., 2000; Broe et al., 2004). Apoptotic astrocytes in FTD have been correlated with the degree of frontotemporal atrophy and significant astrogliosis has been observed to overlap with areas showing disturbed cerebral perfusion (Martinac et al., 2001; Broe et al., 2004). In theory, astrocyte degeneration could cause disruptions similar to those seen in AD and HD, but the possible role of astrocyte degeneration in FTD pathogenesis remains unclear (Su et al., 2000).

MODELING PSYCHOPATHOLOGIES USING HUMAN CELLS

In recent years, a number of astrocyte differentiation methods have been developed and advances on the use of iPSC-derived astrocytes have been reviewed in a recent paper (Zheng et al., 2018). Below, the application of iPSC-derived astrocytes and their use to model frontal cortex defects are discussed. The studies represented are summarized in **Table 1**.

Defects in both the clearance and production of Aβ, associated with AD, can also be seen in iPSC-derived AD astrocytes and appear to involve aberrant lipid metabolism

TABLE 1 | Summary of studies on iPSC-derived astrocytes in modeling frontocortical pathologies.

Disease	Mutation	Astrocyte differentiation	Key findings	Reference
AD	*PSEN* (FAD) *APOE4*+/+ (SAD)	iPSC-derived NPC conversion to astroglia in the presence of CNTF, BMP2, FGF2, EGF.	Both SAD and FAD astrocyted exhibited reduced morphological heterogeneity, aberrant expression of S100β, and altered cytokine secretion. Altered EAAT1 distribution only seen in SAD.	Jones et al., 2017
AD	*PSEN1* Δ*E9*	Expansion of NPCs in suspension culture in the presence of FGF2 and EGF. Astrocyte differentiation in the presence of CNTF and BMP4.	Astrocytes produce Aβ with aberrant uptake. Altered cytokine secretion, increased production of ROS. Induce aberrant Ca2+ signaling in healthy neurons.	Oksanen et al., 2017
AD	$APOE^{\varepsilon 4/\varepsilon 4}$ $APOE^{\varepsilon 3/\varepsilon 3}$	Neural induction in suspension culture followed by neural rosette formation and generation of NPCs. Astrocyte differentiation in the presence of CNTF, BMP4, and Heregulin-β.	ApoE isoforms have distinct properties with $APOE^{\varepsilon 3/\varepsilon 3}$ astrocytes having greater neuroprotective and synaptogenetic potential.	Zhao J. et al., 2017
AD	*APOE4 APOE3*	NPCs generation in an adherent culture. Astrocyte differentiation in the presence of FGF2 and BMP4.	Aberrant production and uptake of Aβ. In 3D culture Aβ starts to accumulates in the organoids. Changes in the gene expressions related to lipid metabolism.	Lin et al., 2018
AD	APP-KO APPswe/swe APP V717F	NPCs were generated in an adherent culture. Astrocyte differentiation in a suspension culture in the presence of FBS and EGF.	Astrocytes have aberrant cholesterol metabolism. Lipoprotein and Aβ endocytosis are impaired.	Fong et al., 2018
HD	*Hit*	NPCs were generated in suspension in the presence of growth factors. Astrocyte differentiation was induced by plating the NPCs in the absence of FGF2.	Generated astrocytes exhibited enhanced cytoplasmic vacuolation under basal conditions.	Juopperi et al., 2012
HD	*Hit*	Astrocyte differentiation of iPSCs in neural differentiation medium in the presence of CNTF.	Blocking soluble TNFα suppresses pathological inflammatory response in astrocytes.	Hsiao et al., 2014
HD	*Hit*	Astrocyte differentiation of iPSCs in neural differentiation medium in the presence of CNTF.	Increased inflammatory response and expression of VEGF-A in HD-astrocytes lead to compromised vascular reactivity.	Hsiao et al., 2015
FTD/ALS	TDP-43 M337V	NPCs were cultured in the presence of LIF and EGF in followed by expansion with FGF2 and EGF. Terminal differentiation into astrocytes induced by growth factor withdrawal.	Astrocytes showed accumulation of cytoplasmic TDP-43 resulting in lowered cell survival.	Serio et al., 2013
FTD	*MAPT* N279K	NPC differentiation induced by lentiviral induction of SOX10 followed by treatment with SAG, PDGF, FGF2, NT3, IGF, and LDN. Astrocyte differentiation in the presence of IGF, CNTF, and dbcAMP	Astrocytes showed changes in *TAU* expression, hypertrophy, increased vulnerability to oxidative stress and altered transcriptomic profile. In co-culture system FTD astrocytes altered responses to oxidative stress in healthy neurons.	Hallmann et al., 2017

(Oksanen et al., 2017; Fong et al., 2018; Lin et al., 2018). When studying the effects of APOE genotype Lin et al. (2018) demonstrated that *APOE4* astrocytes show differences in the transcriptomic profile compared to isogenic *APOE3* cells, as well as a diminished ability in clearing Aβ (Lin et al., 2018). The role of ApoE in the Aβ clearance is still unresolved and some studies claim that ApoE is crucial for the degradation and removal of Aβ, while others have shown that ApoE promotes neurodegeneration (Holtzman et al., 1999; Koistinaho et al., 2004; Liao et al., 2014; Shi et al., 2017). In co-culture studies *APOE3* exhibited a greater ability to promote neuronal support and synaptogenesis (Zhao J. et al., 2017). Different properties of *APOE* isoforms in human astrocytes are in agreement with previous studies in mice (Wang et al., 2005). Jones et al. (2017) studied the function of AD astrocytes generated from iPSCs modeling early-onset FAD with mutation in *PSEN* and late-onset SAD with the *APOE4* genotype. Both FAD and SAD astrocytes showed reduced morphological heterogeneity and aberrant expression of S100β. However, altered distribution of EAAT1 was only seen in SAD astrocytes (Jones et al., 2017). Altered secretion of inflammatory cytokines was found in both FAD and SAD, as well as in astrocytes with the *PSEN1 ΔE9* genotype generated by Oksanen et al. (Jones et al., 2017; Oksanen et al., 2017). *PSEN1 ΔE9* astrocytes also displayed changes in Ca^{2+} homeostasis, mitochondrial metabolism, ROS production and lactate secretion, thus covering all classical features of AD pathology (Oksanen et al., 2017).

Inflammatory responses were studied by Hsiao et al. (2015) in iPSC-derived HD astrocytes and an increase in the expression of VEGF-A, with further up-regulation after inflammatory cytokine treatment, was found. This leads to the enhanced proliferation of endothelial cells and the compromised survival of pericytes. As a result, poor pericyte coverage of blood vessels cause vascular reactivity and disrupts the blood-brain-barrier (Hsiao et al., 2015). Additionally, they demonstrated that the TNFα inhibitor XPro1595 successfully suppressed the inflammatory responses both in human astrocytes as well as primary astrocytes propagated from the brain of a transgenic HD mouse model (R6/2) (Hsiao et al., 2014). Juopperi et al. (2012) showed that HD astrocytes display increased cytoplasmic vacuolization (Juopperi et al., 2012). This phenotype is also present in HD lymphoblasts (Nagata et al., 2004; Martinez-Vicente et al., 2010). The findings in iPSC-derived HD astrocytes are consistent with astrogliosis as a key characteristic of HD pathology.

Frontotemporal dementia astrocytes, derived from iPSCs with mutations in genes encoding microtubule-associated protein TAU (MAPT) and TDP-34, demonstrated an increased susceptibility to oxidative stress and compromised survival (Serio et al., 2013; Hallmann et al., 2017). In M337V *TDP-34* astrocytes, lowered survival paralleled the accumulation of TDP-43 (Serio et al., 2013). This phenomenon has been implicated in astrocyte dysfunction in CTE (Jayakumar et al., 2017). In N279K *MAPT* astrocytes, the expression of 4R-TAU isoform was increased as reported in FTD patients (Ghetti et al., 2015; Hallmann et al., 2017). N279K *MAPT* astrocytes displayed morphological changes and increased GFAP expression, usually linked to reactivity, as well as altered gene expression profiles. In co-culture assays with healthy neurons, N279K *MAPT* astrocytes increased the vulnerability of neurons to oxidative stress (Hallmann et al., 2017). However, M337V *TDP-34* astrocytes did not exert toxic effects on neurons, although astrocytic expression of mutated TDP-43 has been reported to induce neuronal cell death (Tong et al., 2013; Serio et al., 2013) suggesting that other cell types, such as microglia, are required for the neurotoxic effect. Altogether, the results indicate that astrocyte degeneration is a common feature of FTD.

CONCLUSION

An increasing number of studies have connected astrocyte defects to frontal cortex pathologies. Species-specificity of astrocytes poses a challenge in translating results obtained from animal studies to humans, and patient-derived iPSCs offer an alternative to disease modeling. Studies presented above demonstrate that iPSC-derived astrocytes successfully recapitulate various disease phenotypes. Further challenges still include addressing the heterogeneity within the astrocyte population and developing protocols to generate regionally defined human astrocyte subtypes.

AUTHOR CONTRIBUTIONS

U-KP and MN wrote the manuscript in consultation with MC. MC performed the critical revision of the paper.

ACKNOWLEDGMENTS

The authors wish to express their thanks for the financial support of the Academy of Finland, the Arvo and Lea Ylppö Foundation, the Finnish Konkordia Fund, the Finnish Cultural Foundation, and Finnish Brain Foundation.

REFERENCES

Acosta, C., Anderson, H. D., and Anderson, C. M. (2017). Astrocyte dysfunction in Alzheimer disease. *J. Neurosci. Res.* 95, 2430–2447. doi: 10.1002/jnr.24075

Alberini, C. M., Cruz, E., Descalzi, G., Bessieres, B., and Gao, V. (2018). Astrocyte glycogen and lactate: new insights into learning and memory mechanisms. *Glia* 66, 1244–1262. doi: 10.1002/glia.23250

Allen, N. J., and Lyons, D. A. (2018). Glia as architects of central nervous system formation and function. *Science* 362, 181–185. doi: 10.1126/science.aat0473

Bang, J., Spina, S., and Miller, B. L. (2015). Non-Alzheimer's dementia 1: frontotemporal dementia. *Lancet* 386, 1672–1682. doi: 10.1016/S0140-6736(15)00461-4

Bardehle, S., Krüger, M., Buggenthin, F., Schwausch, J., Ninkovic, J., Clevers, H., et al. (2013). Live imaging of astrocyte responses to acute injury reveals selective juxtavascular proliferation. *Nat. Neurosci.* 16:580. doi: 10.1038/nn.3371

Bass, N. H., Hess, H. H., Pope, A., and Thalheimer, C. (1971). Quantitative cytoarchitectonic distribution of neurons, glia, and DNA in rat cerebral cortex. *J. Comp. Neurol.* 143, 481–490. doi: 10.1002/cne.901430405

Bates, G. P., Dorsey, R., Gusella, J. F., Hayden, M. R., Kay, C., Leavitt, B. R., et al. (2015). Huntington disease. *Nat. Rev. Dis. Primers* 1:15005. doi: 10.1038/nrdp.2015.5

Beamer, E., Kovacs, G., and Sperlagh, B. (2017). ATP released from astrocytes modulates action potential threshold and spontaneous excitatory postsynaptic currents in the neonatal rat prefrontal cortex. *Brain Res. Bull.* 135, 129–142. doi: 10.1016/j.brainresbull.2017.10.006

Bobermin, L. D., da Silva, A., Souza, D. O., and Quincozes-Santos, A. (2018). Differential effects of typical and atypical antipsychotics on astroglial cells in vitro. *Int. J. Dev. Neurosci.* 69, 1–9. doi: 10.1016/j.ijdevneu.2018.06.001

Bradford, J., Shin, J.-Y., Roberts, M., Wang, C.-E., Li, X.-J., and Li, S. (2009). Expression of mutant huntingtin in mouse brain astrocytes causes age-dependent neurological symptoms. *Proc. Natl. Acad. Sci. U.S.A.* 106, 22480–22485. doi: 10.1073/pnas.0911503106

Braun, K., Antemano, R., Helmeke, C., Buchner, M., and Poeggel, G. (2009). Juvenile separation stress induces rapid region- and layer-specific changes in S100ss- and glial fibrillary acidic protein-immunoreactivity in astrocytes of the rodent medial prefrontal cortex. *Neuroscience* 160, 629–638. doi: 10.1016/j.neuroscience.2009.02.074

Brockett, A. T., Kane, G. A., Monari, P. K., Briones, B. A., Vigneron, P. A., Barber, G. A., et al. (2018). Evidence supporting a role for astrocytes in the regulation of cognitive flexibility and neuronal oscillations through the Ca^{2+} binding protein S100beta. *PLoS One* 13:e0195726. doi: 10.1371/journal.pone.0195726

Broe, M., Kril, J., and Halliday, G. M. (2004). Astrocytic degeneration relates to the severity of disease in frontotemporal dementia. *Brain* 127(Pt 10), 2214–2220. doi: 10.1093/brain/awh250

Bull, C., Syed, W. A., Minter, S. C., and Bowers, M. S. (2015). Differential response of glial fibrillary acidic protein-positive astrocytes in the rat prefrontal cortex following ethanol self-administration. *Alcohol. Clin. Exp. Res.* 39, 650–658. doi: 10.1111/acer.12683

Cahoy, J. D., Emery, B., Kaushal, A., Foo, L. C., Zamanian, J. L., Christopherson, K. S., et al. (2008). A transcriptome database for astrocytes, neurons, and oligodendrocytes: a new resource for understanding brain development and function. *J. Neurosci.* 28, 264–278. doi: 10.1523/JNEUROSCI.4178-07.2008

Cao, X., Li, L. P., Wang, Q., Wu, Q., Hu, H. H., Zhang, M., et al. (2013). Astrocyte-derived ATP modulates depressive-like behaviors. *Nat. Med.* 19, 773–777. doi: 10.1038/nm.3162

Chai, H., Diaz-Castro, B., Shigetomi, E., Monte, E., Octeau, J. C., Yu, X., et al. (2017). Neural circuit-specialized astrocytes: transcriptomic, proteomic, morphological, and functional evidence. *Neuron* 95, 531–549.e9. doi: 10.1016/j.neuron.2017.06.029

Chanaday, N. L., and Roth, G. A. (2016). Microglia and astrocyte activation in the frontal cortex of rats with experimental autoimmune encephalomyelitis. *Neuroscience* 314, 160–169. doi: 10.1016/j.neuroscience.2015.11.060

Chen, A., Akinyemi, R. O., Hase, Y., Firbank, M. J., Ndung'u, M. N., Foster, V., et al. (2016). Frontal white matter hyperintensities, clasmatodendrosis and gliovascular abnormalities in ageing and post-stroke dementia. *Brain* 139, 242–258. doi: 10.1093/brain/awv328

Colombo, J. A., Lipina, S., Yanez, A., and Puissant, V. (1997). Postnatal development of interlaminar astroglial processes in the cerebral cortex of primates. *Int. J. Dev. Neurosci.* 15, 823–833. doi: 10.1016/S0736-5748(97)00043-9

De Zeeuw, C. I., and Hoogland, T. M. (2015). Reappraisal of Bergmann glial cells as modulators of cerebellar circuit function. *Front. Cell. Neurosci.* 9:246. doi: 10.3389/fncel.2015.00246

Ebrahimi, M., Yamamoto, Y., Sharifi, K., Kida, H., Kagawa, Y., Yasumoto, Y., et al. (2016). Astrocyte-expressed FABP7 regulates dendritic morphology and excitatory synaptic function of cortical neurons. *Glia* 64, 48–62. doi: 10.1002/glia.22902

Estrada-Sanchez, A. M., Montiel, T., Segovia, J., and Massieu, L. (2009). Glutamate toxicity in the striatum of the R6/2 Huntington's disease transgenic mice is age-dependent and correlates with decreased levels of glutamate transporters. *Neurobiol. Dis.* 34, 78–86. doi: 10.1016/j.nbd.2008.12.017

Faideau, M., Kim, J., Cormier, K., Gilmore, R., Welch, M., Auregan, G., et al. (2010). In vivo expression of polyglutamine-expanded huntingtin by mouse striatal astrocytes impairs glutamate transport: a correlation with Huntington's disease subjects. *Hum. Mol. Genet.* 19, 3053–3067. doi: 10.1093/hmg/ddq212

Feresten, A. H., Barakauskas, V., Ypsilanti, A., Barr, A. M., and Beasley, C. L. (2013). Increased expression of glial fibrillary acidic protein in prefrontal cortex in psychotic illness. *Schizophr. Res.* 150, 252–257. doi: 10.1016/j.schres.2013.07.024

Fong, L. K., Yang, M. M., Dos Santos Chaves, R., Reyna, S. M., Langness, V. F., Woodruff, G., et al. (2018). Full-length amyloid precursor protein regulates lipoprotein metabolism and amyloid-beta clearance in human astrocytes. *J. Biol. Chem.* 293, 11341–11357. doi: 10.1074/jbc.RA117.000441

Fuster, J. M. (2002). Frontal lobe and cognitive development. *J. Neurocytol.* 31, 373–385. doi: 10.1023/A:1024190429920

Garcia-Cabezas, M. A., Joyce, M. K. P., John, Y. J., Zikopoulos, B., and Barbas, H. (2017). Mirror trends of plasticity and stability indicators in primate prefrontal cortex. *Eur. J. Neurosci.* 46, 2392–2405. doi: 10.1111/ejn.13706

Garwood, C. J., Ratcliffe, L. E., Simpson, J. E., Heath, P. R., Ince, P. G., and Wharton, S. B. (2017). Review: astrocytes in Alzheimer's disease and other age-associated dementias: a supporting player with a central role. *Neuropathol. Appl. Neurobiol.* 43, 281–298. doi: 10.1111/nan.12338

Ghashghaei, H. T., Weimer, J. M., Schmid, R. S., Yokota, Y., McCarthy, K. D., Popko, B., et al. (2007). Reinduction of ErbB2 in astrocytes promotes radial glial progenitor identity in adult cerebral cortex. *Genes Dev.* 21, 3258–3271. doi: 10.1101/gad.1580407

Ghetti, B., Oblak, A. L., Boeve, B. F., Johnson, K. A., Dickerson, B. C., and Goedert, M. (2015). Invited review: frontotemporal dementia caused by microtubule-associated protein tau gene (MAPT) mutations: a chameleon for neuropathology and neuroimaging. *Neuropathol. Appl. Neurobiol.* 41, 24–46. doi: 10.1111/nan.12213

Giralt, A., Friedman, H. C., Caneda-Ferron, B., Urban, N., Moreno, E., Rubio, N., et al. (2010). BDNF regulation under GFAP promoter provides engineered astrocytes as a new approach for long-term protection in Huntington's disease. *Gene Ther.* 17, 1294–1308. doi: 10.1038/gt.2010.71

Gonzáles-Reyes, R. E., Nava-Mesa, M. O., Vargas-Sánchez, K., Ariza-Salamanca, D., and Mora-Muñoz, L. (2017). Involvement of astrocytes in Alzheimer's disease from a neuroinflammatory and oxidative stress perspective. *Front. Mol. Neurosci.* 10:427. doi: 10.3389/fnmol.2017.00427

Haim, L. B., Ceyzériat, K., Carrillo-de Sauvage, M. A., Aubry, F., Auregan, G., Guillermier, M., et al. (2015). The JAK/STAT3 pathway is a common inducer of astrocyte reactivity in Alzheimer's and Huntington's diseases. *J. Neurosci. 35,* 2817–2829. doi: 10.1523/JNEUROSCI.3516-14.2015

Hallmann, A. L., Arauzo-Bravo, M. J., Mavrommatis, L., Ehrlich, M., Ropke, A., Brockhaus, J., et al. (2017). Astrocyte pathology in a human neural stem cell model of frontotemporal dementia caused by mutant TAU protein. *Sci. Rep.* 7:42991. doi: 10.1038/srep42991

Han, X., Chen, M., Wang, F., Windrem, M., Wang, S., Shanz, S., et al. (2013). Forebrain engraftment by human glial progenitor cells enhances synaptic plasticity and learning in adult mice. *Cell Stem Cell* 12, 342–353. doi: 10.1016/j.stem.2012.12.015

Harris, R. A., Tindale, L., Lone, A., Singh, O., Macauley, S. L., Stanley, M., et al. (2016). Aerobic glycolysis in the frontal cortex correlates with memory performance in wild-type mice but not the APP/PS1 mouse model of cerebral amyloidosis. *J. Neurosci.* 36, 1871–1878. doi: 10.1523/JNEUROSCI.3131-15.2016

Haughey, N. J., and Mattson, M. P. (2003). Alzheimer's amyloid beta-peptide enhances ATP/gap junction-mediated calcium-wave propagation in astrocytes. *Neuromolecular Med.* 3, 173–180. doi: 10.1385/NMM:3:3:173

Holtzman, D. M., Bales, K. R., Wu, S., Bhat, P., Parsadanian, M., Fagan, A. M., et al. (1999). Expression of human apolipoprotein E reduces amyloid-beta deposition in a mouse model of Alzheimer's disease. *J. Clin. Invest.* 103, R15–R21. doi: 10.1172/JCI6179

Hong, Y., Zhao, T., Li, X.-J., and Li, S. (2016). Mutant huntingtin impairs BDNF release from astrocytes by disrupting conversion of Rab3a-GTP into Rab3a-GDP. *J. Neurosci.* 36, 8790–8801. doi: 10.1523/JNEUROSCI.0168-16.2016

Hong, Y., Zhao, T., Li, X. J., and Li, S. (2017). Mutant huntingtin inhibits alphaB-crystallin expression and impairs exosome secretion from astrocytes. *J. Neurosci.* 37, 9550–9563. doi: 10.1523/JNEUROSCI.1418-17.2017

Hsiao, H.-Y., Chen, Y.-C., Huang, C.-H., Chen, C.-C., Hsu, Y.-H., Chen, H.-M., et al. (2015). Aberrant astrocytes impair vascular reactivity in Huntington disease. *Ann. Neurol.* 78, 178–192. doi: 10.1002/ana.24428

Hsiao, H. Y., Chiu, F. L., Chen, C. M., Wu, Y. R., Chen, H. M., Chen, Y. C., et al. (2014). Inhibition of soluble tumor necrosis factor is therapeutic in Huntington's disease. *Hum. Mol. Genet.* 23, 4328–4344. doi: 10.1093/hmg/ddu151

Hsu, E. T., Gangolli, M., Su, S., Holleran, L., Stein, T. D., Alvarez, V. E., et al. (2018). Astrocytic degeneration in chronic traumatic encephalopathy. *Acta Neuropathol.* 136, 955–972. doi: 10.1007/s00401-018-1902-3

Jansen, A. H., van Hal, M., Op den Kelder, I. C., Meier, R. T., de Ruiter, A. A., Schut, M. H., et al. (2017). Frequency of nuclear mutant huntingtin inclusion formation in neurons and glia is cell-type-specific. *Glia* 65, 50–61. doi: 10.1002/glia.23050

Jayakumar, A. R., Tong, X. Y., Shamaladevi, N., Barcelona, S., Gaidosh, G., Agarwal, A., et al. (2017). Defective synthesis and release of astrocytic thrombospondin-1 mediates the neuronal TDP-43 proteinopathy, resulting in defects in neuronal integrity associated with chronic traumatic encephalopathy: in vitro studies. *J. Neurochem.* 140, 645–661. doi: 10.1111/jnc.13867

Jiang, R., Diaz-Castro, B., Looger, L. L., and Khakh, B. S. (2016). Dysfunctional calcium and glutamate signaling in striatal astrocytes from Huntington's disease model mice. *J. Neurosci.* 36, 3453–3470. doi: 10.1523/JNEUROSCI.3693-15.2016

John, C. S., Smith, K. L., Van't Veer, A., Gompf, H. S., Carlezon, W. A. Jr., et al. (2012). Blockade of astrocytic glutamate uptake in the prefrontal cortex induces anhedonia. *Neuropsychopharmacology* 37, 2467–2475. doi: 10.1038/npp.2012.105

Jones, V. C., Atkinson-Dell, R., Verkhratsky, A., and Mohamet, L. (2017). Aberrant iPSC-derived human astrocytes in Alzheimer's disease. *Cell Death Dis.* 8:e2696. doi: 10.1038/cddis.2017.89

Juopperi, T. A., Kim, W. R., Chiang, C. -H., Yu, H., Margolis, R. L., Ross, C. A., et al. (2012). Astrocytes generated from patient induced pluripotent stem cells recapitulate features of Huntington's disease patient cells. *Mol. Brain* 5:17. doi: 10.1186/1756-6606-5-17

Kersaitis, C., Halliday, G. M., and Kril, J. J. (2004). Regional and cellular pathology in frontotemporal dementia: relationship to stage of disease in cases with and without Pick bodies. *Acta Neuropathol.* 108, 515–523. doi: 10.1007/s00401-004-0917-0

Khakh, B. S., Beaumont, V., Cachope, R., Munoz-Sanjuan, I., Goldman, S. A., and Grantyn, R. (2017). Unravelling and exploiting astrocyte dysfunction in Huntington's disease. *Trends Neurosci.* 40, 422–437. doi: 10.1016/j.tins.2017.05.002

Khan, Z. U., Koulen, P., Rubinstein, M., Grandy, D. K., and Goldman-Rakic, P. S. (2001). An astroglia-linked dopamine D2-receptor action in prefrontal cortex. *Proc. Natl. Acad. Sci. U.S.A.* 98, 1964–1969. doi: 10.1073/pnas.98.4.1964

Koistinaho, M., Lin, S., Wu, X., Esterman, M., Koger, D., Hanson, J., et al. (2004). Apolipoprotein E promotes astrocyte colocalization and degradation of deposited amyloid-β peptides. *Nat. Med.* 10, 719–726. doi: 10.1038/nm1058

Lee, W., Reyes, R. C., Gottipati, M. K., Lewis, K., Lesort, M., Parpura, V., et al. (2013). Enhanced Ca^{2+}-dependent glutamate release from astrocytes of the BACHD Huntington's disease mouse model. *Neurobiol. Dis.* 58, 192–199. doi: 10.1016/j.nbd.2013.06.002

Liao, F., Hori, Y., Hudry, E., Bauer, A. Q., Jiang, H., Mahan, T. E., et al. (2014). Anti-ApoE antibody given after plaque onset decreases Aβ accumulation and improves brain function in a mouse model of Aβ amyloidosis. *J. Neurosci.* 34, 7281–7292. doi: 10.1523/JNEUROSCI.0646-14.2014

Liddelow, S. A., Guttenplan, K. A., Clarke, L. E., Bennett, F. C., Bohlen, C. J., Schirmer, L., et al. (2017). Neurotoxic reactive astrocytes are induced by activated microglia. *Nature* 541, 481–487. doi: 10.1038/nature21029

Lievens, J. C., Woodman, B., Mahal, A., Spasic-Boscovic, O., Samuel, D., Kerkerian-Le Goff, L., et al. (2001). Impaired glutamate uptake in the R6 Huntington's disease transgenic mice. *Neurobiol. Dis.* 8, 807–821. doi: 10.1006/nbdi.2001.0430

Lim, D., Iyer, A., Ronco, V., Grolla, A. A., Canonico, P. L., Aronica, E., et al. (2013). Amyloid beta deregulates astroglial mGluR5-mediated calcium signaling via calcineurin and Nf-kB. *Glia* 61, 1134–1145. doi: 10.1002/glia.22502

Lima, A., Sardinha, V. M., Oliveira, A. F., Reis, M., Mota, C., Silva, M. A., et al. (2014). Astrocyte pathology in the prefrontal cortex impairs the cognitive function of rats. *Mol. Psychiatry* 19, 834–841. doi: 10.1038/mp.2013.182

Lin, Y. T., Seo, J., Gao, F., Feldman, H. M., Wen, H. L., Penney, J., et al. (2018). APOE4 causes widespread molecular and cellular alterations associated with Alzheimer's disease phenotypes in human iPSC-derived brain cell types. *Neuron* 98, 1141–1154.e7. doi: 10.1016/j.neuron.2018.05.008

Marathe, S. V., D'Almeida, P. L., Virmani, G., Bathini, P., and Alberi, L. (2018). Effects of monoamines and antidepressants on astrocyte physiology: implications for monoamine hypothesis of depression. *J. Exp. Neurosci.* 12:1179069518789149. doi: 10.1177/1179069518789149

Marina, N., Turovsky, E., Christie, I. N., Hosford, P. S., Hadjihambi, A., Korsak, A., et al. (2018). Brain metabolic sensing and metabolic signaling at the level of an astrocyte. *Glia* 66, 1185–1199. doi: 10.1002/glia.23283

Martinac, J. A., Craft, D. K., Su, J. H., Kim, R. C., and Cotman, C. W. (2001). Astrocytes degenerate in frontotemporal dementia: possible relation to hypoperfusion. *Neurobiol. Aging* 22, 195–207. doi: 10.1016/S0197-4580(00)00231-1

Martinez-Vicente, M., Talloczy, Z., Wong, E., Tang, G., Koga, H., Kaushik, S., et al. (2010). Cargo recognition failure is responsible for inefficient autophagy in Huntington's disease. *Nat. Neurosci.* 13, 567–576. doi: 10.1038/nn.2528

Masliah, E., Alford, M., Mallory, M., and Hansen, L. (1996). Deficient glutamate transport is associated with neurodegeneration in Alzheimer's disease. *Ann. Neurol.* 40, 759–766. doi: 10.1002/ana.410400512

Masters, C. L., Bateman, R., Blennow, K., Rowe, C. C., Sperling, R. A., and Cummings, J. L. (2015). Alzheimer's disease. *Nat. Rev. Dis. Primers* 1:15056. doi: 10.1038/nrdp.2015.56

Merlini, M., Meyer, E. P., Ulmann-Schuler, A., and Nitsch, R. M. (2011). Vascular β-amyloid and early astrocyte alterations impair cerebrovascular function and cerebral metabolism in transgenic arcAβ mice. *Acta Neuropathol.* 12, 293–311. doi: 10.1007/s00401-011-0834-y

Meunier, C., Wang, N., Yi, C., Dallerac, G., Ezan, P., Koulakoff, A., et al. (2017). Contribution of astroglial Cx43 hemichannels to the modulation of glutamatergic currents by D-serine in the mouse prefrontal cortex. *J. Neurosci.* 37, 9064–9075. doi: 10.1523/JNEUROSCI.2204-16.2017

Miguel-Hidalgo, J. J., Baucom, C., Dilley, G., Overholser, J. C., Meltzer, H. Y., Stockmeier, C. A., et al. (2000). Glial fibrillary acidic protein immunoreactivity in the prefrontal cortex distinguishes younger from older adults in major depressive disorder. *Biol. Psychiatry* 48, 861–873. doi: 10.1016/S0006-3223(00)00999-9

Molofsky, A. V., Deneen, B. (2015). Astrocyte development: a guide for the perplexed. *Glia* 63, 1320–1329. doi: 10.1002/glia.22836

Morel, L., Chiang, M. S. R., Higashimori, H., Shoneye, T., Iyer, L. K., Yelick, J., et al. (2017). Molecular and functional properties of regional astrocytes in the adult brain. *J. Neurosci.* 37, 8706–8717. doi: 10.1523/JNEUROSCI.3956-16.2017

Mosconi, L., Sorbi, S., de Leon, M. J., Li, Y., Nacmias, B., Myoung, P. S., et al. (2006). Hypometabolism exceeds atrophy in presymptomatic early-onset familial Alzheimer's disease. *J. Nucl. Med.* 47, 1778–1786.

Nagata, E., Sawa, A., Ross, C. A., and Snyder, S. H. (2004). Autophagosome-like vacuole formation in Huntington's disease lymphoblasts. *Neuroreport* 15, 1325–1328. doi: 10.1097/01.wnr.0000127073.66692.8f

Narita, M., Kuzumaki, N., Narita, M., Kaneko, C., Tamai, E., Khotib, J., et al. (2006). Age-related emotionality is associated with cortical delta-opioid receptor dysfunction-dependent astrogliosis. *Neuroscience* 137, 1359–1367. doi: 10.1016/j.neuroscience.2005.10.067

Neus Bosch, M., Pugliese, M., Andrade, C., Gimeno-Bayon, J., Mahy, N., and Rodriguez, M. J. (2015). Amyloid-beta immunotherapy reduces amyloid plaques and astroglial reaction in aged domestic dogs. *Neurodegener. Dis.* 15, 24–37. doi: 10.1159/000368672

Oberheim, N. A., Takano, T., Han, X., He, W., Lin, J. H. C., Wang, F., et al. (2009). Uniquely hominid features of adult human astrocytes. *J. Neurosci.* 29, 3276–3287. doi: 10.1523/JNEUROSCI.4707-08.2009

Oksanen, M., Petersen, A. J., Naumenko, N., Puttonen, K., Lehtonen, Š., Gubert Olivé, M., et al. (2017). PSEN1 mutant iPSC-derived model reveals severe astrocyte pathology in Alzheimer's disease. *Stem Cell Rep.* 9, 1885–1897. doi: 10.1016/j.stemcr.2017.10.016

Olabarria, M., Noristani, H. N., Verkhratsky, A., and Rodríguez, J. J. (2010). Concomitant astroglial atrophy and astrogliosis in a triple transgenic animal model of Alzheimer's disease. *Glia* 58, 831–838. doi: 10.1002/glia.20967

Parsons, M. P., Vanni, M. P., Woodard, C. L., Kang, R., Murphy, T. H., and Raymond, L. A. (2016). Real-time imaging of glutamate clearance reveals normal striatal uptake in Huntington disease mouse models. *Nat. Commun.* 7:11251. doi: 10.1038/ncomms11251

Phatnani, H., and Maniatis, T. (2015). Astrocytes in neurodegenerative disease. *Cold Spring Harb. Perspect. Biol.* 7:a020628. doi: 10.1101/cshperspect.a020628

Plotkin, J. L., Joshua L., Day, M., Peterson, Jayms D., Xie, Z., Kress, Geraldine J., et al. (2014). Impaired TrkB receptor signaling underlies corticostriatal dysfunction in Huntington's disease. *Neuron* 83, 178–188. doi: 10.1016/j.neuron.2014.05.032

Prevot, V., Dehouck, B., Sharif, A., Ciofi, P., Giacobini, P., and Clasadonte, J. (2018). The versatile tanycyte: a hypothalamic integrator of reproduction and energy metabolism. *Endocr. Rev.* 39, 333–368. doi: 10.1210/er.2017-00235

Rajkowska, G., Miguel-Hidalgo, J. J., Makkos, Z., Meltzer, H., Overholser, J., and Stockmeier, C. (2002). Layer-specific reductions in GFAP-reactive astroglia in the dorsolateral prefrontal cortex in schizophrenia. *Schizophr. Res.* 57, 127–138. doi: 10.1016/S0920-9964(02)00339-0

Reick, C., Ellrichmann, G., Tsai, T., Lee, D. H., Wiese, S., Gold, R., et al. (2016). Expression of brain-derived neurotrophic factor in astrocytes - Beneficial effects of glatiramer acetate in the R6/2 and YAC128 mouse models of Huntington's disease. *Exp. Neurol.* 285, 12–23. doi: 10.1016/j.expneurol.2016.08.012

Reiman, E. M., Chen, K., Alexander, G. E., Caselli, R. J., Bandy, D., Osborne, D., et al. (2004). Functional brain abnormalities in young adults at genetic risk for late-onset Alzheimer's dementia. *Proc. Natl. Acad. Sci. U.S.A.* 101, 284–289. doi: 10.1073/pnas.2635903100

Roberts, R. C., Roche, J. K., and McCullumsmith, R. E. (2014). Localization of excitatory amino acid transporters EAAT1 and EAAT2 in human postmortem cortex: a light and electron microscopic study. *Neuroscience* 277, 522–540. doi: 10.1016/j.neuroscience.2014.07.019

Rodrieguez-Veitez, E., Ni, R., Gulyás, B., Tóth, M., Häggkvist, J., Halldin, C., et al. (2015). Astrocytosis precedes amyloid plaque deposition in Alzheimer APPswe transgenic mouse brain: a correlative positron emission tomography and in vitro imaging study. *Eur. J. Nucl. Med. Mol. Imaging* 42, 1119–1132. doi: 10.1007/s00259-015-3047-0

Semyanov, A. (2019). Spatiotemporal pattern of calcium activity in astrocytic network. *Cell Calcium* 78, 15–25. doi: 10.1016/j.ceca.2018.12.007

Serio, A., Bilican, B., Barmada, S. J., Ando, D. M., Zhao, C., Siller, R., et al. (2013). Astrocyte pathology and the absence of non-cell autonomy in an induced pluripotent stem cell model of TDP-43 proteinopathy. *Proc. Natl. Acad. Sci. U.S.A.* 110, 4697–4702. doi: 10.1073/pnas.1300398110

Sherwood, C. C., Stimpson, C. D., Raghanti, M. A., Wildman, D. E., Uddin, M., Grossman, L. I., et al. (2006). Evolution of increased glia–neuron ratios in the human frontal cortex. *Proc. Natl. Acad. Sci. U.S.A.* 103, 13606–13611. doi: 10.1073/pnas.0605843103

Shi, Y., Yamada, K., Liddelow, S. A., Smith, S. T., Zhao, L., Luo, W., et al. (2017). ApoE4 markedly exacerbates tau-mediated neurodegeneration in a mouse model of tauopathy. *Nature* 549, 523–527. doi: 10.1038/nature24016

Shin, J. Y., Fang, Z. H., Yu, Z. X., Wang, C. E., Li, S. H., and Li, X. J. (2005). Expression of mutant huntingtin in glial cells contributes to neuronal excitotoxicity. *J. Cell Biol.* 171, 1001–1012. doi: 10.1083/jcb.200508072

Sjostedt, E., Fagerberg, L., Hallstrom, B. M., Haggmark, A., Mitsios, N., Nilsson, P., et al. (2015). Defining the human brain proteome using transcriptomics and antibody-based profiling with a focus on the cerebral cortex. *PLoS One* 10:e0130028. doi: 10.1371/journal.pone.0130028

Stroth, N., and Svenningsson, P. (2015). S100B interacts with the serotonin 5-HT7 receptor to regulate a depressive-like behavior. *Eur. Neuropsychopharmacol.* 25, 2372–2380. doi: 10.1016/j.euroneuro.2015.10.003

Su, J. H., Nichol, K. E., Sitch, T., Sheu, P., Chubb, C., Miller, B. L., et al. (2000). DNA damage and activated caspase-3 expression in neurons and astrocytes: evidence for apoptosis in frontotemporal dementia. *Exp. Neurol.* 163, 9–19. doi: 10.1006/exnr.2000.7340

Takahashi, K., Tanabe, K., Ohnuki, M., Narita, M., Ichisaka, T., Tomoda, K., et al. (2007). Induction of pluripotent stem cells from adult human fibroblasts by defined factors. *Cell* 131, 861–872. doi: 10.1016/j.cell.2007.11.019

Takouda, J., Katada, S., and Nakashima, K. (2017). Emerging mechanisms underlying astrogenesis in the developing mammalian brain. *Proc. Jpn. Acad. Ser. B Phys. Biol. Sci.* 93, 386–398. doi: 10.2183/pjab.93.024

Talantova, M., Sanz-Blasco, S., Zhang, X., Xia, P., Akhtar, M. W., Okamoto, S.-I., et al. (2013). Aβ induces astrocytic glutamate release, extrasynaptic NMDA receptor activation, and synaptic loss. *Proc. Natl. Acad. Sci. U.S.A.* 110, E2518–E2527. doi: 10.1073/pnas.1306832110

Tanahashi, S., Yamamura, S., Nakagawa, M., Motomura, E., and Okada, M. (2012). Clozapine, but not haloperidol, enhances glial D-serine and L-glutamate release in rat frontal cortex and primary cultured astrocytes. *Br. J. Pharmacol.* 165, 1543–1555. doi: 10.1111/j.1476-5381.2011.01638.x

Teneka, M. T., Sastre, M., Dumitrescu-Ozimek, L., Dewachter, I., Walter, J., Klockgether, T., et al. (2005). Focal glial activation coincides with increased BACE1 activation and precedes amyloid plaque deposition in APP[V717I] transgenic mice. *J. Neuroinflammation* 2:22. doi: 10.1186/1742-2094-2-22

Tian, G., Kong, Q., Lai, L., Ray-Chaudhury, A., and Lin, C.-L. (2010). Increased expression of cholesterol 24S-hydroxylase results in disruption of glial glutamate transporter EAAT2 association with lipid rafts: a potential role in Alzheimer's disease. *J. Neurochem.* 113, 978–989. doi: 10.1111/j.1471-4159.2010.06661.x

Tong, J., Huang, C., Bi, F., Wu, Q., Huang, B., Liu, X., et al. (2013). Expression of ALS-linked TDP-43 mutant in astrocytes causes non-cell-autonomous motor neuron death in rats. *EMBO J.* 32, 1917–1926. doi: 10.1038/emboj.2013.122

Tong, X., Ao, Y., Faas, G. C., Nwaobi, S. E., Xu, J., Haustein, M. D., et al. (2014). Astrocyte Kir4.1 ion channel deficits contribute to neuronal dysfunction in Huntington's disease model mice. *Nat. Neurosci.* 17, 694–703. doi: 10.1038/nn.3691

Torres-Platas, S. G., Nagy, C., Wakid, M., Turecki, G., and Mechawar, N. (2016). Glial fibrillary acidic protein is differentially expressed across cortical and subcortical regions in healthy brains and downregulated in the thalamus and caudate nucleus of depressed suicides. *Mol. Psychiatry* 21, 509–515. doi: 10.1038/mp.2015.65

Tsai, H.-H., Li, H., Fuentealba, L. C., Molofsky, A. V., Taveira-Marques, R., Zhuang, H., et al. (2012). Regional astrocyte allocation regulates CNS synaptogenesis and repair. *Science* 337, 358–362. doi: 10.1126/science.1222381

Turner, R. C., Lucke-Wold, B. P., Robson, M. J., Lee, J. M., and Bailes, J. E. (2016). Alzheimer's disease and chronic traumatic encephalopathy: distinct but possibly overlapping disease entities. *Brain Inj.* 30, 1279–1292. doi: 10.1080/02699052.2016.1193631

Vasile, F., Dossi, E., and Rouach, N. (2017). Human astrocytes: structure and functions in the healthy brain. *Brain Struct. Funct.* 222, 2017–2029. doi: 10.1007/s00429-017-1383-5

Wallingford, J., Scott, A. L., Rodrigues, K., and Doering, L. C. (2017). Altered developmental expression of the astrocyte-secreted factors hevin and SPARC in the fragile X mouse model. *Front. Mol. Neurosci.* 10:268. doi: 10.3389/fnmol.2017.00268

Wang, C., Wilson, W. A., Moore, S. D., Mace, B. E., Maeda, N., Schmechel, D. E., et al. (2005). Human apoE4-targeted replacement mice display synaptic deficits in the absence of neuropathology. *Neurobiol. Dis.* 18, 390–398. doi: 10.1016/j.nbd.2004.10.013

Xin, W., and Bonci, A. (2018). Functional astrocyte heterogeneity and implications for their role in shaping neurotransmission. *Front. Cell. Neurosci.* 12:141. doi: 10.3389/fncel.2018.00141

Xiu, J., Nordberg, A., Zhang, J. T., and Guan, Z. Z. (2005). Expression of nicotinic receptors on primary cultures of rat astrocytes and up-regulation of the alpha7, alpha4 and beta2 subunits in response to nanomolar concentrations of the beta-amyloid peptide(1-42). *Neurochem. Int.* 47, 281–290. doi: 10.1016/j.neuint.2005.04.023

Zhang, X., Wan, J. Q., and Tong, X. P. (2018). Potassium channel dysfunction in neurons and astrocytes in Huntington's disease. *CNS Neurosci. Ther.* 24, 311–318. doi: 10.1111/cns.12804

Zhang, Y., Sloan, S. A., Clarke, L. E., Caneda, C., Plaza, C. A., Blumenthal, P. D., et al. (2016). Purification and characterization of progenitor and mature human astrocytes reveals transcriptional and functional differences with mouse. *Neuron* 89, 37–53. doi: 10.1016/j.neuron.2015.11.013

Zhao, J., Davis, M. D., Martens, Y. A., Shinohara, M., Graff-Radford, N. R., Younkin, S. G., et al. (2017). APOE ε4/ε4 diminishes neurotrophic function of human iPSC-derived astrocytes. *Hum. Mol. Genet.* 26, 2690–2700. doi: 10.1093/hmg/ddx155

Zhao, T., Hong, Y., Yin, P., Li, S., and Li, X.-J. (2017). Differential HspBP1 expression accounts for the greater vulnerability of neurons than astrocytes to misfolded proteins. *Proc. Natl. Acad. Sci.* 114, E7803–E7811. doi: 10.1073/pnas.1710549114

Zhao, T., Hong, Y., Li, S., and Li, X.-J. (2016). Compartment-dependent degradation of mutant huntingtin accounts for its preferential accumulation in neuronal processes. *J. Neurosci.* 36, 8317–8328. doi: 10.1523/JNEUROSCI.0806-16.2016

Zhao, Z., Nelson, A. R., Betsholtz, C., and Zlokovic, B. V. (2015). Establishment and dysfunction of the blood-brain barrier. *Cell* 163, 1064–1078. doi: 10.1016/j.cell.2015.10.067

Zheng, W., Li, Q., Zhao, C., Da, Y., Zhang, H.-L., and Chen, Z. (2018). Differentiation of glial cells from hiPSCs: potential applications in neurological diseases and cell replacement therapy. *Front. Cell. Neurosci.* 12:239. doi: 10.3389/fncel.2018.00239

Conflict of Interest Statement: The authors declare that the research was conducted in the absence of any commercial or financial relationships that could be construed as a potential conflict of interest.

frontiers in Cellular Neuroscience

BRIEF RESEARCH REPORT
published: 31 July 2019
doi: 10.3389/fncel.2019.00356

Nrf2 Induction Re-establishes a Proper Neuronal Differentiation Program in Friedreich's Ataxia Neural Stem Cells

*Piergiorgio La Rosa[1], Marta Russo[1], Jessica D'Amico[1], Sara Petrillo[1], Katia Aquilano[2], Daniele Lettieri-Barbato[2,3], Riccardo Turchi[2], Enrico S. Bertini[1] and Fiorella Piemonte[1]**

[1] Unit of Neuromuscular and Neurodegenerative Diseases, IRCCS Bambino Gesù Children's Hospital, Rome, Italy, [2] Department of Biology, University of Rome Tor Vergata, Rome, Italy, [3] IRCCS Fondazione Santa Lucia, Rome, Italy

Frataxin deficiency is the pathogenic cause of Friedreich's Ataxia, an autosomal recessive disease characterized by the increase of oxidative stress and production of free radicals in the cell. Although the onset of the pathology occurs in the second decade of life, cognitive differences and defects in brain structure and functional activation are observed in patients, suggesting developmental defects to take place during fetal neurogenesis. Here, we describe impairments in proliferation, stemness potential and differentiation in neural stem cells (NSCs) isolated from the embryonic cortex of the Frataxin Knockin/Knockout mouse, a disease animal model whose slow-evolving phenotype makes it suitable to study pre-symptomatic defects that may manifest before the clinical onset. We demonstrate that enhancing the expression and activity of the antioxidant response master regulator Nrf2 ameliorates the phenotypic defects observed in NSCs, re-establishing a proper differentiation program.

Keywords: Nrf2, Friedreich's Ataxia, neural stem cells, frataxin, neurogenesis, antioxidant, neurodegeneration

OPEN ACCESS

Edited by:
Sara Xapelli,
University of Lisbon, Portugal

Reviewed by:
Juan Antonio Navarro Langa,
University of Regensburg, Germany
Eunchai Kang,
University of Pennsylvania, United States

****Correspondence:***
Fiorella Piemonte
fiorella.piemonte@opbg.net

Specialty section:
This article was submitted to Cellular Neuropathology, a section of the journal Frontiers in Cellular Neuroscience

Received: *16 May 2019*
Accepted: *18 July 2019*
Published: *31 July 2019*

Citation:
La Rosa P, Russo M, D'Amico J, Petrillo S, Aquilano K, Lettieri-Barbato D, Turchi R, Bertini ES and Piemonte F (2019) Nrf2 Induction Re-establishes a Proper Neuronal Differentiation Program in Friedreich's Ataxia Neural Stem Cells. Front. Cell. Neurosci. 13:356. doi: 10.3389/fncel.2019.00356

INTRODUCTION

Friedreich's Ataxia (FRDA) is an early-onset autosomal recessive disease with an incidence of 1:50000, caused by severely reduced levels of frataxin, a mitochondrial protein involved in iron–sulfur cluster synthesis, iron transfer, and antioxidant defense (Romeo et al., 1983; Dürr et al., 1996; Santos et al., 2010; Vaubel and Isaya, 2013). Although no evident signs of the pathology show up in the first 5–10 years of life, a subsequent development of movement coordination loss, cardiac hypertrophy, diabetes and progressive neurodegeneration occurs (Dürr et al., 1996; Folker et al., 2010; Weidemann et al., 2012), resulting in death at young age (Bürk, 2017). Cognitive differences in FRDA patients have also been assessed (Wollmann et al., 2002; Mantovan et al., 2006; De Nobrega et al., 2007; Corben et al., 2011, 2017; Nieto et al., 2013). Thus, even if the progressive degeneration of sensory neurons in the dorsal root ganglia (DRG) and in the dentate nucleus of the cerebellum are observed early upon pathology onset (Bürk, 2017), neuroimaging techniques revealed impairments in white/gray matter structure (Zalesky et al., 2014; Harding et al., 2016; Rezende et al., 2016) and in cerebral functional activation (Georgiou-Karistianis et al., 2012). Reports outlining these defects have been published since a decade (Selvadurai et al., 2018) and several lines of evidence suggest that frataxin deficiency could lead to their insurgence during fetal development (Cossée et al., 2000; Santos et al., 2001; Koeppen et al., 2017). However, studies on the pathogenic mechanism underlying FRDA during the neurogenesis are still lacking.

Recent reports show that a mouse model of the pathology, the Frataxin Knockin/Knockout (KIKO) mouse, manifests neurobehavioral defects on the 9th month of life that closely

recapitulate the clinical human phenotype, including cerebellar ataxia, decreased peripheral sensitivity and motor strength and endurance impairments (Miranda et al., 2002; McMackin et al., 2017). Nevertheless, before the onset of the pathologic symptoms, mitochondrial and synaptic abnormalities are already present in the cerebellum (Lin et al., 2017a,b), suggesting that early pre-symptomatic defects may underlie the clinical onset and contribute to trigger the disease progression. In this context, the KIKO mouse model is a useful tool to search for earliest pathological changes, because it displays a slowly evolving phenotype, while biochemical and functional brain dysregulations arise earlier, thus closely recapitulating the clinical human phenotype (Lin et al., 2017a,b; McMackin et al., 2017; Cotticelli et al., 2019).

Oxidative stress and increased levels of free radicals play an important role in FRDA pathogenesis (Lupoli et al., 2018), where frataxin deficiency has been shown to reduce the expression of Nrf2 (the Nuclear factor erythroid-derived 2)-like 2 transcription factor NE2FL2 either in human FRDA fibroblasts (Paupe et al., 2009; Petrillo et al., 2017) and in mouse models of the disease (D'Oria et al., 2013; Shan et al., 2013; Anzovino et al., 2017; Dinkova-Kostova et al., 2018).

Nrf2 regulates the expression of several antioxidant enzymes and mounting evidences demonstrate an improvement of neurological phenotypes after induction of this signaling pathway (Dinkova-Kostova et al., 2018).

Redox signaling is critical in Nervous System development (Olguín-Albuerne and Morán, 2018) and Nrf2 has a relevant role in the neurogenic process, playing a key function in the regulation of neural stem cells (NSCs) features. In particular, its expression is directly correlated with NSCs proliferation and self-renewal, and its age-dependent down regulation determines the age-related NSCs loss of survival and function, impairing neurogenesis in subventricular zone of the lateral ventricles and in the dentate gyrus of the hyppocampus (Corenblum et al., 2016; Ray et al., 2018). Nrf2 activity and expression also play a role in the neuronal maturation process, as its overexpression and/or induced stabilization determine the increase of the mean length of neuron-differentiated neuroblastoma neuritis (Zhao et al., 2009), although the expression of the transcription factor is reported to constantly decrease throughout the differentiation process (Olguín-Albuerne and Morán, 2018). Importantly, the activation of Nrf2 signaling pathway is neuro-protective for progenitor cells exposed to amyloid beta (Aβ) deposits, a condition resembling the Alzheimer disease (Kärkkäinen et al., 2014), thus potentially representing an early therapeutic target in neurodegeneration.

Moving from these previous findings, in this study we analyzed the Nrf2 expression in NSCs isolated from the embryonic cortex of KIKO FRDA mouse and evaluated if an imbalance of Nrf2 signaling pathway may lead to early phenotypic defects in neurogenesis.

In addition, as two drugs, Sulforaphane (SFN) and EPI-743, are receiving increasing attention as promising candidates for the treatment of neurodegenerative diseases, including FRDA (Zesiewicz et al., 2018; Zhao et al., 2018), we analyzed the induction of Nrf2 pathway in response to those drugs in order to understand if an early activation of the transcription factor may trigger a neuro-regenerative mechanism in FRDA.

METHODS

Ethics Statement

We conducted all mouse experimentations in accordance with accepted standard of humane animal care and with the approval by relevant local (Institutional Animal Care and Use Committee, University of Rome Tor Vergata) and national (Ministry of Welfare, license no. 324/2018-PR) committees. Experiments were carried out according to institutional safety procedures.

NSCs Isolation, Culture, and Immunofluorescence Analysis

Neural stem cells were isolated from Frataxin KIKO C57/BL6 mouse (Charles River Laboratories International Inc., MA, United States) E13.5 (Bard et al., 1998) embryos as previously reported (La Rosa et al., 2016; Svetoni et al., 2017). Clonogenic assays were performed plating 5000 NSCs in 35-mm wells for each experimental point. After 5 days of culture, neurosphere number was counted and NPC clonogenicity expressed as the percentage ratio between plated cells and neurospheres formed. For differentiation assays, 20000 NPCs/well were plated on pre-coated poly-ornithine (Sigma-Aldrich, Saint Louis, MO, United States) and laminin-1 (Sigma-Aldrich) 4-well dishes. Cells were grown in NSCs medium, containing 1% v/v fetal bovine serum (FBS) (Gibco/Thermo-Fisher Scientific, United Kingdom) and incubated in a humidified atmosphere with 6% CO_2, at 37°C, for 3 days. Immunofluorescence staining was performed after cell fixation in 4% (v/v) formaldehyde (Sigma-Aldrich) and permeabilization with 0.1% Triton X-100 in PBS, supplemented with 1% BSA. Samples were incubated with the mouse anti-TUBB3 (1:300, Sigma-Aldrich) primary antibody for 1 h at r.t. and with the FITC-conjugated (1:250) secondary antibody (Jackson ImmunoResearch, Cambridge, United Kingdom) for 1 h at r.t. Hoechst (Invitrogen, CA, United States) was added for 15 min, and fluorescence preserved using the Prolong Gold mounting solution (Invitrogen). 10 randomly fields were taken for each sample using a DMI6000B inverted microscope (Leica, Germany), equipped with a Pan-Neofluar 20X/0.75 objective lens. Data are represented as percentage of positive cells/total cells (evaluated by the number of total nuclei).

RNA Isolation, RT-PCR, and RT-qPCR

Total RNA was extracted from NSCs using Total RNA purification kit (Norgen Biotek Corp., Canada), following manufacturer's instructions. 1 μg RNA was retro-transcribed by M-MLV reverse transcriptase (Invitrogen) and used in quantitative RT-PCR (qPCR) experiments using Sybr green PCR master mix (Applied Biosystem, CA, United States) as described by manufacturer's instructions. All primers used are reported in the table below. GAPDH gene expression was used to normalize qPCR experiments.

Gene	Forward primer (Fw)	Reverse primer (Rv)
Nrf2	5′-TGAGAGGCAGCCATGACT-3′	5′-GTCCTTGTTTTCGGTATT-3′
NQO1	5′-CATCACAGGTGAGCTGAAG-3′	5′-CAGCTTCTTGTGTTCGGCCA-3′
HO-1	5′-TGACACCTGAGGTCAAGCAC-3′	5′-CTCTGACGAAGTGACGCCAT-3′
GAPDH	5′-CCTCGTCCCGTAGACAAAATG-3′	5′-TGAAGGGGTCGTTGATGGC-3′

Immunoblotting

Neural stem cells were lysed in 50 mM Tris–HCl, pH 7.4, containing 100 mM NaCl, 1 mM $MgCl_2$, 0.1 mM $CaCl_2$, 1% NP-40, 0.5% sodium deoxycholate, 0.1% SDS and protease inhibitor cocktail (plus phosphatase and protease inhibitors) (Sigma-Aldrich). Proteins were separated by SDS–PAGE and transferred to polyvinylidene fluoride (PVDF) membranes (Amersham Biosciences Corp., United Kingdom). Antibodies were diluted in 0.1% Tween buffer (+ 5% BSA) as follows: rabbit anti-Nrf2 (1:500, Abcam, United Kingdom), mouse anti-NQO1 (1:2000, Novus Biologicals, United States), rabbit anti-HO-1 (1:2000, Abcam), mouse anti-Tubulin (1:1000, Sigma-Aldrich), rabbit anti-Frataxin (1:1000, Santa Cruz Biotechnology Inc., TX, United States). Signals were detected by enhanced chemiluminescence (ECL) (BioRad, CA, United States).

Complex I Assay

Complex I (NADH:CoQ oxidoreductase, EC 1.6.5.3) activity was measured by following the absorbance decrease of NADH at 340 nm (ε = 6.81 $mM^{-1} \cdot cm^{-1}$) in presence of the specific inhibitor rotenone (10 μM) (Carletti et al., 2014) and normalized for protein content.

ROS Quantification

Three micromolar Dichlorofluorescin–diacetate (DCF–DA) (Sigma-Aldrich) was added to 96-well microplates (Greiner CELLSTAR®, Sigma-Aldrich) and incubated 1 h at 37°C in a humidified 5% CO_2. Relative fluorescence units (RFU, $\lambda_{exc.}$ = 495 nm, $\lambda_{em.}$ = 530 nm), calculated by subtracting blank readings from all measurements, were taken using a plate spectrofluorometer (Enspire, Perkin Elmer). Results were normalized for cell number.

Statistical Analysis

All data are expressed as mean ± SD. Student's *t*-test was performed using Graphpad Prism software (RRID:SCR_002798).

RESULTS

KIKO NSCs Show Proliferation, Clonogenicity, and Differentiation Defects

To analyze if neurodevelopmental defects may occur in FRDA, we isolated NSCs from 13.5 embryonic day of life (E) cortex of KIKO mouse, a well established FRDA animal model, which displays a slowly evolving phenotype despite early biochemical and functional brain deregulations (Lin et al., 2017a,b; Cotticelli et al., 2019), thus closely resembling patient's pathologic progression (McMackin et al., 2017).

In culture, NSCs grow forming neurospheres that consist of a mix of stem and spontaneously differentiating cells (Conti et al., 2003; Galli et al., 2003). Growth curves over 5 days of culture showed a 48% reduction of KIKO NSCs proliferation, respect to WT NSCs (**Figure 1A**), and this was confirmed by 26% decrease of the average neurospheres' diameter (**Figure 1B**). Furthermore, only ∼5% of KIKO NSCs were able to reform spheres upon disaggregation (**Figure 1C**), as assessed by analyses of the NSCs clonogenicity. As the reduced proliferation and clonogenicity of KIKO NSCs could be explained by an increase of spontaneous differentiation events, we further analyzed the KIKO NSCs differentiation index toward neuronal lineage (**Figure 1D**). After 3 days of differentiation, a 1.7-fold increase of neuronal differentiation was observed in KIKO NSCs, respect to WT NSCs, although an overall reduction of neuronal complexity was also evident (**Figure 1D**). These data highlight phenotypic defects in frataxin-deficient NSCs already at early stage of neurogenesis.

Nrf2 Expression and Signaling Is Impaired in KIKO NSCs

Given that the frataxin depletion causes ROS overload and iron-sulfur (Fe-S) cluster proteins impairment in FRDA (Lin et al., 2017b; Abeti et al., 2018; Lupoli et al., 2018), we measured the activity of mitochondrial (Fe-S) Complex I (CI) and ROS levels in KIKO NSCs, in order to validate our model. As shown in **Figure 2**, CI activity was significantly decreased (46%) in KIKO NSCs, whereas ROS increased 3-times respect to WT NSCs, thus confirming the molecular key features of the disease.

As several studies show Nrf2 impairment in post-natal tissues of FRDA patients and in frataxin-deficient cells (Paupe et al., 2009; D'Oria et al., 2013; Shan et al., 2013; Petrillo et al., 2017), we analyzed Nrf2 expression in KIKO and WT NSCs, in order to evidence a potential involvement of the transcription factor in the defects described above. As reported in **Figure 2**, Nrf2 was reduced in KIKO NSCs either as mRNA (20% decrease, A) and as protein level (40% decrease, B). In the same way, a significant decrease of two representative Nrf2 target genes was detected in KIKO NSCs, compared to WT NSCs. In particular, NADPH Quinone Oxidoreductase 1 (NQO1) was 60% reduced as mRNA (**Figure 2A**) and 50% as protein amount (**Figure 2B**), and Heme Oxigenase-1 (HO-1) showed a 50% decrease both as mRNA (**Figure 2A**) and protein level (**Figure 2B**). As expected, a 60% decrease of frataxin expression (mRNA and protein) was also detected in KIKO NSCs (**Figures 2A,B**).

These findings confirm previous studies showing a frataxin-mediated Nrf2 deficiency in cell and mouse models of FRDA

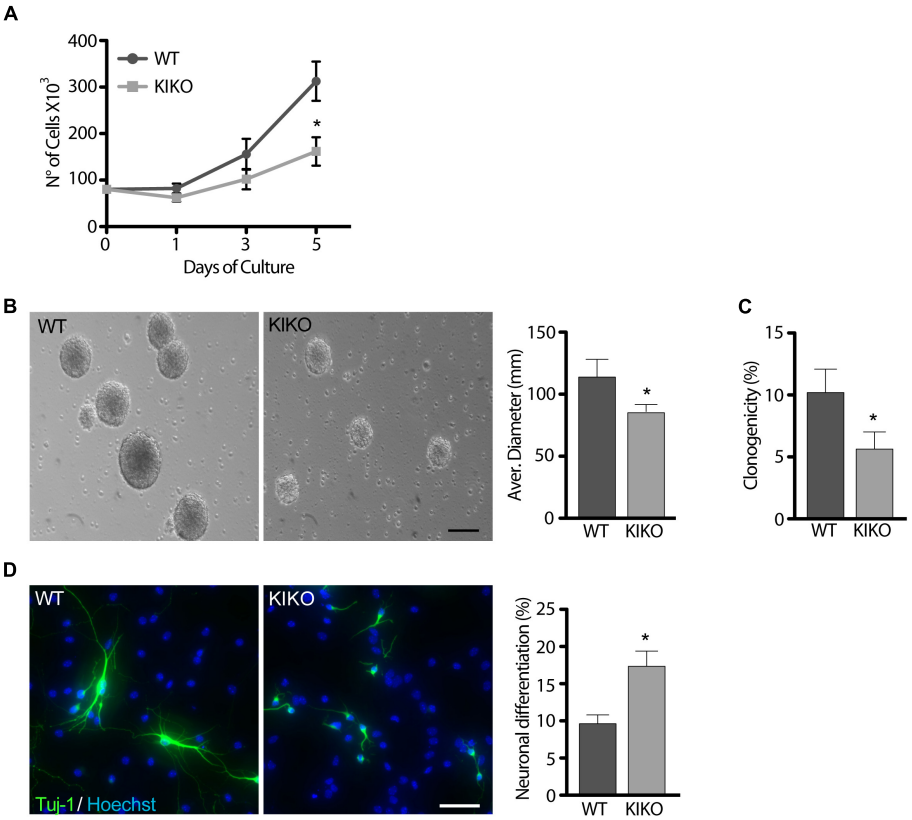

FIGURE 1 | Frataxin depletion determines phenotypic defects in KIKO NSCs and neurons. **(A,B)** analysis of WT and KIKO NSCs proliferation assessed by growth curves experiments over 5 days **(A)**, and diameter evaluation on the fifth day **(B)**. **(C)** Clonogenic assay of WT and KIKO NSCs. Clonogenicity was expressed as the ratio between the observed neurospheres and plated NSCs. **(D)** Immunofluorescence analysis of the neuronal differentiation marker Tuj-1 in WT and KIKO NSCs cultured for 3 days in differentiating conditions. Graph on the right represents (mean ± SD) measurement of number of Tuj-1 positive cells, $^*p < 0.05$. Scale bars = 100 μm.

(Paupe et al., 2009; D'Oria et al., 2013; Piermarini et al., 2016; Anzovino et al., 2017; Petrillo et al., 2017) but, additionally, they represent a progress in understanding the pathogenesis of FRDA because, for the first time, an early impairment of Nrf2 signaling is described already during neurogenesis. Furthermore, given the role of Nrf2 in the neurogenic process (Zhao et al., 2009; Corenblum et al., 2016; Olguín-Albuerne and Morán, 2018; Ray et al., 2018), the defective Nrf2 pathway may also underlie the loss of stemness potential and the increased cell differentiation toward the neuronal lineage evidenced in KIKO NSCs (**Figure 1**).

SFN and EPI-743 Treatments Restore Nrf2 and Nrf2-Target Gene Expression

Nrf2 inducers have been demonstrated to promote the activation of Nrf2/ARE signaling in frataxin silenced motor neurons (Piermarini et al., 2016; Petrillo et al., 2017). Thus, in order to evaluate the effect of Nrf2 activation on the KIKO NSCs defects, we treated KIKO NSCs with the classical Nrf2 inducer SFN and with EPI-743, a para-benzoquinone developed for the treatment of mitochondrial diseases (Enns et al., 2012; Martinelli et al., 2012; Zesiewicz et al., 2018).

qRT-PCR and western blot analyses were performed either under conditions of KIKO NSCs proliferation (**Figures 3A,B**) and following neuronal differentiation (**Figures 3C,D**).

As shown in **Figure 3**, both compounds significantly induce the expression and stability of Nrf2 in proliferating KIKO NSCs, compared to untreated KIKO NSCs, showing a consistent increase of mRNA (**Figure 3A**) and protein amount (**Figure 3B**) already after 2 h treatments (10-fold increase mRNA and 4-fold increase protein level), remaining high throughout 24 h. Also Nrf2 target genes were significantly induced after EPI and SFN treatments, with NQO1 reaching a peak at 6 h drugs (3-fold increase protein amount with EPI and 6-fold increase with SFN), whereas HO-1 showed a growing increase over time (4-fold protein increase with EPI and 6-fold with SFN) (**Figures 3A,B**).

A significant induction of Nrf2 and its down-stream genes was also found after 3 days neuronal differentiation of KIKO NSCs (**Figures 3C,D**), with 1.7- and 2.2-fold increases of protein level, following respectively EPI and SFN 24 h treatments. Similarly, Nrf2 target genes were induced with EPI and SFN both as mRNA (3.6-fold increase, **Figure 3C**) and protein level (1.9-fold increase, **Figure 3D**).

Overall, these findings highlight the effectiveness of the drug-mediated Nrf2 induction in restablishing the antioxidant defense

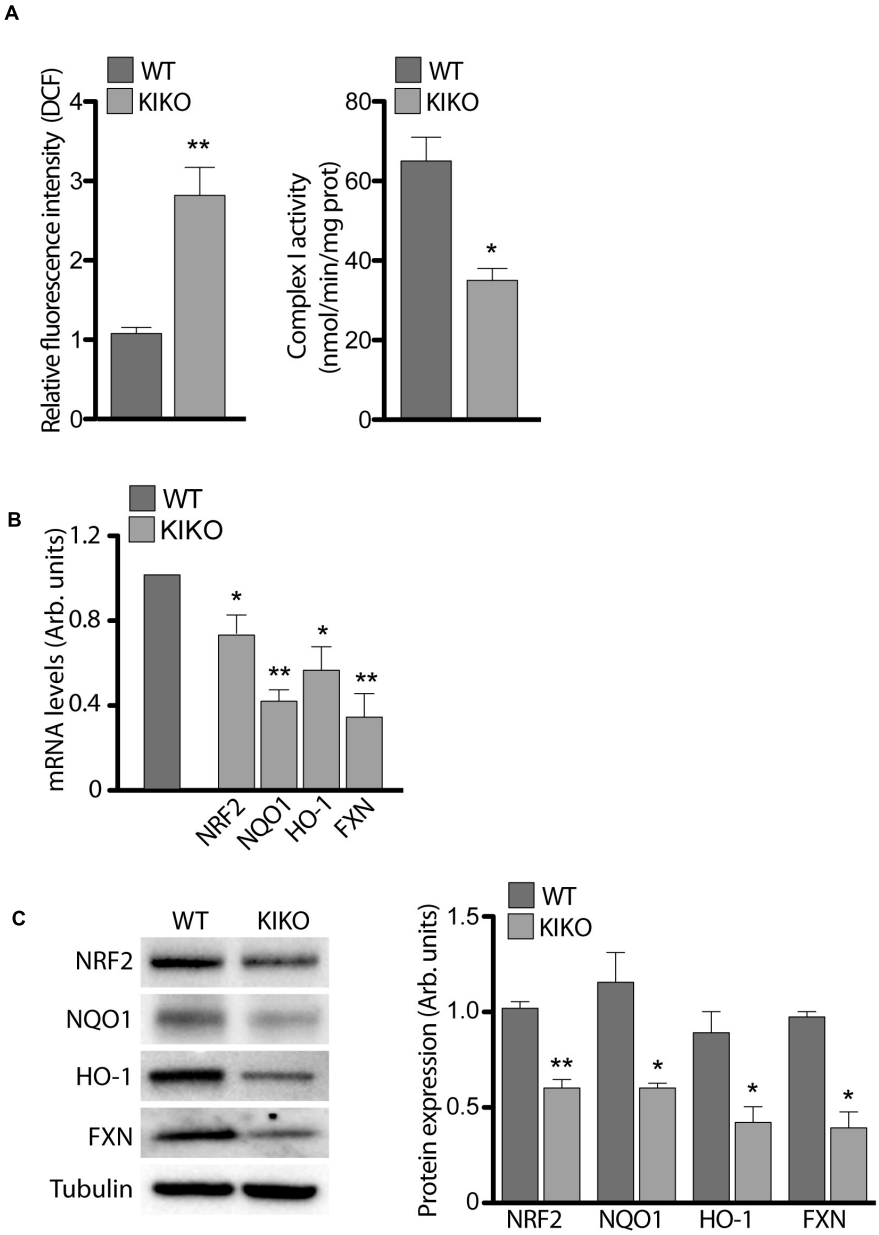

FIGURE 2 | Frataxin depletion determines impairments in NRF-2 expression and signaling. **(A)** ROS determination (graph on the left) and Complex I activity (graph on the right), assessed in WT and KIKO NSCs. Cellular ROS were evaluated by measuring DCF fluorescence, normalized for cell number, while Complex I activity was expressed as nmol/min/mg prot. qPCR **(B)** and Western Blot analyses **(C)** and relative densitometric evaluation (graph on the right) of the expression of the transcription factor Nrf2, its targets (NQO1 and HO-1) and Frataxin, in WT and KIKO NSCs. GAPDH was used for qPCR normalization, while Tubulin was used as Western Blot loading control, $*p < 0.05$ and $**p < 0.01$.

signaling in KIKO NSCs, thus leading to suggest the transcription factor as a potential early target of therapy.

SFN and EPI-743 Revert Phenotypic Defects in KIKO NSCs and Promote Neuronal Complexity and Differentiation

Following the drug-mediated rescue of Nrf2 function, we evaluated the effect of EPI-743 and SFN on KIKO NSCs ROS production (**Figure 2A**). Both treatments consistently reduced ROS overload, either in proliferating condition or during the differentiation process, thus re-balancing the cellular redox environment. Prompted by these results and by previous studies showing that the Nrf2 activation restored neurites' network and axonal re-growth in FRDA silenced neurons (Piermarini et al., 2016; Petrillo et al., 2017), we asked if Nrf2 induction was able to rescue the phenotypic defects observed in KIKO NSCs. As evidenced by growth

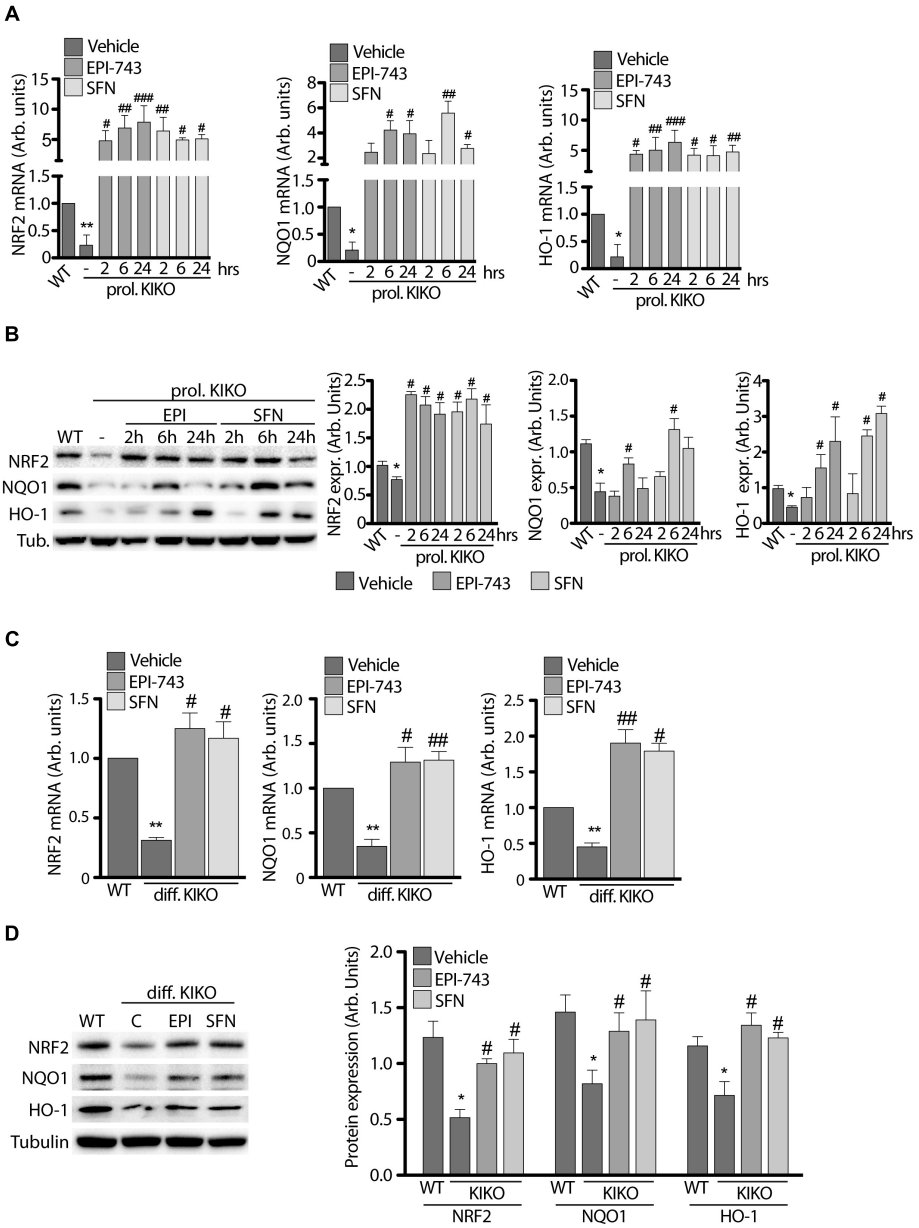

FIGURE 3 | Antioxidant treatment increases NRF2 and downstream gene expression in proliferating and differentiated NSCs. **(A)** qPCR and **(B)** Western Blot analysis with relative densitometric quantification (**B** graphs on the right) of NRF2, NQO1 and HO-1 expression in WT and KIKO NSCs cultured in proliferating conditions and treated for 2, 6, and 24 h with 1 μM EPI-743 or 5 μM SFN. qPCR analyses **(C)** and Western Blot experiments **(D)** of NRF2, NQO1, and HO-1 mRNA and protein expression levels in differentiated WT and KIKO NSCs treated or not with 1 μM EPI-743 or 5 μM SFN during the differentiation protocol. GAPDH was used for qPCR normalization, Tubulin was used as Western Blot loading control. $^{*}p < 0.05$ and $^{**}p < 0.01$ vs. WT. $^{\#}p < 0.05$, $^{\#\#}p < 0.01$, and $^{\#\#\#}p < 0.001$ vs. vehicle-treated KIKO.

curves (**Figure 4A**) and clonogenic assays (**Figure 4B**), both SFN and EPI-743 treatments trigger a positive effect on proliferation (1.7-fold increase) and stemness potential (1.4-fold increase) in KIKO NSCs culture, compared to untreated KIKO NSCs, although this rise was not enough to reach the statistical significance.

Moving from the data reported in **Figure 1C**, showing a consistent increase of spontaneous differentiation events in KIKO NSCs accompanied by a reduction of neuronal complexity, we further tested the efficacy of SFN and EPI-743 on KIKO NSCs neuronal morphology and differentiation rate (**Figure 4C**).

When chronically administrated, EPI-743 and SFN re-established a proper differentiation index in KIKO NSCs, leading to a 28 and 30% decrease of differentiating events, respectively (**Figures 4D,E**). A re-organization of neurites' network was also evidenced following treatments, with a significant increase of

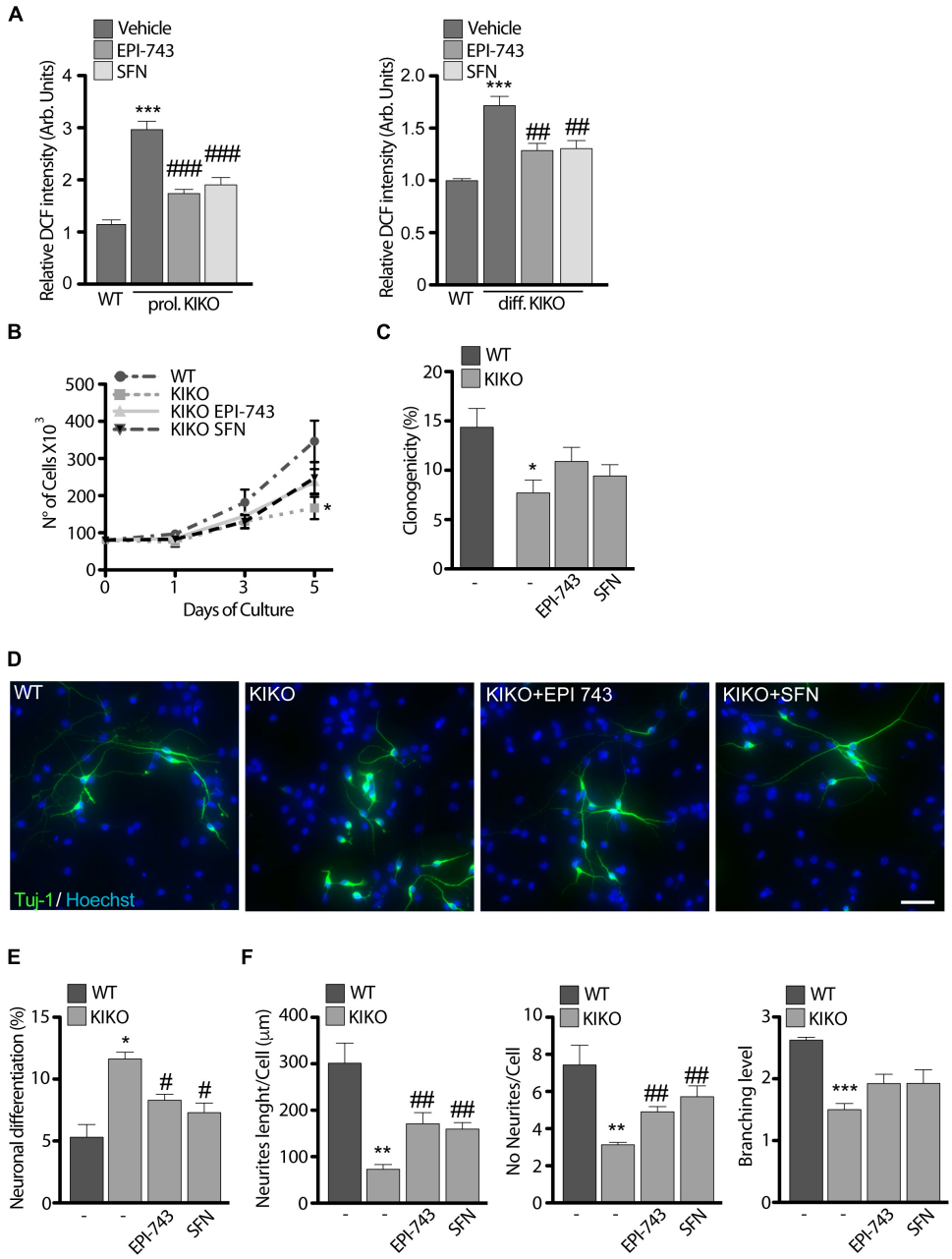

FIGURE 4 | Antioxidant treatment partially re-establishes KIKO NSCs differentiation program toward neuronal lineage. **(A)** ROS determination in WT and KIKO NSCs treated with 1 μM EPI-743 or 5 μM SFN or vehicle in proliferating condition (left graph) or after differentiation (right graph). The fluorescence produced by the oxidation of DCF was normalized for cell number. **(B)** Analysis of WT and KIKO NSCs proliferation, assessed by growth curve over 1, 3, and 5 days of culture in proliferating condition and after treatment with 1 μM EPI-743 or 5 μM SFN. **(C)** Clonogenic assay of WT and KIKO NSCs cultured in proliferating condition and treated with 1 μM EPI-743 or 5 μM SFN or vehicle. Clonogenicity was expressed as the ratio between counted neurospheres and plated cells. **(D)** Representative images of immunofluorescence assay to evaluate NSCs differentiation toward neuronal lineage (Tuj-1 positive cells) in WT and KIKO NSCs treated with vehicle, 1 μM EPI-743 or 5 μM SFN. The graph in panel **(E)** represents measurements of Tuj-1 positive cells number (mean ± SD). **(F)** Analysis of WT and KIKO neuronal complexity, assessed by evaluating average neurites' length (left), average neurites' number (center), and average branching level (right) in samples treated or not with 1 μM EPI-743 or 5 μM SFN along the differentiation protocol. *$p < 0.05$, **$p < 0.01$, and ***$p < 0.001$ vs. WT. #$p < 0.05$, ##$p < 0.01$, and ###$p < 0.001$ vs. vehicle-treated KIKO. Scale bars = 100 μm.

neurites' length (2.4-fold increase with EPI and 2.2-fold increase with SFN) and neurites' number (1.6-fold after EPI and 1.8-fold after SFN) (**Figure 4F**).

These findings show that the drug-mediated Nrf2 activation contributes to a partial recovery of the neuronal morphology and differentiation process in KIKO NSCs. Thus, also based on

the evidence of the pre-symptomatic Nrf2 impairment in KIKO mouse model, we believe that this study paves the way for Nrf2 as an early drug target for FRDA.

DISCUSSION

Although FRDA clinical symptoms manifest between the first and the second decade of life, patients are exposed to frataxin deficiency since development (Bürk, 2017), thus pre-symptomatic defects may contribute to determine the onset and the worsening of FRDA phenotype (Cossée et al., 2000; Santos et al., 2001; Georgiou-Karistianis et al., 2012; Rezende et al., 2016; Selvadurai et al., 2018). Based on this assumption, the evaluation of early pathological changes may be essential to understand the pathogenesis of the disease and to identify new targets for innovative early therapies.

In most cases, indeed, brain samples used for analysis are available from late-stage individuals, thus evidences of early pathological changes can be lost during the disease progression. In this regard, KIKO FRDA mice represent a very useful model to analyze defects in the pre-symptomatic stage of the pathology, because they display a slowly evolving phenotype such as in patients' disease progression, while biochemical and functional brain defects arise earlier (Lin et al., 2017a,b; McMackin et al., 2017; Cotticelli et al., 2019). Furthermore, unlike the lethal prenatally models in which frataxin is completely depleted and the neuron-specific knockouts showing a too severe early onset phenotype (Cossée et al., 2000; Simon et al., 2004), KIKO mice display frataxin levels close to patients' values (20–30% of control levels) (Sahdeo et al., 2014; Lazaropoulos et al., 2015), and neurological signs (i.e., cerebellar gait ataxia, decreased peripheral sensitivity, and motor strength impairment) resembling those occurring in late-onset FRDA patients (McMackin et al., 2017). These neuro-pathological symptoms arise upon the 9th month of life in the KIKO mouse (McMackin et al., 2017), while the deregulation of cerebellar synaptic circuits (Lin et al., 2017b) and mitochondrial impairments (Lin et al., 2017a) occur already at asymptomatic ages of 1st and 3rd months, respectively. Therefore, as reported for other neurodegenerative diseases (Shirendeb et al., 2012; Cai and Tammineni, 2016), we hypothesize that early dysfunctions may be responsible for the onset of FRDA and contribute to address the pathological evolution of the disease.

In light of this, we analyzed NSCs isolated from the cortex of 13.5 days embryonal life (E) of KIKO mice, in order to highlight weather defects were present already during neurogenesis. We investigated the morphological and biochemical phenotype of KIKO NSCs and their proliferative and stemness potential.

Our findings show proliferation and clonogenic defects, premature neuronal differentiation and loss of neuronal complexity in E13.5 KIKO NSCs (**Figures 1A–D**), thus suggesting that frataxin deficiency could induce defects already during neurodevelopment in FRDA and potentially lead to impairments in the white/gray matter structure and connectivity observed in patients (Georgiou-Karistianis et al., 2012; Zalesky et al., 2014; Harding et al., 2016; Rezende et al., 2016).

A tight control of NSCs proliferation, stemness potential and differentiation is critical for a proper brain development (Sun and Hevner, 2014; Taverna et al., 2014), and defects perturbing this balance can lead to the premature exhaustion of stem cells pool, determining the reduction of cortical thickness (Sun and Hevner, 2014; La Rosa et al., 2016). In line with this, two recent studies show thickness and volumetric reduction of cortical lobes in FRDA patients (Rezende et al., 2016; Selvadurai et al., 2016), thus supporting our hypothesis according to which the defects we observed in "*in vitro*" KIKO NSC could resemble the impairments that determine alterations in patients.

Neural stem cells strictly depend on low oxidative environment to maintain their stemness capability (Khacho et al., 2019), and the switch between glycolytic and oxidative metabolism determines an increase of oxidative species that drives the differentiation process (Tormos et al., 2011; Khacho et al., 2016; Zhou et al., 2016). As frataxin deficiency has been reported to enhance production of cellular free radicals in patients and in KIKO cells (Abeti et al., 2018) and Nrf2 deficiency has been described in post-natal FRDA tissues and in frataxin-silenced motor neurons (D'Oria et al., 2013; Piermarini et al., 2016; Petrillo et al., 2017), we evaluated if KIKO NSCs exhibit Nrf2 impairment during neurogenesis. Importantly, the expression of Nrf2 and two target genes (HO-1 and NQO1) is down regulated in KIKO NSCs, respect to the WT NSCs (**Figures 1E,F**), evidencing a defective antioxidant response in FRDA already at early stages of the disease.

Nrf2 is a key factor in neurogenesis regulation, and redox signaling is crucial in nervous system development (Zhao et al., 2009; Kärkkäinen et al., 2014; Olguín-Albuerne and Morán, 2018). Thus, the decrease of Nrf2 levels we detected in KIKO NSCs could be responsible for the reduction of their proliferation and stemness potential, allowing an anticipated differentiation program to take place (**Figures 1A–C**). Notably, it has been previously reported that in the neurogenic niches of the adult brain, the progressive reduction of Nrf2 expression in the stem cell pool correlated with the age-dependent decline of neural progenitors, whereas its overexpression improved NSCs proliferation and regeneration (Zhao et al., 2009; Corenblum et al., 2016). Therefore, the deregulation of Nrf2 expression, evidenced in KIKO NSCs, may underlie the loss of stemness potential and the increased cell differentiation toward the neuronal lineage. Moreover, as in frataxin-silenced neurons the Nrf2-mediated redox imbalance leads to structural impairments and axonal degeneration (Petrillo et al., 2017), we believe that the decrease of Nrf2 expression in KIKO NSCs may also be responsible for defects in the neuronal maturation and in the reduced neuronal complexity (**Figure 1D**). This reduced Nrf2 expression could contribute to explain the recent hypothesis by which the DRG of FRDA patients undergo an early neuronal hypoplasia participating to the late pathologic neuro-degenerative process (Koeppen et al., 2017).

Finally, as no effective therapies have been currently approved for FRDA and the Nrf2 activation was neuroprotective in models of Parkinson's disease and in multiple sclerosis (Benarroch, 2017), we treated KIKO NSCs with two Nrf2 inducers (SFN and EPI-743), known to be effective in frataxin-silenced

motor neurons (Piermarini et al., 2016; Petrillo et al., 2017) and in chronic neurodegenerative diseases (Martinelli et al., 2012; Sadun et al., 2012; Chicani et al., 2013; Tarozzi et al., 2013; Sun et al., 2017; Zhang et al., 2017; Hou et al., 2018; Morroni et al., 2018; Panjwani et al., 2018; Zesiewicz et al., 2018; Zhao et al., 2018).

Both SFN and EPI-743 treatments partially restore proliferation and clonogenicity of KIKO NSCs, although physiological levels were not fully reached (**Figures 4A,B**). Technical limitations in NSCs culture conditions could explain this partial result. NSCs grow as cellular aggregates and, as the growth of the sphere increases, this makes difficult for compounds reaching cells residing inside the spheres. Thus, it is possible that the drugs' effect on proliferation and clonogenic potential occurs in the first days of culture, but becomes less effective as the culture grows. Nevertheless, when SFN and EPI-743 were administrated on spread-cultured differentiating NSCs, a significant rescue of the KIKO NSCs defective phenotype was observed (**Figures 4C–E**), demonstrating that a balanced Nrf2 signaling axis is required so that a proper differentiation process takes place.

Overall, our study highlights two main findings: (1) the Nrf2 signaling pathway is impaired in the pre-clinical KIKO NSCs model; (2) the reduced expression of frataxin leads to phenotypic defects that are partially restored upon drug-driven Nrf2 induction. These findings, besides confirming pathological hallmarks in KIKO NSCs, provide evidences of up-stream neurogenesis defects occurring in FRDA.

It is also important to note that the premature exhaustion of NSCs pool during fetal neurogenesis, due to reduced proliferation and self-renewal together with the increase of neuronal differentiation, may contribute to defects in cortical thickness (La Rosa et al., 2016), thus potentially determining cerebral and cerebellar abnormalities reported in FRDA patients (Selvadurai et al., 2016, 2018). Future studies are needed to "*in vivo*" validate our findings on brain tissues obtained from post-natal KIKO mice, in order to evaluate if neurogenesis deficits may impact on clinical symptoms. This should be of paramount importance for early intervention possibly targeted to Nrf2 activation, taking advantage of highly feasible and tolerable treatments.

DATA AVAILABILITY

Data presented in the manuscript are available from the corresponding author upon request.

AUTHOR CONTRIBUTIONS

PL performed and supervised all the experiments, and analyzed the data. MR cultured the NSCs and performed the clonogenic, growth, and differentiation assays, and western blot analysis. JD'A performed the ROS quantification and Complex I activity assay. SP carried out the qRT-PCR measurements. PL and RT managed the KIKO mice and isolated the NSCs from embryos. KA, DL-B, and EB revised the manuscript. PL and FP designed the experiments, and drafted and edited the manuscript.

FUNDING

This work was supported by the Ricerca Corrente of the Italian Ministry of Health to FP, partially supported by the National Ataxia Foundation (NAF to KA), and by Friedreich's Ataxia Research Alliance (FARA to KA).

ACKNOWLEDGMENTS

The authors wish to thank Dr. Matt Klein and Dr. Jeff Trimmer of the BioElectron Technology Corporation (CA, United States) for kindly providing the EPI-743 compound used in this study.

REFERENCES

Abeti, R., Baccaro, A., Esteras, N., and Giunti, P. (2018). Novel Nrf2-inducer prevents mitochondrial defects and oxidative stress in friedreich's ataxia models. *Front. Cell. Neurosci.* 12:188. doi: 10.3389/fncel.2018.00188

Anzovino, A., Chiang, S., Brown, B. E., Hawkins, C. L., Richardson, D. R., and Huang, M. L. (2017). Molecular alterations in a mouse cardiac model of friedreich ataxia: an impaired Nrf2 response mediated via upregulation of keap1 and activation of the Gsk3β axis. *Am. J. Pathol.* 187, 2858–2875. doi: 10.1016/j.ajpath.2017.08.021

Bard, J. L., Kaufman, M. H., Dubreuil, C., Brune, R. M., Burger, A., Baldock, R. A., et al. (1998). An internet-accessible database of mouse developmental anatomy based on a systematic nomenclature. *Mech. Dev.* 74, 111–120. doi: 10.1016/S0925-477398)00069-

Benarroch, E. E. (2017). Nrf2, cellular redox regulation, and neurologic implications. *Neurology* 88, 1942–1950. doi: 10.1212/WNL.0000000000003946

Bürk, K. (2017). Friedreich ataxia: current status and future prospects. *Cerebellum Ataxias* 4:4. doi: 10.1186/s40673-017-0062-x

Cai, Q., and Tammineni, P. (2016). Mitochondrial aspects of synaptic dysfunction in Alzheimer's disease. *J. Alzheimers Dis.* 57, 1087–1103. doi: 10.3233/JAD-160726

Carletti, B., Piermarini, E., Tozzi, G., Travaglini, L., Torraco, A., Pastore, A., et al. (2014). Frataxin silencing inactivates mitochondrial complex I in NSC34 motoneuronal cells and alters glutathione homeostasis. *Int. J. Mol. Sci.* 15, 5789–5806. doi: 10.3390/ijms15045789

Chicani, C. F., Chu, E. R., Miller, G., Kelman, S. E., and Sadun, A. A. (2013). Comparing EPI-743 treatment in siblings with Leber's hereditary optic neuropathy mt14484 mutation. *Can. J. Ophthalmol.* 48, e130–e133. doi: 10.1016/j.jcjo.2013.05.011

Conti, L., Cattaneo, E., and Papadimou, E. (2003). Novel neural stem cell systems. *Expert Opin. Biol. Ther.* 8, 153–160. doi: 10.1517/14712598.8.2.153

Corben, L. A., Delatycki, M. B., Bradshaw, J. L., Churchyard, A. J., and Georgiou-Karistianis, N. (2011). Utilization of advance motor information is impaired in Friedreich ataxia. *Cerebellum* 10, 793–803. doi: 10.1007/s12311-011-0289-287

Corben, L. A., Klopper, F., Stagnitti, M., Georgiou-Karistianis, N., Bradshaw, J. L., Rance, G., et al. (2017). Measuring inhibition and cognitive flexibility in Friedreich ataxia. *Cerebellum* 16, 757–763. doi: 10.1007/s12311-017-0848-847

Corenblum, M. J., Ray, S., Remley, Q. W., Long, M., Harder, B., Zhang, D. D., et al. (2016). Reduced Nrf2 expression mediates the decline in neural stem cell function during a critical middle-age period. *Aging Cell* 15, 725–736. doi: 10.1111/acel.12482

Cossée, M., Puccio, H., Gansmuller, A., Koutnikova, H., Dierich, A., LeMeur, M., et al. (2000). Inactivation of the Friedreich ataxia mouse gene leads to early embryonic lethality without iron accumulation. *Hum. Mol. Genet.* 9, 1219–1226. doi: 10.1093/hmg/9.8.1219

Cotticelli, M. G., Xia, S., Lin, D., Lee, T., Terrab, L., Wipf, P., et al. (2019). Ferroptosis as a novel therapeutic target for Friedreich's ataxia. *J. Pharmacol. Exp. Ther.* 118:252759. doi: 10.1124/jpet.118.252759

De Nobrega, E., Nieto, A., Barroso, J., and Montón, F. (2007). Differential impairment in semantic, phonemic, and action fluency performance in Friedreich's ataxia: possible evidence of prefrontal dysfunction. *J. Int. Neuropsychol. Soc.* 13, 944–952. doi: 10.1017/S1355617707071202

Dinkova-Kostova, A. T., Kostov, R. V., and Kazantsev, A. G. (2018). The role of Nrf2 signaling in counteracting neurodegenerative diseases. *FEBS J.* 285, 3576–3590. doi: 10.1111/febs.14379

D'Oria, V., Petrini, S., Travaglini, L., Priori, C., Piermarini, E., Petrillo, S., et al. (2013). Frataxin deficiency leads to reduced expression and impaired translocation of NF-E2-related factor (Nrf2) in cultured motor neurons. *Int. J. Mol. Sci.* 14, 7853–7865. doi: 10.3390/ijms14047853

Dürr, A., Cossee, M., Agid, Y., Campuzano, V., Mignard, C., Penet, C., et al. (1996). Clinical and genetic abnormalities in patients with Friedreich's ataxia. *N. Engl. J. Med.* 335, 1169–1175. doi: 10.1056/nejm199610173351601

Enns, G. M., Kinsman, S. L., Perlman, S. L., Spicer, K. M., Abdenur, J. E., Cohen, B. H., et al. (2012). Initial experience in the treatment of inherited mitochondrial disease with EPI-743. *Mol. Genet. Metab.* 105, 91–102. doi: 10.1016/j.ymgme.2011.10.009

Folker, J., Murdoch, B., Cahill, L., Delatycki, M., Corben, L., Vogel, A., et al. (2010). Dysarthria in Friedreich's ataxia: a perceptual analysis. *Folia Phoniatr. Logop.* 62, 97–103. doi: 10.1159/000287207

Galli, R., Gritti, A., Bonfanti, L., and Vescovi, A. L. (2003). Neural stem cells: an overview. *Circ. Res.* 92, 598–608. doi: 10.1161/01.RES.0000065580.02404.F4

Georgiou-Karistianis, N., Akhlaghi, H., Corben, L. A., Delatycki, M. B., Storey, E., Bradshaw, J. L., et al. (2012). Decreased functional brain activation in Friedreich ataxia using the simon effect task. *Brain Cogn.* 79, 200–208. doi: 10.1016/j.bandc.2012.02.011

Harding, I. H., Corben, L. A., Storey, E., Egan, G. F., Stagnitti, M. R., Poudel, G. R., et al. (2016). Fronto-cerebellar dysfunction and dysconnectivity underlying cognitive functioning in Friedreich ataxia: the IMAGE-FRDA study. *Hum. Brain Mapp.* 37, 338–350. doi: 10.1002/hbm.23034

Hou, T. T., Yang, H. Y., Wang, W., Wu, Q. Q., Tian, Y. R., and Jia, J. P. (2018). Sulforaphane inhibits the generation of amyloid-β oligomer and promotes spatial learning and memory in Alzheimer's disease (PS1V97L) transgenic mice. *J. Alzheimers Dis.* 62, 1803–1813. doi: 10.3233/JAD-171110

Kärkkäinen, V., Pomeshchik, Y., Savchenko, E., Dhungana, H., Kurronen, A., Lehtonen, S., et al. (2014). Nrf2 regulates neurogenesis and protects neural progenitor cells against Aβ toxicity. *Stem Cells* 32, 1904–1916. doi: 10.1002/stem.1666

Khacho, M., Clark, A., Svoboda, D. S., Azzi, J., MacLaurin, J. G., Meghaizel, C., et al. (2016). Mitochondrial dynamics impacts stem cell identity and fate decisions by regulating a nuclear transcriptional program. *Cell Stem* 19, 232–247. doi: 10.1016/j.stem.2016.04.015

Khacho, M., Harris, R., and Slack, R. S. (2019). Mitochondria as central regulators of neural stem cell fate and cognitive function. *Nat. Rev. Neurosci.* 20, 34–48. doi: 10.1038/s41583-018-0091-93

Koeppen, A. H., Becker, A. B., Qian, J., and Feustel, P. J. (2017). Friedreich ataxia: hypoplasia of spinal cord and dorsal root ganglia. *J. Neuropathol. Exp. Neurol.* 76, 101–108. doi: 10.1093/jnen/nlw111

La Rosa, P., Bielli, P., Compagnucci, C., Cesari, E., Volpe, E., Farioli Vecchioli, S., et al. (2016). Sam68 promotes self-renewal and glycolytic metabolism in mouse neural progenitor cells by modulating Aldh1a3 pre-mRNA 3'-end processing. *eLife* 5:e20750. doi: 10.7554/eLife.20750

Lazaropoulos, M., Dong, Y., Clark, E., Greeley, N. R., Seyer, L. A., Brigatti, K. W., et al. (2015). Frataxin levels in peripheral tissue in Friedreich ataxia. *Ann. Clin. Transl. Neurol.* 2, 831–842. doi: 10.1002/acn3.225

Lin, H., Magrane, J., Clark, E. M., Halawani, S. M., Warren, N., Rattelle, A., et al. (2017a). Early VGLUT1-specific parallel fiber synaptic deficits, and dysregulated cerebellar circuit in the KIKO mouse model of Friedreich ataxia. *Dis. Model Mech.* 10, 1529–1538. doi: 10.1242/dmm.030049

Lin, H., Magrane, J., Rattelle, A., Stepanova, A., Galkin, A., Clark, E. M., et al. (2017b). Early cerebellar deficits in mitochondrial biogenesis, and respiratory chain complexes in the KIKO mouse model of Friedreich ataxia. *Dis. Model Mech.* 10, 1343–1352. doi: 10.1242/dmm.030502

Lupoli, F., Vannocci, T., Longo, G., Niccolai, N., and Pastore, A. (2018). The role of oxidative stress in Friedreich's ataxia. *FEBS Lett.* 592, 718–727. doi: 10.1002/1873-3468.12928

Mantovan, M. C., Martinuzzi, A., Squarzanti, F., Bolla, A., Silvestri, I., Liessi, G., et al. (2006). Exploring mental status in Friedreich's ataxia: a combined neuropsychological, behavioral and neuroimaging study. *Eur. J. Neurol.* 13, 827–835. doi: 10.1111/j.1468-1331.2006.01363.x

Martinelli, D., Catteruccia, M., Piemonte, F., Pastore, A., Tozzi, G., Dionisi-Vici, C., et al. (2012). EPI-743 reverses the progression of the pediatric mitochondrial disease genetically defined leigh syndrome. *Mol. Genet. Metab.* 107, 383–388. doi: 10.1016/j.ymgme.2012.09.007

McMackin, M. Z., Henderson, C. K., and Cortopassi, G. A. (2017). Neurobehavioral deficits in the KIKO mouse model of Friedreich's ataxia. *Behav. Brain Res.* 316, 183–188. doi: 10.1016/j.bbr.2016.08.053

Miranda, C. J., Santos, M. M., Ohshima, K., Smith, J., Li, L., Bunting, M., et al. (2002). Frataxin knockin mouse. *FEBS Lett.* 512, 291–297. doi: 10.1016/s0014-5793(02)02251-2

Morroni, F., Sita, G., Djemil, A., D'Amico, M., Pruccoli, L., Cantelli-Forti, G., et al. (2018). Comparison of adaptive neuroprotective mechanisms of sulforaphane and its interconversion product erucin in in vitro and in vivo models of parkinson's disease. *J. Agric. Food Chem.* 66, 856–865. doi: 10.1021/acs.jafc.7b04641

Nieto, A., Correia, R., De Nobrega, E., Montón, F., and Barroso, J. (2013). Cognition in late onset Friedreich ataxia. *Cerebellum* 12, 504–512. doi: 10.1007/s12311-013-0457-z

Olguín-Albuerne, M., and Morán, J. (2018). Redox signaling mechanisms in nervous system development. *Antioxid. Redox Signal.* 28, 1603–1625. doi: 10.1089/ars.2017.7284

Panjwani, A. A., Liu, H., and Fahey, J. W. (2018). Crucifers and related vegetables and supplements for neurologic disorders: what is the evidence? *Curr. Opin. Clin. Nutr. Metab. Care* 21, 451–457. doi: 10.1097/MCO.0000000000000511

Paupe, V., Dassa, E. P., Goncalves, S., Auchère, F., Lönn, M., and Holmgren, A. (2009). Impaired nuclear Nrf2 translocation undermines the oxidative stress response in Friedreich ataxia. *PLoS One* 4:e4253. doi: 10.1371/journal.pone.0004253

Petrillo, S., Piermarini, E., Pastore, A., Vasco, G., Schirinzi, T., Carrozzo, R., et al. (2017). Nrf2 inducers counteract neurodegeneration in frataxin-silenced motor neurons: disclosing new therapeutic targets for friedreich's ataxia. *Int. J. Mol. Sci.* 18:E2173. doi: 10.3390/ijms18102173

Piermarini, E., Cartelli, D., Pastore, A., Tozzi, G., Compagnucci, C., Giorda, E., et al. (2016). Frataxin silencing alters microtubule stability in motor neurons: implications for Friedreich's ataxia. *Hum. Mol. Genet.* 25, 4288–4301. doi: 10.1093/hmg/ddw260

Ray, S., Corenblum, M., Anandhan, A., Reed, A., Zhang, D. D., Barnes, C. A., et al. (2018). A role for Nrf2 expression in defining the aging of hippocampal neural stem cells. *Cell Transplant.* 27, 589–606. doi: 10.1177/0963689718774030

Rezende, T. J. R., Silva, C. B., Yassuda, C. L., Campos, B. M., D'Abreu, A., Cendes, F., et al. (2016). Longitudinal magnetic resonance imaging study shows progressive pyramidal and callosal damage in Friedreich's ataxia. *Mov. Disord.* 31, 70–78. doi: 10.1002/mds.26436

Romeo, G., Menozzi, P., Ferlini, A., Fadda, S., Di Donato, S., Uziel, G., et al. (1983). Incidence of Friedreich ataxia in Italy estimated from consanguineous marriages. *Am. J. Hum. Genet.* 35, 523–529.

Sadun, A. A., Chicani, C. F., Ross-Cisneros, F. N., Barboni, P., Thoolen, M., Shrader, W. D., et al. (2012). Effect of EPI-743 on the clinical course of the mitochondrial disease leber hereditary optic neuropathy. *Arch. Neurol.* 69, 331–338. doi: 10.1001/archneurol.2011.2972

Sahdeo, S., Scott, B. D., McMackin, M. Z., Jasoliya, M., Brown, B., Wulff, H., et al. (2014). Dyclonine rescues frataxin deficiency in animal models and buccal cells of patients with Friedreich's ataxia. *Hum. Mol. Genet.* 23, 6848–6862. doi: 10.1093/hmg/ddu408

Santos, M. M., Ohshima, K., and Pandolfo, M. (2001). Frataxin deficiency enhances apoptosis in cells differentiating into neuroectoderm. *Hum. Mol. Genet.* 10, 1935–1944. doi: 10.1093/hmg/10.18.1935

Santos, R., Lefevre, S., Sliwa, D., Seguin, A., Camadro, J. M., and Lesuisse, E. (2010). Friedreich ataxia: molecular mechanisms, redox considerations, and therapeutic opportunities. *Antioxid. Redox Signal.* 13, 651–690. doi: 10.1089/ars.2009.3015

Selvadurai, L. P., Harding, I. H., Corben, L. A., and Georgiou-Karistianis, N. (2018). Cerebral abnormalities in Friedreich ataxia: a review. *Neurosci. Biobehav. Rev.* 84, 394–406. doi: 10.1016/j.neubiorev.2017.08.006

Selvadurai, L. P., Harding, I. H., Corben, L. A., Stagnitti, M. R., Storey, E., Egan, G. F., et al. (2016). Cerebral and cerebellar grey matter atrophy in Friedreich ataxia: the IMAGE-FRDA study. *J. Neurol.* 263, 2215–2223. doi: 10.1007/s00415-016-8252-7

Shan, Y., Schoenfeld, R. A., Hayashi, G., Napoli, E., Akiyama, T., Iodi Carstens, M., et al. (2013). Frataxin deficiency leads to defects in expression of antioxidants and Nrf2 expression in dorsal root ganglia of the Friedreich's ataxia YG8R mouse model. *Antioxid. Redox Signal.* 19, 1481–1493. doi: 10.1089/ars.2012.4537

Shirendeb, U. P., Calkins, M. J., Manczak, M., Anekonda, V., Dufour, B., McBride, J. L., et al. (2012). Mutant huntingtin's interaction with mitochondrial protein Drp1 impairs mitochondrial biogenesis and causes defective axonal transport and synaptic degeneration in huntington's disease. *Hum. Mol. Genet.* 21, 406–420. doi: 10.1093/hmg/ddr475

Simon, D., Seznec, H., Gansmuller, A., Carelle, N., Weber, P., Metzger, D., et al. (2004). Friedreich ataxia mouse models with progressive cerebellar and sensory ataxia reveal autophagic neurodegeneration in dorsal root ganglia. *J. Neurosci.* 24, 1987–1995. doi: 10.1523/jneurosci.4549-03.2004

Sun, T., and Hevner, R. F. (2014). Growth and folding of the mammalian cerebral cortex: from molecules to malformations. *Nat. Rev. Neurosci.* 15, 217–232. doi: 10.1038/nrn3707

Sun, Y., Yang, T., Mao, L., and Zhang, F. (2017). Sulforaphane protects against brain diseases: roles of cytoprotective enzymes. *Austin. J. Cerebrovasc. Dis. Stroke* 4:1054. doi: 10.26420/austinjcerebrovascdisstroke

Svetoni, F., De Paola, E., La Rosa, P., Mercatelli, N., Caporossi, D., Sette, C., et al. (2017). Post-transcriptional regulation of FUS and EWS protein expression by miR-141 during neural differentiation. *Hum. Mol. Genet.* 26, 2732–2746. doi: 10.1093/hmg/ddx160

Tarozzi, A., Angeloni, C., Malaguti, M., Morroni, F., Hrelia, S., and Hrelia, P. (2013). Sulforaphane as a potential protective phytochemical against neurodegenerative diseases. *Oxid. Med. Cell Longev.* 2013:415078. doi: 10.1155/2013/415078

Taverna, E., Gotz, M., and Huttner, W. B. (2014). The cell biology of neurogenesis: toward an understanding of the development and evolution of the neocortex. *Annu. Rev. Cell Dev. Biol.* 30, 465–502. doi: 10.1146/annurev-cellbio-101011-155801

Tormos, K. V., Anso, E., Hamanaka, R. B., Eisenbart, J., Joseph, J., Kalyanaraman, B., et al. (2011). Mitochondrial complex III ROS regulate adipocyte differentiation. *Cell Metab.* 14, 537–544. doi: 10.1016/j.cmet.2011.08.007

Vaubel, R. A., and Isaya, G. (2013). Iron-sulfur cluster synthesis, iron homeostasis and oxidative stress in Friedreich ataxia. *Mol. Cell. Neurosci.* 55, 50–61. doi: 10.1016/j.mcn.2012.08.003

Weidemann, F., Rummey, C., Bijnens, B., Störk, S., Jasaityte, R., Dhooge, J., et al. (2012). The heart in Friedreich ataxia: definition of cardiomyopathy, disease severity, and correlation with neurological symptoms. *Circulation* 125, 1626–1634. doi: 10.1161/circulationha111.059477

Wollmann, T., Barroso, J., Monton, F., and Nieto, A. (2002). Neuropsychological test performance of patients with Friedreich's ataxia. *J. Clin. Exp. Neuropsychol.* 24, 677–686. doi: 10.1076/jcen.24.5.677.1014

Zalesky, A., Akhlaghi, H., Corben, L. A., Bradshaw, J. L., Delatycki, M. B., Storey, E., et al. (2014). Cerebello-cerebral connectivity deficits in Friedreich ataxia. *Brain Struct. Funct.* 219, 969–981. doi: 10.1007/s00429-013-0547-541

Zesiewicz, T., Salemi, J. L., Perlman, S., Sullivan, K. L., Shaw, J. D., Huang, Y., et al. (2018). Double-blind, randomized and controlled trial of EPI-743 in Friedreich's ataxia. *Neurodegener. Dis. Manag.* 8, 233–242. doi: 10.2217/nmt-2018-0013

Zhang, J. C., Yao, W., Dong, C., Yang, C., Ren, Q., Ma, M., et al. (2017). Prophylactic effects of sulforaphane on depression-like behavior and dendritic changes in mice after inflammation. *J. Nutr. Biochem.* 39, 134–144. doi: 10.1016/j.jnutbio.2016.10.004

Zhao, F., Wu, T., Lau, A., Jiang, T., Huang, Z., Wang, X. J., et al. (2009). Nrf2 promotes neuronal cell differentiation. *Free Radic. Biol. Med.* 47, 867–879. doi: 10.1016/j.freeradbiomed.2009.06.029

Zhao, F., Zhang, J., and Chang, N. (2018). Epigenetic modification of Nrf2 by sulforaphane increases the antioxidative and anti-inflammatory capacity in a cellular model of Alzheimer's disease. *Eur. J. Pharmacol.* 824, 1–10. doi: 10.1016/j.ejphar.2018.01.046

Zhou, G., Meng, S., Li, Y., Ghebre, Y. T., and Cooke, J. P. (2016). Optimal ROS signaling is critical for nuclear reprogramming. *Cell Rep.* 15, 919–925. doi: 10.1016/j.celrep.2016.03.084

Conflict of Interest Statement: The authors declare that the research was conducted in the absence of any commercial or financial relationships that could be construed as a potential conflict of interest.

frontiers in Cellular Neuroscience

ORIGINAL RESEARCH
published: 13 September 2019
doi: 10.3389/fncel.2019.00414

Fractalkine Modulates Microglia Metabolism in Brain Ischemia

Clotilde Lauro[1], Giuseppina Chece[1], Lucia Monaco[1], Fabrizio Antonangeli[2], Giovanna Peruzzi[3], Serena Rinaldo[4], Alessio Paone[4], Francesca Cutruzzolà[4] and Cristina Limatola[5,6]*

[1] Department of Physiology and Pharmacology, Sapienza University of Rome, Rome, Italy, [2] Department of Molecular Medicine, Laboratory Affiliated to Istituto Pasteur Italia – Fondazione Cenci Bolognetti, Sapienza University of Rome, Rome, Italy, [3] Center for Life Nano Science@Sapienza, Istituto Italiano di Tecnologia, Rome, Italy, [4] Department of Biochemical Sciences "A. Rossi Fanelli", Sapienza University of Rome, Rome, Italy, [5] Department of Physiology and Pharmacology, Laboratory Affiliated to Istituto Pasteur Italia – Fondazione Cenci Bolognetti, Sapienza University of Rome, Rome, Italy, [6] IRCCS NeuroMed, Pozzilli, Italy

In the CNS, the chemokine CX3CL1 (fractalkine) is expressed on neurons while its specific receptor CX3CR1 is expressed on microglia and macrophages. Microglia play an important role in health and disease through CX3CL1/CX3CR1 signaling, and in many neurodegenerative disorders, microglia dysregulation has been associated with neuroinflammation. We have previously shown that CX3CL1 has neuroprotective effects against cerebral ischemia injury. Here, we investigated the involvement of CX3CL1 in the modulation of microglia phenotype and the underlying neuroprotective effect on ischemia injury. The expression profiles of anti- and pro-inflammatory genes showed that CX3CL1 markedly inhibited microglial activation both *in vitro* and *in vivo* after permanent middle cerebral artery occlusion (pMCAO), accompanied by an increase in the expression of anti-inflammatory genes. Moreover, CX3CL1 induces a metabolic switch in microglial cells with an increase in the expression of genes related to the oxidative pathway and a reduction in those related to the glycolytic pathway, which is the metabolic state associated to the pro-inflammatory phenotype for energy production. The data reported in this paper suggest that CX3CL1 protects against cerebral ischemia modulating the activation state of microglia and its metabolism in order to restrain inflammation and organize a neuroprotective response against the ischemic insult.

Keywords: CX3CL1, microglia, ischemia, neuroprotection, neuroinflammation

OPEN ACCESS

Edited by:
Sandra Henriques Vaz, University of Lisbon, Portugal

Reviewed by:
Renato Socodato, Institute for Molecular and Cellular Biology (IBMC), France
Paula Korhonen, QIMR Berghofer Medical Research Institute, Australia

****Correspondence:***
Clotilde Lauro
clotilde.lauro@uniroma1.it

Specialty section:
This article was submitted to Non-Neuronal Cells, a section of the journal Frontiers in Cellular Neuroscience

Received: *31 January 2019*
Accepted: *27 August 2019*
Published: *13 September 2019*

Citation:
Lauro C, Chece G, Monaco L, Antonangeli F, Peruzzi G, Rinaldo S, Paone A, Cutruzzolà F and Limatola C (2019) Fractalkine Modulates Microglia Metabolism in Brain Ischemia. Front. Cell. Neurosci. 13:414. doi: 10.3389/fncel.2019.00414

INTRODUCTION

CX3CL1 and CX3CR1 in CNS

The chemokine CX3CL1, also known as fractalkine, and its receptor CX3CR1 are expressed by immune and non-immune cells throughout organisms and their expression is cell type-unique in each tissue. In the brain, CX3CL1 is mostly expressed by neurons (Harrison et al., 1998) and its expression is reported on astrocytes upon inflammatory stimulations (Yoshida et al., 2001; Guillemin et al., 2003) while CX3CR1 is expressed on parenchymal microglia (Harrison et al., 1998) and in perivascular, subdural meningeal and choroid plexus macrophages, which, together with microglia, are critical regulators of immune responses in CNS upon neuroinflammation (Jung et al., 2000; Prinz et al., 2011; Goldmann et al., 2013, 2016; Yona et al., 2013). CX3CR1 signaling involves

phospholipase C (PLC), phosphatidylinositol 3-kinases (PI3K) and extracellular signal–regulated kinases (ERKs), and the recruitment of transcription factors such as nuclear factor kappa-light-chain-enhancer of activated B cells (NF-κB) and cyclic adenosine monophosphate response element binding protein (CREB) (Sheridan and Murphy, 2013).

Metabolic Reprograming in the Regulation of the Innate Inflammatory Response

Microglia, under physiological conditions, continuously monitor the surrounding parenchyma by extending and retracting cellular processes to detect alteration of brain homeostasis (Davalos et al., 2005; Nimmerjahn et al., 2005) such as those induced by inflammatory stimuli. Increasing evidence suggest a role of metabolic reprograming in the modulation of the innate inflammatory response (Orihuela et al., 2016). For instance, it is known that polarization toward a pro-inflammatory phenotype induces peripheral macrophages to change from the oxidative phosphorylation to anaerobic glycolysis, so as to increase adenosine triphosphate (ATP) production (Kelly and O'Neill, 2015). Modification of metabolic functions from the ability to promote cell proliferation like anti-inflammatory phenotype to a killing/inhibitory capacity in the pro-inflammatory state, allows macrophages to respond with proper functions in different context (Mills et al., 2000; Rodríguez-Prados et al., 2010; Odegaard and Chawla, 2011; Biswas and Mantovani, 2012). A similar metabolic switch has been well characterized in tumor cells: it is known as the Warburg effect (Warburg, 1956) and permits tumor cells to maintain their increased energy demand (Griffin and Shockcor, 2004). Also microglial cells are capable of an adaptable use of energy substrates: similar to macrophages, when stimulated, they switch among oxidative phosphorylation and glycolytic metabolism. In particular, microglial activation with lipopolysaccharide (LPS) augmented lactate production, diminished mitochondrial oxygen consumption and mitochondrial ATP production, resulting in the increase of glycolysis and the decrease of oxidative phosphorylation (Volobouéva et al., 2013). Moreover, primary rat microglia cultured with increasing glucose concentration (from 10 mM to 50 mM) boosted tumor necrosis factor α (TNFα) secretion (Quan et al., 2011; Zhang et al., 2015). On the other hand, IL-4-stimulated BV-2 cells decreased glucose consumption and lactate production (Gimeno-Bayón et al., 2014) and primary murine microglia stimulated with IL-4/IL-13 maintained an oxidative metabolic state (Orihuela et al., 2016) suggesting that this shift was associated with a reduced need for anabolic reactions. Since neuro-inflammation caused by microglia hyperactivity has been associated with several neurodegenerative diseases (Cartier et al., 2014) and many evidence exist of a metabolic reprograming of microglia in neurodegeneration (Ulland et al., 2017), a metabolic switch toward oxidative metabolism might contribute to afford the healthful role of microglia in some pathophysiological conditions, resulting in the production of metabolites which are beneficial for neurons.

Neuroprotective Activity of CX3CL1 During Ischemia

It was reported that CX3CL1/CX3CR1 signaling in microglia plays important roles in physiological and pathological conditions (Lauro et al., 2015). Many evidence suggest that CX3CL1 has dual activities in the CNS, with either beneficial or detrimental potentials, depending on the activation state of microglia (Lauro et al., 2015). Furthermore, the administration of exogenous CX3CL1 reduces ischemic damage *in vivo* (Cipriani et al., 2011). Ischemia is the second leading cause of death in human and can lead to permanent disability (Johnson et al., 2016). It occurs when cerebral artery blood flow is reduced by a thrombus or atherosclerotic plaque, causing an abrupt deprivation of oxygen and nutrients into the brain. Currently the treatment for cerebral ischemia is reperfusion by thrombolytic administration or surgery, in order to reduce the volume of acute ischemia and improve the clinical outcome. However, only 10–20% of stroke patients receive a prompt therapy because the time window to restore blood flow to a cerebral artery is approximately 4 h from first symptoms and the risk of cerebral hemorrhage is high after this time (Chaudhary et al., 2017). Animal models of cerebral ischemia describe a well-established timing of inflammatory events after brain injury: in particular, it was demonstrated that microglia phenotype changes from anti- to pro-inflammatory with the progression of cerebral ischemia (Fumagalli et al., 2015; Ma et al., 2017). Initially, few minutes after the onset of ischemia, resident microglial cells acquire an anti-inflammatory phenotype, mainly in the peri-infarct region, to constrain brain damage. At 6 days upon ischemic insults, pro-inflammatory microglia predominate in the region close to the infarct zone (Schroeter et al., 1997; Perego et al., 2011). This microglia release reactive oxygen species and pro-inflammatory cytokines that prompt the activation of cerebrovascular endothelial cells and support the adhesion and transmigration of leukocytes into the injured tissue, contributing to the spread of brain damage (Kriz, 2006; Ceulemans et al., 2010; Jin et al., 2010; Grønberg et al., 2013). The inflammatory infiltrate induces anoxic depolarization, perturbs glutamatergic neurotransmission and increases the levels of intracellular calcium, causing the formation of reactive oxygen species and neuronal death (Ceulemans et al., 2010). However, inflammatory cells might also have a protective effects: resident microglia/macrophages achieve phagocytosis and produce neurotropic factors such as neurotrophins and tumor growth factor β1 (TGF β1), both involved in neuroprotection and tissue repair (Jin et al., 2010). Animal models of cerebral ischemia demonstrate that increased pro-inflammatory polarization of microglia is associated with a larger infarct area whereas anti-inflammatory microglia resolve inflammation, limit stroke injury progression and promote tissue reparation (Iadecola and Anrather, 2011). This experimental evidence suggests that a targeted modulation of microglia could be used to reduce the extent of tissue damage. Our previous study showed that CX3CL1 has neuroprotective effect against cerebral ischemia. Here, we investigated the involvement of CX3CL1 in microglia phenotype and metabolic switch toward oxidative metabolism

and the underlying neuroprotective effect toward ischemia injury. The expression profiles of anti- and pro-inflammatory genes and those related to the metabolic reprograming following the inflammatory response were detected *in vitro* after CX3CL1 stimulation of microglial primary cultures and *in vivo* after permanent middle cerebral artery occlusion (pMCAO) in mice, in the presence of CX3CL1, to confirm the *in vitro* data and also to verify a possible role of CX3CL1 in modulating microglia polarization state upon ischemia development. In this paper we demonstrated that CX3CL1 inhibits microglial pro-inflammatory phenotype and induces an increase in the expression of anti-inflammatory genes. Moreover, it induces a metabolic switch with an increased expression of genes related to the oxidative pathway and a reduction in those related to glycolytic one, which is the metabolic state associated to the pro-inflammatory phenotype for energy production, suggesting that CX3CL1 protects against cerebral ischemia injury modulating the activation state of microglia and its metabolism in order to restrain inflammation and activate a neuroprotective response against the ischemic insult.

MATERIALS AND METHODS

Materials

Recombinant human CX3CL1 (cat#300-31) was from Peprotech; IL-4 (cat#12340045) was from Immunotools; LPS (cat#L4391) was from Sigma-Aldrich; anti-Arg1 antibody was from Santa Cruz (cat#sc-271430 RRID:AB_10648473); anti-Actin antibody (cat#A2066) was from Sigma-Aldrich. Secondary antibodies were from DAKO; Microbeads CD11b+ were from Miltenyi Biotec. All cell culture media, fetal bovine serum (FBS), goat serum, penicillin G, streptomycin, glutamine and Hoechst (cat#33342, RRID:AB_10626776) were from Invitrogen; poly-L-lysine (cat#P2636) and papain were from Sigma-Aldrich. Griess reagent kit for Nitrite determination was from Molecular Probe (cat#G-7921), Lactate Assay Kit (cat#MAK064) and Arginase Activity Assay Kit (cat#MAK112) were from Sigma-Aldrich; Seahorse Cell Mito Stress Test Kit for Seahorse XFe Analyzer Respiratory Assay reagents were from Agilent (cat#103015-100).

Animals and Cell Cultures

The experiments described in the present work, were approved by the Italian Ministry of Health in accordance with the guidelines on the ethical use of animals from the European Community Council Directive of September 22, 2010 (2010/63/EU). Wild type mice C57BL/6J (cat# JAX: 000664, RRID:IMSR_JAX:000664) were from Jackson Laboratory.

Microglia Culture and Polarization

Microglial cells were obtained from mixed glia cultures derived from the cerebral cortices of post-natal day 0–2 (p0–p2) *wt* mice. Cortices were chopped and digested in 15 U/ml papain for 20 min at 37°C. Cell suspensions were plated (5×10^5 cells/cm^2) on poly-L-lysine (0.1 mg/ml) coated flasks in growth medium supplemented with 10% FBS. After 9–11 days, cultures were shaken for 2 h at 37°C to detach and collect microglia cells. These procedures gave almost pure microglial cell populations as previously described (Lauro et al., 2010). For microglia polarization, cells were seeded on poly-L-lysine coated 12 well plates (40×10^4 cells), 24-well plate (20×10^4 cells) or 12 mm glass (80×10^3 cells) slides and 2 days after they were treated with LPS 100 ng/ml or IL-4 20 ng/ml for 24 h and with CX3CL1 100 nM for further 24 h.

Form Factor Calculation

Microglia were seeded on 12 mm glass coverslips (80×10^3 cells), treated as reported, fixed, permeabilized, blocked and stained with Alexa-Fluor 488 Phalloidin (Invitrogen) for 20 min together with Hoechst. For the form factor calculation we used 3 different primary microglial culture preparations, 2 glass coverslips for each different conditions and we counted 20 cells for each glass coverslips randomly selected. Fluorescent images were processed using the MetaMorph 7.6.5.0 software (Molecular Device, Sunnyvale, CA, United States), and form factor was calculated according the formula: 4π area/perimeter^2 (Neubrand et al., 2014). Form factor is a parameter taken as 1 for round cells, and correspondingly <1 when the morphology deviates from the spherical shape.

Permanent Middle Cerebral Artery Occlusion (pMCAO)

Mice (25–28 g, 11–12 weeks) were anesthetized with chloral hydrate (400 mg/kg, i.p.). The right middle cerebral artery (MCA) was permanently occluded by electrocoagulation as described previously (Storini et al., 2006). Mice were maintained at 37°C during surgery and sacrificed 24 or 72 h after pMCAO: they were deeply anesthetized and intracardially perfused with ice cold PBS.

Drugs and Administration Protocols

CX3CL1 was dissolved in saline and intra-cerebro-ventricular injected 20 min before pMCAO at 70 pmol/2 μl in mice similar to what was used previously (Cipriani et al., 2011). Anesthetized animals were immobilized on a stereotaxic apparatus (David Kopf Instruments) and injected in the right cerebral ventricle [1 mm lateral and 3 mm deep, according to the atlas of Paxinos and Watson (1998)]. A constant rate of infusion (0.2 μl/min) was maintained with a pump (KD Scientific). Control-operated animals received only vehicles.

Isolation of CD11b$^+$ Cells

Mice 24 and 72 h after ischemia were deeply anesthetized and intracardially perfused with ice cold PBS. Brains were removed, each hemisphere was cut into small pieces and disrupted in a glass-teflon homogenizer. Cell suspension was first applied to a 30-μm cell strainer and then labeled with CD11b$^+$ Microbeads, loaded onto a MACS Column (Miltenyi Biotec) and placed in the magnetic field of a MACS Separator. After removing the magnetic field, CD11b$^+$ cells were eluted and used for RNA extraction. With this procedure we usually obtain around 80-50×10^3 cells from one hemisphere, the viability is about 70% and the purity 99%.

Isolation of Microglia Cells by Fluorescence-Activated Cell Sorting (FACS)

Cell suspensions were obtained as above and passed through a 100 μm nylon cell strainer (Becton Dickinson). The suspension was centrifuged (800 *g*, 10 min, RT), the pellet resuspended in 4 ml of 30% Percoll (Sigma) and overlaid on the top of HBSS. The suspension was centrifuged (14000 *g*, 15 min, RT), the pellet was resuspended in 2% BSA in PBS without Ca^{2+} Mg^{2+}. Single cell suspension was washed in staining buffer (PBS without Ca^{2+} Mg^{2+}, 0.5% BSA, 2 mM EDTA, 0.025% NaN_3). Anti-CD16/32 (clone 24G2) was added (10 min) to prevent non-specific and Fc-mediated binding. Then, cells were stained with the following indicated antibodies for 20 min at 4°C. Directly conjugated mAbs for the following antigens (clone name) were used: CD45.2 APC-eFluor 780 (104) from eBioscience, CD11b PE-Cy7 (M1/70), Ly6C APC (HK1.4), Ly6G PE (1A8) from BioLegend. Cells were sorted using a FACSAriaIII (BD Biosciences) equipped with lasers at 561 and 633 nm, and FACSDiva software (BD Biosciences version 6.1.3). Data were analyzed using FlowJo software (Tree Star, version 9.3.2). Briefly, cells were first gated based on morphology using forward versus side scatter parameters (FSC-A versus SSC-A) and then doublets were excluded considering morphology parameter area versus width (A versus W). Starting from CD45 positive low population, microglia cells were isolated as CD11b positive Ly6C/Ly6G double negative cells. Cells were collected in 1.5 mL eppendorf tubes for later RNA extraction. Following isolation, an aliquot of each tube with sorted cells was evaluated for purity at the same instrument resulting in an enrichment >99% for each sample. With this procedure we obtain around 20×10^3 cells from one hemisphere.

Quantitative Real-Time PCR (RT-qPCR)

Samples were lysed in Trizol reagent (Invitrogen) for isolation of total RNA. The quality and yield of RNAs were verified using NANODROP One (Thermo Fisher Scientific). For RT-qPCR, Reverse transcription reaction was performed in a thermocycler using IScript TM RT Supermix (Biorad) under the following conditions: incubation, 25°C, 5′; reverse transcription, 42°C, 45′; inactivation, 85°C, 5′. Real Time-PCR was carried out in a I-Cycler IQ Multicolor RT-PCR Detection System using SSO Fast Eva Green Supermix (Biorad). The PCR protocol consisted of 40 cycles at 95°C, 30″ and 60°C, 30″. For quantification analysis, the comparative Threshold Cycle (Ct) method was used. The Ct values from each gene were normalized to the Ct value of GAPDH in the same cDNA samples. Relative quantification was performed using the $2^{-\Delta\Delta Ct}$ method (Schmittgen and Livak, 2008) and expressed as fold increase in arbitrary values. Primers sequences are reported in **Table 1**.

Nitric Oxide (NO) Measurement

Nitric Oxide production by microglia cultures was assessed by measuring nitrite accumulation in the culture medium by Griess Reagent Kit according to manufacturer's instructions (Molecular Probes, MA, United States). For the NO measurements we used five different primary microglial culture preparations. The absorbance was measured at 570 nm in a spectrophotometer microplate reader (BioTek Instruments Inc., Winooski, VT, United States).

Arginase Activity Assay Measurement

Arginase activity in microglia cultures was assessed by measuring urea accumulation in the culture medium by Ariginase activity assay Kit according to manufacturer's instructions (Sigma-Aldrich). For the Ariginase activity measurements we used six different primary microglial culture preparations. The absorbance was measured at 430 nm in a spectrophotometer microplate reader (BioTek Instruments Inc., VT, United States).

Lactate Measurement

Lactate production by microglia cultures was assessed by measuring lactate accumulation in the culture medium by Lactate assay Kit according to manufacturer's instructions (Sigma-Aldrich). For the lactate measurements we used three different primary microglial culture preparations. The absorbance was measured at 570 nm in a spectrophotometer microplate reader (BioTek Instruments Inc., Winooski, VT, United States).

Seahorse XF Analyzer Respiratory Assay

Cellular oxygen consumption rate (OCR) and extracellular acidification rate (ECAR) were detected using XF Cell Mito Stress Test (Agilent) measured by the extracellular flux analyzer XFe96 (Seahorse Bioscience, Houston, TX, United States) in the Hyp-ACB Platform in Sapienza University. Microglia were cultured on XFe culture miniplates (coated with poly-L-Lys) for a total of 4 days (40×10^3 cells/well). After 2 days microglia were stimulated with 100 or 10 ng/ml of LPS for 24 h and 100 nM fractalkine for further 24 h. Both treatments show the same trend but only the change observed with 10 ng/ml was statistically significant and therefore only these data were shown. It is likely that 100 ng/ml treatment leads to a dramatic OCR reduction and in such a contest the variation due to CX3CL1 treatment are below the sensibility of the system. The sensor cartridge for XFe analyzer was hydrated in a 37°C non-CO_2 incubator a day before the experiment. According to the manufacturer instructions, stressors concentrations were optimized and added as follows: 1 μM oligomycin as complex V inhibitor, 1 μM FCCP (uncoupler agent) and 0.5 μM rotenone/antimycin A (inhibitors of complex I and III). During sensor calibration, cells were incubated 1 h in a 37°C non-CO_2 incubator in 180 μl assay medium (XF base medium supplemented with 10 mM glucose, 10 mM pyruvate and 2 mM L-glutamine at pH 7.4, was used to wash the cells and replace the growth medium). OCR was normalized for total protein/well/40×10^3 cells. Each sample/treatment was analyzed in at least 8 wells for experiment; the figure represents one sample experiment. Two independent experiments were carried out on two different primary microglial culture preparations.

Western Blotting Analysis

For protein analysis, microglial cells were seeded on 12 well plates (40×10^4 cells) and treated with LPS (100 ng/ml) for 24 h and the day after with CX3CL1 (100 nM) for further 24 h; cells were

TABLE 1 | Sequences of the primers used for RT-qPCR.

Gene	Species	Primer forward	Primer reverse
inos	Mouse	ACATCGACCCGTCCACAGTAT	CAGAGGGGTAGGCTTGTCTC
il1β	Mouse	GCAACTGTTCCTGAACTCAACT	ACTTTTTGGGGTCCGTCAACT
cd86	Mouse	AGAACTTACGGAAGCACCCA	GGCAGATATGCAGTCCCATT
tnfα	Mouse	GTGGAACTGGCAGAAGAG	CCATAGAACTGATGAGAGG
arg1	Mouse	CTCCAAGCCAAAGTCCTTAGAG	AGGAGCTGTCATTAGGGACATC
ym1	Mouse	CAGGTCTGGCAATTCTTCTGAA	GTCTTGCTCATGTGTGTAAGTGA
fizz1	Mouse	CCAATCCAGCTAACTATCCCTCC	ACCCAGTAGCAGTCATCCCA
gapdh	Mouse	TCGCTCCCGTAGACAAAATGG	TTGAGGTCAATGAAGGGGTC
il6	Mouse	GATGGATGCTACCAAACTGGA	TCTGAAGGACTCTGGCTTTG
pgc1a	Mouse	ACAGCTTTCTGGGTGGATTG	TGTCTCTGTGAGGACCGCTA
pparg	Mouse	TCCGTGATGGAAGACCACTCGCA	TCAGCAACCATTGGGTCAGCTCT
tgfb1	Mouse	GGAGAGCCCTGGATACCAAC	AAGTTGGCATGGTAGCCCTT
tgfb1r	Mouse	GCTCCTCATCGTGTTGGTG	CAGTGACTGAGACAAAGCAAAGA
prc	Mouse	GCTTGGCTGTAGGAAACTCAG	CAGTTCTGGGGCTTGTAACC
sirt3	Mouse	ACAGCTACATGCACGGTCTG	TGCTCCCCAAAGAACACAAT
g6pdh	Mouse	TTATCATCATGGGTGCATCG	GTCGTCCACTGTGAGTCGTG
aldoA	Mouse	TTAGTCCTTTCGCCTACCCA	GCGATGTCAGACAGCTCCTT
eno1	Mouse	CACCCTCTTTCCTTGCTTTG	AGATCGACCTCAACAGTGGG
hk1	Mouse	ACCAAAAATACGACCCCCTC	GGGTTATAATCCCGGGAGAG
ldha	Mouse	CCGTTACCTGATGGGAGAGA	TGCCCAGTTCTGGGTTAAGA
pklr	Mouse	GAACACCTCTGCCTTCTGGA	AATGTTCATCCCTGCCTTGA
slc25a15	Mouse	AGTGGTTGGATTGGATCAGC	CATTTCACAAGCTCCGTGG
pkm2	Mouse	CAGCAGGAACCGAAGTACG	TGTGTTCCAGGAAGGTGTCA

washed with PBS and lysed in hot 2× Laemmli buffer, boiled 5 min and sonicated. The same amount of protein samples was separated on 12% SDS-polyacrylamide gel electrophoresis and analyzed by western immunoblot using the following primary antibodies: Arg-1 (1:200, Santa Cruz Biotechnology) PKM2 (1:2000, Cell Signaling), Actin (1:2000 Sigma-Aldrich), HRP-tagged goat anti-mouse and anti-rabbit IgG were used as a secondary antibody (1:2000; Dako). For protein analysis we used four different primary microglial culture preparations. Detection was performed through the chemiluminescent assay Immun-Star Western C Kit (Bio-Rad, CA) and densitometric analysis was carried out with Quantity One software (Bio-Rad, CA).

Statistical Analysis

Data are expressed as the means ± SEM. Student's *t*-test, paired *t*-test, one-way analysis of variance (ANOVA) was performed. A value of $P < 0.05$ was considered significant. All statistical analyses were carried out using the Sigma Plot 11.0 Software (Systat Software GmbH, Erkrath, Germany).

RESULTS

CX3CL1 Induces Change in the Polarization State of Microglia in Culture

Since CX3CL1 is neuroprotective in ischemia (Cipriani et al., 2011) and it is known that neuro-inflammation plays a role in brain damage following ischemic insult (Iadecola and Alexander, 2001; Cheon et al., 2017), we wanted to verify the hypothesis that the neuroprotective effect of CX3CL1 was due to its ability to modulate the phenotype of microglia. For this reason, we used primary murine microglial cells, treated them with CX3CL1 (100 nM) for 24 h and analyzed the expression levels of different anti- (*ym1, arg1, fizz, tgfβ1, tgdβ1r*) and pro- (*inos,* il1β, tnfα, tlr4, cd86, il6) inflammatory genes (Michelucci et al., 2009; Gabrusiewicz et al., 2011) by quantitative real time PCR (RT-qPCR). Data reported in **Figure 1** show that cells exposure to CX3CL1 increased the expression of anti-inflammatory (**Figure 1A**, $n = 8$ $^{**}p < 0.001$, $^{*}p < 0.05$; Student's *t*-test) and lowered the expression of pro-inflammatory genes (**Figure 1B**, $n = 8$ $^{**}p < 0.001$, $^{*}p < 0.05$; Student's *t*-test). Since numerous evidence suggest that upon different activation stages microglial cells switch from the oxidative phosphorylation to the anaerobic glycolysis in order to increase ATP production (Volobouéva et al., 2013; Gimeno-Bayón et al., 2014) we decided to investigate whether CX3CL1 treatment could modify the metabolic repertoire of microglia. Data obtained indicate that CX3CL1 increased the transcription of some genes involved in the oxidative pathway (*pgc1α*, *pgc1β*, *prc*, *sirt3*, *slc25a15*, *pparγ*) (**Figure 1C**, $n = 8$ $^{**}p < 0.001$, $^{*}p < 0.05$; Student's *t*-test) and reduced the expression of others related to the glycolytic pathway (*g6pdh, aldoA, eno1, hk1, ldha, pklr*) (**Figure 1D**, $n = 8$ $^{**}p < 0.001$; Student's *t*-test).

CX3CL1 Induces Shape Changes of Microglia in Culture

The activation state of microglia changes their shape, even if it is not possible to uniquely correlate a specific morphology to a specific phenotype (Kettenmann et al., 2011). We investigated the morphological changes of microglia in culture, upon CX3CL1 stimulation, calculating the "form factor" of single cells, that was calculated as described in the Method section. The form factor is 1 for round cells and correspondingly < 1 when the morphology deviates from the spherical shape. Microglia in culture displayed ramified processes with a small cell body and

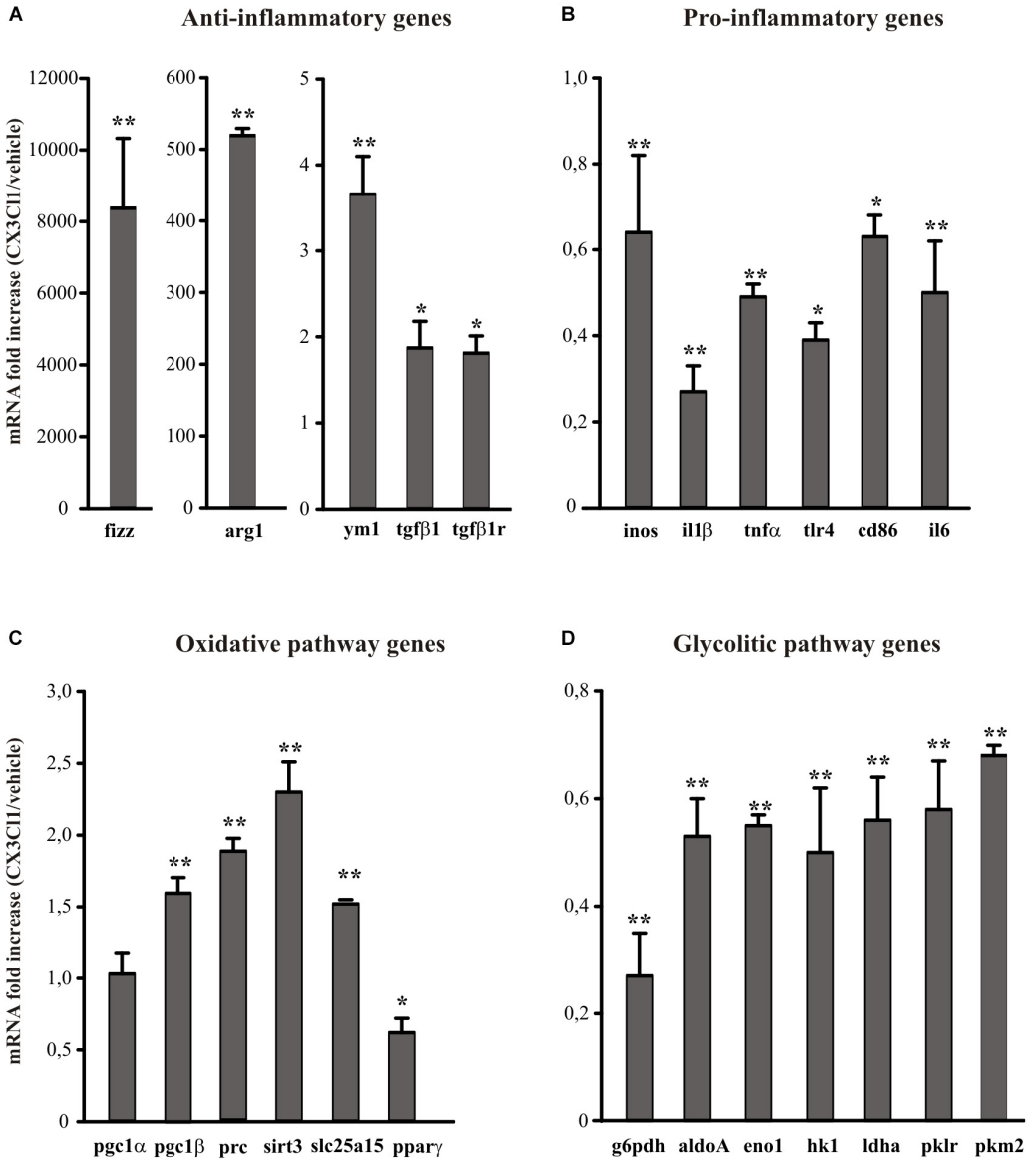

FIGURE 1 | Effects of CX3CL1 in modulating microglia polarization state. Expression analysis by RT-qPCR for mRNAs of anti-inflammatory (**A**: *arg1, ym1*, *fizz, tgfβ1, tgfβ1r*), pro-inflammatory (**B**: *inos, il1β, tnfα, tlr4, cd86, il6*) oxidative pathway (**C**: *pgc1α*, *pgc1β*, *prc*, *sirt3*, *slc25a15 pparγ*) and glycolytic pathway (**D**: *g6pdh, aldoA, eno1, hk1, ldhα, pklr, pkm2*) related genes in primary *wt* microglia treated with CX3CL1 (100 nm, 24 h). For each gene data are expressed as specific mRNA fold increase in CX3CL1 treated cells normalized to specific mRNA expression in vehicle. Statistical analysis: Data are expressed as the mean (±SEM.) of $n = 8$, $^{**}p < 0.001$, $^{*}p < 0.05$, Student's *t*-test.

several long processes (**Figure 2**, not stimulated condition, ns). The results in **Figure 2** show that microglia stimulated with LPS (100 ng/ml, 24 h), significantly change their form factor from 0.26 ± 0.06 (ns) to 0.7 ± 0.05; upon interleukine-4, (IL-4) treatment (20 ng/ml, 24 h) this parameter is similar to not stimulated cells (0.27 ± 0.08) in analogy with what previously reported (Grimaldi et al., 2016). The form factor of cells stimulated with CX3CL1 (0.28 ± 0.05) was similar to untreated cells and CX3CL1/LPS co-treatment significantly reverts the effect of LPS on cell shape variations (form factor: 0.41 ± 0.07) confirming that CX3CL1 efficiently contrasts the effects of inflammatory stimuli on microglial cells ($n = 120$ cells in total for each different conditions, $^{**}p < 0.001$; one-way ANOVA followed by Mann–Whitney Rank Sum *post hoc* test).

CX3CL1 Modulates Microglia Polarization in Pro-inflammatory Conditions *in vitro*

Arginine metabolism via nitric oxide synthase (NOS) or arginase is at the crossroad of the pro- and anti-inflammatory microglia phenotypes (Orihuela et al., 2016). To verify the hypothesis

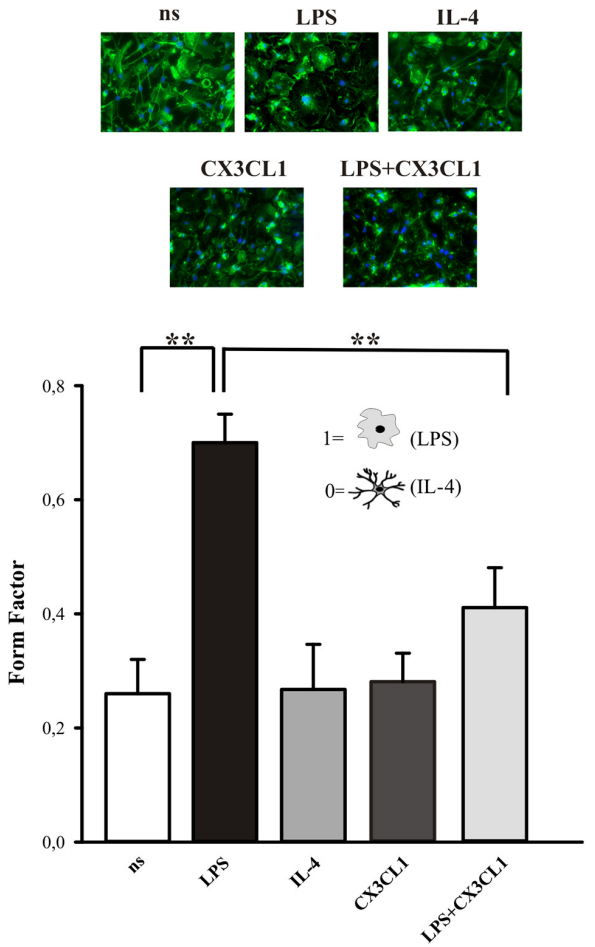

FIGURE 2 | CX3CL1 induces change in microglia shape in culture. **Upper panel:** fluorescence images of microglia in culture stimulated with LPS, IL-4, CX3CL1, LPS + CX3CL1 and stained with Alexa-Fluor 488 Phalloidin. **Lower panel:** form factor analysis of microglia cells treated with LPS (pro-inflammatory stimulus) IL-4 (anti-inflammatory stimulus), CX3CL1, LPS + CX3CL1. Statistical analysis: Data are expressed as the mean (± SEM.) of $n = 20$ cells for each condition, $^{**}p < 0.001$, Student's *t*-test.

that CX3CL1 could modulate microglia phenotype also under pro-inflammatory conditions, we stimulated cells with LPS (100 ng/ml, 24 h) and then with CX3CL1 (100 nM) for additional 24 h, and measured the release of nitric oxide (NO), the production of lactate and the arginase activity in microglia 24 h later. As shown in **Figure 3A**, LPS-induced NO release was significantly reduced by treatment with CX3CL1, bringing it back to the control level ($n = 5$, $^{*}p < 0.05$; One- way ANOVA followed by Holm–Sidak *post hoc* test). In the same conditions we measured the lactate concentration in the medium of cultured microglia: **Figure 3B** shows that the LPS stimulation induced an increase in the lactate production that is reduced after CX3CL1 treatment ($n = 3$, $^{*}p < 0.05$; One- way ANOVA followed by Tukey *post hoc* test). We also decided to analyze the expression of the Pyruvate Kinase isozymes M2 (PKM2) which is an enzyme involved in glycolysis that converts phosphoenolpyruvate to pyruvate and generates ATP. Data obtained by western blot assays reported in **Figure 3D** showed that PKM2 protein levels in microglia markedly increased after LPS exposure while they returned to the control level after CX3CL1 treatment ($n = 3$, $^{*}p < 0.05$; One- way ANOVA followed by Holm–Sidak *post hoc* test). Regarding the arginase activity and arginase 1 (Arg-1) protein expression in microglia, cells were treated as described above and, as shown in **Figure 3C**, CX3CL1 increased arginase activity and reverted the reduction induced by LPS treatment ($n = 6$, $^{*}p < 0.05$; One-way ANOVA followed by Tukey *post hoc* test). Moreover data reported in **Figure 3E** demonstrated that the stimulation with CX3CL1 (100 nM, 24 h) induced an increase in Arg-1 protein in microglia *vs.* not treated cells ($n = 4$, $^{*}p < 0.05$, one-way ANOVA followed by Tukey *post hoc* test) and that the low expression level observed after LPS treatment is back at control level upon CX3CL1 stimulation. To further analyze the effect of fractalkine on the central metabolism, the energetic profile of microglia was assessed through the Cell Mito Stress Test (Agilent) using the extracellular flux analyzer XFe96 (Seahorse Bioscience, Houston, TX, United States). Briefly, this platform allows the determination of the Oxygen Consumption Rate (OCR) under both basal and stressed conditions which is indicative of the mitochondrial function; at the same time the extracellular acidification rate (ECAR) was also measured as an indirect quantification of the glycolytic process. The drugs used to promote the stressed condition target (according to the addition order) (i) complex V, i.e., ATP production; (ii) membrane potential, i.e., by uncoupling electron transfer and proton translocation: (iii) electron transfer chain, i.e., complex I and III. As expected (Volobouéva et al., 2013; Orihuela et al., 2016), LPS treatment (10 ng/ml, 48 h) promoted a deep metabolic re-programing as compared to the untreated sample: the OCR was dramatically reduced (∼65% lower; **Figure 3F**), while ECAR (and therefore glycolysis) was doubled (see **Supplementary Figure S1A**), shifting the aerobic profile of microglia to a glycolytic phenotype upon LPS treatment (see **Supplementary Figure S1B**). In light of this, we investigated whether CX3CL1 is able to attenuate the effect of LPS on the metabolic profile of microglia. Both untreated and LPS-treated samples were incubated with 100 nM CX3CL1 24 h after LPS treatment, and Seahorse analysis was then performed. While CX3CL1 did not affect the energetic profile of the untreated sample (see **Supplementary Figure S2**), in the LPS sample this chemokine promoted a significantly decrease of glycolysis and of OCR even though for the latter to a lower extent (**Figure 3G** and **Supplementary Figure S3**). The same trend was observed also at 100 ng/ml of LPS (data not shown).

CX3CL1 Attenuates Microglial Activation After Ischemia *in vivo*

We have previously demonstrated that exogenous CX3CL1 has a long-lasting neuroprotective action *in vivo* against pMCAO in rodents reducing neurological deficits and infarct size related with cerebral ischemia (Cipriani et al., 2011). We have now decided to investigate how CX3CL1 affects microglia phenotype during ischemia: to this aim mice were subjected to pMCAO,

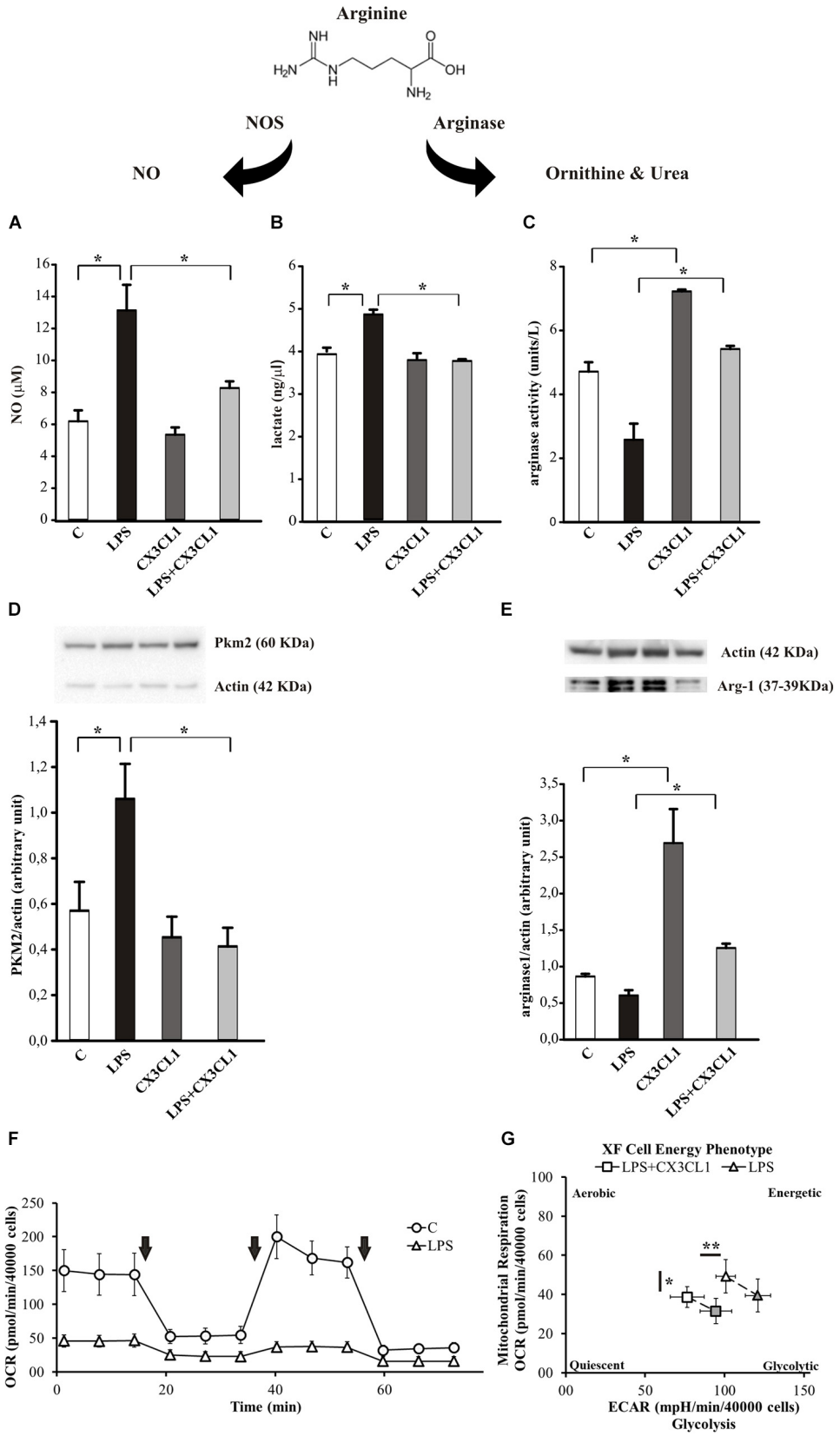

FIGURE 3 | Continued

FIGURE 3 | CX3CL1 modulates microglia phenotype in the context of pro-inflammatory conditions *in vitro*. **(A)** Release of NO by microglia cells not stimulated (C) or stimulated with LPS or CX3CL1 or LPS + CX3CL1; data are expressed as NO concentration (μM). **(B)** Lactate production by microglia cells not stimulated (C) or stimulated with LPS or CX3CL1 or LPS + CX3CL1; data are expressed as lactate concentration (ng/μl). **(C)** Arginase activity in microglia cells not stimulated (C) or stimulated with LPS or CX3CL1 or LPS + CX3CL1; data are expresses as units for liter. **(D)** Western-blot analysis of PKM2 protein expression in microglia cells incubated with vehicle (C) LPS, CX3CL1 or LPS + CX3CL1. At the top, representative image; at the bottom, histogram bar of the quantification of PKM2 expression (data are expressed as PKM2 signal normalized to Actin signal). **(E)** Western-blot analysis of Arg-1 protein expression in microglia cells incubated with vehicle (C) LPS, CX3CL1 or LPS + CX3CL1. At the top, representative image; at the bottom histogram bar of the quantification of Arg1 expression (data are expressed as Arg1 signal normalized to Actin signal). **(F)** Bioenergetic profile of microglial cells: the mitochondrial respiration of microglia, obtained by means of OCR by seahorse experiments, ± 10 ng/ml of LPS (48 h of treatment; triangle and circle, respectively). Arrows indicates the addiction of drugs used to specifically target the mitochondrial function (i.e., oligomycin, FCCP, rotenone + antimycin, in order of addiction). In principle, the first and the third drug lead to a dramatic OCR drop, while FCCP, as uncoupler agent, leads to a maximal oxygen consumption. While this behavior is observed in the untreated sample, LPS treatment abolished this kind of response. In the figure a representative experiment; values reported in the plot are the means of at least 8 replicates ± SD. **(G)** Energetic profile of LPS-treated microglia ± CX3CL1 treatment: the phenotype plot, where both ECAR and OCR are reported on the X and Y-axis, respectively, indicates that the LPS sample (10 ng/ml, open triangle) is more glycolytic than the LPS + CX3CL1-treated one (10 ng/ml + 100 nM, open square). This trend is maintained also under stressed conditions (gray symbols), where FCCP is not able to trigger a maximal respiratory capacity, as expected. In the figure a representative experiment is shown; values reported in the plot are the means of at least 8 replicates ± SD. Statistical analysis: Data are expressed as the mean (± SEM.) **(A)** $n = 5$, $^{**}p < 0.001$ $^{*}p < 0.05$, one-way ANOVA followed by Holm–Sidak *post hoc* test; **(C)** $n = 6$, $^{*}p < 0.05$, one-way ANOVA followed by Tukey *post hoc* test; **(E)** $n = 4$,$^{*}p < 0.05$, one-way ANOVA followed by Tukey *post hoc* test. **(G)** $n = 2$, $^{**}p < 0.001$ $^{*}p < 0.05$, Student's *t*-test.

we verified that CX3CL1-treated mice had a reduced ischemic volume as previously shown (Cipriani et al., 2011), then $CD11b^+$ cells were isolated from the ipsi- and contra-lateral brain hemispheres 24 or 72 h after ischemia and gene expression was analyzed by RT-qPCR. As reported in **Figure 4A**, at 24 h after ischemia $CD11b^+$ cells increased their expression of anti-inflammatory genes (*arg1*, *ym1*, *fizz*, *tgfβ1*, *tgfβ1r*) in the ipsilateral hemisphere, upon CX3CL1 treatment ($n = 6$ mice per group, $^{*}p > 0.05$; Student's *t*-test).

Instead the expression pattern of the pro-inflammatory genes analyzed (*inos, il1β, tnfα, tlr4, cd86, il6*) is less clear: in particular, we observed an increase in the expression of *tnfα*, *cd86* e *tlr4* in CX3CL1 treated mice, while CX3CL1 reduced *il1β* expression ($n = 6$ mice per group, $^{**}p < 0.001$ $^{*}p > 0.05$; Student's *t*-test). Since it was demonstrated that microglia phenotype changes from anti- to pro-inflammatory with the progression of cerebral ischemia (Fumagalli et al., 2015; Ma et al., 2017) we isolated $CD11b^+$ cells from the ipsi- and contra-lateral brain hemispheres of mice at 72 h after ischemia and analyzed by RT-qPCR the same set of genes.

Data reported in **Figure 4C** show that $CD11b^+$ cells isolated from the ipsilateral hemisphere 72 h after ischemia induction, express higher level of pro-inflammatory genes that undergo a significant reduction of expression upon CX3CL1 treatment ($n = 6$ mice per group, $^{*}p > 0.05$; Student's *t*-test). Interestingly, most of the anti-inflammatory genes considered (**Figure 4C**) are still increased in the ipsilateral hemisphere of CX3CL1 treated mice ($n = 6$ mice per group, $^{**}p < 0.001$ $^{*}p > 0.05$; Student's *t*-test). The MACS column system does not permit to distinguish microglia from other myeloid resident cells and from infiltrating immune cells during the ischemic insult, because they can express CD11b as well as CX3CR1. For this reason, we used a new animal cohort and performed gene analysis only on microglia after pMCAO, taking advantage of the fluorescence-activated cell sorting. Starting from CD45 positive low population, microglial cells were isolated as CD11b positive Ly6C/Ly6G double negative cells from both the ipsi- and contra-lateral brain hemispheres, 24 or 72 h after ischemia and gene expression was analyzed by qRT-PCR. With this gating strategy we uncovered a microglia fraction of 80–90% among $CD45^+$ cells at all time points and an immune cell infiltrate ($CD45^{high}$ among $CD45^+$ cells) of 16.37 ± 6.63% saline- *versus* 19.42 ± 5.77% CX3CL1-treated mice at 24 h after ischemia and of 10.87 ± 1.87% saline- *versus* 20.07 ± 2.71% CX3CL1-treated mice at 72 h after ischemia, confirming the chemotactic role of CX3CL1. FACS analysis allowed us to recover an average of 20×10^3 microglial cells per hemisphere, that is not enough to analyze the expression of all the genes taken into consideration in the previous panels; we have therefore chosen only a few of them. Data reported in **Figures 4E,F** confirmed that CX3CL1 treatment increased the expression of the anti-inflammatory genes *arg1* and *ym1* and decreased that of pro-inflammatory gene *inos* on microglial cells isolated from brain hemispheres both 24 and 72 h after ischemia. Regarding the CX3CL1 effect on *il1β* expression in microglial cells after brain ischemia, it induced an increase in the expression of this cytokine 24 h after ischemia while it had an opposite effect after 72 h from ischemic damage ($n = 4$ mice per group, $^{**}p < 0.001$ $^{*}p > 0.05$; Student's *t*-test), contrary to what observed for $CD11B^+$ cells (see **Figures 4B,D**).

CX3CL1 Modulates Microglial Metabolic State After Ischemia *in vivo*

Several evidence suggest a role of metabolic reprograming in the regulation of the innate inflammatory response of microglia (Volobouéva et al., 2013; Gimeno-Bayón et al., 2014). We analyzed the expression profiles of genes related to the glycolytic and oxidative pathways in $CD11b^+$ cells extracted from the ipsi- and contra-lateral brain hemispheres of mice treated with CX3CL1, at 24 and 72 h after ischemia induction.

The analysis of some genes involved in the oxidative pathway (such as *pgc1β*, *sirt3*, *prc*, *slc25a15* and *pparγ*) shows that CX3CL1 increases their expression in the ipsilateral region at 24 h and 72 h after ischemia with the exception of *pparγ* , whose expression is reduced at 24 h (**Figure 5A**, $n = 6$ mice per group, $^{**}p < 0.001$; Student's *t*-test) and of *prc*, that decreased at 72 h (**Figure 5C**, $n = 6$ mice per group, $^{**}p < 0.001$ * $p > 0.05$; Student's *t*-test). On the other hand, among the genes associated with the glycolytic pathway (such as *aldoA, g6pdh, eno1,* and *ldha*), (**Figure 5B**) at 24 h only *aldoA* was reduced ($n = 6$ mice per group,

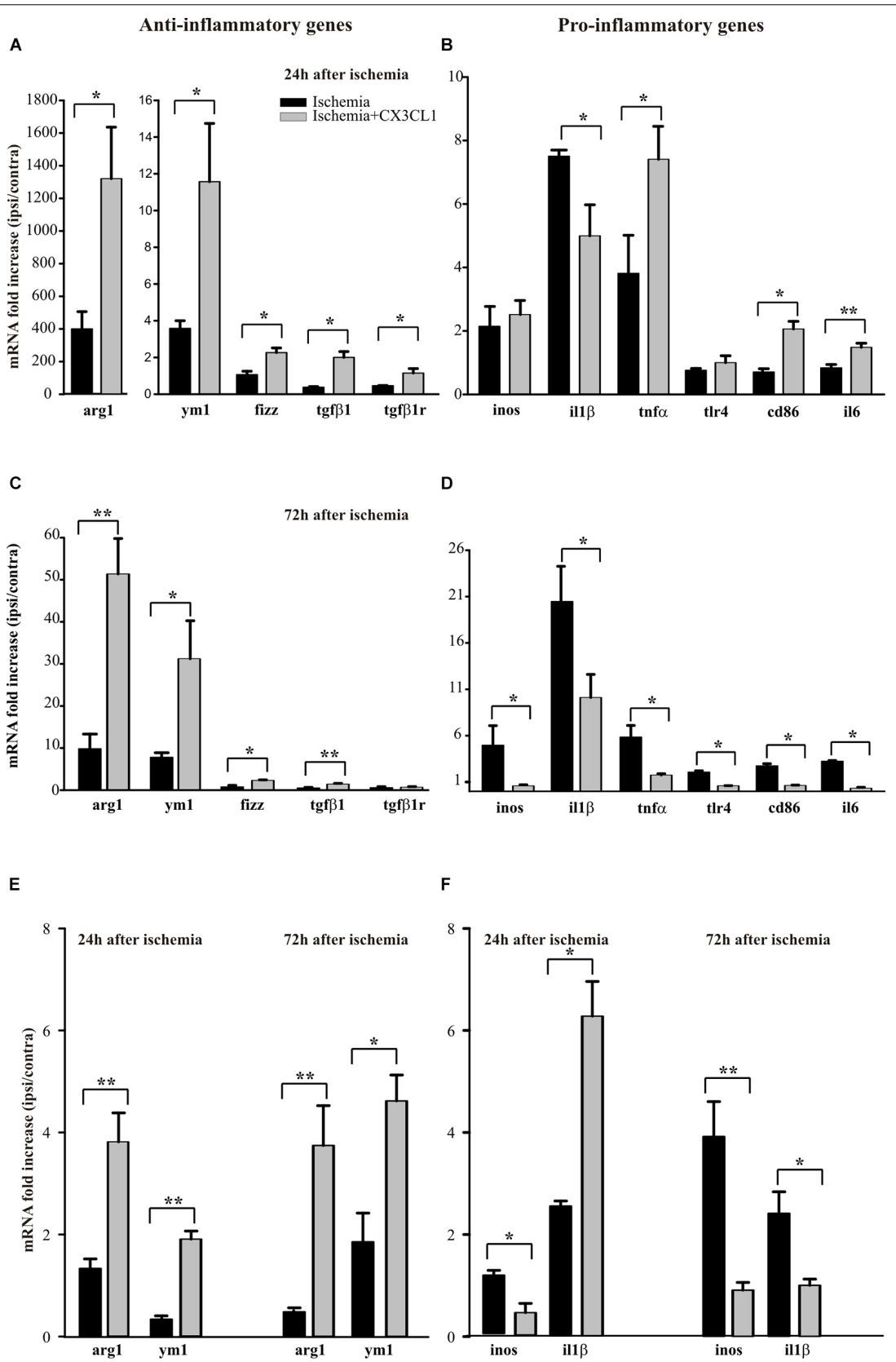

FIGURE 4 | Continued

FIGURE 4 | Effects of CX3CL1 in modulating microglia polarization state after ischemia. Expression analysis by RT-qPCR for mRNAs of anti-inflammatory (*arg1, ym1, fizz, tgfβ1, tgfβ1r*), and pro-inflammatory (*inos, il1β, tnfα, tlr4, cd86, il6*) related genes in $Cd11b^+$ cells extracted from contra- and ipsi-lateral brain hemispheres of mice subjected to pMCAO 24 h **(A,B)** and 72 h **(C,D)** after the insult. Expression analysis by RT-qPCR for mRNAs of anti-inflammatory (*arg1* and *ym1;* **(E)** and pro-inflammatory (*inos* and *il1β*; **F)** related genes in microglial cells sorted by FACS from contra- and ipsi-lateral brain hemisphere cell suspensions of mice subjected to pMCAO 24 h and 72 h after the insult **(E,F)**. For each gene data are expressed as specific mRNA fold increase in the ipsilateral hemisphere of vehicle (black bars) or CX3CL1 treated (gray bars) mice normalized to the mRNA expression for the respective contralateral brain hemisphere. Statistical analysis: Data are expressed as the mean (± SEM.) of $n = 6$ **(A–D)** and $n = 4$ **(E,F)** mice per group, $^{**}p < 0.001$, $^{*}p < 0.05$, Student's *t*-test.

$^{**}p < 0.001$; Student's *t*-test). In contrast 72 h after ischemia they were all reduced upon CX3CL1 treatment (**Figure 5D**; $n = 6$ mice per group, $^{**}p < 0.001$ $^{*}p > 0.05$; Student's *t*-test). We performed a similar analysis on microglial cells isolated from brain hemispheres by fluorescence-activated cell sorting 24 and 72 h after ischemia and what we observed is an increase in the expression of *pgc1β* and *slc25a15* in CX3CL1 treated mice both 24 and 72 h after ischemia (**Figure 5E**, $n = 4$ mice per group, $^{**}p < 0.001$ $^{*}p > 0.05$; Student's *t*-test), while CX3CL1 reduced *pkm2* expression 24 and 72 h after brain damage and ldh*α* expression 72 h after ischemia insult (**Figure 5F**, $n = 4$ mice per group, $^{**}p < 0.001$ $^{*}p > 0.05$; Student's *t*-test).

DISCUSSION

Microglia and Neuroinflammation

Neuroinflammation is associated with the pathophysiology of neurodegenerative disorders (Leszek et al., 2016), and glial activation during neuroinflammation is a common feature in disease progression, resulting in the production of inflammatory cytokines, such as tumor necrosis factor-α (TNF-α), interleukin-1β (IL-1β), reactive oxygen species, and nitric oxide, which can ultimately lead to neuronal loss (Meraz-Ríos et al., 2013). As CNS-resident immune cells, microglia play a key role in maintaining tissue homeostasis, as well as in inducing neurotoxicity (Liddelow et al., 2017). Under normal oxygen conditions, cells usually acquire energy via two mechanisms: glucose is converted to pyruvate via glycolysis which moves to mitochondria to produce ATP through oxidative phosphorylation (Dashty, 2013). Under hypoxic conditions, anaerobic glycolysis converts pyruvate into lactate (Murray, 2006; Hardie, 2007). Immune cells switch from oxidative phosphorylation to aerobic glycolysis, as described in other cell types (Warburg effect) (Warburg, 1956; Vander Heiden et al., 2009), in order to produce metabolic resources necessary to satisfy the request of cell proliferation and activation. This metabolic reprograming plays a key role in the process of the innate inflammatory response; in particular, the pro-inflammatory state is correlated with a shift of energy production from oxidative phosphorylation to aerobic glycolysis (Krawczyk et al., 2010; O'Neill and Hardie, 2013; Orihuela et al., 2016). Moreover, glycolysis inhibition reduces the pro-inflammatory polarization of immune cells, indicating a possible regulatory role in inflammatory cell function (Cheng et al., 2014). When stimulated with LPS/IFN-γ, microglia switch toward a pro-inflammatory phenotype, undergo aerobic glycolysis and release pro-inflammatory cytokines; when stimulated with IL-4/IL-13, they acquire an anti-inflammatory phenotype, with inflammation resolution and tissue repair (Kelly and O'Neill, 2015). In this view, energy demand would be associated with specific functional activities such as change in morphology, phagocytosis and translocation to the injured site of microglial cells (Stence et al., 2001; Koizumi et al., 2007; Fu et al., 2014), and thus may influence the contribution of microglia activation to various neurodegenerative condition. There are evidence of both harmful and protective roles of microglia in stroke (Nakajima and Kohsaka, 2004; Neumann et al., 2006; Neher et al., 2013), and so the precise role and timing of microglia in stroke and cerebral ischemia is debated. Activated microglia produce pro-inflammatory cytokines, nitric oxide and reactive oxygen species inducing an acute and chronic inflammatory response which exacerbates neuronal injury in stroke (Block et al., 2007). Nevertheless, both exogenous and resident proliferating microglia are able to exert neuroprotective action in brain ischemia, through the production of neurotrophic factors (Imai et al., 2007; Lalancette-Hébert et al., 2007; Narantuya et al., 2010). This dual activity of microglia might be explained by the differences in the parenchymal milieu composition produced in injuries of diverse entity and/or at distinct stages of the pathology, which might have various effects on microglia activation (Lai and Todd, 2008). In this contest, the molecular mechanisms through which microglia activate different responses have become an important area of ischemia research. CX3CL1 has been reported to inhibit the release of inflammatory cytokines (Zujovic et al., 2000; Mizuno et al., 2003; Cardona et al., 2006) and reduce microglia activation, keeping these cells in what (before the deep use of transcriptome analysis) has been defined an "off" state (Biber et al., 2007). We previously demonstrated that CX3CL1 is protective against cerebral ischemia (Cipriani et al., 2011). Since it was demonstrated that during the progression of cerebral ischemia microglia phenotype changes from anti- to pro-inflammatory (Fumagalli et al., 2015; Ma et al., 2017) and microglia express CX3CR1, we investigated whether the neuroprotective effect of CX3CL1 in ischemia is due to its ability to change the phenotype of microglia. For this reason, we analyzed the expression profiles of anti- and pro-inflammatory genes and those related to the metabolic reprograming, in the regulation of the inflammatory response both *in vitro* and *in vivo*.

CX3CL1 Modulates the Inflammatory Phenotype of Microglia *in vitro*

In this paper we demonstrate that CX3CL1 drives microglia toward an anti-inflammatory phenotype reducing the expression of pro-inflammatory genes and increasing the expression of

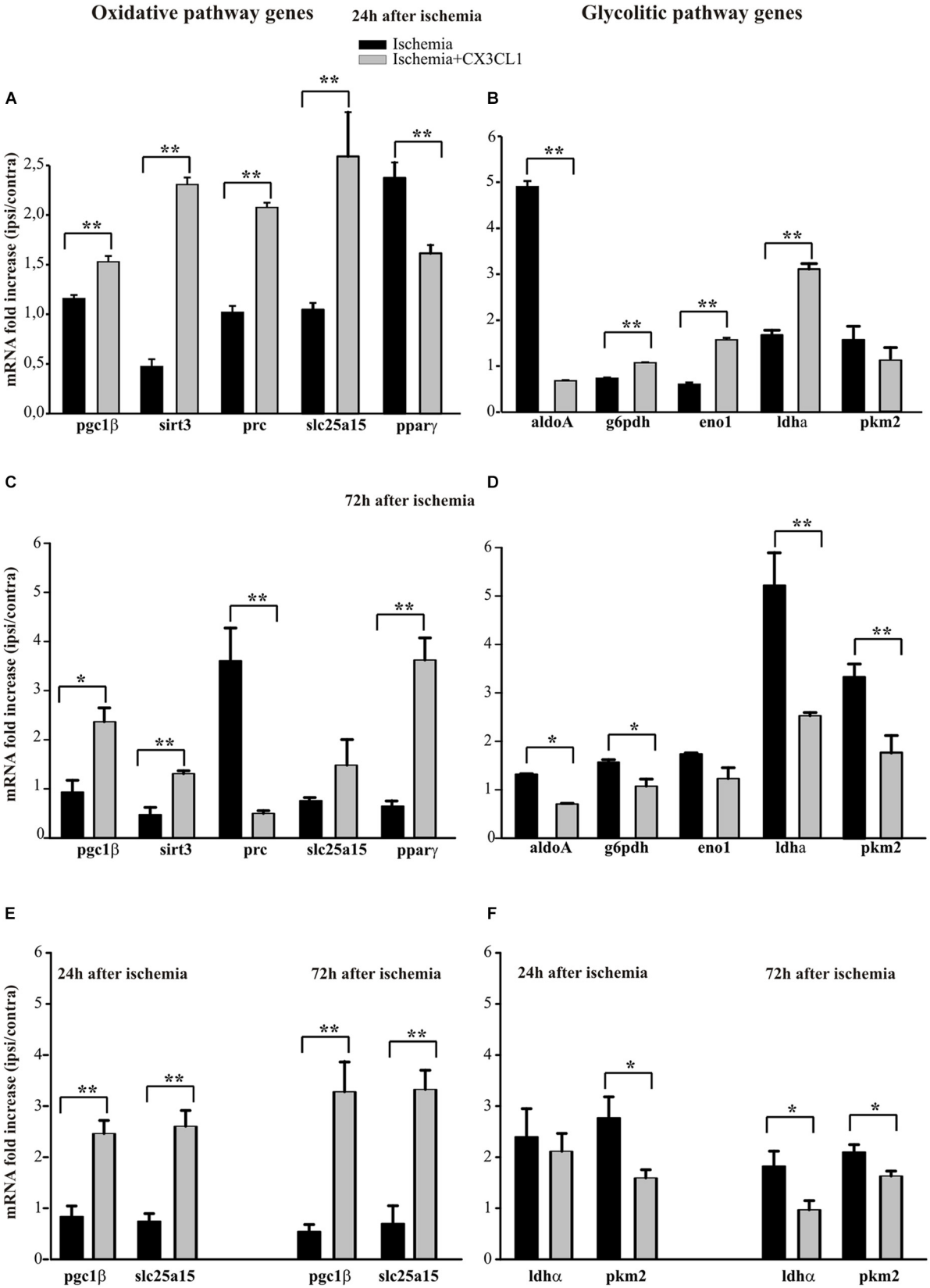

FIGURE 5 | Continued

FIGURE 5 | Effects of CX3CL1 in modulating microglia metabolic state after ischemia. Expression analysis by RT-qPCR for mRNAs of oxidative pathway (*pgc1β*, *sirt3*, *prc*, *slc25a15 pparγ*) and glycolytic pathway (*aldoA, g6pdh, eno1, ldha, pkm2*) related genes in Cd11b$^+$ cells extracted from contra- and ipsi-lateral brain hemispheres of mice subjected to pMCAO 24 h **(A,B)** and 72 h **(C,D)** after the insult. Expression analysis by RT-qPCR for mRNAs of oxidative (*pgc1β* and *slc25a15*; **(E)** and glycolytic pathway (*ldha* and *pkm2*; **(F)** related genes in microglial cells sorted by FACS from contra-and ipsi-lateral brain hemisphere cell suspensions of mice subjected to pMCAO 24 h and 72 h after the insult **(E,F)**. For each gene data are expressed as specific mRNA fold increase in the ipsilateral hemisphere of vehicle (black bars) or CX3CL1 treated (gray bars) mice normalized to the mRNA expression for the respective contralateral brain hemisphere. Statistical analysis: Data are expressed as the mean (± SEM.) of $n = 6$ **(A–D)** and $n = 4$ **(E,F)** mice per group, $^{**}p < 0.001$, $^{*}p < 0.05$, Student's *t*-test.

those related to an anti-inflammatory state. Moreover, CX3CL1 switched the metabolic state of microglia from glycolysis to oxidative pathway, increasing the expression of gene related to oxidative phosphorylation and decreasing those involved in glycolytic metabolism of glucose. These effects are in line with what was observed *in vitro* with NO, lactate and arginase activity in primary microglia in the context of inflammatory environment (induced by LPS stimulation), where CX3CL1 counteracts the acquisition of a pro-inflammatory phenotype. To provide specific experimental data on the bioenergetics profile of microglia following pro-inflammatory activation and CX3CL1 treatment, primary microglia cells were seeded in a Seahorse XF plate in order to detect the cellular oxygen consumption rate (OCR) and extracellular acidification rate (ECAR). First, we observed a normal response pattern for unstimulated primary microglia and a decrease in basal respiration in LPS-treated cells that were unresponsive to the mitochondrial stressors, suggesting an impairment of mitochondrial function. More interesting, while microglia exposed to CX3CL1 maintained a bioenergetics profile similar to control condition, CX3CL1 promoted a significant decrease of glycolysis and OCR in LPS-stimulated microglia, confirming that the different phenotypes of microglia induced by CX3CL1 treatment are associated with different metabolic programing.

CX3CL1 Modulates the Inflammatory Phenotype of Microglia *in vivo*

It is known that injured neurons respond to toxic insults by releasing CX3CL1, which is upregulated, cleaved, and released upon ischemia or excitotoxic insult (Chapman et al., 2000; Tarozzo et al., 2002; Limatola et al., 2005; Noda et al., 2011). The neuroprotective or neurotoxic action of CX3CL1 likely depends on the activation (priming) state of microglia in the different phases of acute and chronic brain diseases (Dénes et al., 2008; Cho et al., 2011; Cipriani et al., 2011; Liu et al., 2011; Pabon et al., 2011; Shan et al., 2011; Fumagalli et al., 2013; Lauro et al., 2015). In this view, we hypothesized that CX3CL1 is neuroprotective, in permanent focal cerebral ischemia, due to its ability to modulate microglia polarization and activation state toward a protective one. To confirm its role in modulating microglia polarization also during ischemia *in vivo*, we isolated CD11b$^+$ cells from the ipsi- and contra-lateral cerebral hemispheres of mice subjected to pMCAO, at 24 and 72 h after ischemic insult, and analyzed the expression of the same genes taken in consideration in the *in vitro* experiments. It was demonstrated that upon acute brain damages, microglia cells produce anti-inflammatory cytokines and trophic factors at the site of injury to promote restorative processes (Neumann et al., 2006; Perego et al., 2011; Hu et al., 2012; Ma et al., 2017). However, over time, microglia acquire a pro-inflammatory phenotype releasing pro-inflammatory cytokines, chemokines, and inducible nitric oxide synthase, which results in the exacerbation of brain damage (Shi and Pamer, 2011). We observed that CX3CL1 changes the phenotype of CD11b+ cells isolated in the pMCAO mice model and that this effect is time dependent, according with the appearance of anti-inflammatory (at 24 h) and pro-inflammatory microglia (at 72 h) (Schroeter et al., 1997; Hu et al., 2012; Fumagalli et al., 2015). In fact, CX3CL1 induced an increase in the expression of several anti-inflammatory and oxidative pathway-related genes already 24 h after ischemia and this effect remained up to 72 h. On the contrary, it down-modulated the expression of several pro-inflammatory and glycolytic pathway markers only at 72 h after the ischemic insult, suggesting that in a way CX3CL1 acts potentiating the function of the anti-inflammatory microglia, trying to prolong this population phenotype. Since CD11b$^+$ cells contain a mixture of myeloid cells, we specifically sorted microglial cells (24 or 72 h after ischemia) from both the ipsi- and contra-lateral brain hemisphere by flow cytometry to specifically analyze their gene expression. With this gating strategy we uncovered a microglia fraction of 80–90% among CD45$^+$ cells and we repeated on these cells the expression analysis for some of the genes evaluated on CD11b$^+$ cells. In this way we confirmed that CX3CL1 induces an increase in the expression of anti-inflammatory and oxidative pathway related genes and decreases that of pro-inflammatory and glycolytic pathway markers on microglia. Since in our experimental condition the immune cell infiltrate (CD45^{high} among CD45$^+$ cells) in CX3CL1-treated mice is about 20%, both at 24 and 72 h after ischemia, we cannot ruled out that what we observed for the CD11b$^+$ cells included the contribution of the infiltrating immune cells. Furthermore, it is possible that CX3CL1 modulates the activation state of these cells too in order to recover the ischemic damage. For example, this would explain the observed differences regarding the CX3CL1 effect on il1β expression. It would be interesting to analyze the infiltrating population and the activation state of these cells in the presence and in the absence of the CX3CL1 stimulus and this will probably be the subject of a subsequent study. Moreover, we interpret that CX3CL1 does not modulate all the markers taken in consideration, because the injury-induced inflammatory processes are dynamic, with spatial and temporal heterogeneity, and/or because some microglial cells have intermediate phenotypes, with the simultaneous expression of pro- and anti-inflammatory genes (Ito et al., 2001; Taylor and Sansing, 2013; Morrison and Filosa, 2013). More interestingly, the ability of CX3CL1 to induce a metabolic switch toward oxidative metabolism in microglia might be necessary to accommodate the beneficial role of anti-inflammatory microglia

and results in the generation of metabolites, which are harmful for neuronal survival. Indeed, CX3CL1 can act in concert with other chemokines, growth factors and metabolites to counteract glutamate excitotoxic damage with a mechanism that involves neurons, microglia and astrocytes (Lauro et al., 2010; Rosito et al., 2014). Considering all these data, we hypothesize that, in addition to limit neuronal damage counteracting excitotoxicity, the release of CX3CL1 in response to ischemic insult might be a physiological response of brain tissue to trigger neuroprotection, modulating the activation state of microglia and its metabolism in order to limit neuro-inflammation and give more time to the cells of the brain parenchyma to organize a neuroprotective response. In this view CX3CL1 may be an important messenger molecule that plays a part in microglia response to extracellular signals during ischemic injuries, linking anti-inflammatory microglia to reduced injury and potential repair and could represent a possible target to modulate microglia phenotype to limit inflammation upon ischemia.

ETHICS STATEMENT

The experiments described in the present work, were approved by the Italian Ministry of Health in accordance with the guidelines on the ethical use of animals from the European Community Council Directive of September 22, 2010 (2010/63/EU).

AUTHOR CONTRIBUTIONS

CLa and CLi contributed to the conception and design of the study. CLa designed and performed all the experiments and statistical analysis and wrote the manuscript. GC performed the *in vivo* experiments. LM performed the real time PCR analysis. FA and GP designed and performed isolation of microglia cells by cell sorting. AP and SR ran and calculated the seahorse experiments. FC supervised the Hyp-ACB facility and data analysis. All authors contributed to the manuscript revision, and read and approved the submitted version.

FUNDING

This work was supported by a grants from the Italian Ministry of Health (RF 2018) and from the Italian Ministry of University and Research (PRIN 2015 E8EMCM_001) to CLi and from Sapienza University of Rome (Italy) for the Hyp-ACB Platform (GA116154C8A94E3D) to FC.

ACKNOWLEDGMENTS

Dr. Giovanna Boumis and Dr. Mariachiara Magnifico are acknowledged for skillful technical support for the experiments performed with the Hyp-ACB Platform.

SUPPLEMENTARY MATERIAL

The Supplementary Material for this article can be found online at: https://www.frontiersin.org/articles/10.3389/fncel.2019.00414/full#supplementary-material

FIGURE S1 | Bioenergetic profile of microglial cells. **(A)** The glycolysis of microglia ± 10 ng/ml of LPS as ECAR parameter of the seahorse experiment reported in **Figure 3F**, indicates that the LPS treatment doubled the basal value. **(B)** The effect of LPS on microglia is reported as phenotype plot. This plot, where both ECAR and OCR are reported on the *X* and *Y*-axis, respectively, indicates that the LPS sample (open triangle) is more glycolytic and less aerobic than the untreated one (open circle). Interestingly, while the untreated responds to stressors as expected (gray circles), by increasing both OCR and ECAR, the LPS sample is quite insensitive to drugs treatment (gray triangles). This could be ascribed to a poor and probably maximal basal mitochondrial activity. In the figure a representative experiment; values reported in the plot are the means of at least 8 replicates ± SD.

FIGURE S2 | Bioenergetic profile of microglial cells. The mitochondrial respiration of microglia, obtained by means of OCR by seahorse experiments, ± 100 nM of CX3CL1 (24 h of treatment; black and empty symbols, respectively). Arrows indicate the addiction of drugs used to specifically target the mitochondrial function (i.e., oligomycin, FCCP, rotenone + antimycin, in order of addiction). Chemokine treatment does not affect the energetic profile. In the figure a representative experiment; values reported in the plot are the means of at least 8 replicates ± SD.

FIGURE S3 | Energetic profile of LPS-treated microglia ± CX3CL1 treatment. LPS sample (10 ng/ml, open triangle) and LPS + CX3CL1-treated one (10 ng/ml + 100 nM, open square). Arrows indicates the addiction of drugs used to specifically target the mitochondrial function (i.e., oligomycin, FCCP, rotenone + antimycin, in order of addiction). In the figure a representative experiment is shown as OCR **(A)** and ECAR **(B)** measurements. Histograms from panels **(C–H)** (LPS sample, black square and LPS + CX3CL1-treated sample, open square) are belong to panels **(A,B)** data, according to Agilent Mito Stress Report generator. Values reported in the plot are the means of at least 8 replicates ± SD.

REFERENCES

Biber, K., Neumann, H., Inoue, K., and Boddeke, H. W. (2007). Neuronal 'On' and 'Off' signals control microglia. *Trends Neurosci.* 30, 596–602. doi: 10.1016/j.tins.2007.08.007

Biswas, S. K., and Mantovani, A. (2012). Orchestration of metabolism by macrophages. *Cell. Metab.* 15, 432–437. doi: 10.1016/j.cmet.2011.11.013

Block, M. L., Zecca, L., and Hong, J. S. (2007). Microglia-mediated neurotoxicity: uncovering the molecular mechanisms. *Nat. Rev. Neurosci.* 8, 57–69. doi: 10.1038/nrn2038

Cardona, A. E., Pioro, E. P., Sasse, M. E., Kostenko, V., Cardona, S. M., Dijkstra, I. M., et al. (2006). Control of microglial neurotoxicity by the fractalkine receptor. *Nat. Neurosci.* 9, 917–924. doi: 10.1038/nn1715

Cartier, N., Lewis, C. A., Zhang, R., and Rossi, F. M. (2014). The role of microglia in human disease: therapeutic tool or target? *Acta Neuropathol.* 128, 363–380. doi: 10.1007/s00401-014-1330-y

Ceulemans, A. G., Zgavc, T., Kooijman, R., Hachimi-Idrissi, S., Sarre, S., and Michotte, Y. (2010). The dual role of the neuroinflammatory response after ischemic stroke: modulatory effects of hypothermia. *J. Neuroinflammation.* 7:74. doi: 10.1186/1742-2094-7-74

Chapman, G. A., Moores, K., Harrison, D., Campbell, C. A., Stewart, B. R., and Strijbos, P. J. (2000). Fractalkine cleavage from neuronal membranes represents an acute event in the inflammatory response to excitotoxic brain damage. *J. Neurosci.* 20:RC87. doi: 10.1523/JNEUROSCI.20-15-j0004.2000

Chaudhary, N., Gupta, M. M., Shrestha, S., Pathak, S., Kurmi, O. P., Bhatia, B. D., et al. (2017). clinicodemographic profile of children with seizures in a

tertiary care hospital: a cross-sectional observational study. *Neurol. Res. Int.* 2017:1524548. doi: 10.1155/2017/1524548

Cheng, S. C., Quintin, J., Cramer, R. A., Shepardson, K. M., Saeed, S., Kumar, V., et al. (2014). mTOR- and HIF-1α-mediated aerobic glycolysis as metabolic basis for trained immunity. *Science* 345:1250684. doi: 10.1126/science.1250684

Cheon, S. Y., Kim, E. J., Kim, J. M., Kam, E. H., Ko, B. W., and Koo, B. N. (2017). Regulation of microglia and macrophage polarization via apoptosis signal-regulating kinase 1 silencing after ischemic/hypoxic injury. *Front. Mol. Neurosci.* 10:261. doi: 10.3389/fnmol.2017.00261

Cho, S. H., Sun, B., Zhou, Y., Kauppinen, T. M., Halabisky, B., Wes, P., et al. (2011). CX3CR1 protein signaling modulates microglial activation and protects against plaque-independent cognitive deficits in a mouse model of Alzheimer disease. *J. Biol. Chem.* 286, 32713–32722. doi: 10.1074/jbc.M111.254268

Cipriani, R., Villa, P., Chece, G., Lauro, C., Paladini, A., Micotti, E., et al. (2011). CX3CL1 is neuroprotective in permanent focal cerebral ischemia in rodents. *J. Neurosci.* 31, 16327–16335. doi: 10.1523/JNEUROSCI.3611-11.2011

Dashty, M. (2013). A quick look at biochemistry: carbohydrate metabolism. *Clin. Biochem.* 46, 1339–1352. doi: 10.1016/j.clinbiochem.2013.04.027

Davalos, D., Grutzendler, J., Yang, G., Kim, J. V., Zuo, Y., Jung, S., et al. (2005). ATP mediates rapid microglial response to local brain injury in vivo. *Nat. Neurosci.* 8, 752–758. doi: 10.1038/nn1472

Dénes, A., Ferenczi, S., Halász, J., Környei, Z., and Kovács, K. J. (2008). Role of CX3CR1 (fractalkine receptor) in brain damage and inflammation induced by focal cerebral ischemia in mouse. *J. Cereb. Blood Flow Metab.* 28, 1707–1721. doi: 10.1038/jcbfm.2008.64

Fu, R., Shen, Q., Xu, P., Luo, J. J., and Tang, Y. (2014). Phagocytosis of microglia in the central nervous system diseases. *Mol. Neurobiol.* 49, 1422–1434. doi: 10.1007/s12035-013-8620-8626

Fumagalli, S., Perego, C., Ortolano, F., and De Simoni, M. G. (2013). CX3CR1 deficiency induces an early protective inflammatory environment in ischemic mice. *Glia* 61, 827–842. doi: 10.1002/glia.22474

Fumagalli, S., Perego, C., Pischiutta, F., Zanier, E. R., and De Simoni, M. G. (2015). The ischemic environment drives microglia and macrophage function. *Front. Neurol.* 8:81. doi: 10.3389/fneur.2015.00081

Gabrusiewicz, K., Ellert-Miklaszewska, A., Lipko, M., Sielska, M., Frankowska, M., and Kaminska, B. (2011). Characteristics of the alternative phenotype of microglia/macrophages and its modulation in experimental gliomas. *PLoS One.* 6:e23902. doi: 10.1371/journal.pone.0023902

Gimeno-Bayón, J., López-López, A., Rodríguez, M. J., and Mahy, N. (2014). Glucose pathways adaptation supports acquisition of activated microglia phenotype. *J Neurosci. Res.* 92, 723–731. doi: 10.1002/jnr.23356

Goldmann, T., Wieghofer, P., Jordão, M. J., Prutek, F., Hagemeyer, N., Frenzel, K., et al. (2016). Origin, fate and dynamics of macrophages at central nervous system interfaces. *Nat Immunol.* 17, 797–805. doi: 10.1038/ni.3423

Goldmann, T., Wieghofer, P., Müller, P. F., Wolf, Y., Varol, D., Yona, S., et al. (2013). A new type of microglia gene targeting shows TAK1 to be pivotal in CNS autoimmune inflammation. *Nat. Neurosci.* 16, 1618–1626. doi: 10.1038/nn.3531

Griffin, J. L., and Shockcor, J. P. (2004). Metabolic profiles of cancer cells. *Nat. Rev. Cancer* 4, 551–561. doi: 10.1038/nrc1390

Grimaldi, A., D'Alessandro, G., Golia, M. T., Grössinger, E. M., Di Angelantonio, S., Ragozzino, D., et al. (2016). KCa3.1 inhibition switches the phenotype of glioma-infiltrating microglia/macrophages. *Cell Death Dis.* 7, e2174. doi: 10.1038/cddis.2016.73

Grønberg, N. V., Johansen, F. F., Kristiansen, U., and Hasseldam, H. (2013). Leukocyte infiltration in experimental stroke. *J. Neuroinflammation.* 10:115. doi: 10.1186/1742-2094-10-115

Guillemin, G. J., Croitoru-Lamoury, J., Dormont, D., Armati, P. J., and Brew, B. J. (2003). Quinolinic acid upregulates chemokine production and chemokine receptor expression in astrocytes. *Glia* 41, 371–381. doi: 10.1002/glia.10175

Hardie, D. G. (2007). Biochemistry. balancing cellular energy. *Science* 315, 1671–1672. doi: 10.1126/science.1140737

Harrison, J. K., Jiang, Y., Chen, S., Xia, Y., Maciejewski, D., McNamara, R. K., et al. (1998). Role for neuronally derived fractalkine in mediating interactions between neurons and CX3CR1-expressing microglia. *Proc. Natl. Acad. Sci. U.S.A.* 95, 10896–10901. doi: 10.1073/pnas.95.18.10896

Hu, X., Li, P., Guo, Y., Wang, H., Leak, R. K., Chen, S., et al. (2012). Microglia/macrophage polarization dynamics reveal novel mechanism of injury expansion after focal cerebral ischemia. *Stroke* 43, 3063–3070. doi: 10.1161/STROKEAHA.112.659656

Iadecola, C., and Alexander, M. (2001). Cerebral ischemia and inflammation. *Curr. Opin. Neurol.* 14, 89–94. doi: 10.1097/00019052-200102000-200102014

Iadecola, C., and Anrather, J. (2011). The immunology of stroke: from mechanisms to translation. *Nat. Med.* 17, 796–808. doi: 10.1038/nm.2399

Imai, F., Suzuki, H., Oda, J., Ninomiya, T., Ono, K., Sano, H., et al. (2007). Neuroprotective effect of exogenous microglia in global brain ischemia. *J. Cereb. Blood Flow Metab.* 27, 488–500. doi: 10.1038/sj.jcbfm.9600362

Ito, D., Tanaka, K., Suzuki, S., Dembo, T., and Fukuuchi, Y. (2001). Enhanced expression of Iba1, ionized calcium-binding adapter molecule 1, after transient focal cerebral ischemia in rat brain. *Stroke* 32, 1208–1215. doi: 10.1161/01.STR.32.5.1208

Jin, A. Y., Tuor, U. I., Rushforth, D., Kaur, J., Muller, R. N., Petterson, J. L., et al. (2010). Reduced blood brain barrier breakdown in P-selectin deficient mice following transient ischemic stroke: a future therapeutic target for treatment of stroke. *BMC Neurosci.* 11:12. doi: 10.1186/1471-2202-11-12

Johnson, W., Onuma, O., Owolabic, M., and Sachdev, S. (2016). Stroke: a global response is needed. *Bull. World Health Organ.* 94 634–634A. doi: 10.2471/BLT.16.181636

Jung, S., Aliberti, J., Graemmel, P., Sunshine, M. J., Kreutzberg, G. W., Sher, A., et al. (2000). Analysis of fractalkine receptor CX3CR1 function by targeted deletion and green fluorescent protein reporter gene insertion. *Mol. Cell Biol.* 20, 4106–4114. doi: 10.1128/mcb.20.11.4106-4114.2000

Kelly, B., and O'Neill, L. A. (2015). Metabolic reprogramming in macrophages and dendritic cells in innate immunity. *Cell Res.* 25, 771–784. doi: 10.1038/cr.2015.68

Kettenmann, H., Hanisch, U. K., Noda, M., and Verkhratsky, A. (2011). Physiology of microglia. *Physiol. Rev.* 91, 461–553. doi: 10.1152/physrev.00011.2010

Koizumi, S., Shigemoto-Mogami, Y., Nasu-Tada, K., Shinozaki, Y., Ohsawa, K., Tsuda, M., et al. (2007). UDP acting at P2Y6 receptors is a mediator of microglial phagocytosis. *Nature* 446, 1091–1095. doi: 10.1038/nature05704

Krawczyk, C. M., Holowka, T., Sun, J., Blagih, J., Amiel, E., DeBerardinis, R. J., et al. (2010). Toll-like receptor-induced changes in glycolytic metabolism regulate dendritic cell activation. *Blood* 115, 4742–4749. doi: 10.1182/blood-2009-10-249540

Kriz, J. (2006). Inflammation in ischemic brain injury: timing is important. *Crit. Rev. Neurobiol.* 18, 145–157. doi: 10.1615/CritRevNeurobiol.v18.i1-2.150

Lai, A. Y., and Todd, K. G. (2008). Differential regulation of trophic and proinflammatory microglial effectors is dependent on severity of neuronal injury. *Glia* 56, 259–270. doi: 10.1002/glia.20610

Lalancette-Hébert, M., Gowing, G., Simard, A., Weng, Y. C., and Kriz, J. (2007). Selective ablation of proliferating microglial cells exacerbates ischemic injury in the brain. *J. Neurosci.* 27, 2596–2605. doi: 10.1523/JNEUROSCI.5360-06.2007

Lauro, C., Catalano, M., Trettel, F., and Limatola, C. (2015). Fractalkine in the nervous system: neuroprotective or neurotoxic molecule? *Ann. N.Y. Acad. Sci.* 1351, 141–148. doi: 10.1111/nyas.12805

Lauro, C., Cipriani, R., Catalano, M., Trettel, F., Chece, G., Brusadin, V., et al. (2010). Adenosine A1 receptors and microglial cells mediate CX3CL1-induced protection of hippocampal neurons against Glu-induced death. *Neuropsychopharmacology* 35, 1550–1559. doi: 10.1038/npp.2010.26

Leszek, J., Barreto, G. E., Gąsiorowski, K., Koutsouraki, E., Ávila-Rodrigues, M., and Aliev, G. (2016). Inflammatory mechanisms and oxidative stress as key factors responsible for progression of neurodegeneration: role of brain innate immune system. *CNS Neurol. Disord. Drug Targets.* 15, 329–336. doi: 10.2174/1871527315666160202125914

Liddelow, S. A., Guttenplan, K. A., Clarke, L. E., Bennett, F. C., Bohlen, C. J., Schirmer, L., et al. (2017). Neurotoxic reactive astrocytes are induced by activated microglia. *Nature* 541, 481–487. doi: 10.1038/nature21029

Limatola, C., Lauro, C., Catalano, M., Ciotti, M. T., Bertollini, C., Di Angelantonio, S., et al. (2005). Chemokine CX3CL1 protects rat hippocampal neurons against glutamate-mediated excitotoxicity. *J. Neuroimmunol.* 166, 19–28. doi: 10.1016/j.jneuroim.2005.03.023

Liu, X., Lu, G., and Shen, J. (2011). Silencing CX3CR1 production modulates the interaction between dendritic and endothelial cells. *Mol. Biol. Rep.* 38, 481–488. doi: 10.1007/s11033-010-0131-131

Ma, Y., Wang, J., Wang, Y., and Yang, G. Y. (2017). The biphasic function of microglia in ischemic stroke. *Prog. Neurobiol.* 157, 247–272. doi: 10.1016/j.pneurobio.2016.01.005

Meraz-Ríos, M. A., Toral-Rios, D., Franco-Bocanegra, D., Villeda-Hernández, J., and Campos-Peña, V. (2013). Inflammatory process in Alzheimer's Disease. *Front. Integr. Neurosci.* 7:59. doi: 10.3389/fnint.2013.00059

Michelucci, A., Heurtaux, T., Grandbarbe, L., Morga, E., and Heuschling, P. (2009). Characterization of the microglial phenotype under specific pro-inflammatory and anti-inflammatory conditions: effect of oligomeric and fibrillar amyloid-beta. *J. Neuroimmunol.* 2010, 3–12. doi: 10.1016/j.jneuroim.2009.02.003

Mills, C. D., Kincaid, K., Alt, J. M., Heilman, M. J., and Hill, A. M. (2000). M-1/M-2 macrophages and the Th1/Th2 paradigm. *J. Immunol.* 164, 6166–6173. doi: 10.4049/jimmunol.164.12.6166

Mizuno, T., Kawanokuchi, J., Numata, K., and Suzumura, A. (2003). Production and neuroprotective functions of fractalkine in the central nervous system. *Brain Res.* 979, 65–70. doi: 10.1016/s0006-8993(03)02867-2861

Morrison, H. W., and Filosa, J. A. (2013). A quantitative spatiotemporal analysis of microglia morphology during ischemic stroke and reperfusion. *J. Neuroinflammation.* 10:4. doi: 10.1186/1742-2094-10-14

Murray, P. J. (2006). Understanding and exploiting the endogenous interleukin-10/STAT3-mediated anti-inflammatory response. *Curr. Opin. Pharmacol.* 6, 379–386. doi: 10.1016/j.coph.2006.01.010

Nakajima, K., and Kohsaka, S. (2004). Microglia: neuroprotective and neurotrophic cells in the central nervous system. *Curr. Drug Targets Cardiovasc. Haematol. Disord.* 4, 65–84. doi: 10.2174/1568006043481284

Narantuya, D., Nagai, A., Sheikh, A. M., Masuda, J., Kobayashi, S., Yamaguchi, S., et al. (2010). Human microglia transplanted in rat focal ischemia brain induce neuroprotection and behavioral improvement. *PLoS One* 5:e11746. doi: 10.1371/journal.pone.0011746

Neher, J. J., Emmrich, J. V., Fricker, M., Mander, P. K., Théry, C., and Brown, G. C. (2013). Phagocytosis executes delayed neuronal death after focal brain ischemia. *Proc. Natl. Acad. Sci. U.S.A.* 110, E4098–E4107. doi: 10.1073/pnas.1308679110

Neubrand, V. E., Pedreño, M., Caro, M., Forte-Lago, I., Delgado, M., and Gonzalez-Rey, E. (2014). Mesenchymal stem cells induce the ramification of microglia via the small RhoGTPases Cdc42 and Rac1. *GLIA* 62, 1932–1942. doi: 10.1002/glia.22714

Neumann, J., Gunzer, M., Gutzeit, H. O., Ullrich, O., Reymann, K. G., and Dinkel, K. (2006). Microglia provide neuroprotection after ischemia. *FASEB J.* 20, 714–716. doi: 10.1096/fj.05-4882fje

Nimmerjahn, A., Kirchhoff, F., and Helmchen, F. (2005). Resting microglial cells are highly dynamic surveillants of brain parenchyma in vivo. *Science* 308, 1314–1318. doi: 10.1126/science.1110647

Noda, M., Doi, Y., Liang, J., Kawanokuchi, J., Sonobe, Y., Takeuchi, H., et al. (2011). Fractalkine attenuates excito-neurotoxicity via microglial clearance of damaged neurons and antioxidant enzyme heme oxygenase-1 expression. *J. Biol. Chem.* 286, 2308–2319. doi: 10.1074/jbc.M110.169839

Odegaard, J. I., and Chawla, A. (2011). Alternative macrophage activation and metabolism. *Annu. Rev Pathol.* 6, 275–297. doi: 10.1146/annurev-pathol-011110-130138

O'Neill, L. A., and Hardie, D. G. (2013). Metabolism of inflammation limited by AMPK and pseudo-starvation. *Nature* 493, 346–355. doi: 10.1038/nature11862

Orihuela, R., McPherson, C. A., and Harry, G. J. (2016). Microglial M1/M2 polarization and metabolic states. *Br. J. Pharmacol.* 173, 649–665. doi: 10.1111/bph.13139

Pabon, M. M., Bachstetter, A. D., Hudson, C. E., Gemma, C., and Bickford, P. C. (2011). CX3CL1 reduces neurotoxicity and microglial activation in a rat model of Parkinson's disease. *J. Neuroinflammation.* 8:9. doi: 10.1186/1742-2094-8-9

Paxinos, G., and Watson, C. (1998). *A Stereotaxic Atlas of the Rat Brain*. New York, NY: Academic Press.

Perego, C., Fumagalli, S., and De Simoni, M. G. (2011). Temporal pattern of expression and colocalization of microglia/macrophage phenotype markers following brain ischemic injury in mice. *J. Neuroinflammation.* 8:174. doi: 10.1186/1742-2094-8-174

Prinz, M., Priller, J., Sisodia, S. S., and Ransohoff, R. M. (2011). Heterogeneity of CNS myeloid cells and their roles in neurodegeneration. *Nat. Neurosci.* 14, 1227–1235. doi: 10.1038/nn.2923

Quan, Y., Jiang, C. T., Xue, B., Zhu, S. G., and Wang, X. (2011). High glucose stimulates TNFα and MCP-1 expression in rat microglia via ROS and NF-κB pathways. *Acta Pharmacol. Sin.* 32, 188–193. doi: 10.1038/aps.2010.174

Rodríguez-Prados, J. C., Través, P. G., Cuenca, J., Rico, D., Aragonés, J., Martín-Sanz, P., et al. (2010). Substrate fate in activated macrophages: a comparison between innate, classic, and alternative activation. *J. Immunol.* 185, 605–614. doi: 10.4049/jimmunol.0901698

Rosito, M., Lauro, C., Chece, G., Porzia, A., Monaco, L., Mainiero, F., et al. (2014). Trasmembrane chemokines CX3CL1 and CXCL16 drive interplay between neurons, microglia and astrocytes to counteract pMCAO and excitotoxic neuronal death. *Front. Cell. Neurosci.* 8:193. doi: 10.3389/fncel.2014.00193

Schmittgen, T. D., and Livak, K. J. (2008). Analyzing real-time PCR data by the comparative C(T) method. *Nat. Protoc.* 3, 1101–1108. doi: 10.1038/nprot.2008.73

Schroeter, M., Jander, S., Huitinga, I., Witte, O. W., and Stoll, G. (1997). Phagocytic response in photochemically induced infarction of rat cerebral cortex. The role of resident microglia. *Stroke* 28, 382–386. doi: 10.1161/01.STR.28.2.382

Shan, S., Hong-Min, T., Yi, F., Jun-Peng, G., Yue, F., Yan-Hong, T., et al. (2011). New evidences for fractalkine/CX3CL1 involved in substantia nigral microglial activation and behavioral changes in a rat model of Parkinson's disease. *Neurobiol. Aging* 32, 443–458. doi: 10.1016/j.neurobiolaging.2009.03.004

Sheridan, G. K., and Murphy, K. J. (2013). Neuron-glia crosstalk in health and disease: fractalkine and CX3CR1 take centre stage. *Open Biol.* 3:130181. doi: 10.1098/rsob.130181

Shi, C., and Pamer, E. G. (2011). Monocyte recruitment during infection and inflammation. *Nat. Rev. Immunol.* 11, 762–774. doi: 10.1038/nri3070

Stence, N., Waite, M., and Dailey, M. E. (2001). Dynamics of microglial activation: a confocal time-lapse analysis in hippocampal slices. *Glia* 33, 256–266. doi: 10.1002/1098-1136(200103)33:3<256::aid-glia1024>3.0.co;2-j

Storini, C., Bergamaschini, L., Gesuete, R., Rossi, E., Maiocchi, D., and De Simoni, M. G. (2006). Selective inhibition of plasma kallikrein protects brain from reperfusion injury. *J. Pharmacol. Exp. Ther.* 318, 849–854. doi: 10.1124/jpet.106.105064

Tarozzo, G., Campanella, M., Ghiani, M., Bulfone, A., and Beltramo, M. (2002). Expression of fractalkine and its receptor, CX3CR1, in response to ischaemia-reperfusion brain injury in the rat. *Eur. J. Neurosci.* 15, 1663–1668. doi: 10.1046/j.1460-9568.2002.02007.x

Taylor, R. A., and Sansing, L. H. (2013). Microglial responses after ischemic stroke and intracerebral hemorrhage. *Clin. Dev. Immunol.* 2013:746068. doi: 10.1155/2013/746068

Ulland, T. K., Song, W. M., Huang, S. C., Ulrich, J. D., Sergushichev, A., Beatty, W. L., et al. (2017). TREM2 maintains microglial metabolic fitness in Alzheimer's Disease. *Cell* 170, 649.e13–663.e13. doi: 10.1016/j.cell.2017.07.023

Vander Heiden, M. G., Cantley, L. C., and Thompson, C. B. (2009). Understanding the warburg effect: the metabolic requirements of cell proliferation. *Science* 324, 1029–1033. doi: 10.1126/science.1160809

Volobouеva, L. A., Emery, J. F., Sun, X., and Giffard, R. G. (2013). Inflammatory response of microglial BV-2 cells includes a glycolytic shift and is modulated by mitochondrial glucose-regulated protein 75/mortalin. *FEBS Lett.* 587, 756–762. doi: 10.1016/j.febslet.2013.01.067

Warburg, O. (1956). On respiratory impairment in cancer cells. *Science* 124, 269–270. doi: 10.1126/science.124.3215.267

Yona, S., Kim, K. W., Wolf, Y., Mildner, A., Varol, D., Breker, M., et al. (2013). Fate mapping reveals origins and dynamics of monocytes and tissue macrophages under homeostasis. *Immunity* 38, 79–91. doi: 10.1016/j.immuni.2012.12.001

Yoshida, H., Imaizumi, T., Fujimoto, K., Matsuo, N., Kimura, K., Cui, X., et al. (2001). Synergistic stimulation, by tumor necrosis factor-alpha and interferon gamma, of fractalkine expression in human astrocytes. *Neurosci. Lett.* 303, 132–136. doi: 10.1016/S0304-3940(01)01699-1698

Zhang, X., Dong, H., Zhang, S., Lu, S., Sun, J., and Qian, Y. (2015). Enhancement of LPS-induced microglial inflammation response via TLR4 under high glucose conditions. *Cell Physiol. Biochem.* 35, 1571–1581. doi: 10.1159/000373972

Zujovic, V., Benavides, J., Vigé, X., Carter, C., and Taupin, V. (2000). Fractalkine modulates TNF-alpha secretion and neurotoxicity induced by microglial activation. *Glia* 29, 305–315. doi: 10.1002/(sici)1098-1136(20000215)29:4<305::aid-glia2>3.0.co;2-v

Conflict of Interest Statement: The authors declare that the research was conducted in the absence of any commercial or financial relationships that could be construed as a potential conflict of interest.

Advantages of publishing in Frontiers

OPEN ACCESS
Articles are free to read for greatest visibility and readership

FAST PUBLICATION
Around 90 days from submission to decision

HIGH QUALITY PEER-REVIEW
Rigorous, collaborative, and constructive peer-review

TRANSPARENT PEER-REVIEW
Editors and reviewers acknowledged by name on published articles

Frontiers
Avenue du Tribunal-Fédéral 34
1005 Lausanne | Switzerland

Visit us: www.frontiersin.org
Contact us: info@frontiersin.org | +41 21 510 17 00

REPRODUCIBILITY OF RESEARCH
Support open data and methods to enhance research reproducibility

DIGITAL PUBLISHING
Articles designed for optimal readership across devices

FOLLOW US
@frontiersin

IMPACT METRICS
Advanced article metrics track visibility across digital media

EXTENSIVE PROMOTION
Marketing and promotion of impactful research

LOOP RESEARCH NETWORK
Our network increases your article's readership